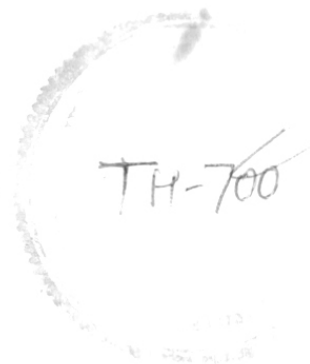


**MOLECULAR RECOGNITION BASED APPROACHES  
TO NUCLEASE MODEL SYSTEMS: SYNTHESIS AND  
STUDIES OF OLIGONUCLEOTIDES CONJUGATED  
WITH AMINE LIGANDS**

A THESIS  
SUBMITTED TO THE  
UNIVERSITY OF POONA

FOR THE DEGREE OF  
DOCTOR OF PHILOSOPHY  
IN CHEMISTRY



**T. P. PRAKASH**



NATIONAL CHEMICAL LABORATORY

PUNE-411 008

DECEMBER 1993

## CERTIFICATE

Certified that the work incorporated in the thesis entitled "*Molecular Recognition Based Approaches to Nuclease Model Systems: Synthesis and Studies of Oligonucleotides Conjugated with Amine Ligands*" submitted by **Mr. T. P. Prakash** was carried out by the candidate under my supervision. Such material as has been obtained from other sources has been duly acknowledged in the thesis.



**(K.N.Ganesh)**

**Research Guide**


**December 1993**

## CANDIDATES DECLARATION

I hereby declare that the thesis entitled "*Molecular Recognition Based Approaches to Nuclease Model Systems: Synthesis and Studies of Oligonucleotides Conjugated with Amine Ligands*" submitted for Ph. D. Degree to the University of Poona has not been submitted by me for a degree to any other University.

National Chemical Laboratory

Pune-411 008



(T. P. Prakash)

## ACKNOWLEDGEMENTS

I express my deep sense of gratitude to my research guide Dr. K. N. Ganesh for his untiring guidance during the entire course of this investigation. His enthusiasm, perseverance and fruitful discussion always inspired me to understand and indulge more into the wonderful world of science.

I record my sincere thanks to the Director National Chemical Laboratory and Dr. S. Rajappa, for permitting me to work in this premier laboratory and providing the necessary infrastructure for carrying out this work.

My sincere thanks are due to Prof. Andrew Hamilton, University of Pittsburgh for mass spectral analysis and Prof. Craig Wilcox for providing the HOSTEST programme.

I thank Prof. A. S. Kolaskar for allowing me to use computer facility at Bioinformatics center, University of Poona. I acknowledge the assistance from National 500 MHz NMR facility, Tata Institute of Fundamental Research, Bombay.

I greatly appreciate assistance and helpful discussion with Dr. Rajamohanam, Dr. Krishna Kumar and Mr. George Samuel regarding NMR spectral analysis and Mr. S. M. Likhite, Mrs. M. V. Mane and Mrs. Sunita Kunte for HPLC analysis.

My thanks are also due to the staff of I. R, Mass Spectroscopy, Microanalysis and Library facilities for their service.

I am grateful to Dr.(Mrs.) V. A. Kumar, Mrs. Anita Gunjal, Dr. A. A. Natu, Dr. T. Pathak and Dr. M. S. Shashidhar, Dr. Mayadevi, Dr. T. P. Mohandas for their help and

suggestions during the course of this work.


I thank my lab mates, Devender, Vidhya, Manjari, Raju, Dinesh, Anand, Gopalakrishna, Vasant, Shakthivel, Sanjib, Renil, Rajeev, Gangamani, Tanya, Lakshmi, Pawar and Sunil for their help and creating a lively lab atmosphere.

I am thankful to my hostel friends Jayant, Prasad, Sagun, Satyanarayana, Gagan, Prakash, Ganesh, Murali, Vivek, Billy, Jose, Rane, Abhay, Anuj, etc. for their company and encouragement.

I am indebted to my parents and my wife for their sacrifice and encouragement throughout my Ph. D. work.

I am obliged to Mr. K. P. Ahamed (KAYAMCO) and M. K. Raghavan for the financial support during my early stage of education.

Finally, I acknowledge CSIR (INDIA) and people of INDIA for a fellowship which enabled me to submit this thesis.

  
T. P. Prakash.

# CONTENTS

Page No

## PUBLICATIONS

## ABSTRACT

## ABBREVIATIONS

### CHAPTER 1 INTRODUCTION TO VARIOUS APPROACHES TO CHEMICAL NUCLEASES

1.1	<i>Introduction</i>	1
1.2	<i>Nucleases</i>	1
1.3	<i>Structure of Catalytic Sites of Nucleases</i>	6
1.4	<i>Chemistry of Phosphate Ester Hydrolysis</i>	12
1.5	<i>Nature's Selection of Phosphates: The Chemical Logic</i>	15
1.6	<i>Nuclease Models</i>	16
1.7	<i>ATPase Mimics</i>	31
1.8	<i>Artificial Receptors for Transition State Stabilization of Phosphoryl-Transfer Reactions</i>	32
1.9	<i>Rationale for The Present Work</i>	33
1.10	<i>References</i>	34

### CHAPTER 2 SYNTHESIS OF MACROCYCLIC POLYAMINES [16]-N<sub>3</sub> AND [21]-N<sub>4</sub> and THEIR COMPLEXATION STUDIES WITH NUCLEOTIDYL PHOSPHATES

2.1	<i>Introduction</i>	40
2.2	<i>Properties of Macrocyclic Polyamines</i>	43
2.3	<i>Objectives of Present Work</i>	51
2.4	<i>Present Work</i>	51
2.5	<i>Conclusion</i>	74
2.6	<i>Experimental</i>	75
2.7	<i>References</i>	81

**CHAPTER 3 SYNTHESIS AND CONFORMATIONAL STUDIES OF d(TpA)  
AND r(UpA) CONJUGATED AT C8 AND C5' WITH AMINES**

3.1	<i>Introduction</i>	84
3.2	<i>Nuclease Models</i>	84
3.3	<i>Objective of Present Work</i>	86
3.4	<i>Present Work</i>	89
3.5	<i>Conformational Studies of Dinucleotides by <sup>1</sup>H NMR Spectroscopy</i>	129
3.6	<i>Conformational Studies of Dinucleotides by <sup>31</sup>P NMR Spectroscopy</i>	136
3.7	<i>Conclusion</i>	137
3.8	<i>Experimental</i>	138
3.9	<i>References</i>	156

**CHAPTER 4 STUDIES ON METAL ION MEDIATED HYDROLYSIS OF  
MODIFIED DINUCLEOTIDES**

4.1	<i>Introduction</i>	159
4.2	<i>Results and discussion</i>	161
4.3	<i>Relevance to RNA Mechanism</i>	186
4.4	<i>Conclusion</i>	188
4.5	<i>Experimental</i>	188
4.6	<i>References</i>	193

**CHAPTER 5 AMINE TETHERED OLIGONUCLEOTIDES: SYNTHESIS  
AND BIOPHYSICAL STUDIES**

5.1	<i>Introduction</i>	196
5.2	<i>Present Objectives</i>	198
5.3	<i>Results and Discussion</i>	199
5.4	<i>Conclusion</i>	230
5.5	<i>Experimental</i>	231
5.6	<i>References</i>	246

## LIST OF PUBLICATIONS.

1. Macrocyclic polyamines [16]-N<sub>3</sub> and [21]-N<sub>4</sub> and study of their ATP complexation by <sup>31</sup>P nuclear magnetic resonance spectroscopy, **Prakash, T. P.**; Rajamohanam, P.; Ganesh, K. N. *J. Chem. Soc. Perkin Trans. I* **1991**, 1273-1278.
2. <sup>31</sup>P NMR study of amine-ATP complexation and conformational differences between 3'-5' and 2'-5'-RNA, Ganesh, K. N.; **Prakash, T. P.**; Gopalakrishnan, V.; Rajamohanam, P. R. in *Magnetic Resonance Current Trends* Khetrpal, C. L.; Govil, G. (eds.), Narosa Publishing House: New Delhi, **1991**, 156-170.
3. 8-Amino(2-aminoethyl)-2'-deoxyadenosine incorporation into DNA by solid phase synthesis, **Prakash, T. P.**; Ganesh, K. N. *Bio-Organic and Medicinal Chemistry Letters* **1993**, **3**, 689-692.
4. Synthesis and conformational studies of d(TpA) and r(UpA) conjugated with histamine and ethylenediamine, **Prakash, T. P.**; Krishna Kumar, R.; Ganesh, K. N. *Tetrahedron* **1993**, **49**, 4035-4050.
5. Approaches to nuclease models: synthesis and conformational studies of dTprA conjugated with histamine at C8(A) and ethylenediamine at C5' (T), **Prakash, T. P.**; Krishna Kumar, R.; Ganesh, K. N. *Nucleosides and Nucleotides* **1993**, **12**, 713-728.
6. Synthesis of site-specific oligonucleotide polyamine conjugates, **Prakash, T. P.**; Kumar, V.; Ganesh, K. N. (Communicated, **1993**)
7. Self cleavage of C8-Histamino-rUpA in presence of Zinc chloride: Mechanistic mimic of ribonuclease, **Prakash, T. P.**; Likhite, S. M.; Ganesh, K. N. (Manuscript under preparation).



## PAPERS PRESENTED AT SYMPOSIA

1. Synthesis of macrocyclic polyamines and their interaction with nucleotide components, **Prakash, T. P.**; Rajmohan, P. R.; Ganesh, K. N.  
Post-IUPAC symposium on the synthesis of natural products, February 12-13, 1990, Indian Institute of Science, Bangalore, India.
2.  $^1\text{H}$  and  $^{31}\text{P}$  NMR in study of oligonucleotides and their conjugates, Ganesh, K. N.; **Prakash, T. P.**; Rajamohan, P. R.  
Indo-Soviet symposium on magnetic resonance, January 14-16, 1991, Indian Institute of Science, Bangalore, India.
3. Molecular recognition in aqueous media: nucleotidyl phosphate complexation by amines, **Prakash, T. P.**, Krishna Kumar, R. Ganesh, K. N.  
Fourth national symposium on bio-organic chemistry, January 27-29, 1992, BARC, Bombay, India.

## ABSTRACT

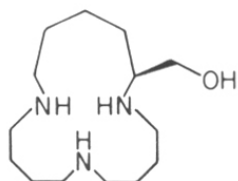
### **Chapter I: Introduction to various approaches to chemical nucleases**

Nucleic acids are the carriers of genetic information in biological systems. The basic chemical linkage that keeps the nucleobase monomers held covalently together is the phosphodiester moiety. There are many cellular processes, such as replication, recombination, repair and restriction cleavage where these phosphate diester bonds are cleaved. In biological systems, all enzymes associated with the above function have one thing in common: they all perform either hydrolysis or transesterification of phosphodiester bonds. Hence an understanding and mimicking of their function assumes importance.

In this chapter, a review of various common structural features of nucleases as found from reported crystallographic structures is presented. The design and studies of various nucleases model systems is also discussed. Amino and imidazole groups are most commonly found as active functional groups at the catalytic site of nucleases (natural & mimics). Interaction of these functional groups with the phosphate backbone of nucleic acids through electrostatic and/or hydrogen bonding activate the phosphate esters towards hydrolytic cleavage. This inspired us to study inter and intra molecular amine-phosphate interactions in model nucleotides which is also the genesis of the present work.

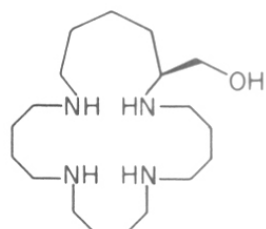
### **Chapter II: Synthesis of macrocyclic polyamines [16]ane N<sub>3</sub> and [21]ane N<sub>4</sub> and their complexation studies with nucleotidyl phosphates**

This chapter describes synthesis of two polyazamacrocycles **1** and **2**. The two macrocycles differ in the number of nitrogen atoms in the macrocycle and hence in their



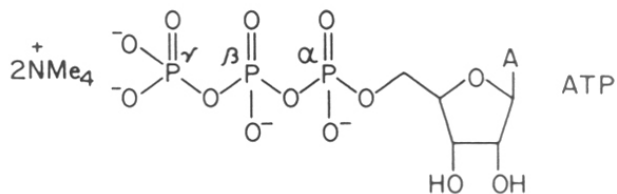
$N_3$  [16]

1



$N_4$  [21]

2

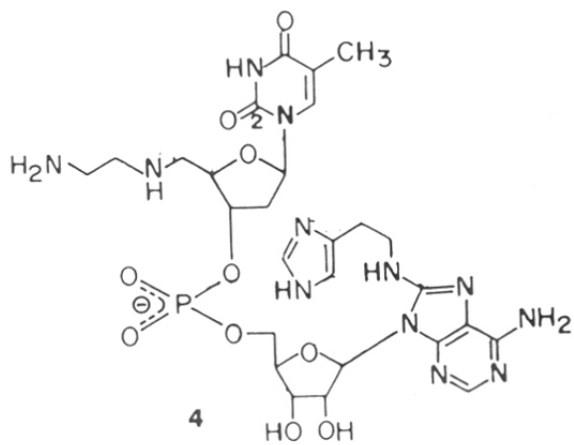
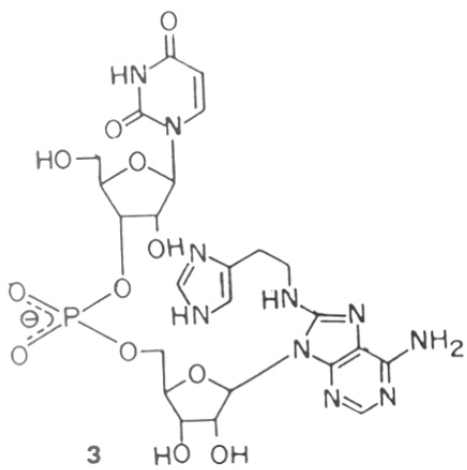
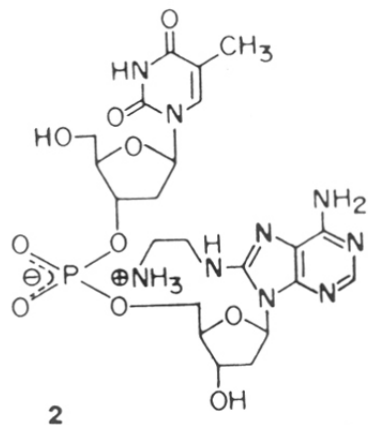
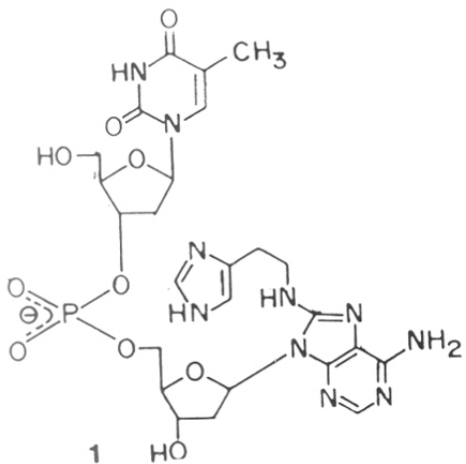


nature and size of the cavity available for complexation of anions. The macrocyclization was achieved by condensation of lysine ditosylate with appropriate components in the presence of  $Cs_2CO_3$ . The complexation of polyamines **1** and **2** with ATP was studied by  $^{31}P$  NMR spectroscopy, which indicated a specific recognition of  $\gamma$ -phosphorus of  $ATP(NMe_4$  salt) by polyamines. The measurement of binding constants by  $^{31}P$  NMR indicated that ATP binds compound **2** about 35 times stronger than it does with compound **1**. The binding curves indicated a definite 1:1 stoichiometry for **2**:ATP binding. The mononucleotides, AMP, cAMP and dinucleotide TpT did not show significant complexation with either **1** or **2**. The binding of ATP by macrocyclic polyamines **1** and **2** and the presence of a hydroxymethyl side chain to link with a nucleophile may aid rational design of chemical nucleases.

### **Chapter III: Synthesis and conformational studies of d (TpA) and r (UpA) conjugated at C8 and C5' with amines**

Binding via molecular recognition and hydrolytic cleavage of DNA and RNA are important biological processes. Enzymes that act on nucleic acids such as ribonuclease, DNA polymerase I, *E. Coli* alkaline phosphatase, endo and exo restriction nucleases, contain either metal ions ( $Zn^{2+}$ ,  $Mg^{2+}$ ) or positively charged amino acid residues (arginine, lysine or protonated histidine) in their active sites for recognition/interaction with negatively charged phosphate group. The active sites also contain amino acids with nucleophilic side chains such as aspartic acid, tyrosine and histidine which mediate phosphate hydrolysis by either general or specific base catalysis. Currently, attention in several laboratories is focussed on molecular recognition of phosphate function which is a chemical pre-requisite for effecting its hydrolysis. Incorporation of active site functional groups of nucleases (enzyme mimicking) may potentially have several applications in oligonucleotide therapeutics.

The main aim of this work was to synthesise dinucleotides **1-4** containing amines conjugated with bases, conformational studies of the base modified dinucleotides and metal ion mediated cleavage reactions. The synthetic possibility of conjugating amino and imidazole containing side chains to C8 of adenosine or C5' of nucleosugars is demonstrated. Solution phase phosphotriester chemistry was used for their synthesis and all compounds were well characterised by the  $^1H$ ,  $^{31}P$ ,  $^{13}C$  NMR and mass spectroscopy. The purity was established by HPLC analysis and conformational analysis was carried out by a first order analysis of  $^1H$ - $^1H$  coupling constants. This indicated that due to base modification, S conformer population of sugar residue increases compared to sugar residue in unmodified dinucleotide. An analysis of spectroscopic data also suggests an intramolecular interaction of the conjugated ligand with internucleotidic



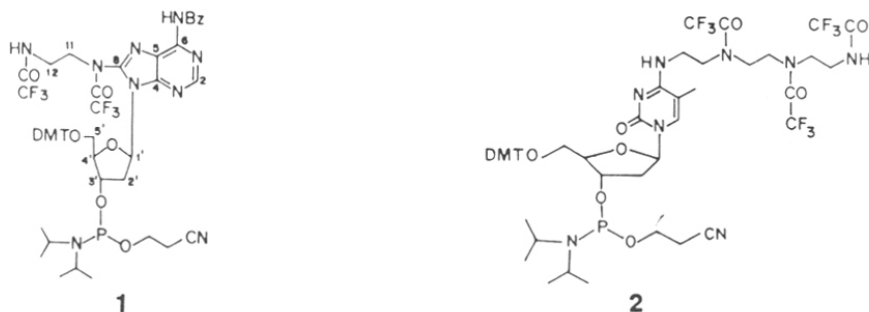
phosphate. These dinucleotides are first of a group of compounds designed to model electrostatic and hydrogen bonding interactions present in the active site of ribonucleases.

#### **Chapter IV: Studies on metal ion mediated hydrolysis of modified dinucleotides**

In this chapter metal ion promoted cleavage of dinucleotides conjugated with histamine **1**, **2** and **3** and ethylenediamine **4** and the unmodified dinucleotide r(UpA) **5**, (synthesized as in Chapter III) were investigated. It was envisaged that the covalently linked catalytic imidazole, in proximity to the phosphate, may accelerate hydrolysis or transesterification reaction. It was indeed found that in presence of  $Zn^{2+}$ , the hydrolysis of C8-histamino ribodinucleotide **3** was 10-15 times faster than that of unmodified ribodinucleotide r(UpA). It was observed that the modified dinucleotide **3** was hydrolyzed in presence of  $ZnCl_2$  whereas other modified dinucleotides **1**, **2** and **4** did not react. The product analysis by HPLC suggested that the reaction involves cleavage of P-O5' bond with the formation of C8-histamino dA and 2',3'-cUMP in the first step. This intermediate subsequently got hydrolysed in a slower reaction to a mixture of 2' and 3' uridine monophosphates. Thus, mechanistically, the reaction is a true enzyme mimic since it went through 2',3'cyclic-UMP as an intermediate, as in ribonucleases, generated in first step by an intramolecular attack of 2'-OH on phosphodiester bond. The thermodynamic activation energy computed from kinetic parameters for the reaction of **3** was less than that of r(UpA) by 4 kcal/mole. While the reaction exhibited a relatively favorable enthalpic activation, the entropic change was unfavorable.

#### **Chapter V: Amine tethered oligonucleotides:- synthesis and biophysical studies**

This chapter reports on synthesis of di and polyamine tethered oligonucleotides and studies on structural variations induced by these modifications. For unambiguous synthesis of such modified oligonucleotides, suitably pre-modified monomer was intro



duced at the desired position in the oligonucleotide sequence. In view of the importance of polyamines such as spermine, spermidine etc. in influencing DNA structure in addition to the diamine conjugated oligonucleotides, those with polyamine conjugates were also synthesized. For this purpose the protected phosphoramidite monomers **1** and **2** containing tethered polyamines were chemically synthesised. These modified monomers were incorporated at the specific positions on DNA chain during the oligonucleotide synthesis using an automated DNA synthesizer. Trifluoroacetyl group was used for N-protection of the side chain amino groups. Successful incorporation of the modified monomer into the sequence was unambiguously established by synthesis of a trinucleotide containing this modified monomer in milligram quantity for its characterization by  $^1\text{H}$  NMR spectroscopy. The stability of modified oligonucleotides were investigated by UV melting experiments. The ability of modified nucleoside monomers in base pairing with complementary nucleoside were also studied by  $^1\text{H}$  NMR titrations and binding constants were evaluated. The convenient synthetic approaches described in this chapter show the possibility of incorporating intelligent, nucleophilic and metal complexing functional groups into the oligonucleotide sequences.

## ABBREVIATIONS

Ac <sub>2</sub> O	- Acetic anhydride
aq	- aqueous
CH <sub>3</sub> CN	- acetonitrile
CHCl <sub>3</sub>	- chloroform
Hist.	- Histamine
EDA	- Ethylenediamine
cm	- centimeter
dA	- deoxy Adenosine
dG	- deoxy Guanosine
dC	- deoxy Cytidine
dT	- deoxy Thymidine
DTT	- Dithiothreitol
DCM	- dichloromethane
DCE	- dichloroethane
DNase	- deoxyribonuclease
DMF	- dimethylformamide
EtOH	- ethanol
EDTA	- Ethylene diamine tetraacetic acid
Fig	- figure
FPLC	- Fast protein liquid chromatograph
g	- grams
HPLC	- High pressure liquid chromatography
hr(s).	- hour(s)
M	- Molar
MHz	- Megahertz



mM	- millimolar
mmol	- millimole
MeOH	- methanol
min	- minute (s)
nm	- nanometers
NMR	- Nuclear magnetic resonance
PAGE	- Polyacrylamide gel electrophoresis
RPC	- reverse phase chromatography
RT	- room temperature
RNA	- ribonucleic acid
TEAA	- triethylammonium acetate
TEAB	- triethylammonium bicarbonate
TLC	- Thin layer chromatography
Tris	- Tris (hydroxymethyl) methylamine (2-amino-2-(hydroxymethyl)-1,3 propanediol)
$\mu\text{Ci}$	- microcurie
$\mu\text{g}$	- microgram
$\mu\text{l}$	- microlitre
$\mu\text{M}$	- micromolar
UV	- ultraviolet
THF	- Tetrahydrofuran
AcOH	- Acetic acid
aq.	- aqueous
Bz	- Benzoyl
DABCO	- 1,4-Diazabicyclo[2.2.2]octane
DCA	- Dichloroacetic acid
DMTCI	- Dimethoxytrityl chloride

DNA	- Deoxyribonucleic acid
MSCl	- 1-Mesitylenesulphonyl chloride
MSNT	- 1-(2-Mesitylenesulphonyl)-3-nitro-1,2,4-triazole
NMI	- N-Methyl Imidazole
NaHCO <sub>3</sub>	- Sodium bicarbonate
RNase	- Ribonuclease
TEA	- Triethylamine

## **CHAPTER 1**

# **INTRODUCTION TO VARIOUS APPROACHES TO CHEMICAL NUCLEASES**

## 1.1 INTRODUCTION

Nucleic acids are the carriers of genetic information in biological systems. The basic chemical linkage that keeps the nucleobase monomers held covalently together is the phosphodiester moiety. There are many cellular processes, such as replication, recombination, repair and restriction cleavage where these phosphate diester bond have to be cleaved. In biological systems, all the enzymes associated with the above function have one thing in common: they all perform either hydrolysis or transesterification of phosphodiester bonds. Hence an understanding and mimicking of their function assumes importance.

## 1.2 NUCLEASES

All biological systems contain nucleases, which are enzymes that catalyse the breakdown of nucleic acids.<sup>1,2</sup> The ribonucelase are specific for RNA substrates whereas deoxyribonucleases act only on DNA; a third class of non specific nucleases phosphodiesterases are active against both types of nucleic acids. The main features of nuclease action used as a basis for classification are

- (i) substrate specificity (i.e., action on RNA, DNA or both) and sequence specificity (restriction enzymes)
- (ii) mode of attack (endonucleases or exonucleases)
- (iii) mode of phosphodiester bond cleavage, (product is either 3'-phosphate and 5' OH termini) or 5'-phosphate and 3'-OH termini (**Fig. 1**)

Table I : Selected Nucleases

Enzyme	Source	Type	Product	Specificity
Pancreatic RNase	Mammalian pancrease	Endonuclease	3'-PO <sub>4</sub> , 5'-OH	3' side of pyrimidine
RNase T1	Aspergillus Oryzae	Endonuclease	3'-PO <sub>4</sub> , 5'-OH	3' to Guanosine
S1Nuclease	Aspergillus	Endonuclease	5'-PO <sub>4</sub> , 3'-OH	Single-strand RNA or DNA
Exoribo nuclease H	Retroviruses	Exonuclease	5'-PO <sub>4</sub> , 3'-OH	RNA of RNA:DNA duplex
Pancreatic deoxy ribonuclease (DNase I)	Pancreas	Endonuclease	3'-PO <sub>4</sub> , 5'-OH	Pu-p-Py bond
Deoxyribo nuclease II	Porcine Spleen	Endonuclease	3'-PO <sub>4</sub> , 5'-OH	No specificity
E. Coli Exonuclease I	E. Coli.	Exonuclease	5'-PO <sub>4</sub> , 3'-OH	Single stranded DNA

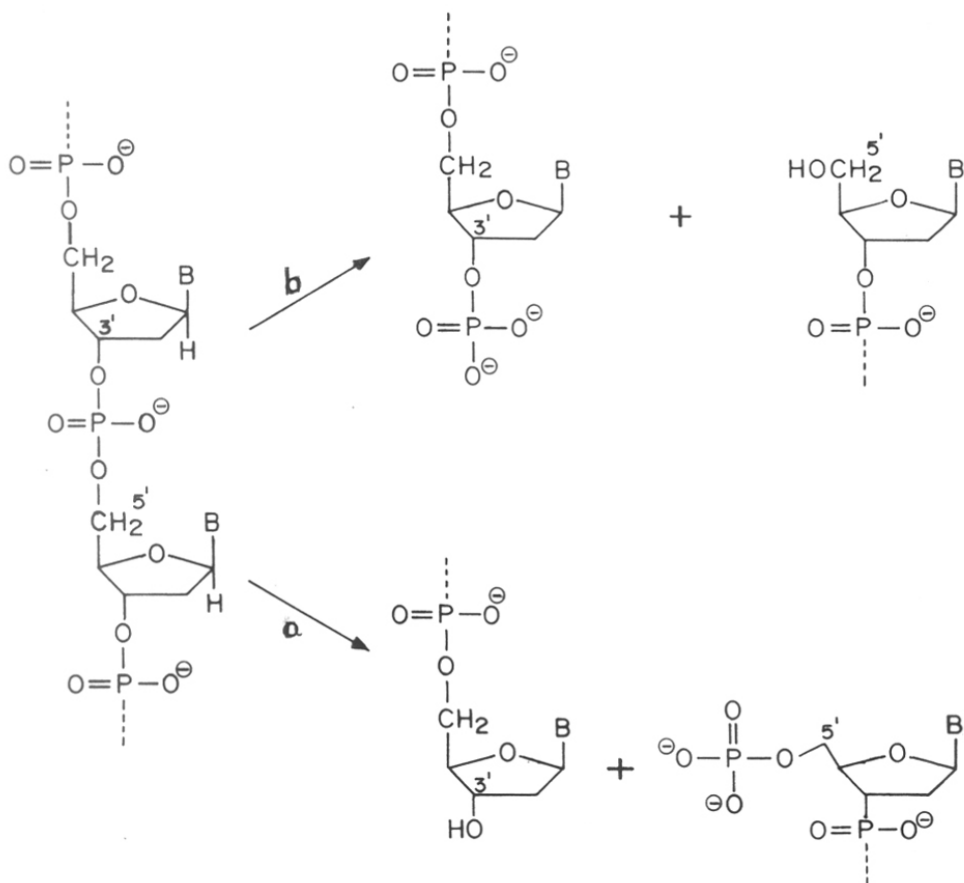


Fig. 1. (a) Cleavage generates 5'-phosphate and 3'-hydroxyl termini  
 (b) Cleavage generates 3'-phosphate and 5'-hydroxyl termini.

### 1.2.1 Non-specific endonucleases

These are endonucleases, which cleave nucleic acids by attacking at points within the polymer chain. These enzymes act on both RNA as well as DNA substrate. Micrococcal nuclease found in cultures of *Staphylococcus* degrade DNA to a mixture of nucleoside and oligonucleotides both with 3'-phosphate termini.<sup>3</sup> It preferentially attacks RNA and heat-denatured DNA. *Neurospora crassa* nucleases has been purified from conidia of *Neurospora* and they act upon DNA or RNA to give oligonucleotides with a 5'-phosphate terminus. Nuclease  $P_1$  from *Penicillium citrinum* splits 3',5'-phosphodi-

ester bonds in RNA and single-stranded DNA as well as 3'-phosphomonoester bonds in mononucleotides and oligonucleotides. It is also a  $Zn^{2+}$  dependent enzyme<sup>4</sup> with optimum activity at 70°C.

### 1.2.2 Non-specific exonucleases<sup>4</sup>

Exonucleases are enzymes which cleave nucleic acids from one end of the chain (exolytic). The venoms of several species of snakes contain a phosphodiesterase which is commonly employed in the preparation of nucleoside 5'-phosphates. Snake Venom phosphodiesterase hydrolyses RNA to nucleoside 5'-monophosphates starting at the 3'-hydroxyl end of the chain (3'→5' exonucleolytic activity). Spleen phosphodiesterase hydrolyses RNA to nucleoside 3'-monophosphates starting at the 5'-hydroxyl end (5'→3' exonucleolytic activity). Both act on mixture of oligonucleotides produced by spleen deoxyribonucleases action on DNA.

### 1.2.3 Riboendonucleases which form 5'-phosphate groups: "a-type"

RNase IV from *E. Coli*<sup>5</sup> cleave a number of RNAs at specific sites by an unknown mechanism of recognition. The 26S RNA of the bacteriophage R17 is cleaved at five sites in a short section of RNA, generating 15S and 22S fragments. It seems likely that the enzymes recognize some features of the secondary structure of the substrate and Adams et al.<sup>6</sup> related the cleavage sites to the proposed secondary structure of the phage RNA.

### 1.2.4 Endoribonucleases which form 3'-phosphate: "b-type"

Pancreatic ribonucleases (Ribonucleases A) first purified by Dubos and Thompson<sup>7</sup> and crystallized by Kunitz<sup>4</sup> is remarkably resistant to heat, inactive on DNA and is strongly antigenic. This enzyme cleaves the ester bond between the 3'-phosphate and the 5'-oxygen of the ribose of pyrimidine nucleotide. Ribonuclease T<sub>1</sub> obtained from

*Aspergillus Oryzae* specifically hydrolyses -GpX- phosphate bond of RNA between 3'-phosphate side of G and the 5'-OH group of adjacent nucleotide. Ribonuclease I from *E. Coli*. digests single-stranded RNA with no absolute base specificity although it hydrolyses poly U faster than other homopolymers. Ribonucleases U<sub>2</sub>, from *Ustilago sphaerogena* hydrolyses phosphodiester bonds in two separable steps; transphosphorylation and hydrolysis<sup>4</sup>.

### 1.2.5 Ribonucleases acting on RNA:DNA hybrids (RNase H)

RNase H first described by Stein and Hausen<sup>4</sup> digests the RNA component of an RNA:DNA hybrid. All RNase H's characterized so far produce 5'-phosphate and 3'-hydroxyl termini. Some produce oligomers 2 to 9 nucleotides in length while others generate mono and dinucleotides. The role of RNase H is unknown but recent experiments with *E. Coli* mutants<sup>8</sup> suggest that, in this organism at least, the enzyme plays a role in the initiation of the replication of the bacterial chromosome and is the information of a primer for DNA polymerase. RNase H enzyme is important in antisense technology based on use of synthetic oligonucleotide for inhibition of gene expression. The binding of specific synthetic oligonucleotides to mRNA results the formation of RNA:DNA hybrids which are the substrates for RNase H enzyme. As a result the RNA of the hybrid will be digested and thereby protein synthesis is inhibited.

### 1.2.6 Restriction endonucleases

Restriction endonucleases are found in a wide variety of prokaryotes.<sup>9</sup> Their biological role is to cleave DNA molecules foreign to system. The cells own DNA is not degraded because corresponding site recognized by its restriction enzyme are methylated. These enzymes recognize specific base sequences in double-helical DNA and cleave both strands of the duplex. Restriction enzymes are highly useful as a tool for analysis of chromosomal structure, sequencing very long DNA molecules, isolation of



genes and for designing new DNA fragments for cloning and expression. A unique characteristic of cleavage sites of these enzymes is that the sequences are self complementary and sites of cleavage are symmetrically located on both strands with respect to the two fold axis. Some of the sequences recognized by few restriction enzymes are given in the **Table II**. In comparison to other nucleases, these enzymes have DNA recognition characteristics at level of specific sequences.

Table II: Examples of Restriction Endonucleases. Arrows Shows Cleavage Site

$\begin{array}{c} \downarrow \\ 5' \text{ GGATCC } 3' \\ 3' \text{ CCTAGG } 5' \\ \uparrow \end{array}$	Bam H I	$\begin{array}{c} \downarrow \\ 5' \text{ GAATTC } 3' \\ 3' \text{ CTTAAG } 5' \\ \uparrow \end{array}$	Eco R <sub>1</sub>
$\begin{array}{c} \downarrow \\ 5' \text{ GGCC } 3' \\ 3' \text{ CCGG } 5' \\ \uparrow \end{array}$	Hae III	$\begin{array}{c} \downarrow \\ 5' \text{ GCGC } 3' \\ 3' \text{ CGCG } 5' \\ \uparrow \end{array}$	Hna I
$\begin{array}{c} \downarrow \\ 5' \text{ CTCGAG } 3' \\ 3' \text{ GAGCTC } 5' \\ \uparrow \end{array}$	Xho I		

### 1.3 STRUCTURE OF CATALYTIC SITES OF NUCLEASES

#### 1.3.1 Ribonuclease A

This is perhaps one of the most widely studied enzyme, both from the structural point as well as understanding of enzymatic activity. RNase recognizes the pyrimidine bases uracil and cytidine and cleave RNA next to these residues. Studies on ribonuclease A indicated the participation of at least three amino acid residues in the active site: 2 histidines (Hist.-12 and Hist.-119) and one lysine (Lys.-41). RNA hydrolysis by this enzyme (**Figure 2**) proceeds by two steps: (i) transesterification and (ii) hydrolysis. At physiological pH, one of the two imidazole ring is protonated while the other is not.

The two imidazole rings function as a general acid-base catalytic system

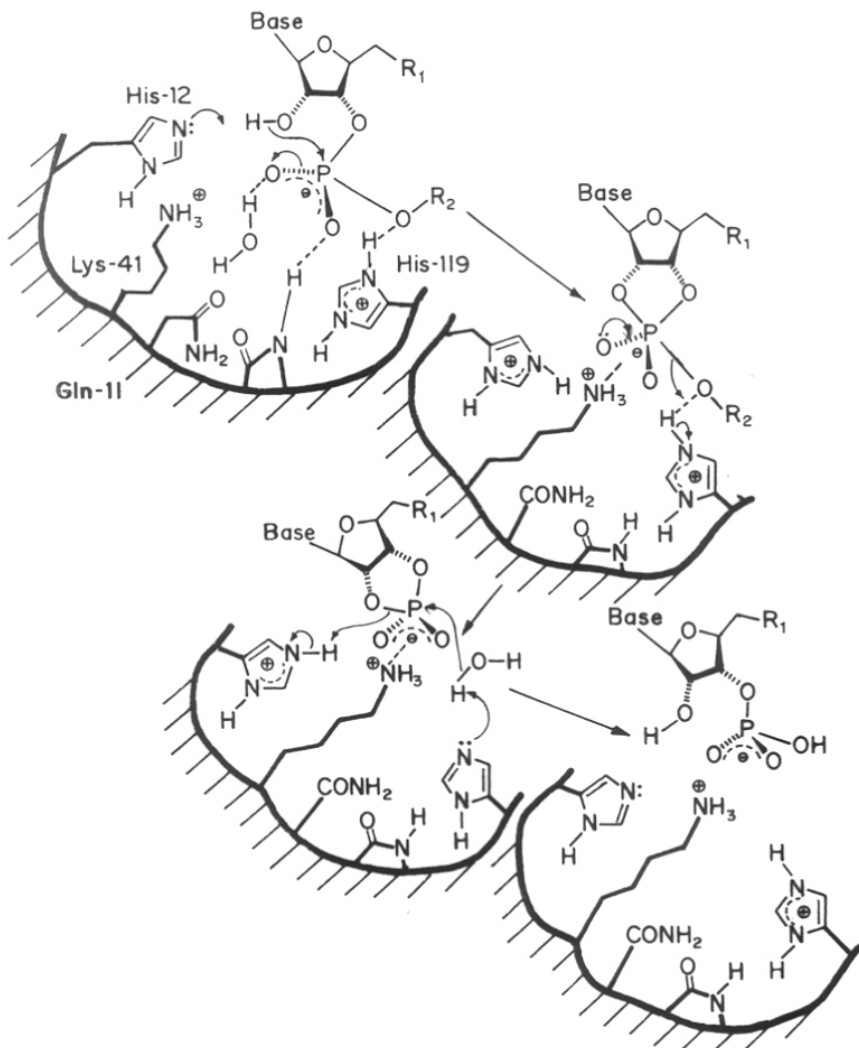


Fig. 2. Mechanism for the ribonuclease catalyzed hydrolysis of RNA. Amino acid residue number refers to its position relative to the N-terminal amino acid of the polypeptide (protein chain).

while the cationic lysine aids in the stabilization of the pentacoordinate phosphorane intermediate.<sup>10</sup> The phosphate substrate is bound by means of two hydrogen bonds between the phosphoryl oxygen and an amide backbone hydrogen and a hydrated glutamine residue. These hydrogen bonds increase the electrophilicity of the phosphorus atom. An important hydrogen bond occurs between the protonated imidazole ring and the oxygen atom of the substrate that is involved in cleavage. This hydrogen bond facilitates complete proton transfer from the imidazole ring to P-O- during the hydrolysis (**Figure 2**). Ribonuclease has a well-defined binding cleft for the substrate.<sup>11</sup> In it are located His-12, His-119 and the side chain of Lys-7, Lys-41 and Lys-66.

Two possible mechanisms have been suggested for phosphate hydrolysis depending upon the relative geometry of the incoming and leaving groups during the displacement process. Referring to the plane defined by the three equatorial ligands, the stereochemical mechanism is inline if the nucleophile enters on one side of the plane and the leaving group departs on the other side. On the other hand, if the nucleophile attacks from one side of the plane containing the leaving group the mechanism is termed "adjacent". According to the preference rules, the adjacent mechanism will require a pseudorotation to transform the leaving group from an equatorial to apical geometry. After an extensive study<sup>11</sup> on the mechanism of hydrolysis it was concluded that RNase hydrolysis proceeds via adjacent mechanism which involves pseudorotation as a step in bond cleavage.

### 1.3.2 Staphylococcal Nuclease<sup>12</sup>

This enzyme consists of a single polypeptide chain (Mr 16900) and crystal structure of its complex with thymidine 3',5' diphosphate has been solved at 1.5 Å resolution.<sup>12</sup> This has given intimate details concerning substrate binding (**Figure 3**) and the mechanism of hydrolysis. The 5'-phosphate group of thymidine 3'-5'-diphosphate in the

enzyme inhibitor complex is hydrogen bonded to the positively charged side chains of

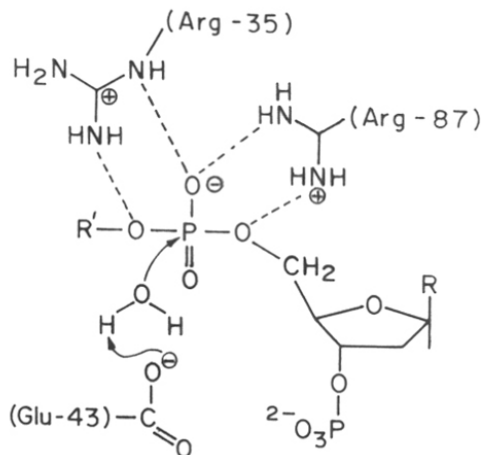


Fig. 3. Mechanism for the Staphylococcal nuclease catalyzed hydrolysis of DNA and RNA.

Arg-35 and Arg-87 which activate the phosphate to nucleophilic attack. Calcium ion is known to be essential for enzyme activity and is present in the active site bound by carboxylates of Asp-21 and Arg 40 and it coordinates with the phosphate to further activate it towards nucleophilic attack. Glu-43 is positioned to act as a general-base catalyst for the attack of  $\text{H}_2\text{O}$ . Thus this enzyme's activity is based on co-ordinated functions of arginine and glutamic acid.

### 1.3.3 Ribonuclease $T_1$

Ribonuclease  $T_1$  resembles Ribonuclease A in<sup>13</sup> function. These are not homologous in amino acid sequences or three-dimensional structure. RNase  $T_1$  found to be specific to guanine and adenine or they are non specific. Due to its high specificity for single-stranded RNA, Rnase  $T_1$  has found versatile application as a tool in RNA sequencing and mapping studies. Detailed crystallographic studies<sup>14</sup> on RNase  $T_1$  complexed with guanosine 2'-phosphate (**Figure 4**) has given much insight into the catalytic site of RNase  $T_1$ . From this and from the information known from numerous biochemical stud-

ies<sup>14</sup> reaction mechanism of RNase T<sub>1</sub> as proposed consists of

- (i) activation of Glu-58 is by His-40 to act as a base for abstraction of the O2'-H proton

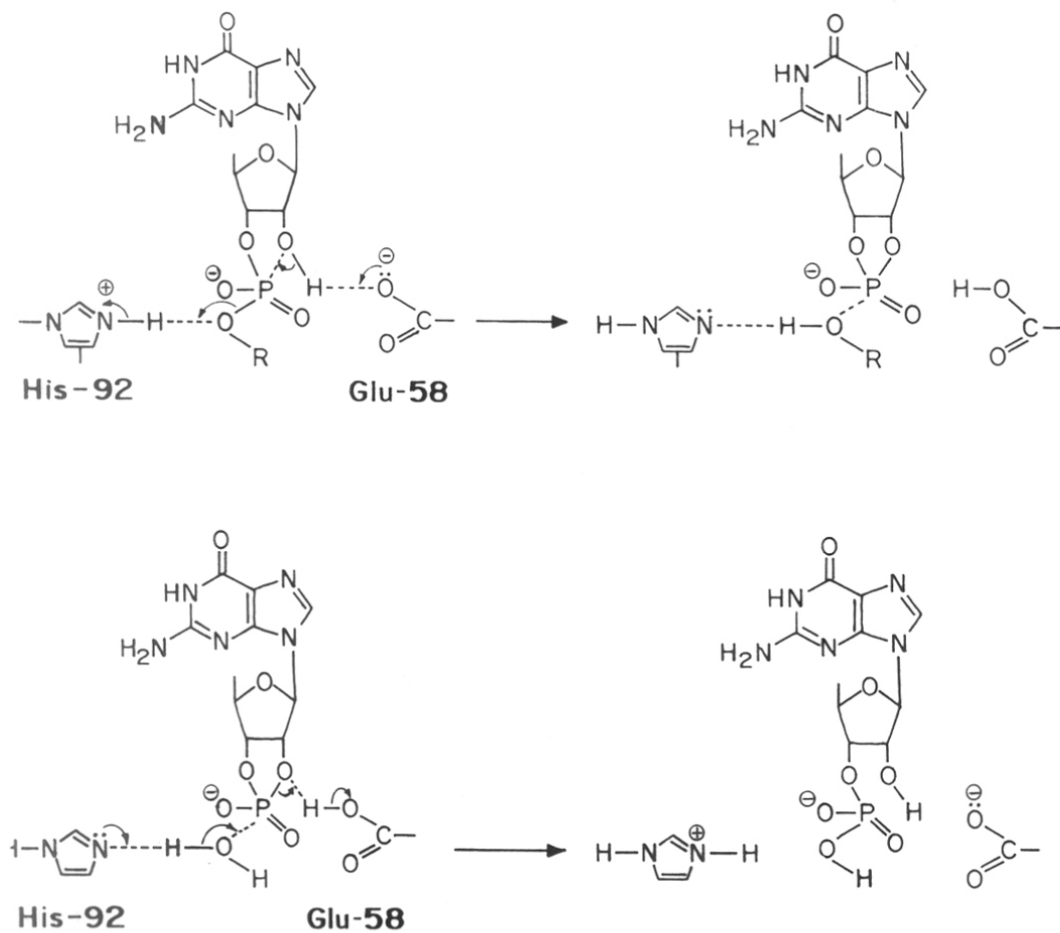


Fig. 4. Most probable mechanism for phosphodiester bond hydrolysis by RNase T<sub>1</sub>.

- (ii) intramolecular attack of  $O(2')^-$  on phosphodiester bond
- (iii) protonation of the leaving alkoxidyl  $O(5')$  from the protonated His 92
- (iv) hydrolysis of the newly formed terminal guaninyl-2'3'-cyclic phosphate is by a water molecule activated by His 92
- (v) protonation of the leaving  $O(2')$  from Glu-58 and the terminal Guanosine 3'-phosphate.

#### 1.3.4 RNase S

Richards, Wyckoff and coworkers<sup>15</sup> have reported a number of crystallographic studies on RNase S, which reveal the involvement of His-119, His-12 and Ly-41 at the substrate binding site. Interaction between these amino acid side chains and the substrate occurs via phosphate group and 2'-hydroxyl group of the dinucleotide. Hydrogen bonds also exist between the ribose, pyrimidine base and Thr-45, Asn-44 and Ser-123 in the so called  $\beta_1$ -site and between the adenine (of the dinucleotide UpA) moiety and Gln-111 and Asn-71 in the  $\beta_2$  binding site.

There are several common chemical principles of RNase mechanism of action showed by all the ribonucleases:

- (i) electrophilic activation of the phosphate group by metal ions or imidazolium ions
- (ii) imidazole acting as acceptors
- (iii) nucleophilic attack from internal 2'-OH which is deprotonated by active base or  $Asp\ COO^-$
- (iv) leaving group stabilization by lysine (RNase A) or aspartic acid (RNase  $T_1$ )
- (v) stereochemical requirement (pseudorotation)
- (vi) stabilization of purine/pyrimidine-binding/recognition

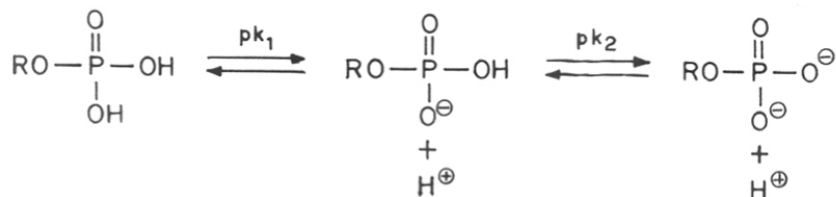
## 1.4 CHEMISTRY OF PHOSPHATE ESTER HYDROLYSIS

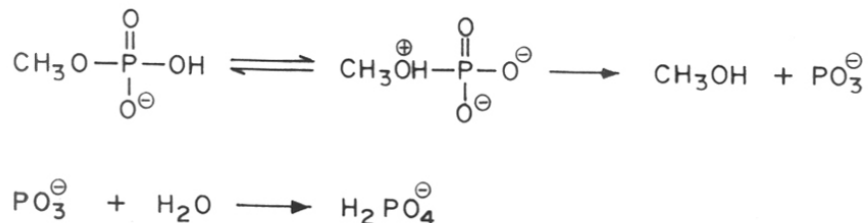
Apart from their important presence in nucleic acids DNA and RNA, phosphate esters and phosphoanhydrides are present as components of many other biological constituents. For e. g. most coenzymes are esters of phosphonic or phosphoric acid. The principal reservoirs of biochemical energy ATP and many essential intermediates in biochemical synthesis and degradations such as creatine phosphates, phosphoryl pyruvate etc. are composed of phosphate functional groups. Understanding of the nature of hydrolytic cleavage of phosphate esters therefore assumes importance. In deed, there is a vast body of literature on mechanistic aspects of hydrolysis of biological and non biological phosphates.

### 1.4.1 Phosphomonoesters

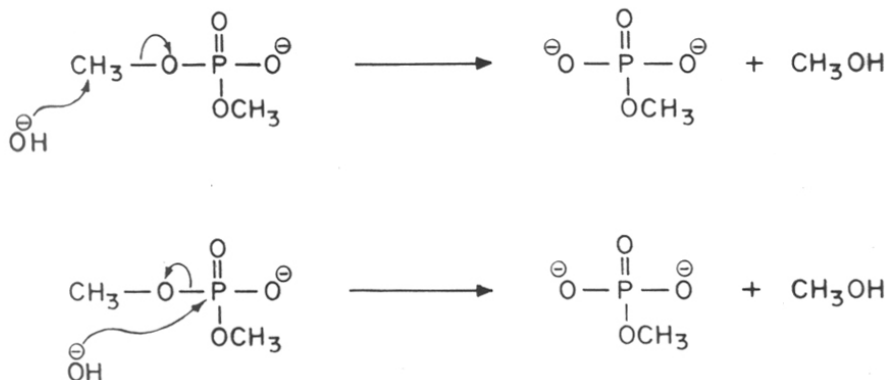
Phosphate monoesters such as adenosine monophosphate and methyl phosphate are normally resistant towards hydrolysis.<sup>16</sup> The mono substituted phosphate esters have two ionizable groups with pKa's of around 1.0 and 6.5<sup>17</sup> with three potentially reactive species (**Scheme 1**). The maximum rate of hydrolysis of monoesters of phosphoric acid occurs at pH 4 where the major species present is the mono protonated monoanion. The pathway postulated for its decomposition is by way of monomeric metaphosphate (**Scheme 2**).

#### SCHEME 1



**SCHEME 2****1.4.2 Phosphodiester**

The non-cyclic disubstituted phosphate esters are the most stable of the phosphate esters. Since the diesters have an ionizable group with a pKa of around 1.5, two reactive species are potentially possible. In strongly alkaline solutions, the hydrolysis of dimethyl phosphate is first order with respect to the concentration of the hydroxide ion and ester. The primary mechanism involves a nucleophilic attack on the carbon with a small percentage of attack occurring at the phosphorus (**Scheme 3**). Under acidic conditions, disubstituted esters are hydrolyzed via mechanisms involving either cleav-

**SCHEME 3**



age at P-O or C-O bond. Some confusion seems to exist as to the exact amount of P-O cleavage but values of 20-30 % have been reported.<sup>17</sup> If a hydroxyl or other nucleophile is present vicinal to the diester, the reactivity is markedly increased, for e. g. RNA gets hydrolyzed very much faster than DNA due to the presence of 2'-hydroxyl group.

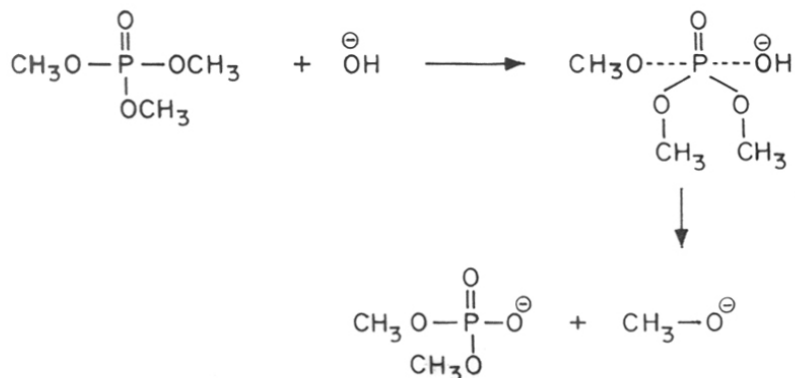
### 1.4.3 Phosphotriesters

Under alkaline conditions phosphatetriesters undergo rapid hydrolysis initially to diesters followed by a slower reaction to other species and the hydrolysis is characterized by following features:

- (i) the reaction is first order with respect to the hydroxide ion and the ester
- (ii) the reaction involves entirely P-O bond cleavage and
- (iii) there is no exchange between the P-O bond and water.

The mechanism which best fits this observation is a concerted, nucleophilic attack of the hydroxyl ion on the phosphorus, with a concomitant displacement of the methoxide ion as shown below (**Scheme 4**).

#### SCHEME 4



## 1.5 NATURES SELECTION OF PHOSPHATES: THE CHEMICAL LOGIC

Most of the biological phosphates remain ionized at physiological pH. The importance of keeping these molecules in ionized state is of vital necessity for the living organisms from the point of storage of metabolites within the cell membranes. Electrically neutral molecules are partially soluble in lipids and may pass through membrane and help their retention within the cell enclosure. Further, electrostatic interaction of the positive and negative charges constitutes a simplest and strong mode of molecular interaction. The negative charge on phosphates are important for binding of metabolites and coenzymes with enzymes and in packing of nucleic acids.

Since nucleic acids are carriers of genetic information, the retention of their chemical integrity is foremost to the organisms. Phosphodiester<sup>18</sup> linkage used by nature is ideal for this purpose since, the group is ionized at physiological pH and the group has chemical stability toward hydrolytic, thermal and oxidative conditions. The preference for the phosphate diester linkage in nucleic acids can further be understood if one considers other possible choices. Esters (e. g. EtOAc) survive neutral pH of the biological environment at ambient temperature for a month (1 molecule hydrolysed/  $10^6$ / month) but at higher acidity or basicity, the hydrolysis is even faster ( $1/10^6$ /sec.). Esters would not have survived the early stage of evolution where pH was far from neutrality. Amide<sup>18</sup> linkages, of course, clash directly with protein chemistry and function and not suitable as a genetic linker. Also, both esters and amides are neutral molecules and hence have drawbacks. The pKa and chemical characteristics of other groups such as citrate, arsenate etc. are unsuitable. The phosphate triesters are hydrolyzed at somewhat lower rates than ethylacetate, but being neutral have other disadvantages. Monoanionic phosphodiesters are most suitable as a chemical theme for backbone structure since nucleophiles (eg.  $\text{OH}^-$ ) are repelled by the negative charge of the phosphodiester anion and are enormously stable against alkaline conditions. Phospho-

monoesters can decompose by a mechanism other than normal nucleophilic attack and hence suitable as metabolic intermediates.

Enzymes cleave phosphodiesterases with enormous ease (high rate) and this is possible due to specific configuration of their side chains in the active site which decrease the chemical stability of phosphates by appropriate molecular interactions. One of the objective of this thesis is to rationalise approaches towards design of artificial, chemical nucleases based on understanding of the strategies employed by various enzymes.

## 1.6 NUCLEASE MODELS

The development of genetic engineering and in particular, human genome project, has called for requirement of DNA cleaving molecules with specificities beyond that provided by restriction enzymes. As a result, the field of "chemical nucleases" has emerged to provide chemical alternative for these enzymes.

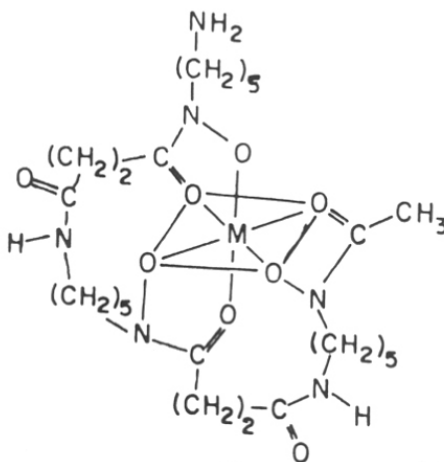
Broadly, three approaches have emerged. One is the oxidative damage of sugar residues which leads to subsequent cleavage of DNA or RNA backbone. A second method is electrophilic modification of a base that results in removal of base moieties and creation of "abasic" sites in DNA/RNA chain. The sugar-phosphate backbone is prone to fragmentation at these "abasic" sites. Both these methods consequent in split of base/sugar units at the point of cleavage and are not exactly "enzyme mimics". The product obtained cannot be "religated" to original DNA unlike those formed in restriction enzyme digests. Alternatively, reaction proceeding via hydrolysis of phosphodiester backbone would have distinct advantage over base modification or its oxidative counterparts: (i) it does not require redox cofactors to initiate reaction or generation of oxy radical species to mediate the reaction. (ii) it would generate fragments that are chemi-

cally competent for ligation by enzymatic reactions. Accordingly there has been considerable interest in developing DNA and RNA hydrolytic catalysts or "nuclease mimics".

### 1.6.1 Oxidative degradation model systems

1,10-Phenanthroline-copper was the first synthetic co-ordination complex demonstrated to have an efficient nucleolytic activity.<sup>19</sup> Subsequently, there are many such complexes reported which are capable for bringing oxidative damage to DNA. A few such examples are ferrous-EDTA<sup>20</sup>, various metalloporphyrins<sup>21</sup> and octahedral complexes of 4,7-diphenyl-1,10-phenanthroline<sup>22</sup> etc. Bleomycin, an antibiotic derived from *Streptomyces verticillus*, nicks DNA via metal ion in an oxygen dependent reaction and has provided important mechanistic rules for structure based design of chemical nucleases.<sup>23</sup>

Recently, it has been demonstrated that Cu(II), Co(III) and Ni(ii) complexes **1** of a siderophore chelating drug Desferal

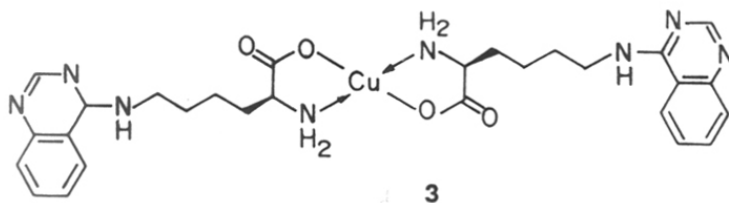
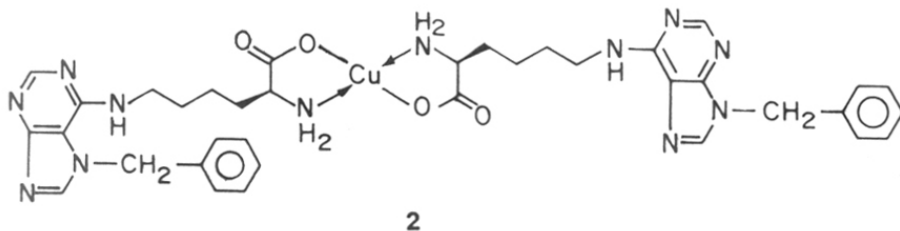


**1**

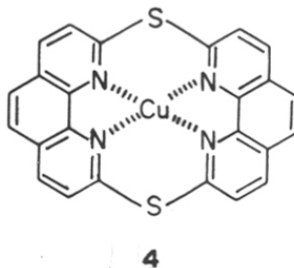
M = Cu(II); Co(III); Ni(II).

cleave DNA.<sup>24</sup> Copper complexes of  $\alpha$ -amino carboxylate units of coded amino acids L-lysine derivative **2** and **3** cleave double stranded DNA.<sup>25</sup>

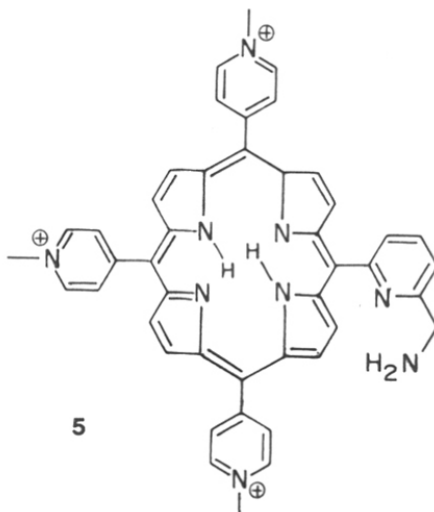
PR  
577.155(043)  
PRA



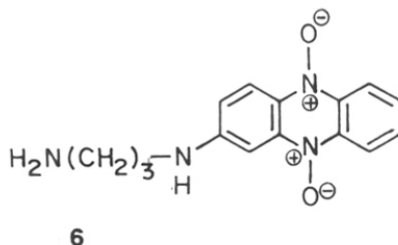
Copper complex **4** binds and cleaves DNA in the presence of a reducing agent under aerobic conditions.<sup>26</sup>



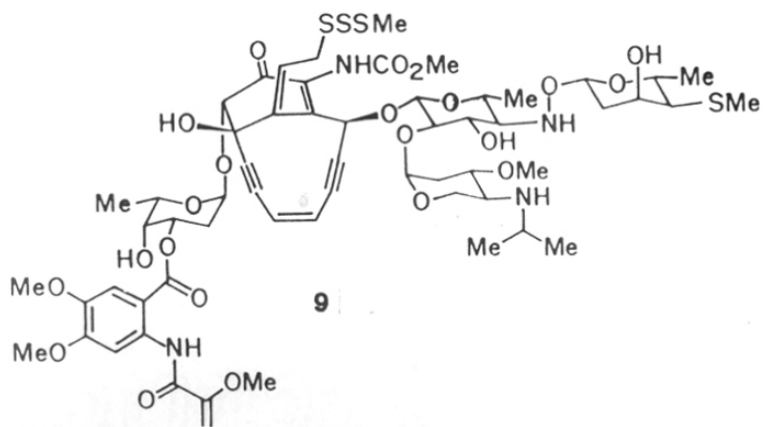
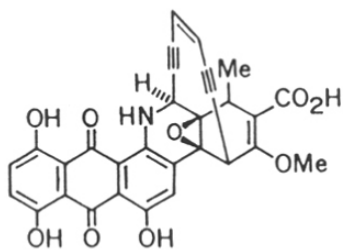
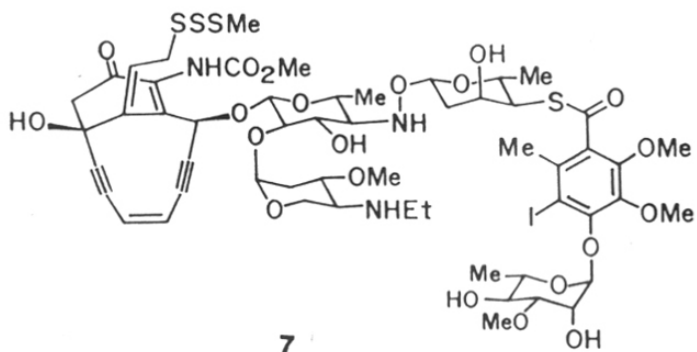
In the presence of high intensity visible light and oxygen, various water soluble porphyrins induce single-strand scission in DNA.<sup>27</sup> This method has potential for photodynamic therapy. DNA cleavage was also observed with metallo derivatives of meso-tetra(4-N-methylpyridyl)porphyrin (Fe(III), Mn(III) and Co(III)), but these porphyrins generally required reduced forms of oxygen for activity.<sup>28</sup> The Cu(II)-**5** system produced extensive DNA cleavage in 1 mM DTT and 1 mM DTT/1 mM hydrogen peroxide.<sup>29</sup>

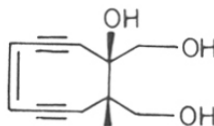


Phenazine-N-oxide derivative **6** upon incubation with  $\phi$ x174 replicative form DNA in the presence of dithiothreitol (DTT), effected cleavage of the plasmid DNA anaerobically in the presence of both DTT and NADPH.<sup>30</sup>



It has recently been discovered that Calicheamicin **7**, Dynemicin **8** and Esperamicin **9**, a new class of antibiotics containing "ene-diyne" moiety induce DNA scission.<sup>31</sup> The mechanism of scission reaction involves a Bergman cyclization of "ene-diyne" system to benzenoid diradical which initiate DNA cleavage chemistry. The cyclization is triggered by binding of the drug to DNA. Synthetic models designed on this chemistry have led to potent synthetic analogues **10**.<sup>31</sup>

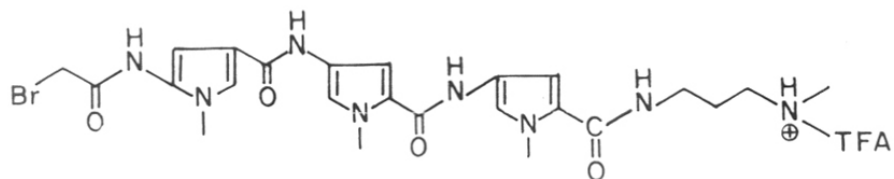




10

### 1.6.2 Electrophilic modification of base

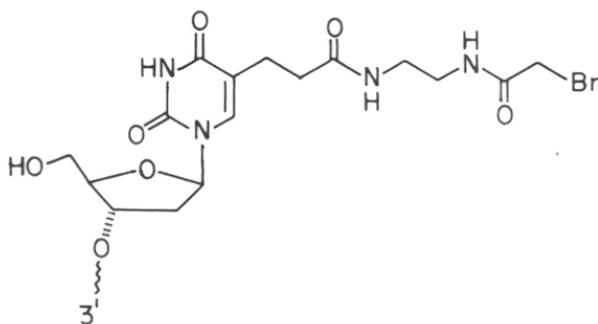
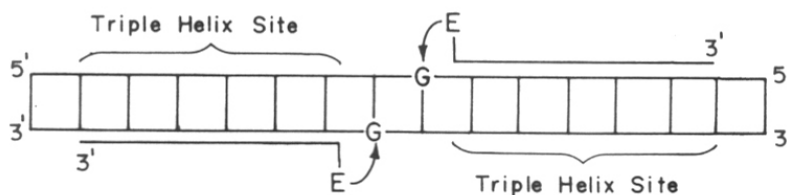
Reactive alkylating agents and electrophiles bring about N'-modification of purines making these sites facile for subsequent depurination which finally leads to cleavage of DNA. Some of the active electrophiles capable of this are  $-S^+(Me)_3$ , nitrogen mustards and bromoacetyl group. A purposeful use of this is to conjugate them with DNA binding moieties such as intercalators, groove binders, peptides or even complementary oligonucleotides. Two examples of such a strategy are cited here. Distamycin a tripeptide from the natural products binds to five base pair site with a preference for A, T rich region.<sup>32</sup> This tripeptide was attached to an electrophile (bromoacetyl) on the amino end close to the A, T sequences in the minor groove of DNA proximal to the N<sup>3</sup> of adenine.<sup>33</sup> Foot printing studies revealed that N-bromoacetyl distamycin **11** binds rapidly to a 167 base pair restriction fragment at four AT rich sites, each five base pairs in size 5'-TTTAA, GTTA, AATT and GAAT. But cleavage occurs only at a single site at GTTA site in this 167 base pair fragment indicating the sequence specificity achievable in this approach.



11



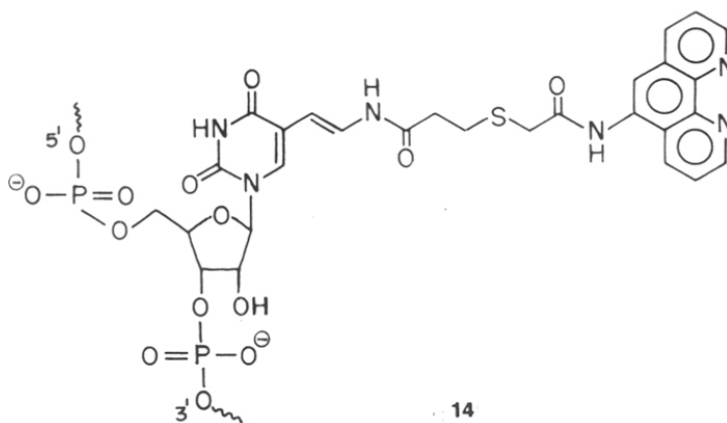
Nondiffusible electrophile N-bromoacetyl attached to the 6-position of thymine **12** at the 5'-end of a pyrimidine oligodeoxy ribonucleotide affords sequence specific alkylation of a guanine, located 2 base pairs to the 5'-side of a local triple-helix complex<sup>34</sup> **13**. N-Bromoacetyl oligodeoxyribonucleotides bind adjacent inverted purine tracts on double-helical DNA by triple-helix formation and alkylate single guanine position on opposite strands at 37°C (pH 7.4).

**12****13**

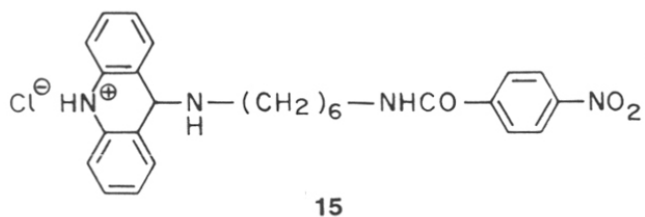
### 1.6.3 Site specific cleavage of Nucleic acids

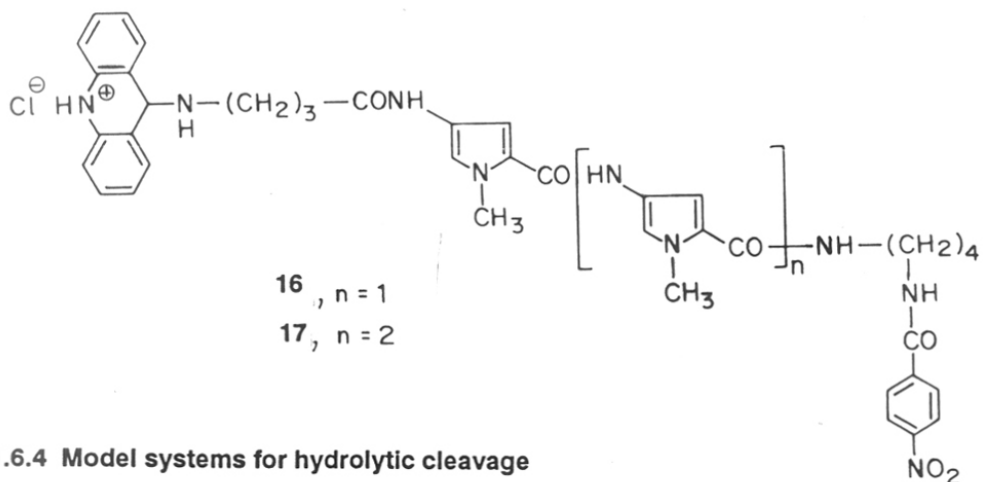
Pyrimidine oligonucleotides bind duplex DNA sequence specifically at homopurine sites to form a triple helix structure. Dervan has extensively utilized this property of DNA to target cleavage moiety to a specific site.<sup>35</sup> The cleavage of a naturally occurring 18 base pair sequence, 5'-A<sub>4</sub>G<sub>4</sub>G<sub>6</sub>G<sub>4</sub>GA-3', that occur once within the 48502 base pair of bacteriophage genome by an oligonucleotide-EDTA probe has been reported,<sup>36</sup> with

considerable specificity and efficiency. Bleomycin was conjugated to the oligonucleotide and its copper complex was found to cleave complementary oligonucleotides<sup>31</sup>. The specificity and the nuclease activity of 1,10-phenanthroline-copper has been altered by conjugating the ligand at its 5-position to proteins, peptides and nucleic acids. RNA linked to the chemical nuclease 1,10-phenanthroline-copper **14** cuts double stranded DNA of complementary sequence.<sup>19</sup>



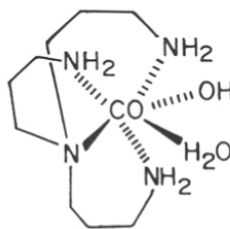
Shinomoya<sup>37</sup> et al. synthesised two novel photocleaving compounds **15**, **16** and **17** containing an intercalator and a photocleaving moiety attached through spacer. Their ability to induce photocleavage at specific sites of DNA was assessed by photoinduced nicking of supercoiled pBR322 DNA.





#### 1.6.4 Model systems for hydrolytic cleavage

As described before phosphate esters are very much resistant to the hydrolysis. Jik Chin<sup>38</sup> et al. have demonstrated that metal complexes such as **18** accelerate the hydrolysis of these monoesters. Adenosine monophosphate (AMP) can be hydrolyzed using the cobalt(II) complex **18**.

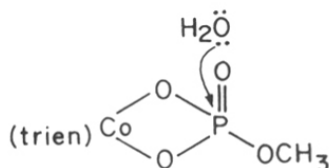


**18**

Hydrolysis of polyphosphates are effected by substantially inert<sup>39</sup>  $\text{cis-N}_4\text{Co}(\text{OH})(\text{OH}_2)^{2+}$  complexes. Hydrolysis of ATP and ADP are effected by two moles of  $\text{trien}_2\text{Co}(\text{OH})(\text{OH}_2)^{2+}$  per moles of poly phosphates<sup>40</sup> while that of linear triphosphate ( $\text{P}_3\text{O}_{10}^{5-}$ ) is enhanced by  $10^4$  times relative to free triphosphate by three moles of cyclen- $\text{Co}(\text{OH})\text{OH}_2^{2+}$ .

In 1969 Farrell<sup>41</sup> et al. reported the acceleration of the hydrolysis of methylphosphate bound to the triethylene tetramine cobalt (III) ion **19**. The hydrolysis of methylphosphate

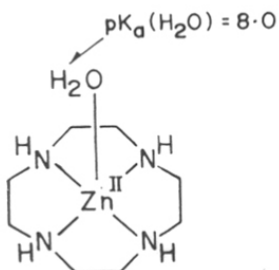
bound to the triethylene tetramine cobalt (III) ion is much faster than the hydrolysis of either dimethyl phosphate bound to the same cation or methylphosphate bound to the pentaamine cobalt (III) ion.



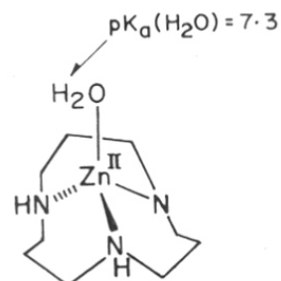
19

Jik Chin and Xian Zou<sup>42</sup> studied the effects of four Co (III) complexes  $[\text{Co}(\text{trien})(\text{OH})(\text{OH}_2)]^{2+}$ ,  $[\text{Co}(\text{en})_2(\text{OH})(\text{OH}_2)]^{2+}$ ,  $[\text{Co}(\text{dien})(\text{OH})(\text{OH}_2)]^{2+}$  and  $[\text{Co}(\text{en})_2(\text{OH})(\text{NH}_3)]^{2+}$  on the rate of hydrolysis of bis(p-nitrophenyl)phosphate, p-nitrophenyl phosphate and bis-(2,4-dinitrophenyl)phosphate at 50 °C under neutral pH. At pH 7.0, the cobalt bound phosphodiester  $[\text{Co}(\text{en})_2(\text{OH})[\text{OP}(\text{O})(\text{OC}_6\text{H}_4\text{NO}_2)_2]]^+$  is cleaved  $10^7$  times more rapidly than the free phosphodiester, whereas the corresponding cobalt-bound phosphomonoester  $[\text{Co}(\text{en})_2(\text{OH})[\text{OP}(\text{O})_2\text{OC}_6\text{H}_4\text{NO}_2]]$  was cleaved  $10^4$  times more rapidly than the unbound phosphodiester.

The zinc (II) complexes of macrocycles **20** and **21** promote the hydrolysis of tris(4-nitrophenyl)phosphate and bis(4-nitrophenyl)phosphate. Kinetic studies show that reactive species commonly is L-Zn(II)-OH<sup>-</sup> where L is the macrocycle<sup>43</sup>.

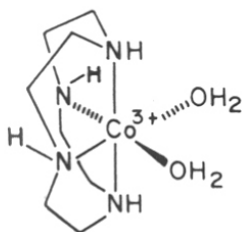
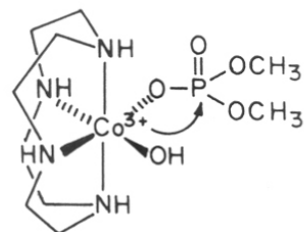


20

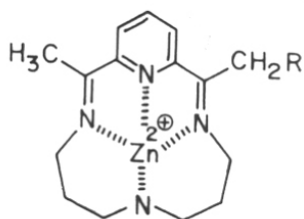


21

Hydrolysis of dimethyl phosphate by using a polyaza metal complex was achieved by Jik Chin<sup>44</sup> et al. By using the cobalt complex **22** they could hydrolyze dimethylphosphate at 60°C at neutral pH. The proposed mechanism of **22** promoted hydrolysis of dimethyl phosphate involves co-ordination of the diester to the metal complex, followed by intramolecular metal hydroxide attack **23**.

**22****23**

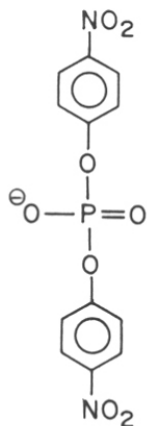
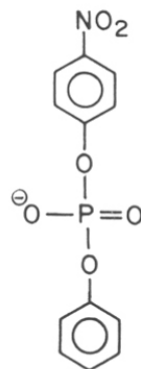
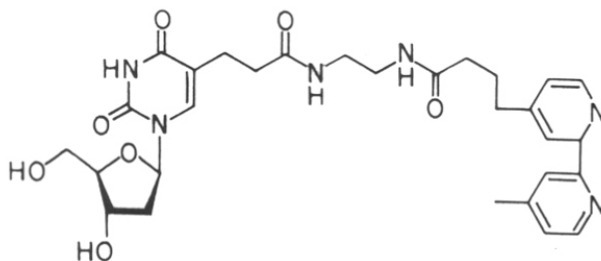
A tetra co-ordinated Zn complex **24** of a tetraazamacrocyclic was found to catalyze the hydrolysis<sup>45</sup> of diphenyl p-nitrophenylphosphate (DPPNPP) in aqueous acetonitrile. The principal products are derived from loss of p-nitrophenol. Zinc macrocycle complex carrying long alkyl chain **25** was more effective in the hydrolysis of DPPNPP than its parent macrocycle Zinc complex.

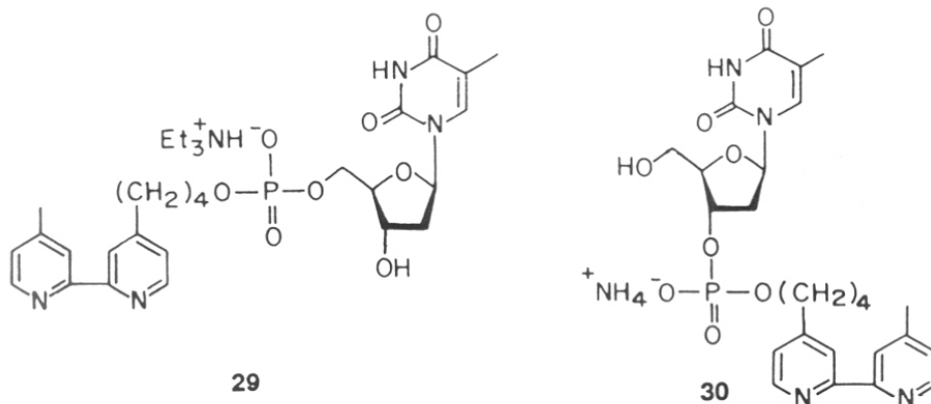


**24** , R = H

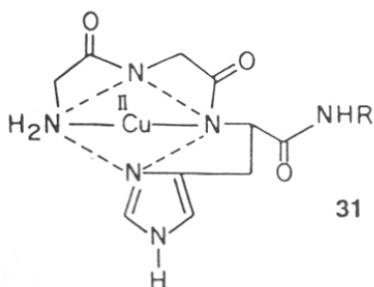
**25** , R = C<sub>16</sub>H<sub>33</sub>

Hydrolysis of phosphate diesters **26** and **27** was catalyzed by  $\text{Cu}(\text{bpy})^{2+}$  in aqueous solution at 75 °C in the pH range 5.8-8.3. Greater than 1000 turnovers and 200 turnovers per  $\text{Cu}(\text{bpy})^{2+}$  were observed in the hydrolysis of **26** and **27** respectively.<sup>46</sup> Hydrolysis of diethyl-4-nitrophenylphosphate (DEPNPP) to diethylphosphate proceeds 1600 fold more rapidly with 1mM  $\text{Cu}(\text{bpy})^{2+}$  at pH 6.4 and 75°C than without metal complex catalyst.<sup>47</sup> As an extension to this nucleoside-2,2'-bipyridyl(bpy) conjugates were synthesized<sup>48</sup> **28**, **29**, **30** and were shown to hydrolyze RNA at 37 °C and neutral pH.

**26****27****28**

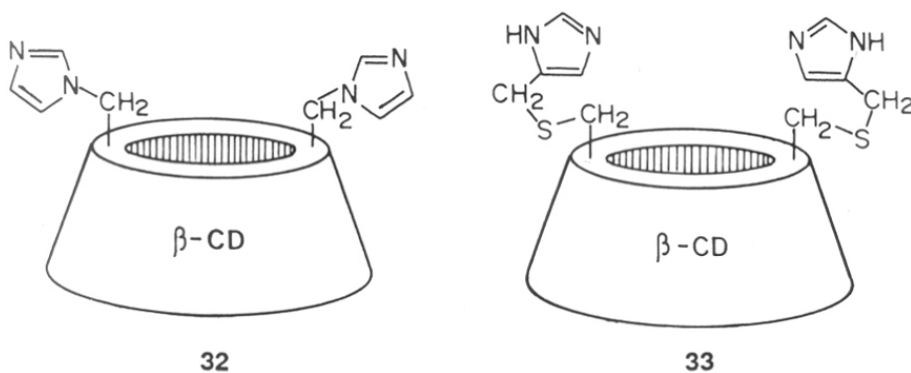


Mack et al.<sup>49</sup> has attached a tripeptide, H-Gly-Gly-His-OH (GGH) which is a consensus sequence for the copper-binding domain of serum albumin, to the amino terminus of the DNA-binding domain of Hin recombinase (residue 139-190) to afford a new 55-residue protein, GGH (Hin 139-190) and showed that in presence of Cu(II), and other necessary cofactors cleavage of DNA occurs at one of the four sites by oxidative degradation of deoxyribose. In presence of Ni(AcO)<sub>2</sub> and monoperoxyphthalic acid, the sequence specificity and efficiency of the DNA cleavage by GGH (Hin 139-190) are remarkably altered. The nickel-mediated DNA cleavage process that occurs at all four binding sites, is more rapid and efficient and is chemically activated by 1 equivalent of an oxygen atom donor. The tripeptide GGH binds Cu (II) in a 1:1 complex over the pH range 6.5-11 with a dissociation constant of  $1.2 \times 10^{-6} \text{ M}^{-1}$ . A crystal structure of Cu(II)-GGH reveals square-planar complexation of the Cu(II) by an imidazole nitrogen, two deprotonated peptide nitrogens and the terminal amino group **31**.

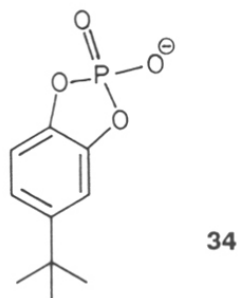


In an another approach to achieve the site specificity of nucleases, the K84C nuclease was linked directly to the 3'-thiol group of the terminal thymidine and the ability of this hybrid nuclease to sequence-specific hydrolysis of supercoiled DNA was demonstrated.<sup>50</sup> An another study to achieve a targeted delivery of nucleases comprised of a  $\lambda$  repressor-Staphalococcal nuclease hybrid protein<sup>51</sup>. The repressor domain of the hybrid nuclease binds specifically to its recognition sequence,  $\lambda$  operator OR1 or OL1 and delivers the nuclease activity to DNA sequences adjacent to the repressor binding site.

Breslow<sup>52</sup> in an elegant way demonstrated the cleavage of ribodinucleotide r(UpU) by imidazole buffer. The reaction shows kinetic behavior that indicates a sequential bifunctional mechanism, in which the imidazolium ion acts first. This mechanism is related to simultaneous bifunctional cleavage of RNA by the enzyme ribonuclease. Cyclodextrin-bisimidazoles<sup>52a</sup> **32** and **33** were synthesized as enzyme mimic and it was demonstrated that for the hydrolysis of cyclic phosphate esters of 4-t-butylcatecol **34** proceeds via simultaneous bifunctional mechanism.

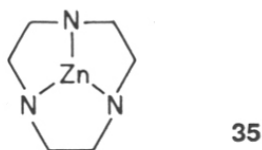




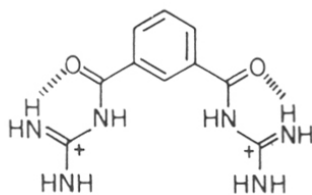


Ribonucleases cleave RNA to fragments having the 3'-terminal phosphates. In an attempt to mimic this selectivity of ribonucleases Komiyama<sup>53</sup> used  $\beta$ -cyclodextrin to attain regioselective cleavage of 2'3'-cyclic monophosphates of cytidine, uridine, adenosine and guanosine to corresponding 3'-monophosphates at pH 11.08, 20°C.

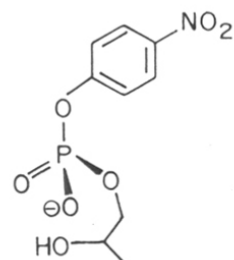
Morrow et al.<sup>54</sup> used Zinc complexes **35** to hydrolyze adeny-3',5'-uridine-3'-monophosphate (ApUp) in water at 64 °C and pH 7. Catalytic behavior is observed for transesterification of ApUp by **35**, with five turnovers observed under conditions of excess ApUp.



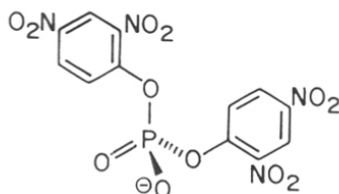
Andrew Hamilton et al.<sup>55</sup> have designed a synthetic receptor **36** based on active site of staphalococcal nuclease and showed acceleration of hydrolytic cleavage of phosphodi-esters **37** and **38** by this receptor. Anslyn et al.<sup>56</sup> have designed and synthesised a water soluble staphalococcal nuclease mimic **39** and demonstrated that receptor **39** enhanced the rate of imidazole-catalyzed RNA hydrolysis.



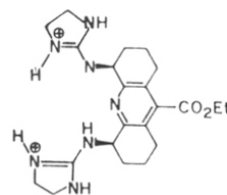
36



37



38



39

### 1.7 ATPase MIMICS

ATP, the "currency of energy" in biological system is hydrolyzed by ATPase enzymes. Some important aspects of this reaction are the requirement of magnesium ion for the reaction and formation of a covalent enzyme-phosphoryl complex. The metal ion effects and covalent catalysis, have been shown to mimic by the low molecular weight polyammonium macrocycles.

Complexation of biologically relevant molecules such as adenosine triphosphate (ATP) by polyammonium macrocycles was observed by Lehn<sup>57</sup> in 1981. Among different polyammonium macrocycles, with varying degrees of affinity for ATP, The hexaaza-dioxa macrocycle [24]N<sub>6</sub>O<sub>2</sub> **40** was most efficient at catalyzing the dephosphorylation of ATP<sup>58</sup> (Figure 5) at pH 7.0. as followed by <sup>31</sup>P NMR, and the reaction showed first order kinetics.

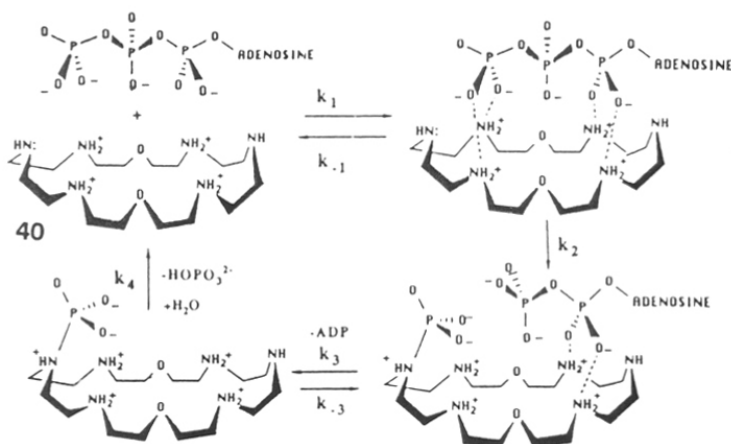
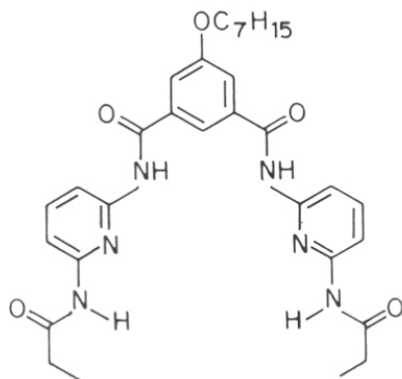


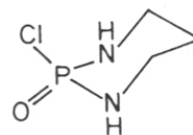
Fig. 5. Schematic representation of the sequence of reactions for ATP dephosphorylation catalyzed by macrocycle 40

## 1.8 ARTIFICIAL RECEPTORS FOR TRANSITION STATE STABILIZATION OF PHOSPHORYL-TRANSFER REACTIONS

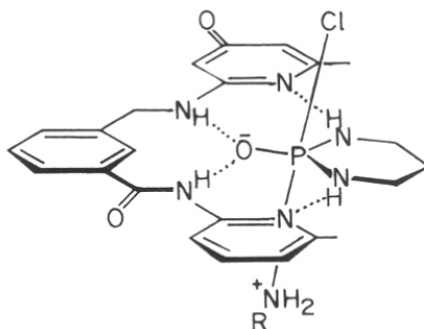
Preferential complexation and stabilization of transition state is one of the important step in enzyme catalyzed reactions. Construction of synthetic receptors and spatial features of transition-state structures is a useful strategy to develop artificial enzymes. Hamilton et al.<sup>59</sup> have demonstrated the design and synthesis of artificial receptor **41** which accelerated the phosphoryl-transfer reaction. **41** was designed to be complementary to the postulated transition state. It was observed that the receptor **41** causes a 10 fold acceleration in the rate of reaction between **42** and n-butylamine. This rate enhancement was attributed to the special hydrogen environment provided by the receptor **41** to stabilize the trigonal-bipyramidal intermediate **43**.



41



42



43

## 1.9 RATIONALE FOR THE PRESENT WORK

The review presented so far clearly highlights that amino groups are the most commonly found functional groups at the catalytic site of nucleases (natural & mimics). Interaction of these functional groups with the phosphate back bone of nucleic acids through electrostatic or hydrogen bonding activate the phosphate esters towards hydrolytic cleavage. This inspired us to study inter and intra molecular amine-phosphate interactions in model nucleotides which is the genesis of the present work.

There are many features of polyammonium macrocycles which makes them good enzyme mimics. In polyprotonated form they are soluble in water. The high positive charge density and potential hydrogen bond capacity promote complex formation with biologically relevant anionic substrates. Pendant functionality can also be placed at virtually any position on the ring. With these points in mind two novel macrocyclic polyamines [16]-N<sub>3</sub> and [21]-N<sub>4</sub> having a pendant hydroxyl group have been designed and synthesised. Their complexation with nucleotidyl phosphates and molecular recognition properties were studied. This constitutes the second chapter of this thesis,

Imidazole moiety of the histidine and amino moiety of the lysine present at the catalytic site of the nucleases play crucial role in catalyzing the hydrolysis of DNA or RNA. In order to understand the interaction of these amino functionality with phosphate anion and possible catalysis, dinucleotides conjugated with these amines were designed and conformational studies of these novel dinucleotides form the subject matter of the chapter III. Hydrolytic cleavage of these modified dinucleotides achieved in presence of metal ions is described in the chapter IV. Successful incorporation of amine-tethered monomers into oligonucleotide sequences is demonstrated in the chapter V.

## 1.10 REFERENCES

1. Laskowski, M. *Adv. Enzymol*, **1967**, *29*, 165.
2. Barnard, E. A. *Annu. Rev. Biochem.*, **1965**, *38*, 677.
3. Grossman, L.; Moldave, K. (eds) *Methods Enzymology*, **1980**, 65.
4. Adams, R. L. P.; Knowler, J. T.; Leader, D. P. (eds) *The Biochemistry of the Nucleic Acids*, Chapman and Hall: New York, **1986**.
5. Shen, V.; Schlessinger, D. in *The Enzymes* (ed. P. D. Boyer) Academic Press: New York, **1982**, *15*, p 501.

6. Adams, J. M.; Cory, S.; Spahr, P. F. *Eur. J. Biochem.*, **1972**, *29*, 469.
7. Dubos, R. J.; Thompson, R. H. S. *J. Bio. Chem.*, **1938**, *124*, 501.
8. (a) Ogawa, T.; Pickett, G. G.; Kogoma, T.; Kornberg, A. *Proc. Natl. Acad. Sci. U. S. A.*, **1984**, *81*, 1040.  
(b) Kogoma, T. *Proc. Natl. Acad. Sci. U. S. A.*, **1984**, *81*, 7845.
9. Stryer, L. *Biochemistry*, (ed) W. H. Freeman and company, New York, **1981**.
10. Deakyne, C. A.; Allen, L. C. *J. Am. Chem. Soc.*, **1979**, *101*, 3951.
11. (a) Cantor, C. R. Ed. *Bioorganic Chemistry, A Chemical Approach to Enzyme Action*, Springer Verlag: New York, **1981**.  
(b) Kartha, G.; Bello, J.; Harker, D. *Nature, London*, **1967**, *213*, 862.  
(c) Wyckoff, H. W.; Tsernoglou, D.; Hanson, A. W.; Knox, J. R.; Lee, B.; Richards, F. M. *J. Biol. Chem.*, **1970**, *245*, 305.
12. Fersht, A. *Enzyme Structure and Mechanism* W. H. Freeman and company, New York, **1985**.
13. Pace, C. N.; Heinemann, U.; Hahn, U.; Saenger, W. *Angew. Chem. Int. Ed. Engl.*, **1991**, *30*, 343.
14. (a) Takahashi, K.; Moore, S. *Enzyme*, **1982**, *15*, 435.  
(b) Takahashi, K. *Biochemistry*, **1970**, *67*, 833.  
(c) Eckstein, F.; Schulz, H. H.; Ruterjans, H.; Haar, W.; Maurer, W. *Biochemistry*, **1972**, *11*, 3507.  
(d) Nishikawa, S.; Morioka, H.; Kim, H. J.; Fuchimura, K.; Tanaka, T.; Uesugi, S.; Hakoshima, T.; Tomita, K. -I.; Ohtsuka, E.; Ikehara, M. *Biochemistry*, **1987**, *26*, 8620.
15. (a) Richards, F. M.; Wyckoff, H. W. (eds) in : *The Enzymes*, Academic Press: New York, **1971**, *4*, p 647.  
(b) Wyckoff, H. W.; Tsernoglou, D.; Hanson, A. W.; Knox, J. R.; Lee, B.; Richards, F. M. *J. Biol. Chem.*, **1970**, *247*, 305.

- (c) Allewell, N. M.; Mitsui, Y.; Wyckoff, H. W. *J. Biol. Chem.*, **1973**, *248*, 5291.
- (d) Wodak, S. Y.; Liu, M. Y.; Wyckoff, H. W. *J. Mol. Biol.*, **1977**, *116*, 855.
16. (a) Chin, J. *Acc. Chem. Res.*, **1991**, *24*, 145.
- (b) Guthrie, J. P. *J. Am. Chem. Soc.*, **1977**, *99*, 3991
17. Singleton, Jr.; R. *J. Chem. Ed.*, **1973**, *50*, 538.
18. Westheimer, F. H. *Science*, **1987**, *235*, 1173.
19. (a) Sigman, D. S.; Graham, D. R.; Aurora, D. V.; Stern, A. M. *J. Biol. Chem.*, **1979**, *254*, 12269.
- (b) Sigman, D. S.; Chen, C. B.; *Ann. Rev. Biochem.*, **1990**, *59*, 207.
- (c) Chen, C. B.; Gorin, M. B.; Sigman, D. S. *Proc. Natl. Acad. Sci. U. S. A.*, **1993**, *90*, 4206.
20. (a) Hertzberg, R. P.; Dervan, P. B. *J. Am. Chem. Soc.*, **1982**, *104*, 313.
- (b) Schultz, P. G.; Taylor, J. S.; Dervan, P. B. *J. Am. Chem. Soc.*, **1982**, *104*, 6861.
- (c) Tullius, T. D.; Dambroski, B. A. *Pro. Natl. Acad. Sci., U. S. A.*, **1986**, *83*, 5469.
21. (a) Ward, B.; Skorobogaty, A.; Dabrowiak, J. C. *Biochemistry*, **1986**, *25*, 6875.
22. Barton, J. K. *Science*, **1986**, *233*, 727.
23. (a) Stubbe, J.; Kozarich, J. W. *Chem. Rev.*, **1987**, *87*, 1107.
- (b) Kozarich, J. W.; Worth, L. Jr.; Frank, B. L.; Christner, D. F.; Vanderwall, D. E.; Stubbe, J. *Science*, **1989**, *245*, 1396.
24. Joshi, R. R.; Ganesh, K. N. *Biochem. Biophys. Res. Commun.*, **1992**, *182*, 588.
25. Ranganathan, D.; Patel, B. K.; Mishra, R. K. *J. Chem. Soc. Chem. Commun.*, **1993**, 337.
26. Hirai, M.; Shinozaka, K.; Sawai, H.; Ogawa, S. *Chemistry Letters*, **1992**, 2023.
27. Praseuth, D.; Gaudemer, A.; Verlac, J.; Kralic, I.; Sissoef, I.; Guille, E. *Photochem. Photobiol.*, **1986**, *44*, 717.
28. (a) Fiel, R. J.; Beerman, T. A.; Mark, E. H.; Datta Gupta, N. *Biochem, Biophys. Res. Commun.*, **1982**, *107*, 1067.

- (b) Foquet, E.; Pratviel, G.; Bernadou, J.; Meunier, B. *J. Chem. Soc. Chem. Commun.*, **1987**, 1169.
- (c) Ward, B.; Rehfuess, R.; Dabrowiak, J. C. *J. Biomolec. Struct. Dynam.* **1987**, *4*, 685.
- (d) Bromley, S. D.; Ward, B. W.; Dabrowiak, J. C. *Nucleic Acids. Res.*, **1986**, *14*, 9133.
29. Groves, J. T.; Farrell, T. P. *J. Am. Chem. Soc.*, **1989**, *111*, 4998.
30. Nagi, K.; Carter, B. J.; Xu, J.; Hecht, S. M. *J. Am. Chem. Soc.*, **1991**, *113*, 5099.
31. (a) Nicolaou, K. C.; Ogawa, Y.; Zuccarello, G.; Kataoka, H. *J. Am. Chem. Soc.*, **1988**, *110*, 7247.
- (b) Zarytova, V. F.; Sergeev, D. S.; Godovikova, T. S. *Bioconjugate Chemistry*, **1993**, *4*, 189.
- (c) Nicolaou, K.C.; Dai, W. -M. *Angew. Chem. Int. Ed. Engl.*, **1991**, *30*, 1387.
32. (a) For a comprehensive review see Zimmer, C. *Prog. Nucl. Acid. Res. Mol. Biol.*, **1975**, *15*, 285.
33. Baker, B. F.; Dervan, P. B. *J. Am. Chem. Soc.*, **1989**, *111*, 2700.
34. Povsic, T. J.; Strobel, S. A.; Dervan, P. B. *J. Am. Chem. Soc.*, **1992**, *114*, 5934.
35. Dreyer, G. B.; Dervan, P. B. *Biochemistry* **1985**, *82*, 968.
36. Strobel, S. A.; Moser, H. E.; Dervan, P. B. *J. Am. Chem. Soc.*, **1988**, *110*, 7927.
37. Shinomiya, M.; Kuroda, R. *Tet. Lett.*, **1993**, *33*, 2697.
38. Chin, J.; Banaszczyk, M. *J. Am. Chem. Soc.*, **1989**, *111*, 4103.
39. (a) Creaser, I. I.; Haight, G. P.; Peachey, R.; Robinson, W. T.; Sargeson, A. M. *J. Chem. Soc. Chem. Commun.*, **1984**, 1568.
- (b) Haight, G. P.; Hambley, T. W.; Hendry, P.; Lawrance, G. A.; Sargeson, A. M. *J. Chem. Soc. Chem. Commun.*, **1985**, 488.
- (c) Jones, D. R.; Lindoy, L. F.; Sargeson, A. M. *J. Am. Chem. Soc.*, **1983**, *105*, 7327.



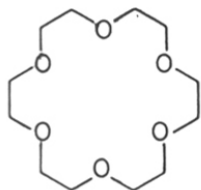
- (d) Harrowfield, J. MacB.; Jones, D. R.; Lindoy, L. F.; Sargeson, A. M. *J. Am. Chem. Soc.*, **1980**, *102*, 7733.
40. Hediger, M.; Milburn, R. M. *J. Inorg. Biochem.*, **1982**, *16*, 165.
41. Farrell, F. J.; Kjellstrom, W. A.; Spiro, T. G. *Science (Washington D. C)*, **1969**, *164*, 320.
42. Chin, J.; Zou, X. *J. Am. Chem. Soc.*, **1988**, *110*, 223.
43. Koike, T.; Kimura, E. *J. Am. Chem. Soc.*, **1991**, *113*, 8935.
44. Kim, J. H.; Chin, J. *J. Am. Chem. Soc.*, **1992**, *114*, 9792.
45. Gellman, S. H.; Petter, R.; Breslow, R. *J. Am. Chem. Soc.*, **1986**, *108*, 2388.
46. Morrow, J. R.; Trogler, W. C. *Inorg. Chem.*, **1988**, *27*, 3387.
47. Morrow, J. R.; Trogler, W. C. *Inorg. Chem.*, **1989**, *28*, 2330.
48. Modak, A. S.; Gard, J. K.; Merriman, M. C.; Winkeler, K. A.; Bashkin, J. K.; Stern, M. K. *J. Am. Chem. Soc.*, **1991**, *113*, 283.
49. (a) Mack, D. P.; Iverson, B. L.; Dervan, P. B. *J. Am. Chem. Soc.*, **1988**, *110*, 7572.  
(b) Mack, D. P.; Dervan, P. B. *J. Am. Chem. Soc.*, **1990**, *112*, 4604.
50. Corey, D. R.; Pei, D.; Schultz, P. G. *J. Am. Chem. Soc.*, **1989**, *111*, 8523.
51. Pei, D.; Schultz, P. G. *J. Am. Chem. Soc.*, **1990**, *112*, 4579.
52. (a) Breslow, R.; Anslyn, E.; Huang, D. -L. *Tetrahedron*, **1991**, *47*, 2365.  
(b) Breslow, R. *Acc. Chem. Res.*, **1991**, *24*, 317.  
(c) Breslow, R.; Xu, R. *Proc. Natl. Acad. Sci. U. S. A.*, **1993**, *90*, 1201.
53. (a) Komiyama, M. *J. Am. Chem. Soc.*, **1989**, *111*, 3046.  
(b) Komiyama, M.; Takeshige, Y. *J. Org. Chem.*, **1989**, *54*, 4936.
54. Shelton, V. M.; Morrow, J. R. *Inorg. Chem.*, **1991**, *30*, 4295.
55. Jubian, V.; Dixon, R. P.; Hamilton, A. D. *J. Am. Chem. Soc.*, **1992**, *114*, 1120.
56. Smith, J.; Ariga, K.; Anslyn, E. V. *J. Am. Chem. Soc.*, **1993**, *115*, 362.
57. Dietrich, B.; Hosseini, M. W.; Lehn, J. -M.; Sessions, R. B. *J. Am. Chem. Soc.*, **1981**, *103*, 1282.

58. (a) Hosseini, M. W.; Lehn, J. -M.; Mertes, M. P. *Helv. Chim. Acta.*, **1983**, *66*, 2454.  
(b) Hosseini, M. W.; Lehn, J. M.; Moggiora, L.; Mertes, K. B.; Mertes, M. P. *J. Am. Chem. Soc.*, **1987**, *109*, 537.  
(c) Hosseini, M. W.; Lehn, J. W.; Jones, K. C.; Plute, K. E.; Mertes, K. B.; Mertes, M. P. *J. Am. Chem. Soc.*, **1989**, *111*, 6330.  
(d) Hosseini, M. W.; Blacker, A. J.; Lehn, J. M. *J. Am. Chem. Soc.*, **1990**, *112*, 3896.
59. Tecilla, P.; Chang, S. K.; Hamilton, A. D. *J. Am. Chem. Soc.*, **1990**, *112*, 9586.

**CHAPTER 2**  
**SYNTHESIS OF MACROCYCLIC POLYAMINES [16]-N<sub>3</sub> AND [21]-N<sub>4</sub>**  
**AND THEIR COMPLEXATION STUDIES WITH**  
**NUCLEOTIDYL PHOSPHATES**

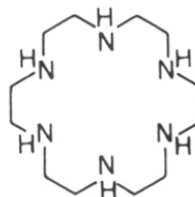
## 2.1 INTRODUCTION

In 1967 Pederson reported the synthesis of a new class of molecules "macrocylic polyethers" crown ethers.<sup>1</sup> Since then considerable knowledge on the fundamental chemistry of these compounds has accumulated and newer applications have emerged. These encompass almost every field of chemistry.<sup>2-6</sup> The nitrogen analogues of crown ethers (1), polyazacrowns (2), have emerged as efficient ligands for transition metals and heavy metal ions.<sup>7</sup> Interest in macrocyclic polyamines has also led to extensive studies on thermodynamics and kinetics of their complexation.



18-membered  
macrocyclic  
hexaether  
([18] crown-6)

1



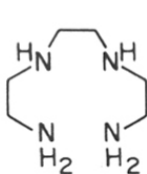
18-membered  
macrocyclic  
hexamine  
([18] azacoronand-6)

2

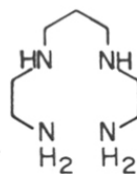
The versatility of azacrowns is well illustrated by numerous reports on their ability to act as receptors for a variety of anions, cations and neutral molecules depending on their protonation states. Moreover, the observation that lower degrees of saturation have important biological functions have also aroused great interest in these molecules. Metallo complexes of macrocyclic polyamines<sup>8</sup> and porphyrins<sup>9</sup> function as O<sub>2</sub> carriers and activators, promote photosynthesis and form the basic structure of vitamin B<sub>12</sub>. Introduction of functionalised side-chains into macrocyclic receptors in a defined way may provide means to impart additional features such as catalysis or transport and enable conjugation of the complexones to the bioactive molecules.

Structurally macrocyclic polyamines may be viewed as an extended form of linear polyamines<sup>10-13</sup> with one lower degree of saturation (**Scheme 1**). The Structures and the abbreviated nomenclature of some of the saturated polyamines are given in the Table I.

**SCHEME 1**



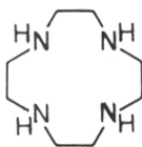
Trien



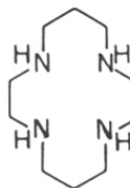
2,3,2-tet

Linear tetraamines

One lower degree  
of saturation  
↓



Cyclen



Cyclam

Macrocyclic tetraamines

More lessening in the  
degree of saturation  
↓

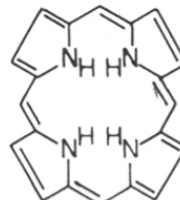
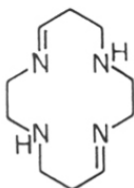
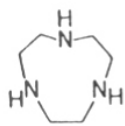
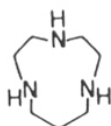
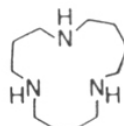
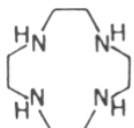
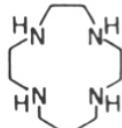
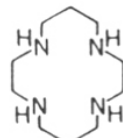


TABLE I

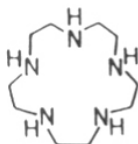
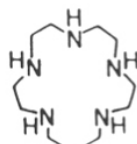
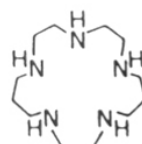
## Triamines

[9]ane N<sub>3</sub>[10]ane N<sub>3</sub>[14]ane N<sub>3</sub>  
(Cyclic spermidine)

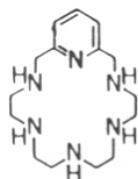
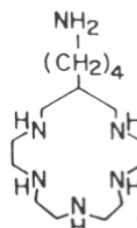
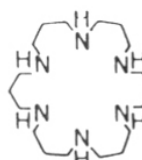
## Tetraamines

[12]ane N<sub>4</sub>  
(Cyclen)[13]ane N<sub>4</sub>[14]ane N<sub>4</sub>  
(Cyclam)

## Pentaamines

[15]ane N<sub>5</sub>[16]ane N<sub>5</sub>[17]ane N<sub>5</sub>

## Hexaamines

Py [18]ane N<sub>6</sub>[16]ane N<sub>5</sub>  
BuNH - tailing[24]ane N<sub>6</sub>

## 2.2 PROPERTIES OF MACROCYCLIC POLYAMINES

Macrocyclic polyamine systems have rigid conformations due to intramolecular N-H<sup>+</sup>..N hydrogen bondings. In contrast to the wide dispersion of cationic charge in linear polyamine systems, the geometric proximity of various nitrogens in macrocyclic polyammonium systems result in a condensation of positive charge in a narrow space. Unlike other cationic systems such as metal ions, macrocyclic polyammonium ions can hydrogen bond with oxyanions via NH<sup>+</sup> protons leading to stronger complexation through ion-pairs.

### 2.2.1 Protonation properties

One of the important properties which distinguishes macrocyclic polyamines from their linear counterparts is seen in the successive protonations. The nitrogen of macrocyclic polyamines show a higher basicity for the first protonation and a sudden drop at subsequent stages of protonation. **Table II** illustrates comparative protonation constants for some of macrocyclic polyamines in comparison with those values for their linear analogues. The diminishing change in the basicity of the second and especially the third amine of a linear polyamine upon cyclization is attributed to the conformational restraint imposed by the cyclic structure. Here three of the N orbitals containing non-bonding electron pairs are directed towards the center of the cavity. The increased electron density in the macrocyclic cavity facilitates the first H<sup>+</sup> uptake resulting in the higher K<sub>1</sub> value. The prior presence of the first proton retards the uptake of second protonation due to the proximal effect. The third protonation constant of macrocyclic is further reduced due to the electrostatic repulsion from the already coordinated protons. Additional strains also inhibit proton entry into the nitrogen cavity. As the ring size increases the value of K<sub>4</sub> and K<sub>5</sub> become higher, converging to the corresponding values for the linear polyamine, tetren.

Table II: Protoantion Constants of Polyamines

Polyamine	log K <sub>1</sub>	log K <sub>2</sub>	log K <sub>3</sub>	log K <sub>4</sub>	log K <sub>5</sub>
<u>Triamines</u>					
[9]ane N <sub>3</sub> <sup>14</sup>	10.59	6.88	<1		
[10]ane N <sub>3</sub> <sup>15a</sup>	10.85	6.76	<1		
Spermidine <sup>15b</sup>	10.89	9.81	8.34		
<u>Tetraamines</u>					
[12]ane N <sub>4</sub> <sup>15c</sup>	10.70	9.70	1.73	<1	
Spermine <sup>15c</sup>	10.80	10.02	8.85	7.96	
<u>Pentaamines</u> <sup>15d</sup>					
[15]ane N <sub>5</sub>	10.85	9.65	6.00	1.74	1.2
tetren	10.36	9.65	8.50	4.70	2.40

### 2.2.2 Binding to Anions

Macrocyclic polyamine cations containing more than one proton within the cavity can hydrogen bond with oxyanions. In these complexes the NH<sup>+</sup> protons, assist in the association of ion-pairs. Macrocyclic polyamines possessing greater number of protons can form stronger ion-pairs with polyoxyanions.

The formation of ion-pair between carboxylate anions and macromonocyclic polyamines lead to altered electrophoretic mobility<sup>16</sup>. It was observed that certain polycarboxylates used as buffers or electrolytes strongly influence the sequence and migration distance of some polyamines (Table III). In acetate or lactate buffers (at pH ~6) the polyamines moved as anticipated while in citrate buffer at same pH, some larger polyamines such as cyclic spermine ([16]ane N<sub>4</sub>, [17]ane N<sub>4</sub>, [15]-[17]ane N<sub>5</sub> and [18]ane N<sub>6</sub>



Table III: Electrophoretic mobilities of polyamines in various buffers.

0.1 M buffer (pH)	[15]ane N <sub>5</sub>	[16]ane N <sub>5</sub>	[17]ane N <sub>5</sub>	[18]ane N <sub>6</sub>	tetren
Acetate (5.8)	0.9	1.1	0.9	1.1	1.2
Lactate (5.8)	1.0	1.0	0.9	0.9	1.1
Malonate (5.9)	0.7	0.7	0.6	0.4	0.9
Succinate (5.8)	0.7	0.7	0.7	0.5	0.8
Malate (5.7)	0.7	0.8	0.7	0.4	0.8
Fumarate (5.8)	0.9	0.9	1.0	0.8	1.0
o-Phthalate (6.0)	0.6	0.9	0.5	0.3	0.5
m-Phthalate (5.4)	0.8	0.9	0.8	0.7	1.0
Citrate (6.0)	0.3	0.0	-0.2	-0.9	0.0

showed less migration. The smaller macrocycles ([12]-[14]ane N<sub>4</sub>) were unaffected. The larger macrocycles may bind two carboxylate groups as shown in **Fig. 1**. The smaller macrocycles (eg. [13]ane N<sub>3</sub> or [12]-[15]ane N<sub>4</sub>) form dipositive cations that weakly bind to polycarboxylate anions. In contrast to macrocyclic spermines, pentamines and hexamines that contain three more NH<sup>+</sup> at pH 7 bind with di and tricarboxylate anions in 1:1 association.<sup>16</sup> For a given receptor molecule, the anions most strongly complexed are usually the smallest and most highly charged ones. The stability sequence with [18]ane N<sub>6</sub>.3H<sup>+</sup> is oxalate > malonate > maleate > succinate > fumarate. The tricarboxylate anion, citrate, binds more strongly than any dicarboxylate anion, indicating to ion-pair formation in these systems.

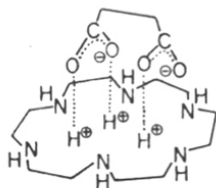


Fig. 1 A model for 1:1 complex of [18]ane  $N_6.3H^+$  with citrate.

In biological anion transport systems, the complexed species are often phosphate anions rather than dicarboxylate anions<sup>17, 18</sup>. This has triggered several studies on phosphate anions with macrocyclic polyazacrowns. Macrocyclic polyamines having more than three protons form stable 1:1 complexes with inorganic phosphate, AMP, ADP and ATP at physiological pH. The stability order for all the polyamines is  $ATP^{4-} > ADP^{3-} > AMP^{2-}$ . Despite having the same anionic charge as inorganic phosphate, AMP forms more stable complexes<sup>19</sup> with [18]- $N_6$  by a factor of 10 or 100. The extra stability for the AMP complex comes from an additional interaction of adenine base (Fig. 2)

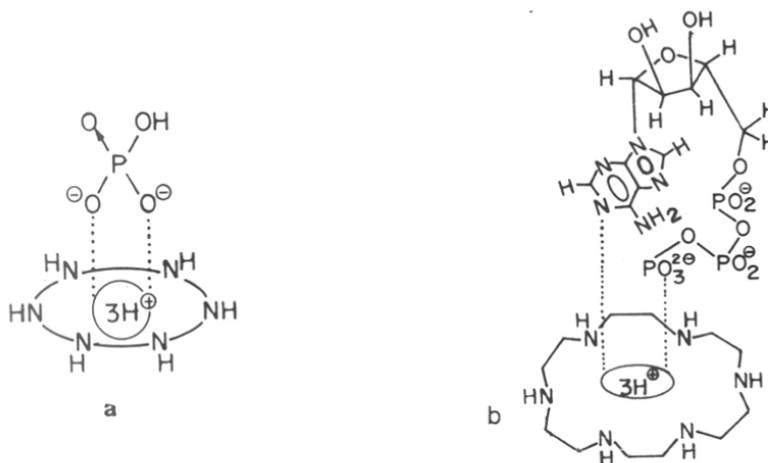
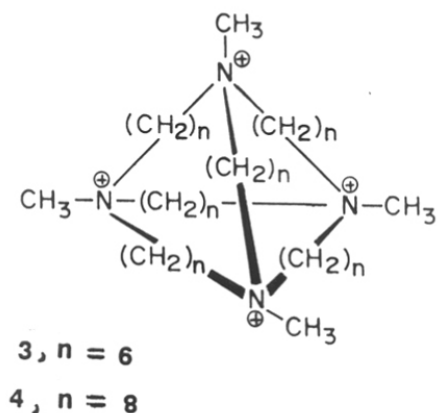


Fig. 2 a) Structure of [18]ane  $N_6.3H^+$ - $HPO_4^{2-}$  complex.  
b) Structure for 1:1 Complex of [18]ane  $N_6.3H^+$  with ATP at neutral pH.

The selective complexation of biologically important anions is of particular interest, especially if the ligands are converted into selective anion carriers by attachment of lipophilic hydrocarbon chain.

Macrocyclic tetraammonium compounds **3** and **4** form stable 1:1 inclusion complexes with anionic<sup>20</sup> molecules such as halides, carbonates, phosphates, AMP, ATP etc. The stability of inclusion complexes depends on electrostatic as well as hydrophobic interactions. Whereas complexes of **3** are dominated by the electrostatic component, the hydrophobic interaction play the main role of stabilization part in complexes of **4**.

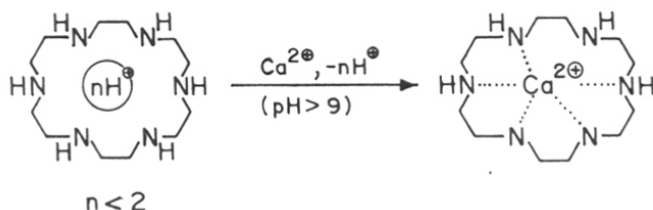


### 2.2.3 Complexation with cations

Compared to O-donor in crown ethers, N-donor in polyaza macrocycles is soft. Hence polyazamacrocycles tend to bind strongly with softer metal ions such as transition metals. Inherently, macrocyclic polyethers are better in complexing hard metal ions (eg. alkali metals or alkaline earth metals<sup>21a</sup>) compared to polyazamacrocycles-transition metal ion complexation. Macrocyclic hexamines turned out to be exceptional. [18]ane

$N_6^{21b}$  and its homologues<sup>22</sup> can form 1:1 complex (**Scheme 2**) in aqueous alkaline solution containing  $K^+$ ,  $Ca^{2+}$ ,  $Sr^{2+}$  or  $La^{3+}$  (**Table IV**). While [18] crown-6 has a higher affinity for  $K^+$  than  $Ca^{2+}$ , [18]ane  $N_6$  displays an opposite preference. The strong coordinate bonding character of  $Ca^{2+}$ -[18]ane  $N_6$  may account for its higher stability compared to

### **SCHEME 2**



$Ca^{2+}$ -18-crown-6 whose bonding nature is mostly electrostatic. Replacement of an amine donor of [18]ane  $N_6$  by an O donor ([18]ane  $N_5O$ ) or a pyramidal N donor (Py [18]ane  $N_6$ ) reduces the affinity for metal ions except for  $Ca^{2+}$ .

Table IV: Stability Constants of  $M^+$ -Ligand Complexes,  $I = 0.2$  M,  $25^\circ\text{C}$ .

Ion	[18]ane $N_6^{21b}$ log $K M^{-1}$	18-Crown <sup>21a</sup> log $K M^{-1}$
Na <sup>+</sup>	nil	0.8
K <sup>+</sup>	0.8	2.03
Ca <sup>2+</sup>	2.5	0.5>
Cr <sup>2+</sup>	3.2	2.7
Pb <sup>2+</sup>	14.1	4.3

In addition to the ring nitrogens, those present in the side arms may also be involved in co-operatively binding<sup>22</sup> to the cations (**Fig. 3**).

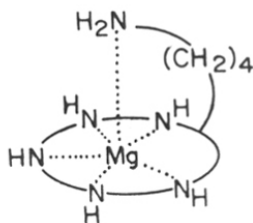


Fig. 3 Structure for  $\text{Mg}^{2+}$ -n-BuNH<sub>2</sub>-[16]ane N<sub>6</sub>.

#### 2.2.4 Recognition of neutral molecules

The macrocyclic hexamine [18]ane N<sub>6</sub> was found to recognize derivatives of catechol<sup>23</sup> (**See Table V**). It interacts with all of these donor compounds in neutral pH solution to form 1:1 coplexes.

Table V: Association constants K for [18]ane N<sub>6</sub> [L] with catechols<sup>23</sup> (A) at 25°,  
I = 0.2 M

Catechol	Complex formula	K (M <sup>-1</sup> )
Catechol	H <sub>3</sub> L <sup>3+</sup> -H <sub>2</sub> A <sup>0</sup>	1.6 x 10 <sup>2</sup>
Dopamine	H <sub>3</sub> L <sup>3+</sup> -H <sub>3</sub> A <sup>+</sup>	1.1 x 10 <sup>3</sup>
Dopa	H <sub>3</sub> L <sup>3+</sup> -H <sub>3</sub> A <sup>0</sup>	3.7 x 10 <sup>3</sup>
Adrenaline	H <sub>3</sub> L <sup>3+</sup> -H <sub>3</sub> A <sup>+</sup>	1.0 x 10 <sup>3</sup>
Resorcinol	H <sub>3</sub> L <sup>3+</sup> -H <sub>2</sub> A <sup>0</sup>	1.3 x 10 <sup>3</sup>

Catechol derivatives, regardless of the residual groups, binds with [18]ane  $N_6 \cdot 3H^+$ . The interaction would occur at the O-dihydroxy benzene and the complexation is not appreciably perturbed by the residual  $NH_3^+$ ,  $CO_2^-$ ,  $NH_2^+-CH_3$  groups. Thus the structure of catecholamine complex is postulated as shown in Fig. 4.

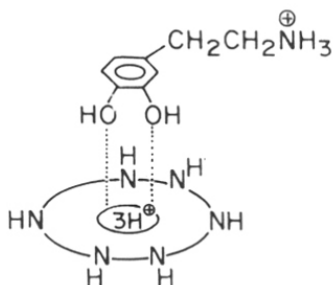


Fig. 4 Structure of complex [18]ane  $N_6$ -catecholamine.

### 2.2.5 Ion transport

$N,N'$ -Bisstearyl derivative of 1,4-diazabicyclo[2.2.2]octane selectively extract nucleotides from aqueous solution to chloroform solution<sup>24</sup>. The order of nucleotide affinity is  $ATP > ADP > AMP$  which is same as their relative transport rate. The mode of interaction of ADP and ATP are proposed to be as shown in Fig. 5.

Saphrin a  $22\pi$ -electron pentapyrrolic expanded porphyrin successfully transported GMP and other nucleotide monophosphates<sup>25</sup>.

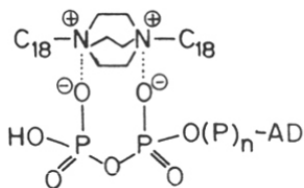
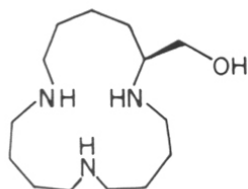
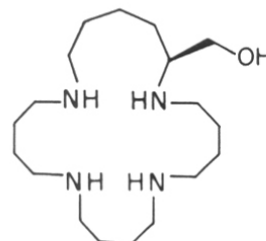


Fig. 5 Structure for 1:1 complex of 1,4-diazabicyclo [2.2.2] octane with ADP ( $n = 0$ ) and ATP ( $n = 1$ ).

## 2.3 OBJECTIVES OF PRESENT WORK

The main aim of this work was to synthesise two macrocyclic polyamines **5** and **6** and study their complexation with nucleotidyl phosphates. The two macrocycles differ in the number of nitrogen atoms in the macrocycle and hence their nature and size of the cavity available for complexation of anions.

**5****6**

This chapter consists of the synthetic methodology used to achieve the synthesis of these macrocyclic polyamines starting from a single common precursor, lysine. This is followed by their structural characterization by spectroscopic methods and studies on their complexation with various biological phosphate anions such as ATP, AMP,  $\alpha$ ,  $\beta$ -cAMP and dinucleotide TpT.

## 2.4 PRESENT WORK

### 2.4.1 Synthesis: General strategy for macrocyclization

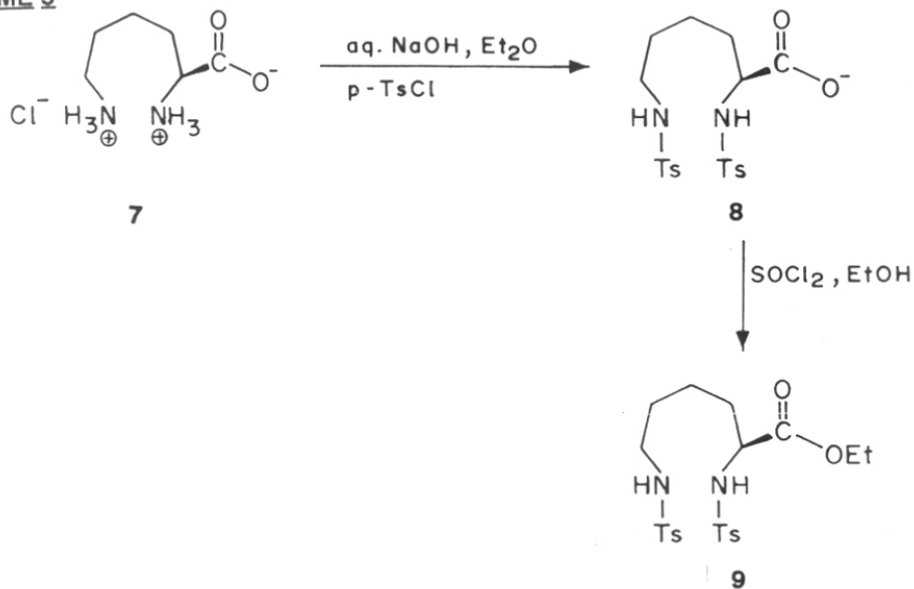
Macrocyclization using high dilution techniques<sup>26</sup> or template synthesis<sup>27</sup> are widely used synthetic procedures in the chemical synthesis of macrocyclic polyamines. Most popular method involves the cyclization of the sodium salt of a linear ditosylamide with a tosylated diol as reported by Richman and Atkins<sup>28</sup>. More recently,<sup>29</sup> several large-ring macrocyclic amines have been synthesized using  $\text{Cs}_2\text{CO}_3$  to deprotonate the ditosylamide in DMF followed by slow addition of a dibromoalkane. This method gave

excellent yields for 17-28 membered rings but low yields for 11-12 membered rings.<sup>29</sup> A comparison of methods for synthesis of a 28-membered diamine macrocycle using  $\text{Cs}_2\text{CO}_3$  for deprotonation and performing the reaction using the sodium salt suggested that a combined ion-pair/template effect may be operative. This gives  $\text{Cs}^{2+}$  a significant advantage over the smaller  $\text{Na}^+$  for closure of ring of this size. With this background it was decided to use  $\text{Cs}_2\text{CO}_3$  assisted macrocyclization procedure in DMF for macrocyclization reaction.

### 2.4.2 Synthesis of macrocyclic polyamine [16]ane $\text{N}_3$ **5**

$\alpha, \omega$ -Ditosyllysinecarboxyester **9** was prepared from lysine monohydrochloride **7** (Scheme 3) and  $\alpha$ -carboxy group of compound **9** was the progenitor of the hydroxymethyl side arm in the target macrocycles. Its lower homologue ornithine has been used previously,<sup>30</sup> for synthesis of macrocycles [15]- $\text{N}_3$  and [18]- $\text{N}_4$ . The extra methylene group of lysine enables an increase in the N-N distance in northern half of the macrocycle. The N,N'-ditosylamide **8** was prepared from L-lysine monohydrochloride **7**.

**SCHEME 3**

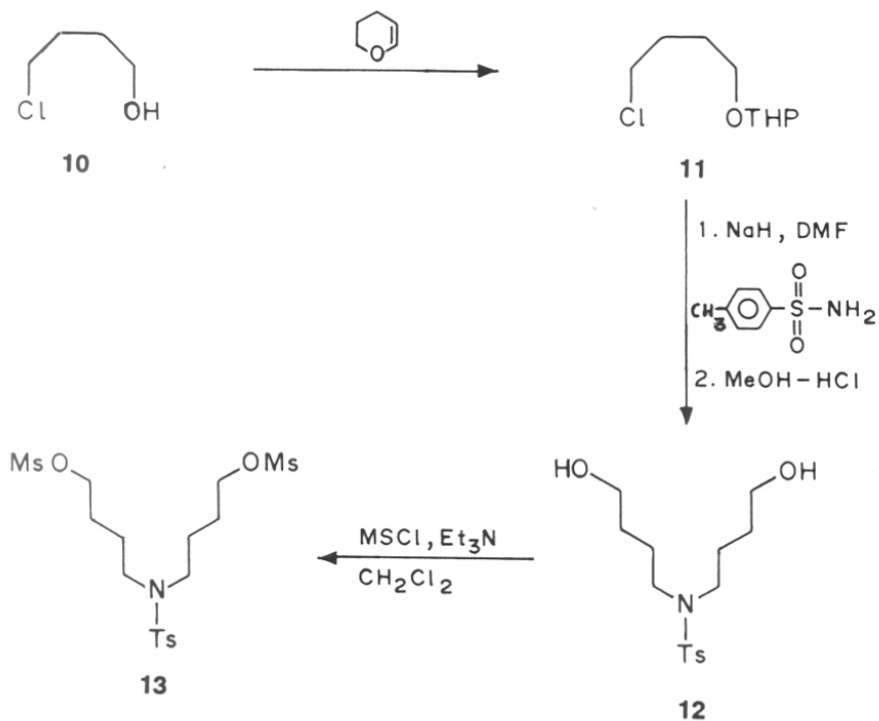


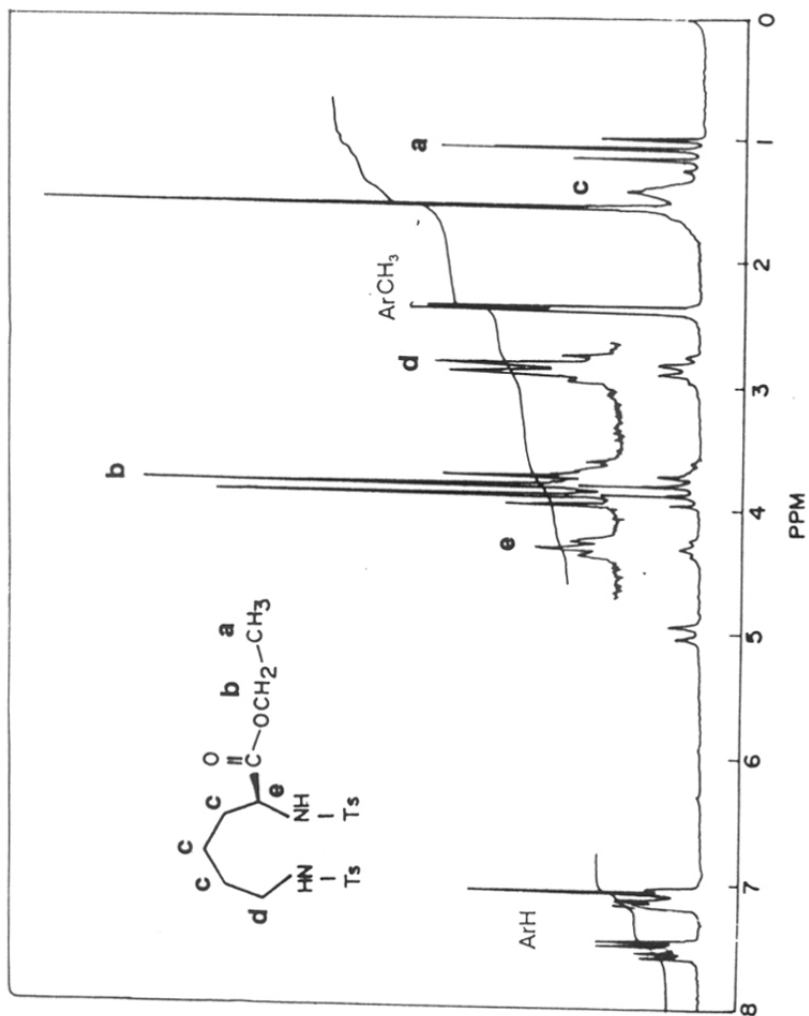


Treatment of lysine with p-toluenesulphonyl chloride in an alkaline solution (pH 12.0) gave the ditosyl derivative **8**. This product was purified by column chromatography and characterized by  $^1\text{H}$  NMR. Appearance of characteristic doublets at 7.44 ppm and 7.83 ppm due to aromatic proton confirmed the formation of N,N'-ditosylate. This on esterification with ethanol- $\text{SOCl}_2$  gave **9** in about 84% yield and well characterized by spectroscopic methods (Fig. 6).

The other segment **13** of the macrocycle **5** was synthesized by a standard chain extension alkylation (Scheme 4). 4-Chlorobutanol was protected at hydroxy group as tetrahydropyranyl derivative. Alkylation of p-toluenesulphonamide with 4-chloro-tetrahydropyranyl-2-yloxy butane **11** gave the bis-alkylated product, which on deprotection

**SCHEME 4**



Fig. 6 90 MHz  $^1\text{H}$  NMR Spectrum of **9** in  $\text{CDCl}_3$ .

of tetrahydropyranyl protecting group with methanolic HCl yielded N-tosyl- $\omega,\omega'$ -diol **12** in 36% yield. The appearance of peaks at 7.41 and 7.77 ppm (Ar-H), 3.18 ppm (4H, 2 x N-CH<sub>2</sub>) and 3.6 ppm (OCH<sub>2</sub>) in <sup>1</sup>H NMR spectra (Fig. 7) confirmed the successful alkylation. This was then converted into corresponding methanesulfonate by treatment with methane sulfonyl chloride to afford **13** in 74 % yield. A sharp singlet at 3 ppm in <sup>1</sup>H NMR spectrum showed (Fig. 8) presence of methanesulfonyl moiety in **13**.

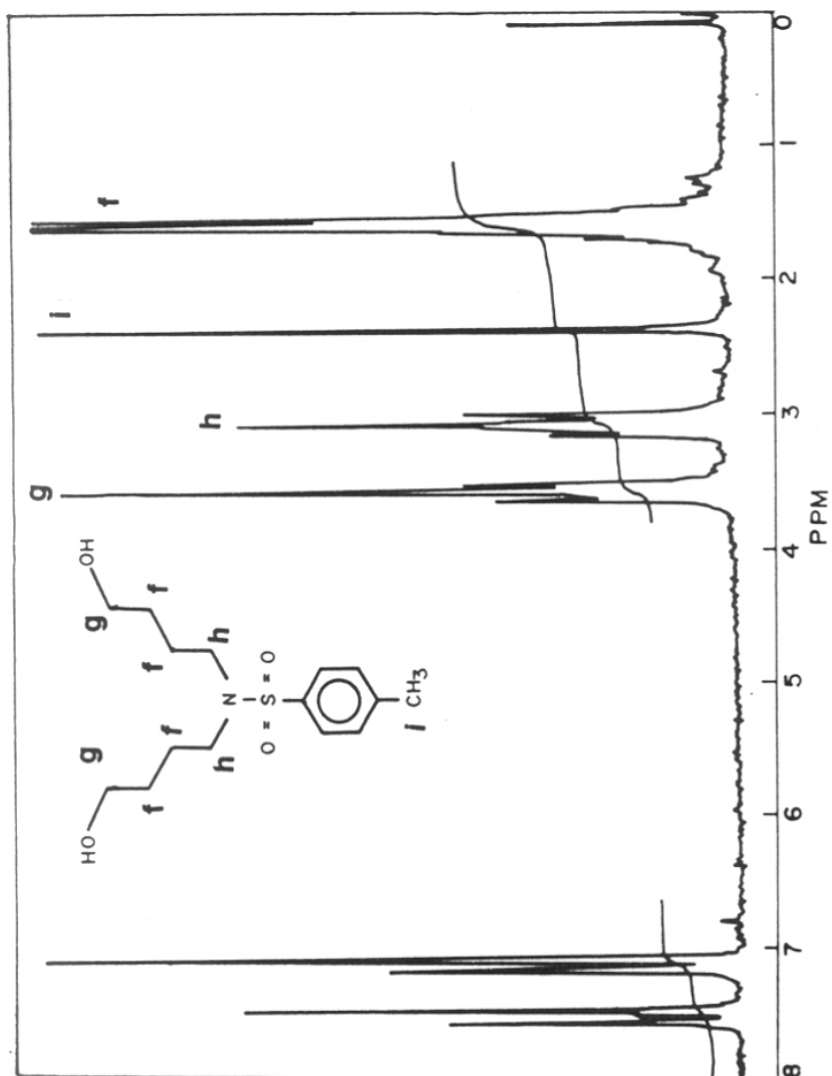
The synthesis of macrocyclic polyamines is easily effected through a cyclic bis N-alkylation reaction using metal-ion promoted templation. Among several methods known in literature to effect macrocyclisation,<sup>26-29</sup> the Cs<sub>2</sub>CO<sub>3</sub> method<sup>29</sup> seemed to be a good choice for cyclisations involving 17-28 membered rings.

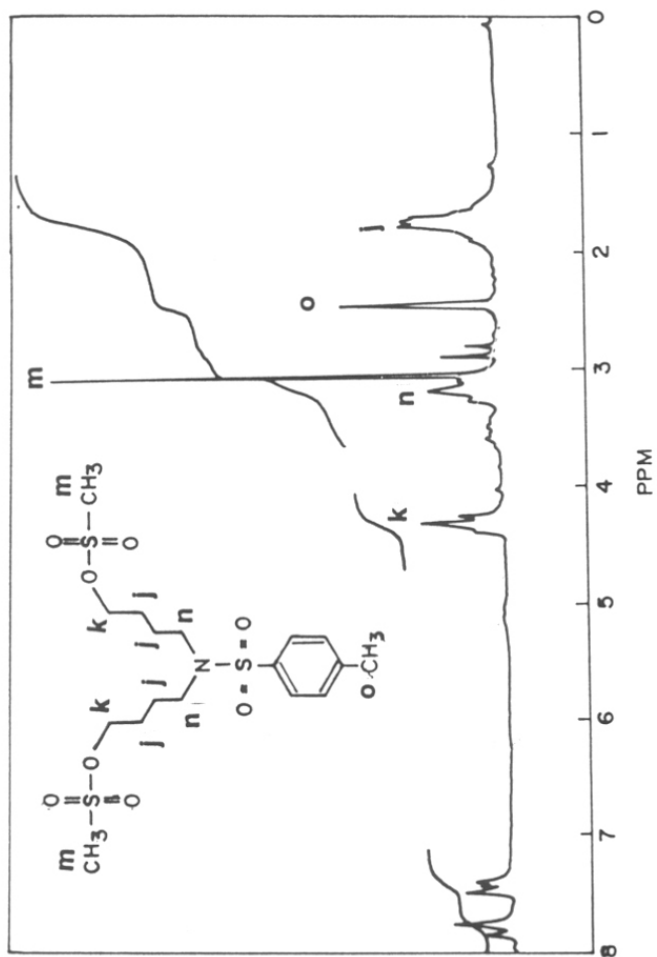
The bis mesylate compound **13** was coupled with ditosylate **9** in presence of Cs<sub>2</sub>CO<sub>3</sub> in dimethylformamide to get **14** (Scheme 5). The cyclisation was conducted by simultaneous dropwise addition of separate solutions of **9** and **13** to a suspension of Cs<sub>2</sub>CO<sub>3</sub> in DMF followed by heating overnight. The macrocycle **14** was obtained in 33% yield after column purification by silica gel chromatography.

The proof for cyclisation in **14** was by <sup>1</sup>H NMR (Fig. 9) which gave evidence for the presence of both cyclisation components in cyclised product:

- (i) the absence of methyl resonances due to mesyl group at 3.0 ppm.
- (ii) the presence of protons due to tosyl groups (Ar-CH<sub>3</sub>) at 2.4ppm,
- (iii) the non equivalent resonance patterns and the increase in the integral values of various methylenes.

Though the enantiomeric purity, was not been determined, the stereogenic carbon is unlikely to epimerize under the cyclisation reaction conditions<sup>29</sup>.

Fig. 7.  $^1\text{H}$  NMR spectrum of **12** in  $\text{CDCl}_3$  (90 MHz).

Fig. 8.  $^1\text{H}$  NMR spectrum of **13** in  $\text{CDCl}_3$  (90 MHz).

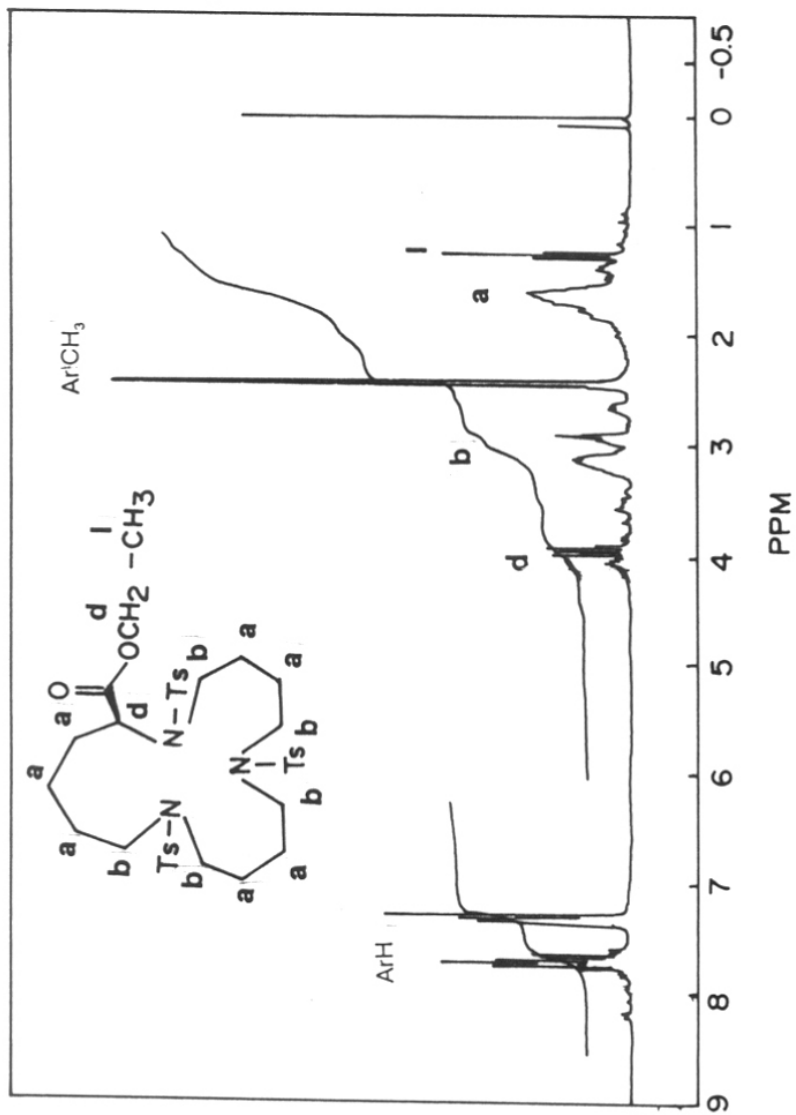
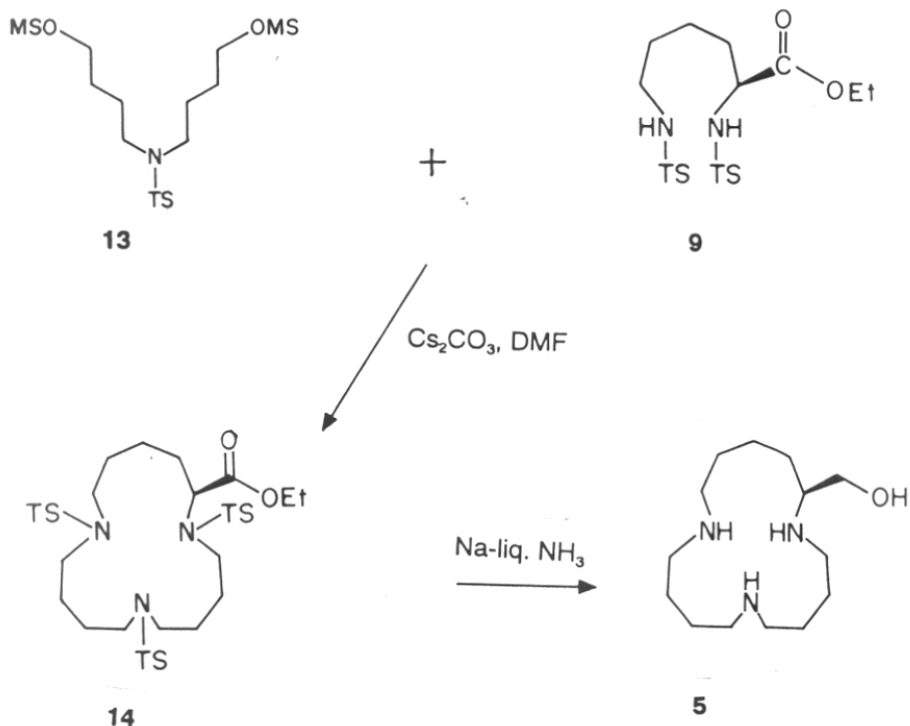


Fig. 9.  $^1\text{H}$  NMR spectrum of **14** in  $\text{CDCl}_3$  (300 MHz).

**SCHEME 5**

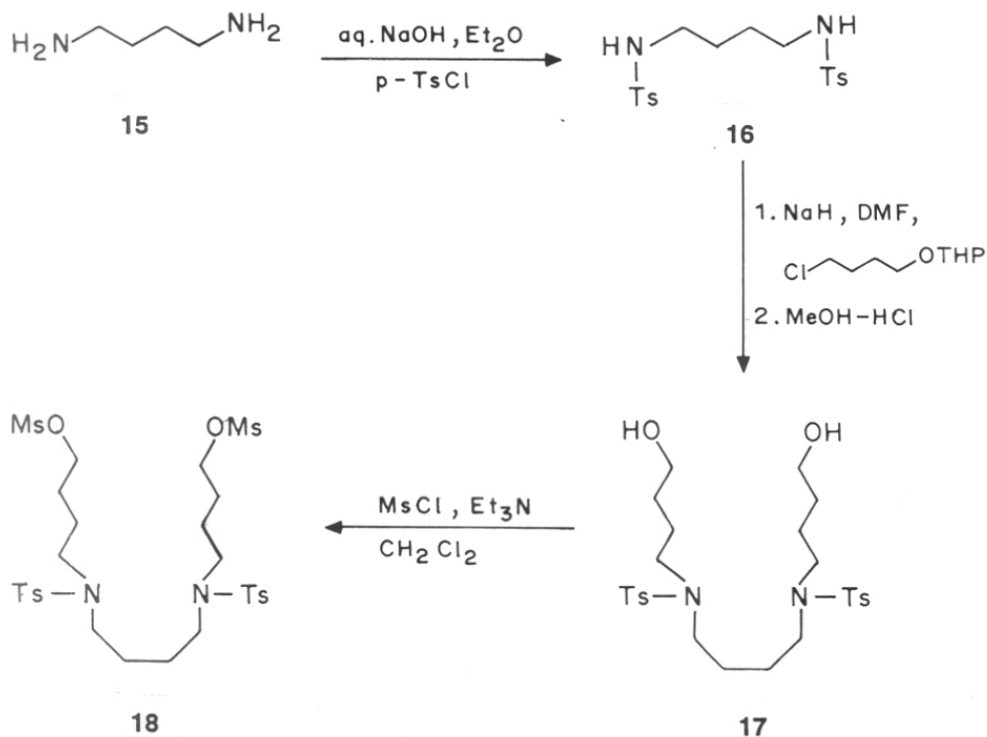
The protected macrocycle **14** on treatment with sodium/liquid ammonia underwent simultaneous detosylation and reduction of the side arm carboxy group to give the macrocyclic polyamine **5**. Among several reagents that were employed for detosylation ( $\text{LiAlH}_4$ , Na-Hg amalgam,  $\text{HBr-CH}_3\text{COOH}$ ) the most effective was sodium in liquid ammonia. This reagent also caused the desired reduction of the pendant carboethoxy ester function into hydroxymethyl group. The product macrocyclic polyamine **5** was extremely water soluble and care was taken to minimise the isolation losses. The physical and chemical data are consistent with structure **5** (see exptl).

### 2.4.3 Synthesis of macrocyclic polyamine [21]ane **N<sub>3</sub>** **6**

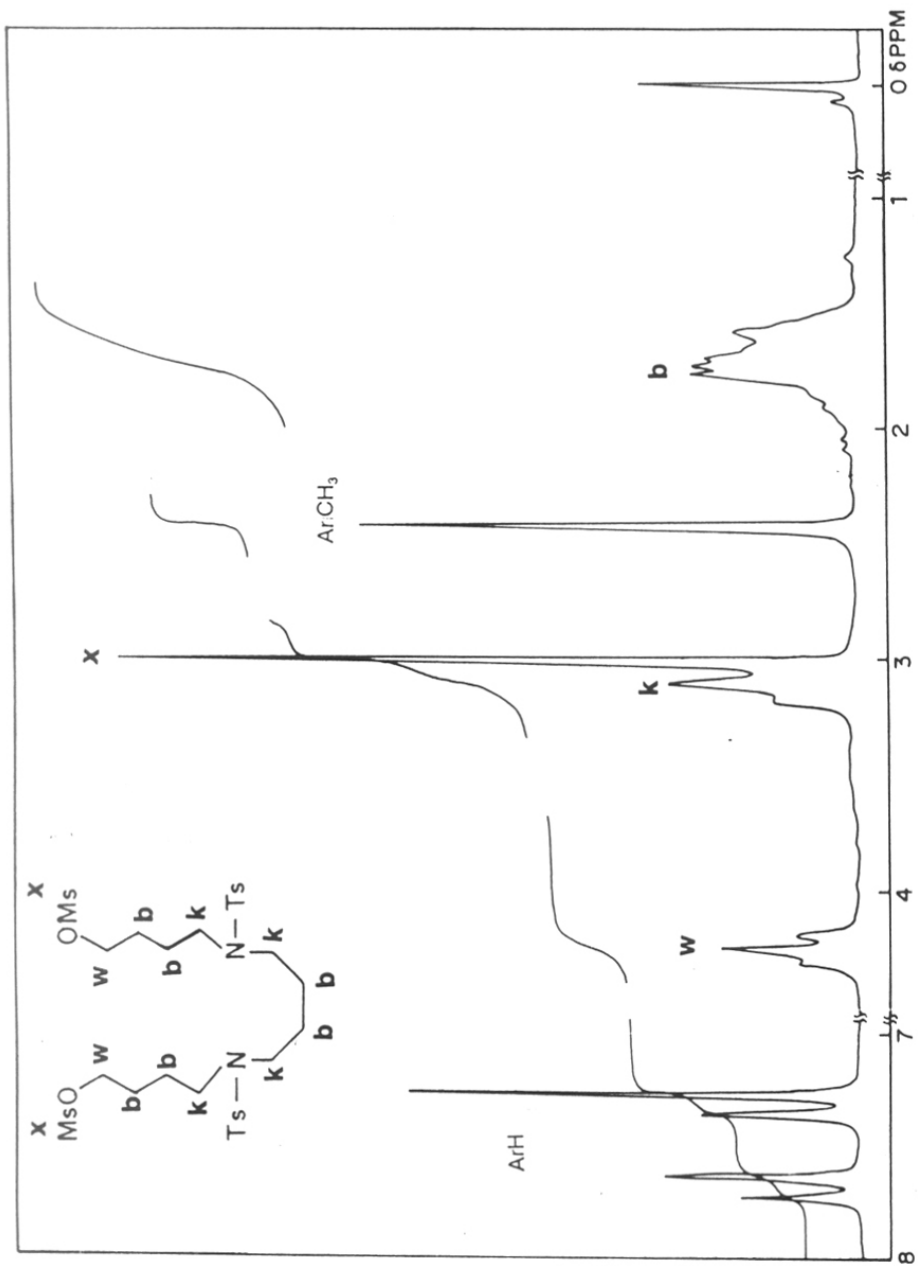
This was achieved by cyclization coupling of appropriate components **18** and **9**. The component **18** was synthesized from a suitable precursor by chain extension alkyla-

tion as before. Since this is a symmetrical compound it can be easily obtained by bis-N alkylation of precursor tosylamide **16**. The N,N'-ditosylamide **16** was prepared from 1,4-diaminobutane **15** by treatment with p-toluenesulfonyl chloride in diethyl ether and aq. NaOH (**Scheme 6**). The compound **17** was synthesised in 2 steps: by alkylation of N,N'-ditosyltetramethylene-1,4-diamine **16** with 1-chloro-4-(tetrahydropyran-2-yloxy)butane **11** to give the bisalkylated product, which was then deprotected with methanol-HCl to give **17** in 34% yield. The formation of bisalkylated product was indicated by an increase in the number of methylene protons at 1.57 ppm. **17** was then converted into dimesyl derivative **18** by treatment with methanesulfonyl chloride in presence of triethylamine in 73% yield. Appearance of sharp singlet at 3 ppm (**Fig. 10**) indicated formation of bis methanesulfonate.

### **SCHEME 6**

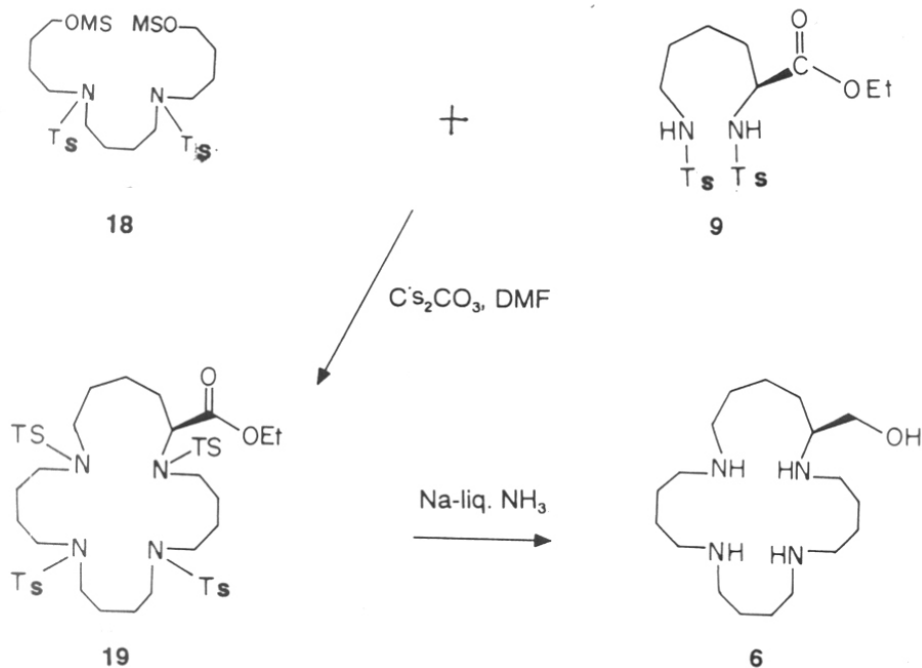




Fig. 10.  $^1\text{H}$  NMR spectrum of **18** in  $\text{CDCl}_3$ .

The cyclization was achieved by simultaneous addition of separate solutions of **18** and **9** in dry DMF to a suspension of  $\text{Cs}_2\text{CO}_3$  in DMF followed by heating (**Scheme 7**) overnight at  $80^\circ\text{C}$ . The macrocycle **19** was obtained in 37% yield.  $^1\text{H}$  NMR spectroscopy gave evidence for the formation of cyclised product **19** (**Fig. 11**) include the absence of methyl resonance due to mesyl group at 3 ppm, presence of protons due to the tosyl groups (Ar-Me) at 2.4 ppm, the non-equivalent resonance pattern and an increase in the integral value of various methylenes. **19** was detosylated by means of sodium in liquid ammonia which was accompanied by a simultaneous reduction of side-arm ester to afford the target polyamine **6** which was isolated and characterized by spectroscopic methods (**Fig. 12**).

**SCHEME 7**



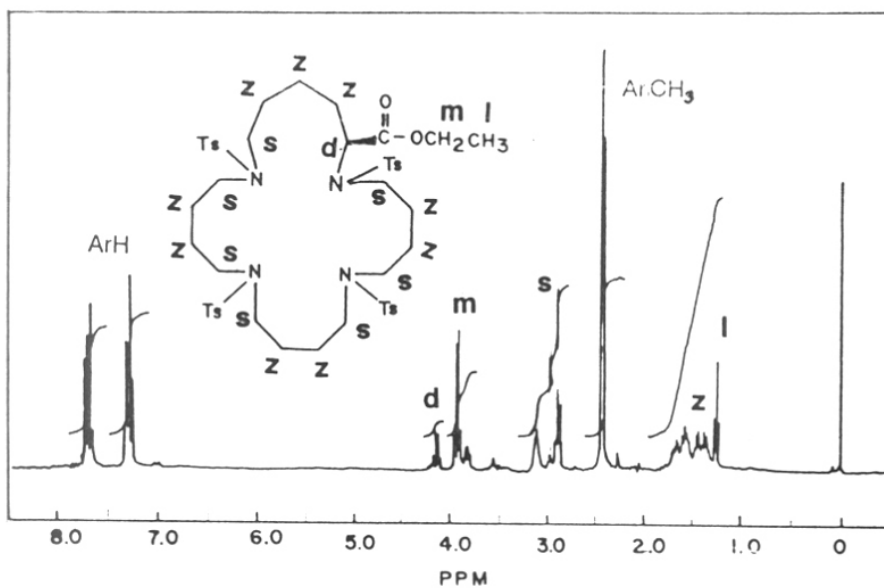


Fig. 11.  $^1\text{H}$  NMR spectrum of **19** in  $\text{CDCl}_3$ .

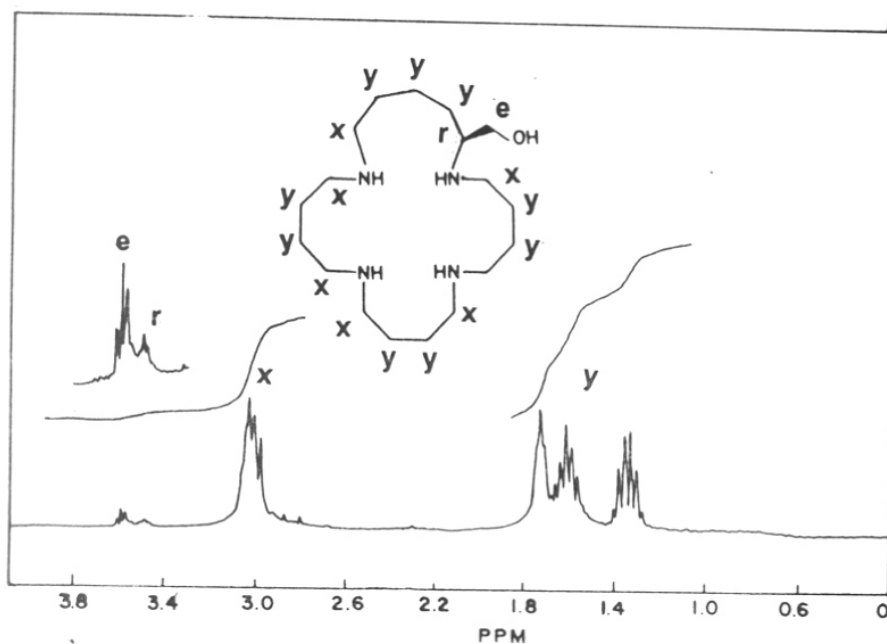


Fig. 12.  $^1\text{H}$  NMR spectrum of **6** in  $\text{CDCl}_3$ .

#### 2.4.4 Studies on complexation of macrocyclic polyamines **5** and **6** with nucleotidyl phosphates

$^{31}\text{P}$  NMR chemical shifts are sensitive to changes in the electronic environment and the geometry of the phosphate ligand. Hence the phosphate binding ability of polyamines **5** and **6** was investigated by  $^{31}\text{P}$  NMR. A solution of tetramethylammonium salt of ATP ( $(\text{NMe}_4)_2\text{-ATP}3\text{H}_2\text{O}$ , (20 mM)) in 20% $\text{D}_2\text{O}$ - $\text{H}_2\text{O}$  (pH 6.8) was individually titrated with stoichiometric amounts of an aqueous solution of cyclic polyamine hydrochlorides **5** and **6**. The results are shown in **Fig. 13** and **Fig. 14**. ATP shows a well resolved  $^{31}\text{P}$  spectrum with peaks corresponding to  $\alpha$ ,  $\beta$ ,  $\gamma$  clearly separated. It was seen that upon incremental addition of macrocyclic polyamine **6** only the  $\gamma$ -phosphorus of ATP exhibited significant upfield shifts. The magnitude of shift was a function of the added polyamine concentration. The polyamine **5** also induced similar  $^{31}\text{P}$  shift changes in ATP upon binding. This behavior in  $^{31}\text{P}$  NMR resonance indicates that ATP binds strongly to **5** and **6**. A similar binding experiment with the disodium salt of ATP resulted in a 30% broadening of  $^{31}\text{P}$  resonances without significant shift for any of the phosphorous resonances.

**Figure 15** depict the results of complexation studies as followed by  $^{31}\text{P}$  NMR. The upfield shift seen specifically for the  $\gamma$ -phosphorus of ATP indicates that this is sufficiently sensitive to polyamine **6** binding and is the main target for macrocyclic polyamine-ATP complexation. The magnitude of the upfield shifts observed was a function of added polyamine **6** concentration and for  $\gamma$ -phosphorus, a limiting value of 4.5 ppm was obtained. On further polyamine addition, no significant effect was observed. Compared to this, the limiting shifts for  $\beta$ -and  $\alpha$ -phosphorus atoms of ATP were about 1.0 and 0.5ppm respectively.

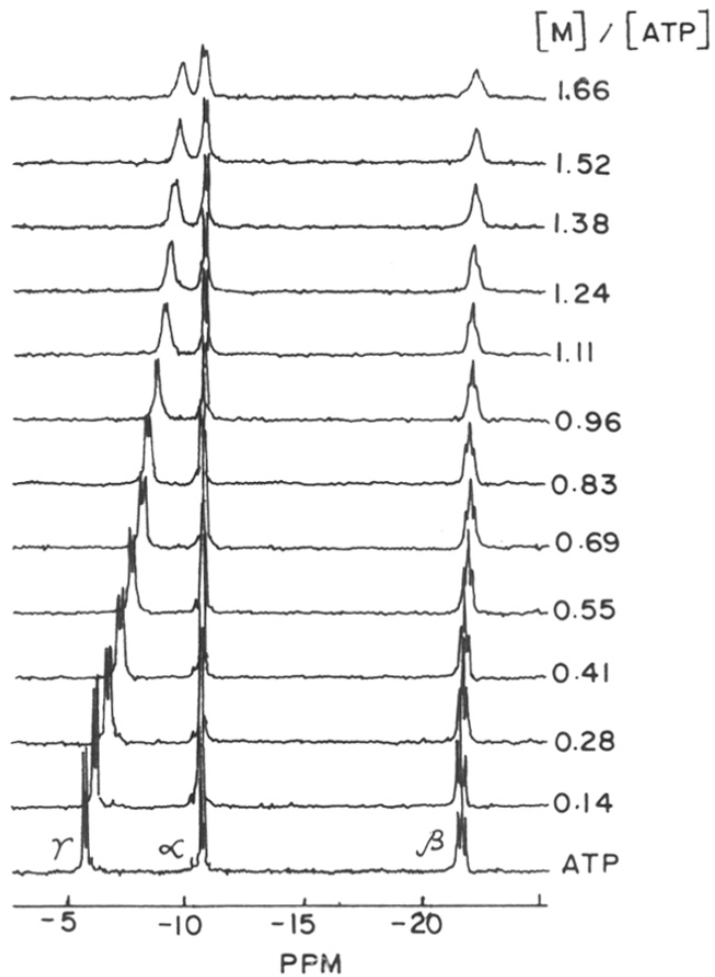


Fig. 13.  $^{31}\text{P}$  NMR (121.5 MHz) spectra of  $(\text{NMe}_4)_2\text{-ATP}$  upon addition of polyamine  $[\text{M}]$ ,  $[\text{16-}\text{N}_3]$ , **5**. Conditions: 0.02 M ATP; 20%  $\text{D}_2\text{O-H}_2\text{O}$ , pH 6.8; 21°C. The polyamine-ATP quotients ( $[\text{M}]/[\text{ATP}]$ ) are indicated in the right side.

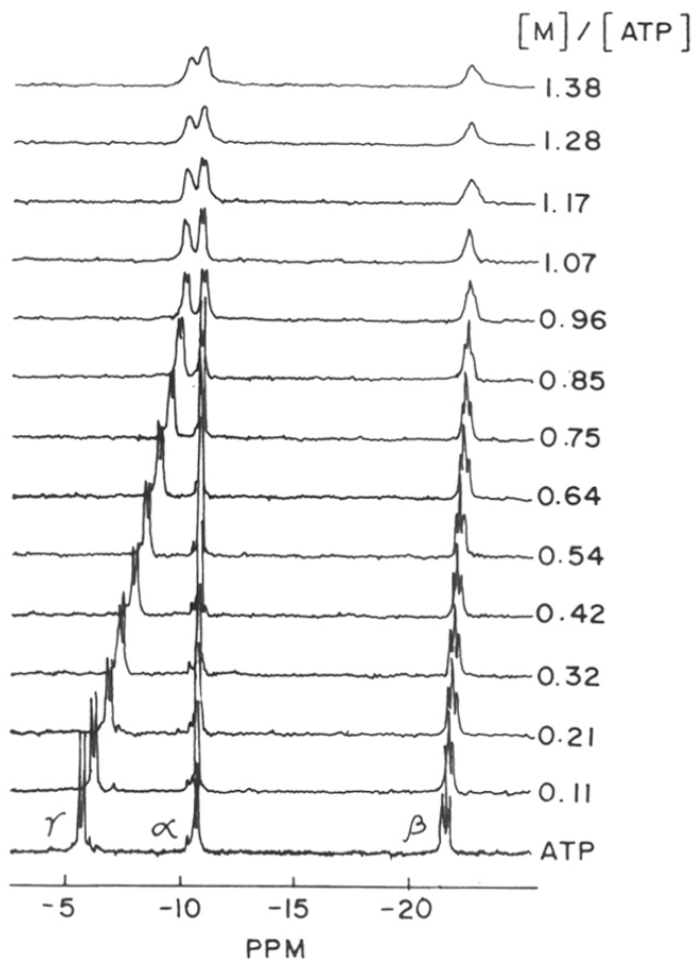


Fig. 14.  $^{31}\text{P}$  NMR (121.5 MHz) spectra of  $(\text{NMe}_4)_2\text{-ATP}$  upon addition of polyamine [M],  $^{24}\text{-N}_4$ , **6**. Conditions: 0.02 M ATP; 20%  $\text{D}_2\text{O-H}_2\text{O}$ , pH 6.8; 21°C. The polyamine-ATP quotients ( $[M]/[ATP]$ ) are indicated in the right side

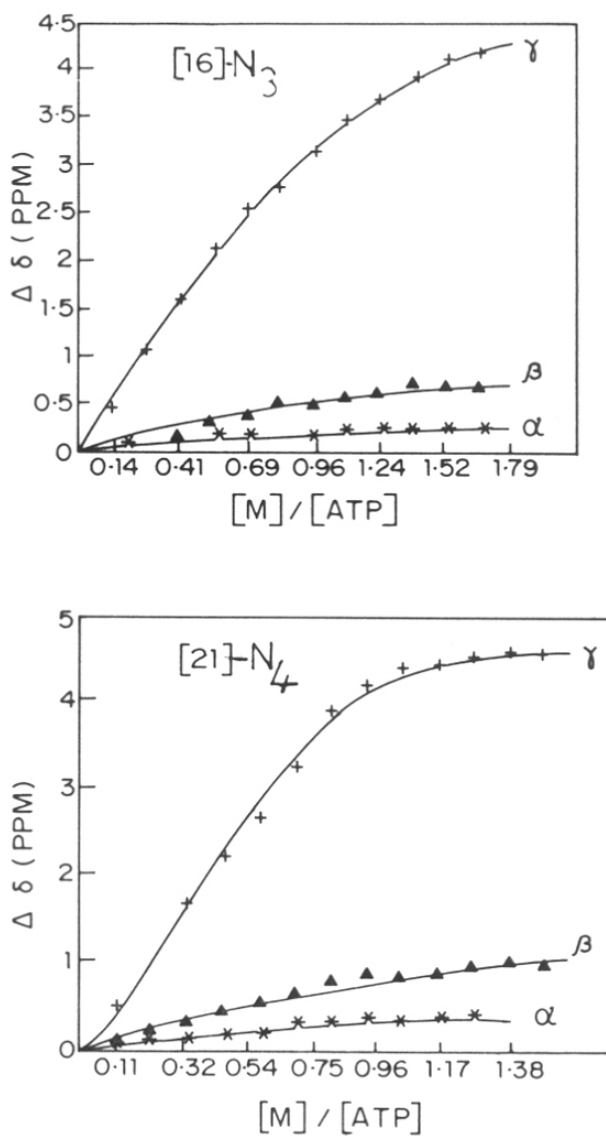


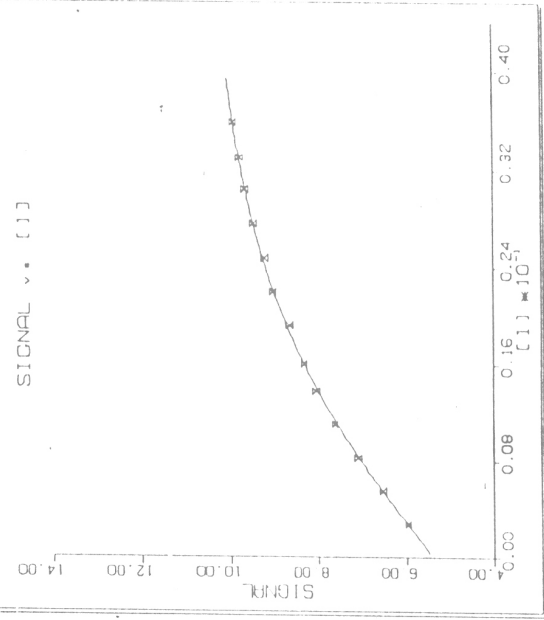
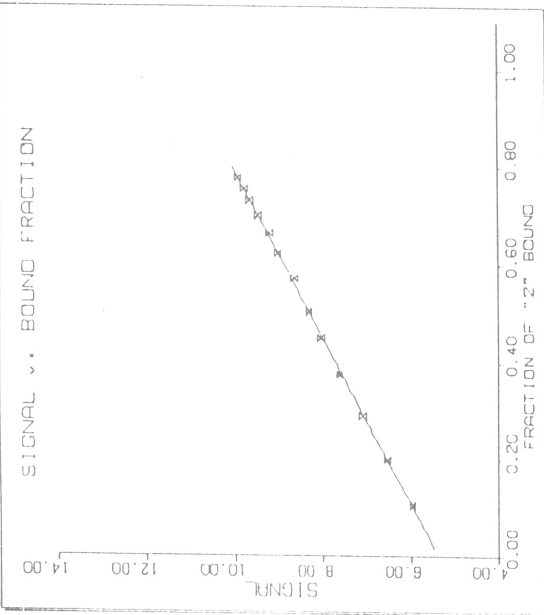
Fig. 15. Plot of shift in  $^{31}\text{P}$  NMR resonances of  $\alpha$ ,  $\beta$  and  $\gamma$  -phosphorus atoms as a function of added polyamine  $[M]$ ,  $[16]-N_3$  and  $[21]-N_4$ .

The lower aza homologue [16]-N<sub>3</sub> **5** effected qualitatively a similar upfield shift of the <sup>31</sup>P resonance from ATP, with the  $\gamma$ -phosphorus displaying shifts of a higher magnitude than the less significant shifts from  $\beta$ - and  $\alpha$ -phosphorus atoms. However, in contrast to [21]-N<sub>4</sub> (**6**), no plateau was observed in the binding curve, even beyond the addition of molar equivalents of polyamines. The magnitude of the shift itself is about the same order (4.3ppm) in both cases. The <sup>31</sup>P NMR data were analyzed using HOSTEST-II software,<sup>31</sup> a programme designed to assist investigations in molecular recognition. Association constants  $K_a$  of  $1.72 \times 10^2 \text{M}^{-1}$  for **5** (Fig. 16) and  $6.3 \times 10^3 \text{M}^{-1}$  for **6** (Fig. 17) were obtained. These values interestingly indicate that the macrocycle [21]-N<sub>4</sub> **6** binds about 35 times stronger to ATP than [16]-N<sub>3</sub> (**5**). Thus, although both polyamines act as receptors for the  $\gamma$ -P of ATP and induce similar magnitude of upfield shifts, the [21]-N<sub>4</sub> (**6**) is remarkably a better receptor than [16]-N<sub>3</sub> (**5**). Further, it can be seen from the binding isotherms that **6** binds ATP at a definite stoichiometry of 1:1 whereas that for **5** is not so well defined.

It has earlier been reported<sup>32</sup> that <sup>31</sup>P chemical shift of phosphorus moiety is highly sensitive to O-P-O bond angle, with a change of 1° inducing as much as 4 ppm shift differences. The complexation shifts in ATP may therefore be attributed to the conformational changes the triphosphate group undergoes upon association with the polyammonium cation of macrocycle. The data in Fig. 15 indicates that though overall shift upon complexation to triamine **5** and tetramine **6** are similar in magnitude, the slope of the binding curves are somewhat different. In the limit of infinitely strong binding, a straight line with a change to zero slope at a 1:1 stoichiometry would be expected. For complexation of **6** with ATP, the binding curve is not only steeper but also resembles more closely to the theoretically expected one for a bimolecular association. Because of the dependence of <sup>31</sup>P chemical shift of phosphates on the O-P-O



HOSTEST II SUMMARY  
 HOSTEST II PROGRAM ©1989, 1990 BY C.S. WILCOX. ALL RIGHTS RESERVED



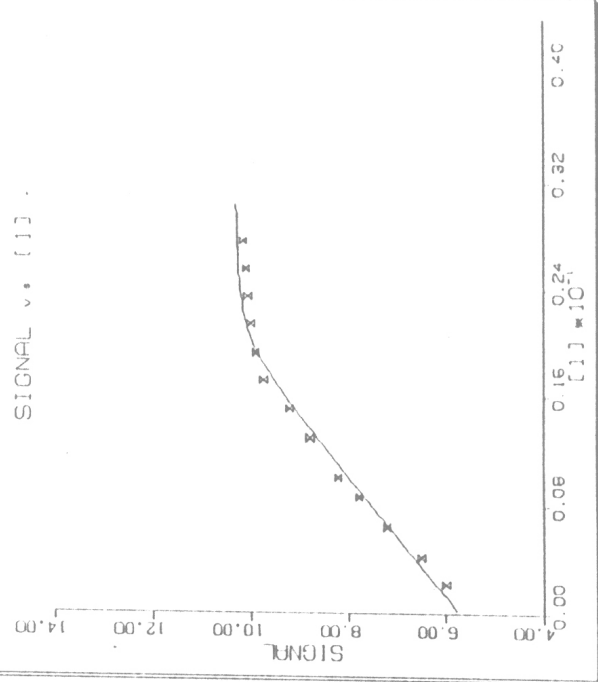
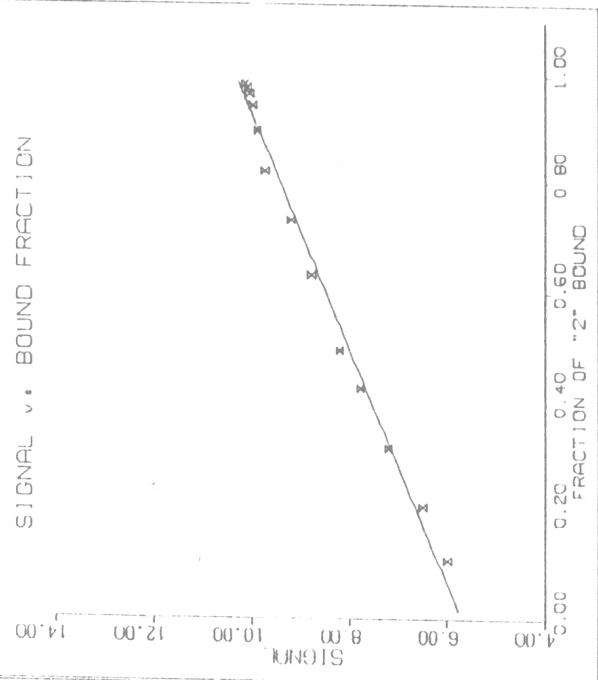
COMPONENT 1 : N3  
 COMPONENT 2 : H  
 C2) = 0.000 \* 1 + C.02000 ; RES = 0.000  
 RANGE OF [1] : 0.002800 0.035800 ; H : \* H NOT DEFINED  
 RANGE OF \*P\* : 0.60 0.78 ; M : \* M VARIES  
 CHEMIST : REF : P. 22-OCTOBER-1989 FERNANDO GA  
 SHYAMA RECEPTOR-N-CBZ-GLUTAMIC ACID TITRATION

PARAMETER	BEST VALUE	INTERVALS OF 50% CONFIDENCE
DISSOCIATION CONSTANT	0.00560723	0.00546572 0.00616267
ASSOCIATION CONSTANT	172.	163. 162.
SIGNAL OF COMPLEX	11.215	11.140 11.293
SIGNAL OF FREE SOLUTE	5.366	5.355 5.373
F OF RESIDUALS (REL. %)	0.9717	0.9603 0.9811
DURBIN-WATSON VALUE	1.61	1.58 1.59

LIMITS DEFINED BY REGRESSION LINE

Fig. 16. Computation of association constant for the complex [16]-N<sub>3</sub>-ATP by using HOSTEST II programme.

HOSTEST II SUMMARY  
 HOSTEST II PROGRAM ©1989, 1990 BY C.S. WILCOX. ALL RIGHTS RESERVED



COMPONENT	N4	TEMPERATURE	23.0
COMPONENT 2	***	SOLVENT	620
COEFF	0.000 x (1.0 - 0.02000) ASD=0.000	pH	pH NOT DEFINED
RANGE OF [1]	0.002200	M	VARIABLES
RANGE OF [2]	0.99	ELECTROLYTE	NONE
CHEMIST	REF 24-22-OCTOBER-1989	PERMANENCE OF	PERMANENCE OF
PARAMETER		BEST VALUE	INTERVALS OF SC. CONFIDENCE
DISSOCIATION CONSTANT	0.00015873	0.00000578	0.00037936
ASSOCIATION CONSTANT	6900.	173092.	2555.
SIGNAL OF COMPLEX	10.364	10.190	10.539
SIGNAL OF FREE SOLUTE	5.688	5.739	5.552
F OF RESIDUALS	3.7863	4.0529	3.8773
SCHEMATIC VALUE	0.45	0.58	0.44

Fig. 17. Computation of association constant for the complex [21]-N<sub>4</sub>-ATP by using HOSTEST II programme.

geometry in a major way compared to the electronic shielding parameters, the magnitude of the shift is not a true indication of strength of binding.

The weaker binding of [16]-N<sub>3</sub> (**5**) may be attributed to either or both of the following reasons:

(i) the macrocycle is not in fully protonated form at the reaction pH, and (ii) the complexation is non-stoichiometric with multiple species contribution apparently leading to an overall weak association.

It has been reported previously that non-fully protonated macrocyclic polyamines may show lower stability constants<sup>16a</sup>. Present results suggest that the sum of charge-charge interactions (electronic) may contribute to the association in a major way, causing the tetraprotonated receptor **6** interacting strongly with the tetraanion ATP.<sup>4-</sup> An assumption in suggesting such a possibility is that there are no inherent conformational differences in the polyamines **5** and **6**. Earlier work<sup>30</sup> has also indicated that the tetrammonium receptor [18]-N<sub>4</sub> with a larger ring size is a slightly better binding unit than its triammonium analog [15]-N<sub>3</sub>.

The binding studies of the mononucleotides AMP (Fig. 18) and the 3',5'-cyclic AMP (Fig. 19) and a dinucleotide TpT were similarly carried out in order to understand the specificity associated with the binding. In all cases, broadening of <sup>31</sup>P resonances of ATP from 9Hz (linewidth at half height) upto 30Hz was observed without much changes in chemical shift.

It was noticed that the sodium salt of ATP does not bind strongly to the macrocycles **5** and **6**. The phosphate resonances of ATP are only broadened without much shifts. However the tetramethylammonium salt of ATP displayed significant binding to **5**

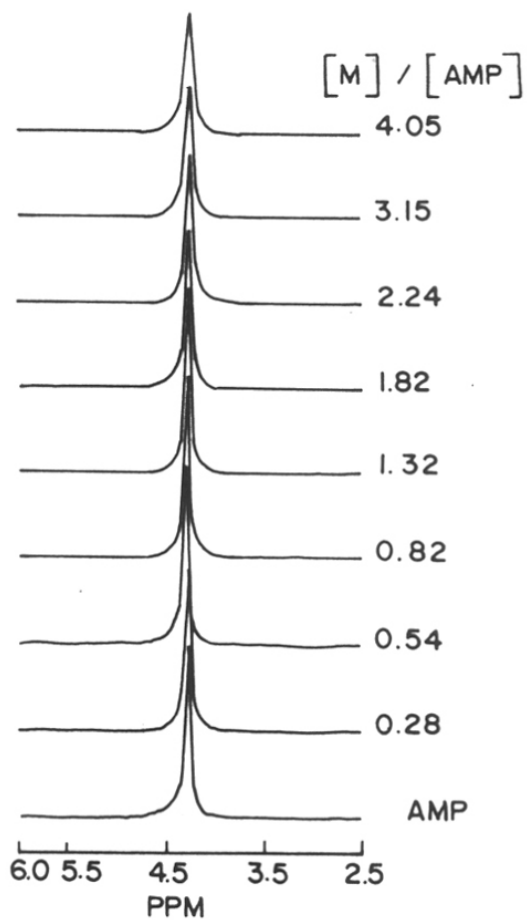


Fig. 18.  $^{31}\text{P}$  NMR (121.5 MHz) spectra of  $(\text{NMe}_4)_2\text{-AMP}$  upon addition of polyamine  $[\text{M}]$ ,  $[\text{24-N}_4]$ , **6**. Conditions: 0.02 M ATP; 20%  $\text{D}_2\text{O-H}_2\text{O}$ , pH 6.8; 21°C. The polyamine-ATP quotients ( $[\text{M}]/[\text{ATP}]$ ) are indicated in the right side.

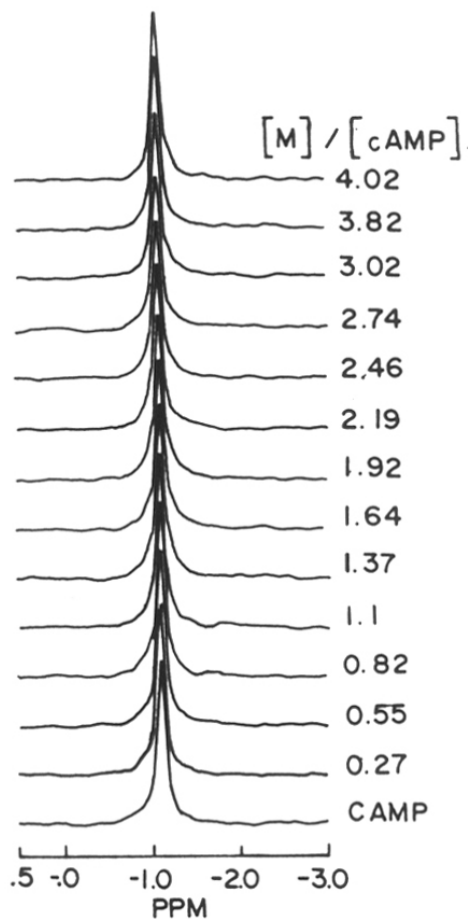


Fig. 19.  $^{31}\text{P}$  NMR (121.5 MHz) spectra of  $(\text{NMe}_4)_3\text{-}3',5'\text{-cAMP}$  upon addition of polyamine  $[\text{M}]$ ,  $[\text{24-N}_4]$ , **6**. Conditions: 0.02 M ATP; 20%  $\text{D}_2\text{O-H}_2\text{O}$ , pH 6.8; 21°C. The polyamine-ATP quotients ( $[\text{M}]/[\text{ATP}]$ ) are indicated in the right side.

and **6**. This counter-ion effect is perhaps due to the fact that, while the bulky macrocycle cannot displace a hard metal ion such as  $\text{Na}^+$  from the anion shell, the spatially concentrated positive charge in macrocyclic polyamines can effectively compete with a soft point-charged counterion such as  $\text{N}^+\text{Me}_4$ . It was also noticed similar counterion differences as well effect the binding of linear polyamines spermine and spermidine with ATP. Due to the mechanistic nature of interaction between ATP and a hard metal ion,<sup>33</sup> the binding of polyammonium macrocycles to ATP may effect a much larger conformational changes in O-P-O bond geometry than that seen due to binding of isocationic metal ions. The linking of the pendant hydroxymethyl group to side chains containing nucleophilic groups such as imidazole, thiol, carboxylate or organometallics may effect a catalytic hydrolysis of bound ATP which is a topic of current interest due to its applications in design of artificial chemical nucleases<sup>34</sup>.

## 2.5 CONCLUSIONS

Chapter II demonstrates the synthesis of two novel macrocyclic polyamines **5** and **6** possessing a hydroxymethyl side chain. The macrocyclization was achieved by condensation of lysineditosylate **9** with appropriate components **13** and **18** in the presence of  $\text{Cs}_2\text{CO}_3$  to obtain **14** and **19**. The complexation of polyamines **5** and **6** with ATP was studied by  $^{31}\text{P}$  NMR spectroscopy, which indicated a specific recognition of  $\gamma$ -phosphorus of  $\text{ATP}(\text{NMe}_4 \text{ salt})$  by polyamines. The measurement of binding constants by  $^{31}\text{P}$  NMR indicated that ATP binds compound **6** ca. 35 times stronger than it does with compound **5**. The binding curves indicated a definite 1:1 stoichiometry for **6**:ATP binding. The mononucleotides, AMP, cAMP and dinucleotide TpT did not show significant complexation with either compound **5** or **6**. The binding of ATP by macrocyclic polyamines **5** and **6** and the presence of a hydroxymethyl side chain to link with a nucleophile may aid rational design of chemical nucleases.

## 2.6 EXPERIMENTAL

All melting points are uncorrected and all compounds gave satisfactory C,H analysis. TLC analyses were done on precoated silica gel plates (E Merck, Art. No.5554) and the solvent systems used were: A,  $\text{CHCl}_3/\text{MeOH}(10\%)$ , B,  $\text{CH}_2\text{Cl}_2$ . The spots were identified by iodine detection, ninhydrin spray or by acid spray (60%  $\text{HClO}_4$ -EtOH) depending on the nature of compounds. Lysine monohydrochloride, 1,4-butane-diamine, 4-chloro-1-butanol, cesium carbonate (all from Aldrich) and 1,2-dihydropyran (Merck) were used without further purification. THF was distilled over sodium-benzophenone and DMF was dried by keeping overnight over KOH pellets, followed by distillation under vacuum. Silica gel column chromatography was carried out by using 100-200 mesh silica gel.  $^1\text{H}$  and  $^{31}\text{P}$  NMR spectra were recorded on MSL300 or WH 90 (Bruker). IR spectra were recorded with a Perkin-Elmer 599-B double beam IR spectrometer. Mass spectra were run on a Finnigan MAT 1020 automated GC/MS instrument.

### 2.6.1 N,N'-ditosylbutane-1,4-diamine 16

To a solution of 1,4-diaminobutane (10 g, 113 mmol) in 1M aq. NaOH (450 ml), a solution of p-toluenesulfonylchloride (43.4 g, 230 mmol) in diethylether (150 ml) was added slowly with cooling. Reaction mixture was stirred for 4 hrs. at room temperature. The separated ethereal layer was evaporated to yield crude N,N'-ditosyl-1,4-diaminobutane. This was purified by column chromatography over silica gel and eluted with EtOAc/hexane to yield **20** (23.3 g, 85%). It was recrystallised from MeOH to a pale yellow solid, m.p. 139°C. IR (Nujol)  $\text{cm}^{-1}$ : 3370 (N-H), 1600,1480 (aromatic), 1320 and 1160 (O=S=O);  $^1\text{H}$  NMR (acetone- $d_6$ )  $\delta$  1.47 (m, 4H, 2 x  $-\text{CH}_2-$ ), 2.38 (s, 6H, 2 x  $\text{Ar-CH}_3$ ), 2.78 (t, J = 3 Hz, 4H, 2 x N- $\text{CH}_2$ ), 7.31 (d, J = 8Hz, 4H, Ar-H), 7.67 (d, J = 8 Hz, 4H, Ar-H).

### 2.6.2 1-Chloro-4-(tetrahydropyran-2-yloxy)butane 11

To a mixture of 4-chloro-1-butanol (10.85 g, 100 mmol) and 3,4-dihydro-2-pyran (10.09 g, 120 mmol) phosphorous oxychloride (0.5 ml) was added slowly while cooling in an ice-bath. The reaction mixture was stirred at room temperature for 3 hrs. after which it was diluted with diethyl ether (50 ml) and washed with aq. KOH (5%, 2 x 50 ml). The ethereal layer was dried and evaporated to afford crude product **11** which was purified by distillation (b.p.82-84°C/2 mm, yield 90%). <sup>1</sup>H NMR (CCl<sub>4</sub>) δ 4.53 (m, 1H, CH<sub>2</sub>-O-CH<sub>2</sub>-O), 3.56 (overlapping multiplets, 6H, 2 x OCH<sub>2</sub>, CH<sub>2</sub>Cl), 1.75(m, 10H, 5 x CH<sub>2</sub>)

### 2.6.3 N,N-Bis(4-hydroxybutyl)totuene-p-sulfonamide 12

To a solution of p-toluenesulfonamide (9.26 g, 54 mmol) in dry DMF (25 ml), NaH (1g, 43 mmol) was added and the mixture was stirred for 30 min. 1-chloro-4-(tetrahydropyran-2-yloxy)-butane **11** (5 g, 26 mmol) was then added and heated at 70-75°C for 4 hrs. The reaction mixture was cooled and further batches of NaH (1 g, 43 mmol) and 1-chloro-4-(tetrahydropyran-2-yloxy)-1-butane (5 g, 26 mmol) were added and heated overnight (70-75°C). The reaction progress was monitored by the disappearance of **11** (TLC, solvent system A). The separated solid was filtered and the filtrate concentration under vacuum gave a brown oil. This was dissolved in 10% aq. HCl (150 ml, 36%) in MeOH and the mixture was stirred overnight to remove the tetrahydropyranyl group. Evaporation of the mixture under reduced pressure gave a residue which was dissolved in CH<sub>2</sub>Cl<sub>2</sub> (70 ml) and washed successively with aq.NaHCO<sub>3</sub> (2 x 75 ml) and water (2 x 75 ml). The organic phase was dried and concentrated to obtain a brown solid which was purified by column chromatography and eluted with EtOAc/hexane to yield the pure product **12** (5.1 g, yield 30%). m.p. 69-70°C; IR (Nujol) cm<sup>-1</sup> 3300-3450 (O-H), 1040 (C-O), 1150, 1330 (O=S=O); <sup>1</sup>H NMR (CDCl<sub>3</sub>): δ 1.6 (m,



8H, 4 X  $-\text{CH}_2-$ ), 2.4 (s, 3H,  $\text{Ar}-\text{CH}_3$ ), 3.18 (t,  $J = 6$  Hz, 4H, 2 X  $\text{N}-\text{CH}_2$ ), 3.68 (t,  $J = 6$  Hz, 4H, 2 X  $-\text{O}-\text{CH}_2$ ), 7.41 (d,  $J = 8$  Hz, 2H,  $\text{Ar}-\text{H}$ ) and 7.77 (d,  $J = 8$  Hz, 2H,  $\text{Ar}-\text{H}$ ). Mass spectrum ( $m/z$ ), 314 [ $\text{M}^+-1$ ].

**2.6.4 N,N'-Bis(4-hydroxybutyl)-N,N'-tetramethylenedi(toluenep-sulphonamide) 17**  
 N,N'-Ditosyl-1,4-diaminobutane (7.6 g, 19 mmol) was dissolved in dry DMF (50 ml) and NaH (0.8 g) was added and the mixture was stirred for 30 min. Compound **11** (3.64 g, 18.92 mmol) was added and the mixture heated for 4hrs. at 75-80°C. After the mixture had cooled, a second portion of NaH (0.8 gm) was added followed by addition of more compound **11** and heating at 75-80°C for further 40 hrs. Work-up was repeated as above to afford pure **17** (3.49 g, yield 34%) as a pale yellow gum. IR (Neat)  $\text{cm}^{-1}$  3300-3500 (O-H), 1075 (C-N), 1310 and 1140 (O=S=O);  $^1\text{H NMR}$  ( $\text{CDCl}_3$ )  $\delta$  1.57 (m, 12H, 6 X  $-\text{CH}_2-$ ), 2.4 (s, 6H, 2 X  $\text{Ar}-\text{CH}_3$ ), 3.09 (t,  $J = 5$  Hz, 8H, 4 x  $\text{N}-\text{CH}_2$ ), 3.6 (t,  $J = 5$  Hz, 4H, 2 x  $-\text{O}-\text{CH}_2$ ), 7.27 (d,  $J = 8$  Hz, 4H,  $\text{Ar}-\text{H}$ ), 7.64 (d,  $J = 8$  Hz, 4H,  $\text{Ar}-\text{H}$ ).

#### 2.6.5 2,6-Bis(tosylamino)hexanoic Acid **8**

To a stirred solution lysine monohydrochloride (5 g, 82 mmol) dissolved in aq. NaOH (1 M, 390 ml), p-toluenesulfonylchloride (39 g, 200 mmol) dissolved in diethylether (375 ml) was added and the reaction mixture stirred for 14 hrs. at room temperature. The aq. layer was separated and acidified with aq. HCl (1M). The precipitated oily material was extracted with  $\text{CH}_2\text{Cl}_2$  (3 x 200 ml) and the residue obtained on evaporation was dissolved in NaOH (1 M, 100 ml) and precipitated with aq. HCl (1 M, 75 ml) to obtain a white solid of **8** (28.8 g, yield 75 %). m.p. 152°C; IR ( $\text{CHCl}_3$ )  $\text{cm}^{-1}$  1730 (C=O), 1320 and 1170 (O=S=O);  $^1\text{H NMR}$  ( $\text{CDCl}_3$ )  $\delta$  1.31 (m, 6H,  $-\text{CH}_2$ ), 1.62 (m, 2H,  $-\text{CH}_2-$ ), 2.4 (s, 6H, 2 x  $\text{Ar}-\text{CH}_3$ ), 2.75 (t,  $J = 6$  Hz, 2H,  $\text{N}-\text{CH}_2$ ), 3.82 (t,  $J = 5.5$  Hz, 1H,  $\text{N}-\text{CH}-\text{CO}$ ), 7.44 (d,  $J = 8$  Hz, 4H,  $\text{Ar}-\text{H}$ ), 7.83 (d,  $J = 8\text{Hz}$ , 4H,  $\text{Ar}-\text{H}$ ).

### 2.6.6 Ethyl 2,6-Bis(tosylamino)hexanoate 9

Thionyl chloride (17.78 g, 150 mmol) was gradually added to a cooled suspension of N,N'-ditosyl-2,6-diaminohexanoic acid (23.37 g, 50 mmol) in abs. EtOH (75 ml). The reaction mixture was refluxed for 4 hrs. and the excess of EtOH was evaporated off. The residue was coevaporated three times with dry benzene to remove excess thionylchloride. The product was dissolved in  $\text{CHCl}_3$ , washed successively with  $\text{NH}_4\text{OH}$  and water (2 x 100 ml). Removal of solvent from organic layer gave crude product **9** which was purified by filtration through column of silica gel (TLC grade) and eluted with ethylacetate/MeOH to give a solid (20.85, yield 84%). m.p. 124°C; IR ( $\text{CHCl}_3$ )  $\text{cm}^{-1}$  1740 (C=O), 1170 and 1340 (O=S=O), 1230 (-CO-O);  $^1\text{H}$  NMR ( $\text{CDCl}_3$ )  $\delta$  1.1 (t, J = 7 Hz, 3H,  $\text{CH}_3$ ), 1.29-1.8 (m, 6H, 3 x  $-\text{CH}_2$ ), 2.4 (s, 3H, Ar- $\text{CH}_3$ ), 2.42 (s, 3H, Ar- $\text{CH}_3$ ), 2.9 (q, J = 6 Hz, 2H,  $-\text{N}-\text{CH}_2$ ), 3.9 (q, J = 7 Hz, 2H, O- $\text{CH}_2$ ), **4.3** (t, J = 6 Hz, N- $\text{CH}-\text{CO}-$ ), 7.25 (d, J = 8 Hz, 4H, Ar-H) and 7.69 (d, J = 8 Hz, 4H, Ar-H)

### 2.6.7 4,4'-Tolune-p-sulphonyliminodibutyl Bismethanesulphonate 13

N,N-Bis(4-hydroxybutyl)-p-toluenesulfonamide **12** (2.0 g, 6 mmol) and  $\text{NEt}_3$  (2.3 g, 24 mmol) were dissolved in  $\text{CH}_2\text{Cl}_2$  (25 ml) and solution was chilled to -5 °C. Methanesulfonylchloride was added dropwise while the temperature was kept below 0°C. After 1 hr. the mixture was worked up by washing successively with ice-water (2 x 30 ml), 10% aq. HCl (2 x 30 ml), aq.  $\text{NaHCO}_3$  (2 x 30 ml) and brine. On concentration of  $\text{CH}_2\text{Cl}_2$  layer yielded a brown oil was produced which was purified by column chromatography on silica gel. Elution with EtOAc/hexane yielded **13** (2.2 g, yield 74%). m.p. 65-66°C; IR ( $\text{CHCl}_3$ )  $\text{cm}^{-1}$  1176 and 1351 (O=S=O);  $^1\text{H}$  NMR ( $\text{CDCl}_3$ )  $\delta$  1.7 (m, 8H, 4 x  $-\text{CH}_2-$ ), 2.4 (s, 3H, Ar- $\text{CH}_3$ ), 3.0 (s, 6H, 2 x  $\text{SO}_2-\text{CH}_3$ ), 3.1 (t, J = 6Hz, 4H, 2 x  $-\text{N}-\text{CH}_2$ ), 4.2 (t, J = 6 Hz, 4H, 2 x  $-\text{CH}_2-\text{O}-\text{SO}_2$ ), 7.4 (d, J = 8 Hz, 2H, Ar-H), 7.79 (d, J = 8Hz, 2H, Ar-H).

**2.6.8 4,4'-[N,N'-Tetramethylene-N,N'-bis(tolune-p-sulphonyl)diamino]dibutyl  
Bis(methanesulphonate) 18**

Compound **18** was prepared as above from 3.1 g (6 mmol) of **17** and methanesulfonylchloride (1.56 g, 14 mmol) in 73% yield. m.p. 118-120°C; IR (CHCl<sub>3</sub>) cm<sup>-1</sup> 1176 and 1351 (O=S=O); <sup>1</sup>H NMR (CDCl<sub>3</sub>) δ 1.42-2.0 (m, 12H, 6 x -CH<sub>2</sub>-), 2.42 (s, 6H, 2 x Ar-CH<sub>3</sub>), 3.0 (s, 6H, SO<sub>2</sub>-CH<sub>3</sub>), 3.1 (t, J = 7 Hz, 8H, 4 x -N-CH<sub>2</sub>-), 4.24 (t, J = 6 Hz, 4H, 2 x -CH<sub>2</sub>-O-SO<sub>2</sub>), 7.31 (d, J = 8 Hz, 4H, Ar-H), 7.69 (d, J = 8 Hz, 4H, Ar-H).

**2.6.9 (S)-Ethyl-1,6,11-tritosyl-1,6,11-triazacyclohexadecane-13-carboxylate 14**

Ethyl N,N'-ditosyllysinate **9** (2.85 g, 6 mmol) was dissolved in dry DMF (600 ml) and Cs<sub>2</sub>CO<sub>3</sub> (3.27 g, 17 mmol) was added and stirred for 30 min. To this was added a solution of **13** in dry DMF (240 ml), dropwise over 6-7 hr. The mixture was then heated at 80°C for 36 hrs. DMF was removed under reduced pressure and the residue was diluted with CH<sub>2</sub>Cl<sub>2</sub> (50 ml) and then the usual work up gave a brown gum which was purified on column chromatography using EtOAc/hexane as eluent to obtain **14** (1.52 g, yield 33%), m.p. 97°C. IR (CHCl<sub>3</sub>) cm<sup>-1</sup> 1740 (C=O), 1140 and 1320 (O=S=O); <sup>1</sup>H NMR (CDCl<sub>3</sub>) δ 1.25 (t, J = 6 Hz, 3H, CH<sub>3</sub>), 1.3-1.9 (m, 14H, 7 x -CH<sub>2</sub>), 2.4 (s, 9H, Ar-CH<sub>3</sub>), 2.8-3.3 (m, 10H, N-CH<sub>2</sub>), 3.97 (overlapping m, 3H, N-CH-CO, O-CH<sub>2</sub>), 7.25 (d, J = 8 Hz, 6H, Ar-H) and 7.68 (d, J = 8 Hz, 6H, Ar-H).

**2.6.10 (S)-Ethyl-1,6,11,16-tetratosyl-1,6,11,16-tetraazacycloheicosane-17-carboxylate 19**

Compound **19** was prepared according to the procedure described above from ethyl N,N'-ditosyllysinate **9** (2.61 g, 6 mmol) in dry DMF (570 ml), Cs<sub>2</sub>CO<sub>3</sub> (5.03 g, 26 mmol) and **18** (4 g, 6 mmol) in dry DMF (228 ml) in 37% yield (1.82 g). m.p. 88°C; [α]<sub>577</sub> = 5.41° (C=4.82, CHCl<sub>3</sub>); IR (CHCl<sub>3</sub>) cm<sup>-1</sup> 1740 (C=O), 1080 (C-N), 1140 and

1320 (O=S=O);  $^1\text{H NMR}$  ( $\text{CDCl}_3$ )  $\delta$  1.24 (t,  $J = 7$  Hz, 3H,  $-\text{CH}_3$ ), 1.6 (m, 18H, 9 x  $-\text{CH}_2-$ ), 2.4 (s, 12H, 4 x Ar- $\text{CH}_3$ ), 3.09 (m, 14H, 7 x N- $\text{CH}_2$ ), 4.13 (q,  $J = 7$  Hz, 1H, N- $\text{CH}-\text{CO}_2$ ), 3.9 (m, 2H, O- $\text{CH}_2-$ ), 7.28 (d,  $J = 8$  Hz, 8H, Ar- $\text{H}$ ); 7.67 (d,  $J = 8$  Hz 8H, Ar- $\text{H}$ ).

### 2.6. 11 (S)-(1,6,11-Triazacyclohexadecan-13-yl)methanol 5

A solution of **14** (1 g, 1.3 mmol) in dry THF (30 ml) was slowly added to a solution of liquid  $\text{NH}_3$  (260 ml) and sodium metal. When blue colour of the liquid ammonia disappeared, more sodium was added until the blue colour persisted and the reaction mixture was stirred at  $-78^\circ\text{C}$  for 4 hrs.  $\text{NH}_4\text{Cl}$  (4 g) was added and  $\text{NH}_3$  was slowly allowed to boil off. The solvent was evaporated off and the residue was dissolved in aq. AcOH (0.1 M, 30 ml); the solution was washed with diethyl ether (2 x 30 ml). The aq. layer was neutralised (pH 7) with  $\text{NaHCO}_3$  and the mixture was extracted with  $\text{CH}_2\text{Cl}_2$  (1 x 25 ml) to compound **5** a dark yellow gum of **5** (0.26 g, yield 77%). Dissolution of the gum in aq. HCl (1 M, 20 ml) followed by lyophilisation to obtain a yellow solid of the corresponding trihydrochloride. m.p.  $266^\circ\text{C}$  (decomp); IR (free amine, neat)  $\text{cm}^{-1}$  3200-3440 (O-H, N-H), 1050 (C-N);  $^1\text{H NMR}$  ( $\text{D}_2\text{O}$ )  $\delta$  1.6-1.9 (m, 14H), 3-3.3 (m, 10H, N $\text{CH}_2$ ), 3.5-3.75 (m, 3H, N- $\text{CH}$ -,  $\text{CH}_2$ -OH), MS (m/z) 256 [ $\text{M}^+-1$ ].

### 2.6. 12 (S)-(1,6,11,16-Tetraazacycloheneicosan-17-yl)methanol 6

**6** was prepared by following the same procedure as above from **19** (1.44 g, 2 mmol) in dry THF (70 ml), liquid  $\text{NH}_3$  (300 ml) in yield of 73% (0.46 g). Tetrahydrochloride, m.p.  $280^\circ\text{C}$  (decom);  $[\alpha]_{\text{D}} = +6.98^\circ$  ( $C = 0.47$ ,  $\text{H}_2\text{O}$ ); IR (free amine, neat)  $\text{cm}^{-1}$  ; 3300, 3190 (N-H, O-H), 1620  $\text{cm}^{-1}$  (N-H), 1040 (C-N);  $^1\text{H NMR}$  ( $\text{CDCl}_3$ )  $\delta$  1.21-1.61 (m, 18H, 9 x  $-\text{CH}_2-$ ), 2.88-3.15 (m, 14H, 7 x N- $\text{CH}_2$ ), 3.48 (t, 1H, N- $\text{CH}-\text{CH}_2\text{OH}$ ), 3.6 (t, 2H,  $\text{CH}_2$ -OH).

## 2.6. 13 Complexation studies of macrocyclic polyamines with nucleotidyl phosphates

Tetramethyl ammonium salt of the ATP was prepared from disodium salt of ATP. A solution of ATP disodium salt in water was titrated with 1 M solution of tetramethyl ammonium hydroxide in methanol. It was then purified by size exclusion chromatography (sephadex G-10, 2 x 12 cm) and characterised by  $^1\text{H}$  and  $^{31}\text{P}$  NMR. Solution of polyamines were prepared by addition of solid hydrochloride salt of macrocyclic polyamines **5** and **6** in 0.02 M solution of nucleotide phosphates [(NMe<sub>4</sub>)<sub>2</sub>ATP, (NMe<sub>4</sub>)<sub>2</sub>AMP, (NMe<sub>4</sub>)cAMP, TpT] and adjusted the pH to 6.8. Incremental amounts of this solution was then titrated to 0.02 M solution of nucleotidyl phosphates in water D<sub>2</sub>O mixture (8:2).  $^{31}\text{P}$  NMR spectrum was recorded at each addition.

## 2.7 REFERENCES

1. Pedersen, C. J. *J. Am. Chem. Soc.* **1967**, *89*, 2495, 7017.
2. Cram, D. J.; Cram, J. M. *Science* **1974**, *183*, 803.
3. Izatt, R. M.; Christensen, J. J. (ed.) *Synthetic Multidentate macrocyclic Compounds* Academic Press **1978**.
4. (a) Christensen, J. J.; Eatough, D. J.; Izatt, R. M. *Chem. Rev.* **1974**, *74*, 351.  
(b) Izatt, R. M.; Bradshaw, J. S.; Nielson, S. A.; Lamb, J. D.; Christensen, J. J. *Chem. Rev.* **1985**, *85*, 271.
5. Melson, G. A. (ed.) *Co-ordination Chemistry of Macrocyclic Compounds* Plenum Press: New York and London, **1979**.
6. Izatt, R. M.; Christensen, J. J. (ed.) *Progress in Macrocyclic Chemistry* Wiley-Interscience: New York, Vol. I, **1979** and Vol. II, **1981**.
7. Izatt, R. M.; Pawlak, K.; Bradshaw, J. S. *Chem. Rev.* **1991**, *91*, 1721.
8. Busch, P. H.; Farmery, K. J.; Goedken, V.; Kotavic, V.; Melnyk, A. C.; Speratic, C. R.; Tokel, N. *Adv. Chem. Ser. No. 100* **1971**, 44.

9. Dolphin, D. (ed.) *The Phophyrins* Academic Press, Vol I-VII, 1979.
10. Collman, J. P.; Shneider, P. W. *Inorg. Chem.* **1960**, *5*, 138.
11. Iitaka, Y.; Shina, M.; Kimura, E. *Inorg. Chem.* **1974**, *13*, 2886.
12. Hinz, F. P.; Margerum, D. W. *J. Am. Chem. Soc.* **1974**, *96*, 4993.
13. Kodama, M.; Kimura, E. *J. Chem. Soc. Chem. Comm.* **1975**, 326.
14. Kodama, M.; Kimura, E. *J. Chem. Soc., Dalton Trans.* **1977**, 1473.
15. (a) Kodama, M.; Kimura, E. *J. Chem. Soc., Dalton Trans.* **1978**, 1081.  
(b) Kimura, E.; Yatsunami, T. *Chem. Pharm. Bull. Jpn.* **1980**, *28*, 994.  
(c) Kodama, M.; Kimura, E. *J. Chem. Soc. Dalton Trans* **1976**, 116.  
(d) Kodama, M.; Kimura, E. *J. Chem. Soc., Dalton Trans.* **1978**, 104.
16. (a) Kimura, E.; Sakonaka, A.; Yatsunami, T.; Kodama, M. *J. Am. Chem. Soc.* **1981**, *103*, 3041.  
(b) Yatsunami, T.; Sakonaka, A.; Kimura, E. *Anal. Chem.* **1981**, *53*, 477.
17. Robinson, B. H.; Williams, G. R. *Biochem. Biophys. Acta.* **1970**, *216*, 63.
18. Palmieri, F.; Prezioso, G.; Quagliariello, E.; Klingenberg, M. *Eur. J. Biochem.* **1971**, *22*, 66.
19. Kimura, E.; Kodama, M.; Yatsunami, T. *J. Am. Chem. Soc.* **1982**, *104*, 3182.
20. Schmidtchen, F. P. *Angew. Chem. Int. Ed. Engl.* **1981**, *20*, 466.
21. (a) Poonia, N. S.; Bajaj, A. V. *Chem. Rev.* **1979**, *79*, 389.  
(b) Kodama, M.; Kimura, E.; Yamaguchi, S. *J. Chem. Soc. Dalton Trans.* **1980**, 2536.  
(c) Izatt, R. M.; Terry, R. E.; Haymore, B. L.; Hansen, L. D.; Dalley, N. K.; Avondet, A. G.; Christensen, J. J. *J. Am. Chem. Soc.* **1976**, *98*, 7620.
22. Fujioka, H.; Kimura, E.; Kodama, M. *Chem. Lett.* **1982**, 737.
23. Kimura, E.; Watanabe, A.; Kodama, M. *J. Am. Chem. Soc.* **1983**, *105*, 2063.
24. (a) Tabushi, I.; Imuta, J.; Seko, N.; Kobuke, Y. *J. Am. Chem. Soc.* **1978**, *100*, 6287.  
(b) Tabushi, I.; Kobuke, Y.; Imuta, J. *J. Am. Chem. Soc.* **1981**, *103*, 6152.

25. Furuta, H.; Cyr, M. J.; Sessler, J. L. *J. Am. Chem. Soc.* **1991**, *113*, 6677-6678.
26. Rossa, L.; Vogtle, F. *Top. Curr. Chem.* **1983**, *113*, 1.
27. Laidler, D. A.; Stoddart, J. F. *In The Chemistry of Functional Groups* Patai, S., (ed.), Wiley; New York, **1980**, part I.
28. Richman, J. E.; Atkins, T. J. *J. Am. Chem. Soc.* **1974**, *96*, 2268.
29. Vriesema, B. K.; Buter, J.; Kellogg, R. M. *J. Org. Chem.* **1984**, *49*, 110.
30. (a) Marecek, J. F.; Burrows, C. J. *Tetrahedron Lett.* **1986**, *27*, 5943.  
(b) Marecek, J. F.; Fischer, P. A.; Burrows, C. J. *Tetrahedron Lett.* **1988**, *29*, 6231.
31. Wilcox, C. S. in *Frontiers in Supramolecular Organic Chemistry and Photochemistry* Schneider, H.; Durr, H, (eds.), VCH: Weinheim, **1990**.
32. (a) Cozzone, P. J.; Jardetzky, O. *Biochemistry* **1976**, *15*, 4853.  
(b) Gorenstein, G. (ed) *<sup>31</sup>P NMR* Academic Press: New York, **1984**.
33. Ramirez, F.; Merececk, J. F. *Biochim. Biophys. Acta.* **1980**, *589*, 21.
34. (a) Hosseini, M. W.; Blacker, A. J.; Lehn, J. M. *J. Am. Chem. Soc.* **1990**, *112*, 3896.  
(b) Bashkin, J. K.; Gard, J. K.; Modak, A. K. *J. Org. Chem.* **1990**, *55*, 5125.

## CHAPTER 3

### SYNTHESIS AND CONFORMATIONAL STUDIES OF d(TpA) AND r(UpA) CONJUGATED AT C8 AND C5' WITH AMINES



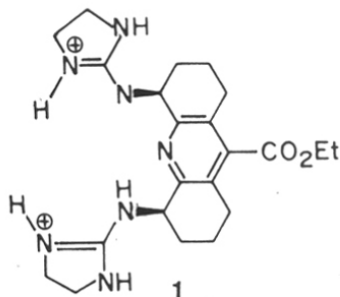
### 3.1 INTRODUCTION

Binding via molecular recognition and hydrolytic cleavage of DNA and RNA are important biological processes<sup>1,2</sup>. Enzymes that act on nucleic acids such as ribonuclease,<sup>3</sup> DNA polymerase I,<sup>4</sup> *E. Coli* alkaline phosphatase,<sup>5</sup> endo and exo restriction nucleases,<sup>4</sup> contain either metal ions<sup>6</sup> ( $Zn^{2+}$ ,  $Mg^{2+}$ ) or positively charged amino acid residues (arginine, lysine or protonated histidine) in their active sites for recognition-interaction with negatively charged phosphate group. The active sites also contain amino acids with nucleophilic side chains such as aspartic acid, tyrosine and histidine which mediate phosphate hydrolysis by either general or specific base catalysis. Currently, attention in several laboratories are focussed on study on molecular recognition of phosphate function which is a chemical pre-requisite for effecting its hydrolysis.

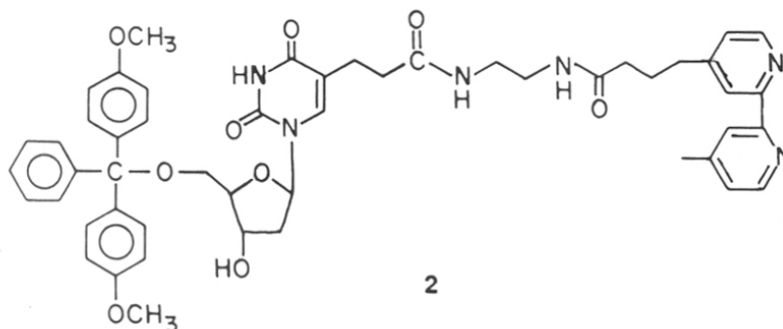
### 3.2 NUCLEASE MODELS

There are many approaches attempted in the literature to mimic the nuclease activity due to its potential application for multiple purpose, including health related goals such as the coupling of RNA hydrolytic catalyst to antisense DNA<sup>7</sup> for use in mRNA gene therapy<sup>8</sup>. Several metal complexes<sup>9,10</sup> have been widely used to achieve efficient cleavage, but their utility is complicated by associated lability and toxicity.<sup>10</sup>

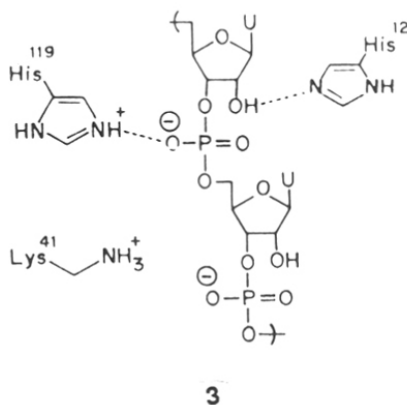
Enzyme mimicing by incorporation of active site functional groups of nucleases may potentially lead to reaching nature's enormous hydrolytic rate.<sup>11</sup> A successful approach in this direction was reported by Smith et al.<sup>12</sup> They designed **1**, which possesses an amino imidazoline group pre organized by a relatively rigid spacer.



Modak et al.<sup>13</sup> synthesised oligonucleotide bipyridyl conjugate **2** and demonstrated the cleavage of RNA by its copper complexes. In an elegant way Breslow et al.<sup>11</sup> have shown that imidazole buffer can catalyze cleavage of ribonucleotides. Attempts have been made to incorporate imidazole moieties into the oligonucleotide through amide linkages at C5 of the pyrimidine and C2 of purine nucleosides<sup>14</sup> to design chemical nucleases. Very recently Chin et al.<sup>15</sup> have achieved the hydrolysis of unactivated dimethylphosphate by using cobalt complex.



None of the model systems reported so far possess the entire complementary side chain present in the active site of the ribonuclease (**3**). Also, no report exists in the literature where active functional groups (Imidazole/NH<sub>2</sub>) of the ribonuclease catalytic

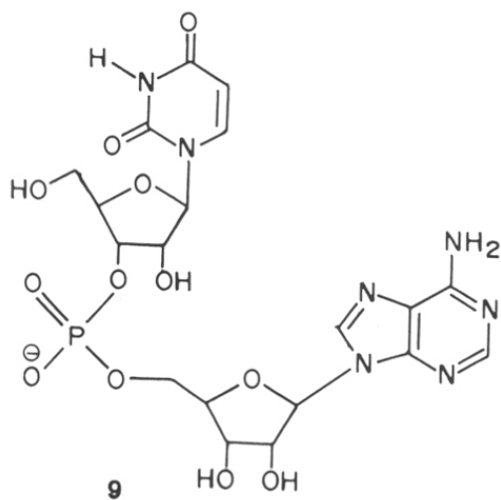
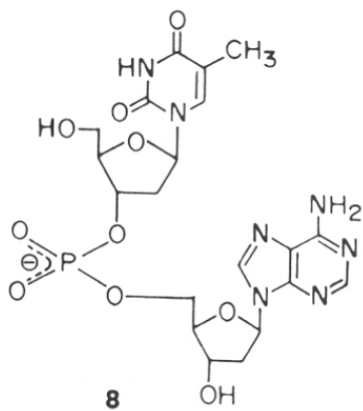


site are juxtaposed close to the phosphate backbone of the nucleotides. As a first step towards achieving the complete complementary catalytic site, we undertook synthesis and studies of molecules where these active functional groups are positioned very close in proximity to the phosphate backbone.

### 3.3 OBJECTIVE OF PRESENT WORK

The main aim of this work was to synthesize dinucleotides **4-9** with base conjugated with amines, conformational studies of the base modified dinucleotides and metal ion mediated cleavage reactions. Solution phase phosphotriester chemistry was used for their synthesis and all compounds were well characterised by the  $^1\text{H}$ ,  $^{31}\text{P}$ ,  $^{13}\text{C}$  NMR and mass spectroscopy. Purity was established by HPLC analysis. Conformational analysis was carried out by a first order analysis of  $^1\text{H}$ - $^1\text{H}$  coupling constants. Metal-ion mediated cleavage of the phosphodiester backbone of these base modified dinucleotides were carried out and it will be discussed in the chapter IV.



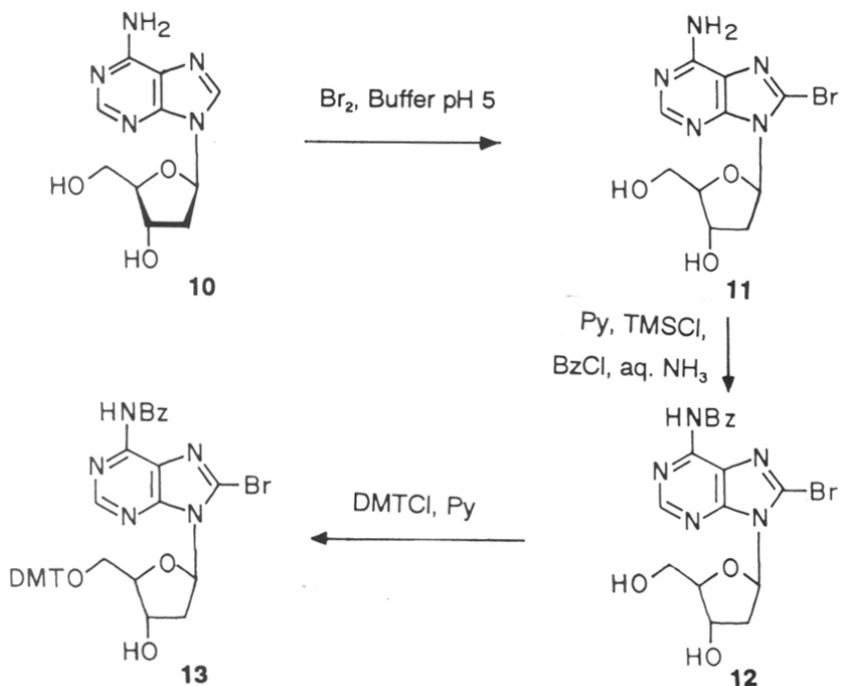


### 3.4 PRESENT WORK

#### 3.4.1 Synthesis of 8-bromo-5'-dimethoxytrityl-N<sup>6</sup>-Bz-2'-deoxyadenosine

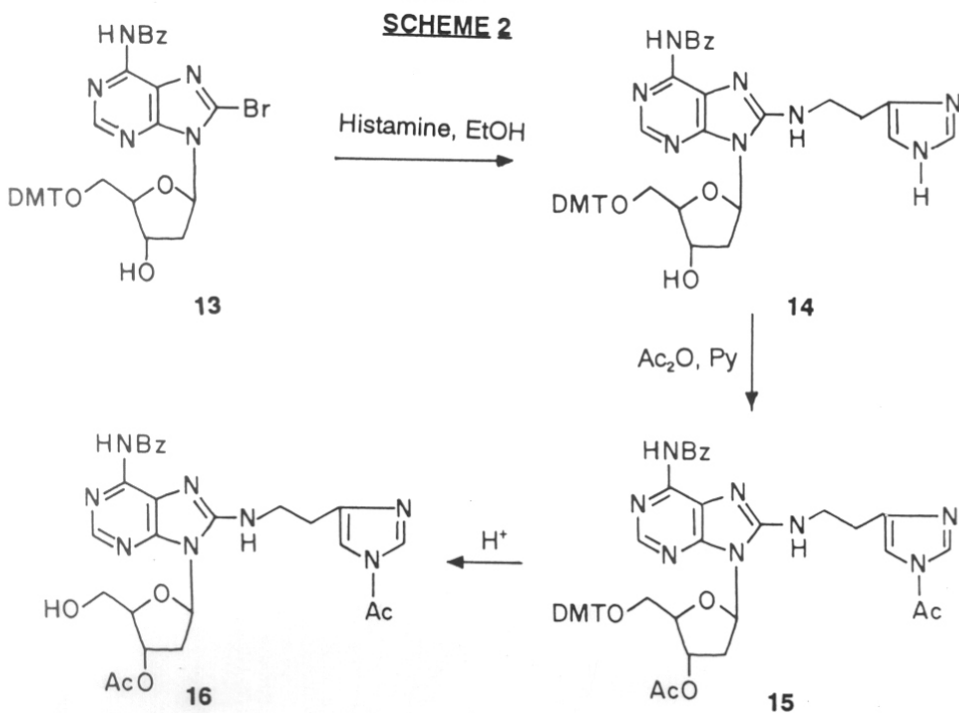
Treatment of 2'-deoxyadenosine **10** with bromine-water<sup>16</sup> in sodium acetate buffer (pH 5.0) gave 8-bromo-2'-deoxyadenosine **11**. The disappearance of H8 proton signal in <sup>1</sup>H NMR spectrum showed the formation of 8-bromo-2'-deoxyadenosine. This was N<sup>6</sup> benzoylated by treatment with trimethylsilyl chloride and benzoyl chloride in pyridine (transient protection method<sup>17</sup>) to yield **12** (Scheme 1). It was then 5'-O-protected with 4,4'-dimethoxytrityl (DMT) group to give **13**.

#### SCHEME - 1



### 3.4.2 Synthesis of C8 conjugated histamine and ethylenediamine-2'-deoxyadenosine

C8 conjugated histamino-**14** (**Scheme 2**) or ethylenediamino- 2'-deoxy adenosine **17** (**Scheme 3**) was obtained by treatment of **13** with excess of either histamine or 1,2-diaminoethane respectively. The structural proof for **14** and **17** were obtained from  $^1\text{H}$  NMR spectra which had characteristic signals for imidazole peaks at 7.52 ppm, 6.61 ppm and methylene protons at 3.6 ppm and 2.6 ppm for compound **14** and additional methylene protons at 3.0 ppm and 2.73 ppm for compound **17**. Compounds **14** and **17** were converted into their corresponding N,3'-O-acetyl derivatives (**15** and **18**) by reaction with acetic anhydride-pyridine. Detritylation with 2% dichloroacetic acid (DCA) in dichloromethane (DCM) to generate the 5'-hydroxyl terminal blocks **16** and **19**. Compounds **16** and **19** were well characterized by  $^1\text{H}$  and  $^{13}\text{C}$  NMR spectroscopy (Fig. 1, 2, 3 and 4).



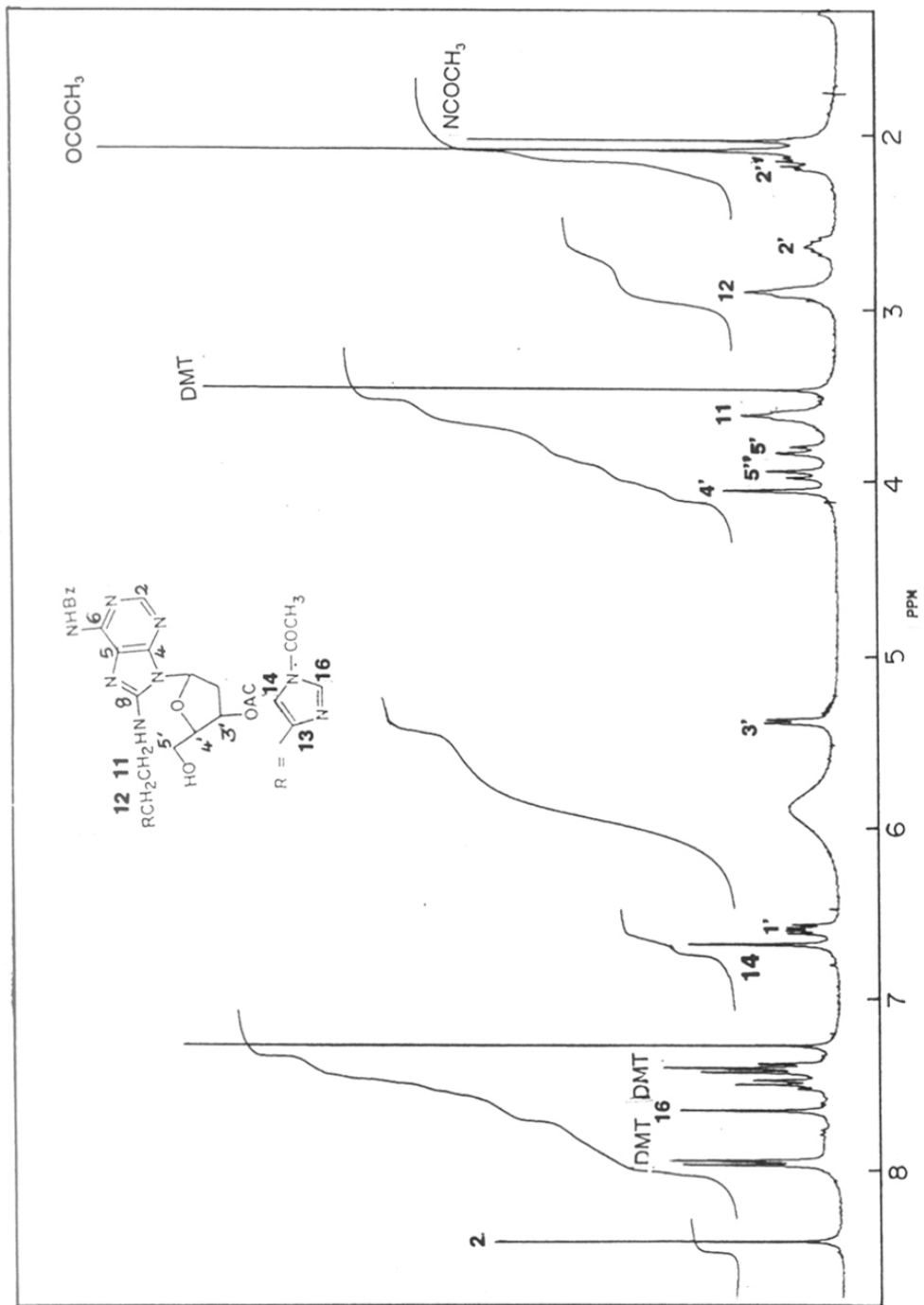


Fig. 1 300 MHz  $^1\text{H}$  NMR spectrum of 16.



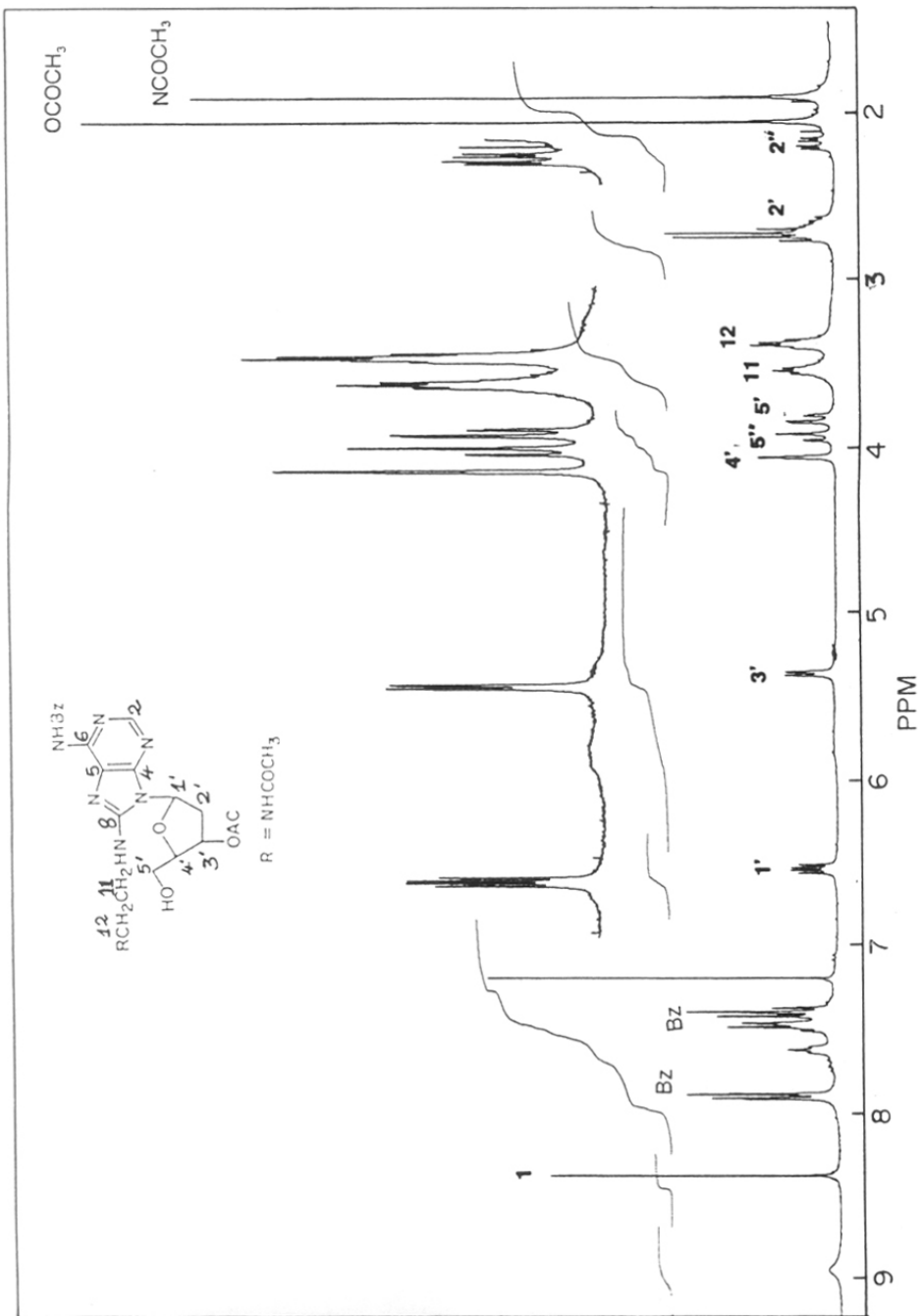
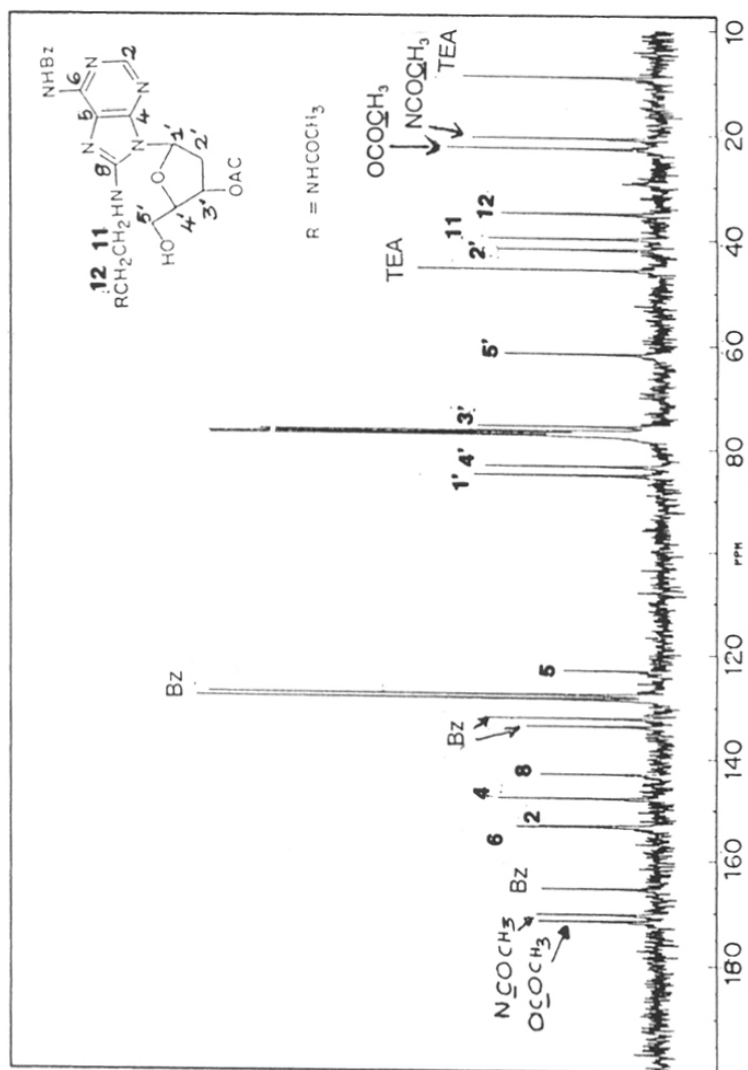


Fig. 2 300 MHz <sup>1</sup>H NMR spectrum of **19** in CDCl<sub>3</sub>.

Fig. 3 <sup>13</sup>C NMR spectrum of **19** in CDCl<sub>3</sub>.

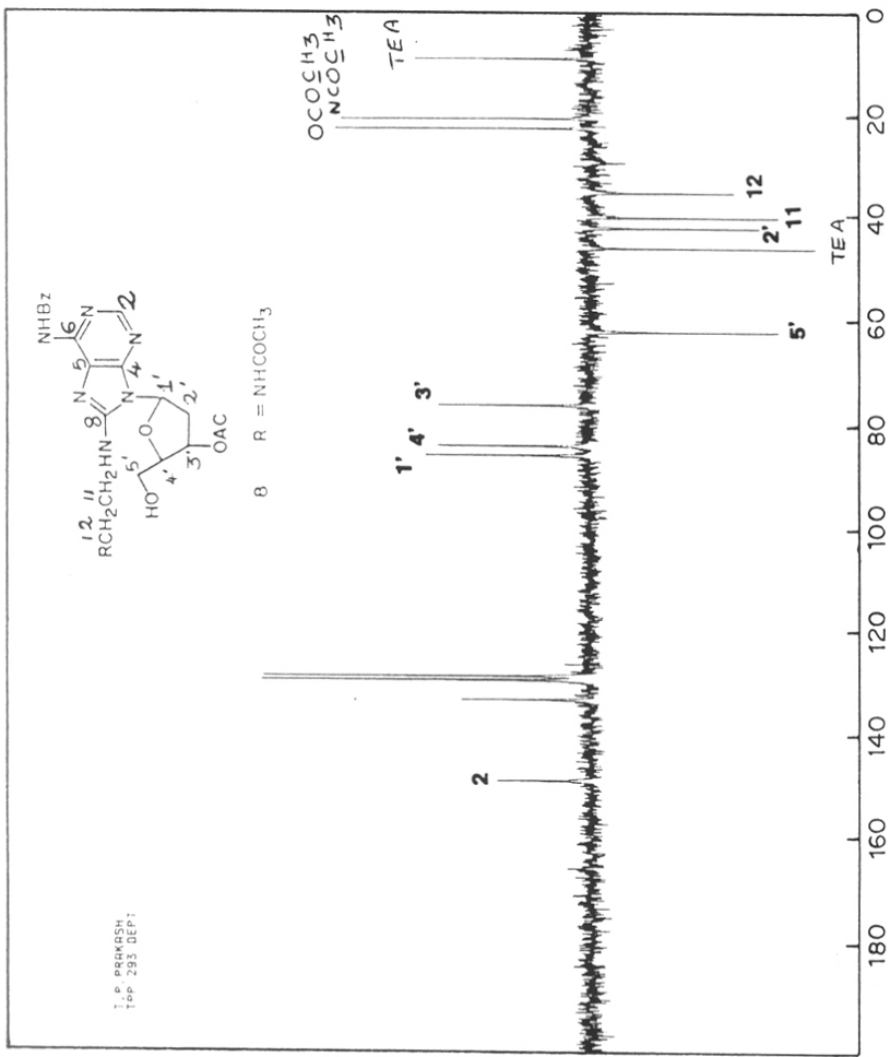
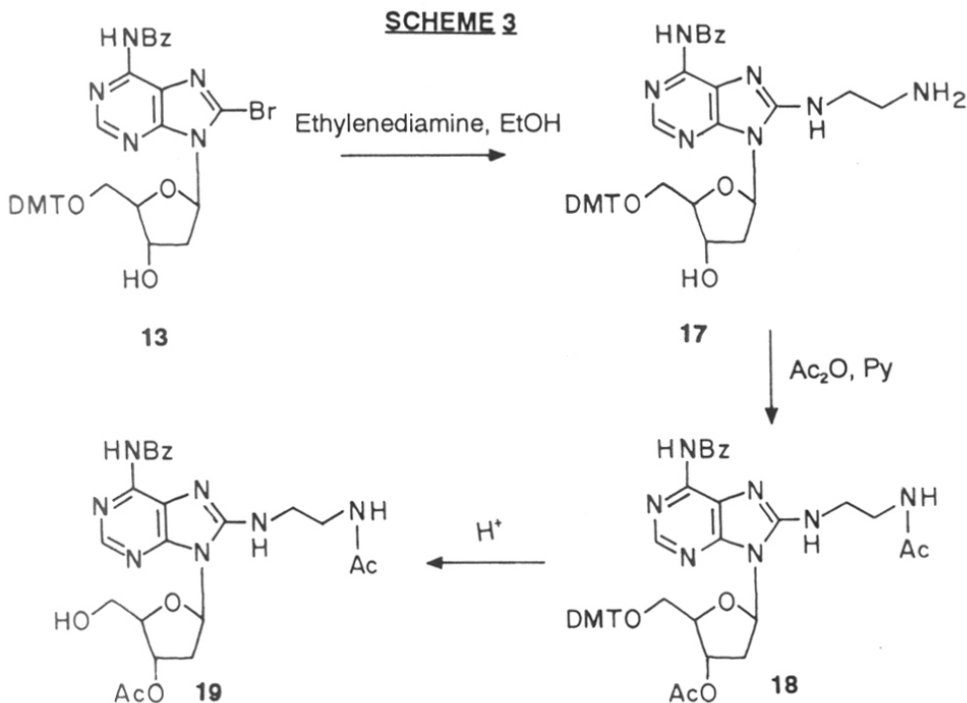


Fig. 4 INEPT spectrum of 19.

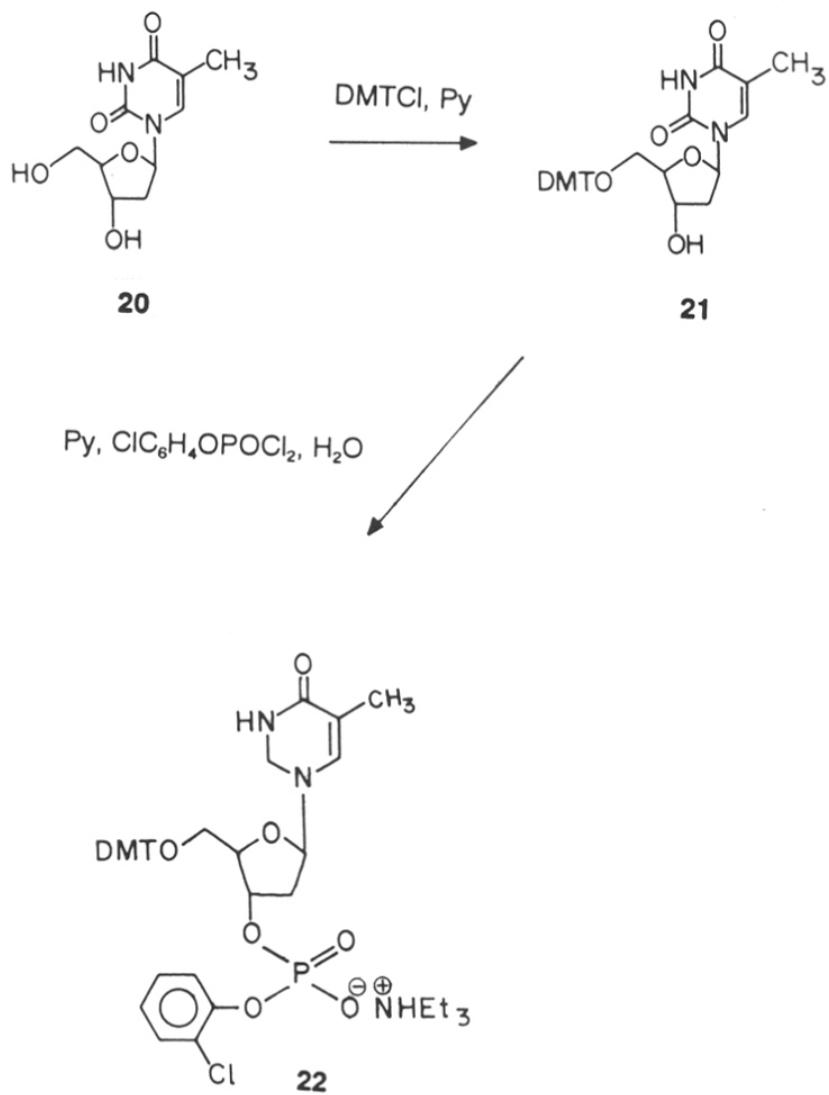


### 3.4.3 Synthesis of Thymidine monomer 22

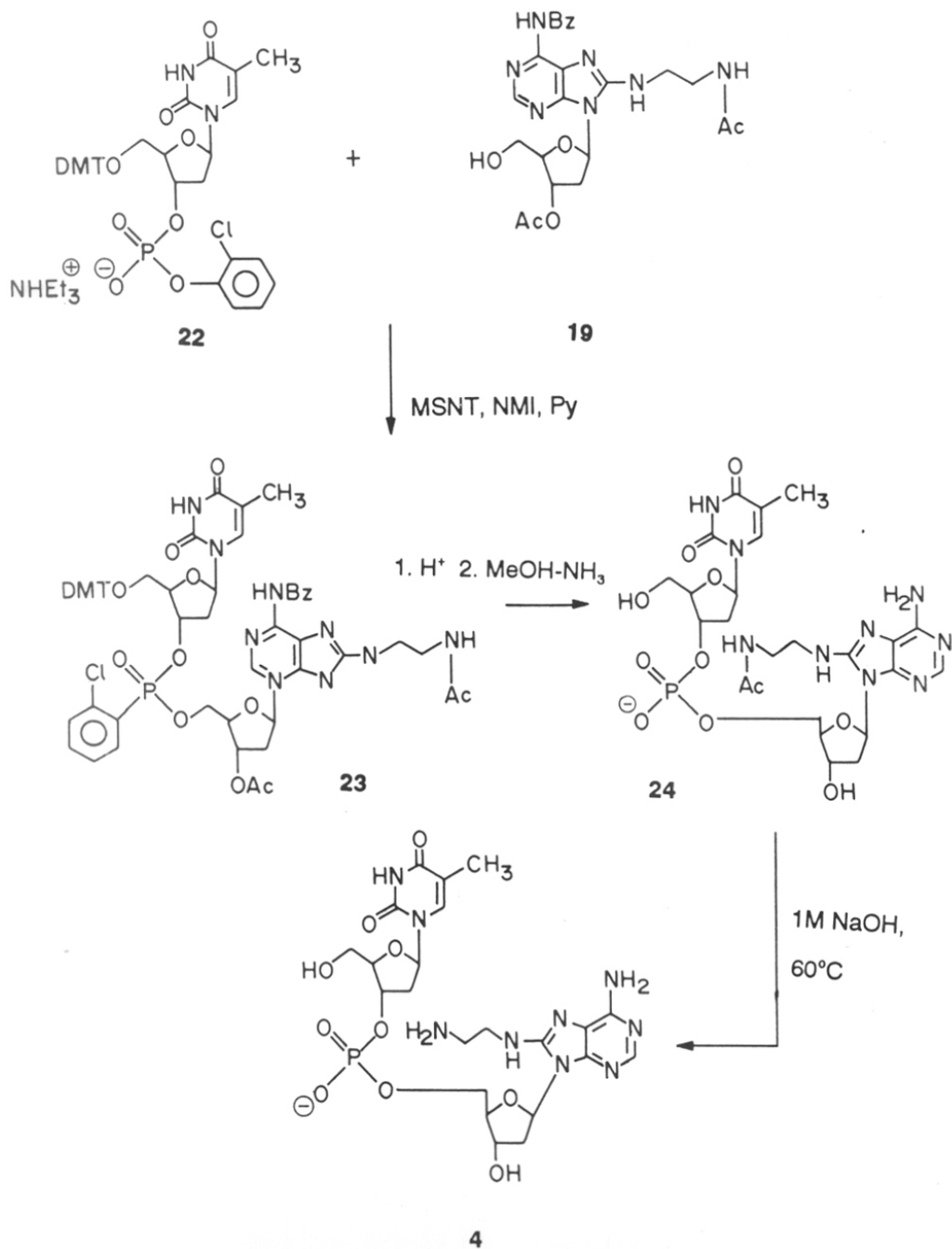
The triethylammonium [5'-O-DMT-thymidine-3'-O-(2-chlorophenyl)phosphate] **22** was synthesised according to the reported procedure.<sup>18</sup> 5'-Hydroxyl of the thymidine **20** (Scheme 4) was selectively protected by 4,4'-dimethoxytrityl group to obtain **21** which was treated with (2-chlorophenyl)dichlorophosphate to obtain **22**. This was then purified by column chromatography and characterized by <sup>1</sup>H and <sup>31</sup>P NMR (-5.77 ppm and -6.13 ppm).

### 3.4.4 Synthesis of 8-ethylenediamine and 8-histamine d(TpA) **4** and **5**

The triethylammonium [5'-O-DMT-thymidine-3'-O-(2-chlorophenyl)phosphate] **22** was condensed with **19** or **16** in presence of 2-mesitylenesulphonyl-3-nitrotriazole (MSNT) and N-methylimidazole (NMI) to generate the protected dinucleotides **23** (Scheme 5) and **25** (Scheme 6), respectively. No side products due to N-phosphonyla-

**SCHEME 4**

**SCHEME-5**



tion (as seen in  $^{31}\text{P}$  NMR spectrum) or 5'-sulphonylation were observed. The product dinucleotides were separated from the excess reactants on a short silica gel column using DCM containing MeOH as eluent. The dinucleotides **25** and **23** on sequential deprotection by treatment with 2% DCA-DCM to remove 5'-DMT group and MeOH- $\text{NH}_3$  to effect cleavage of the  $\text{N}^6$ -benzoyl, 3'-O-acetyl and 2-chlorophenyl groups, yielded the desired products **5** and **24**. These compounds were purified by ion-exchange column chromatography. The  $^1\text{H}$  NMR of **5** (Fig. 5) and **24** (Figure 6), clearly indicated that while the N-acetyl group of C8 side chain in **5** was completely removed during ammonolysis, the N-acetate of ethylenediamine chain in **24** remained intact (1.99 ppm,  $-\text{NCOCH}_3$ ). This N-acetyl group was fully hydrolyzed by treatment of **24** with aq. NaOH (1M) at  $60^\circ\text{C}$  to give **4**. Analysis of **4** by  $^1\text{H}$  and  $^{31}\text{P}$  NMR (Fig. 7) showed that the internucleotide phosphate link was unaffected under these reaction conditions. Control reaction with unmodified d(TpA) with aq. NaOH (1 M),  $60^\circ\text{C}$  and analysis confirmed the stability of phosphate linkage. These results are supported by a literature precedent<sup>19</sup> where the N-acetyl group of a dC analog could be deblocked only under the above conditions without affecting the internucleotide linkage. Figure 8 shows the HPLC purity of the dinucleotides **4** and **5**. Dinucleotides **4** and **5** were well characterized by  $^1\text{H}$  (1D and 2D) and  $^{31}\text{P}$  NMR (Fig. 9, 10, 11, 12) spectroscopy.

#### 3.4.5 Synthesis of dinucleotide 6

The model dinucleotide **6** carrying double conjugation (C5' of T and C8 of A) was synthesized by an analogous route involving coupling of **31** and **36**. In **36** TFA group was preferred to acetate since alkylamino acetates are resistant to ammonolysis and use of aq. NaOH is undesirable in ribonucleotide synthesis. The trifluoroacetyl as a N-protector is known to be compatible with oligonucleotide synthesis conditions.<sup>20</sup>

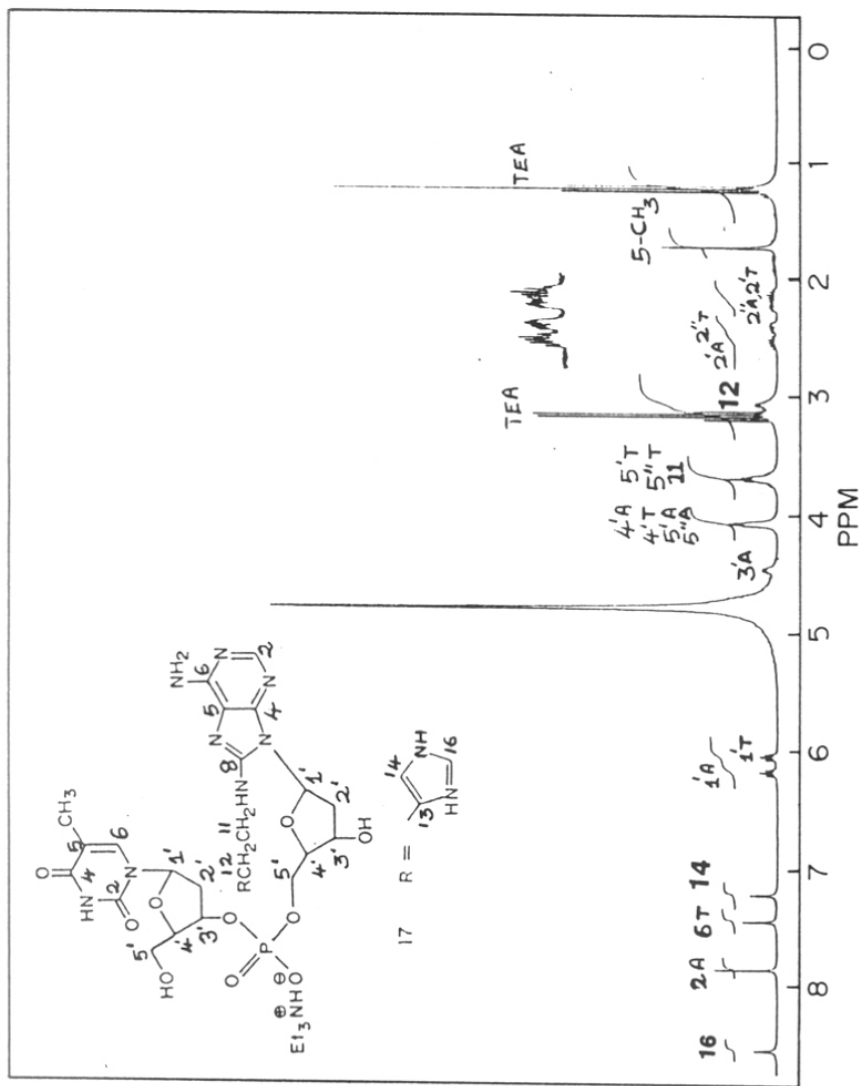
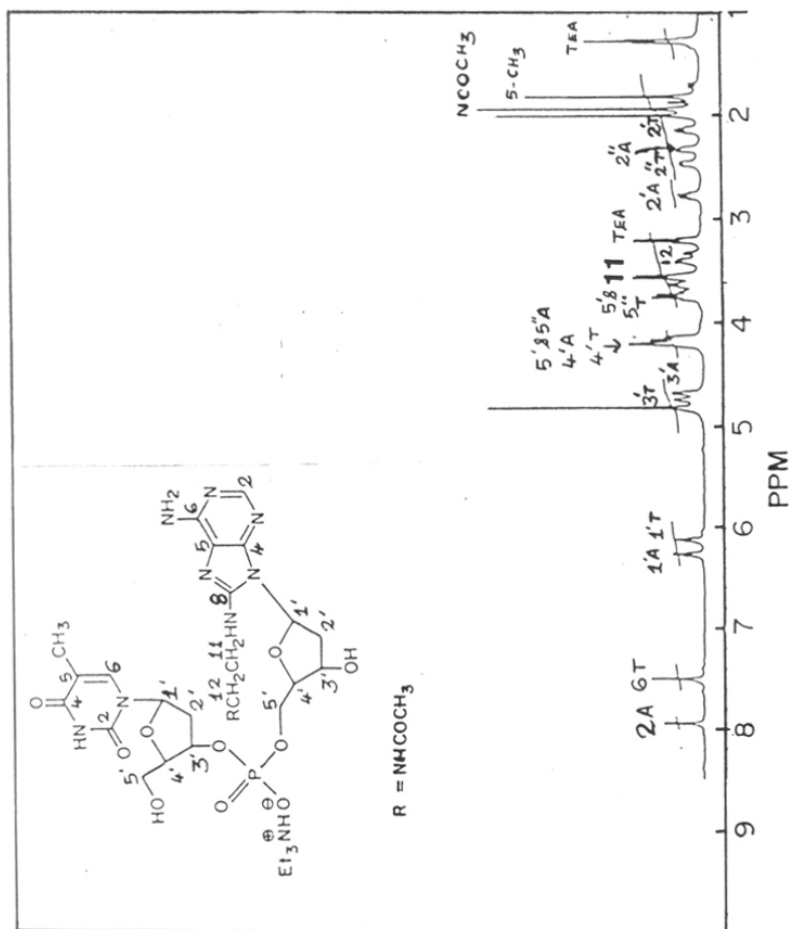
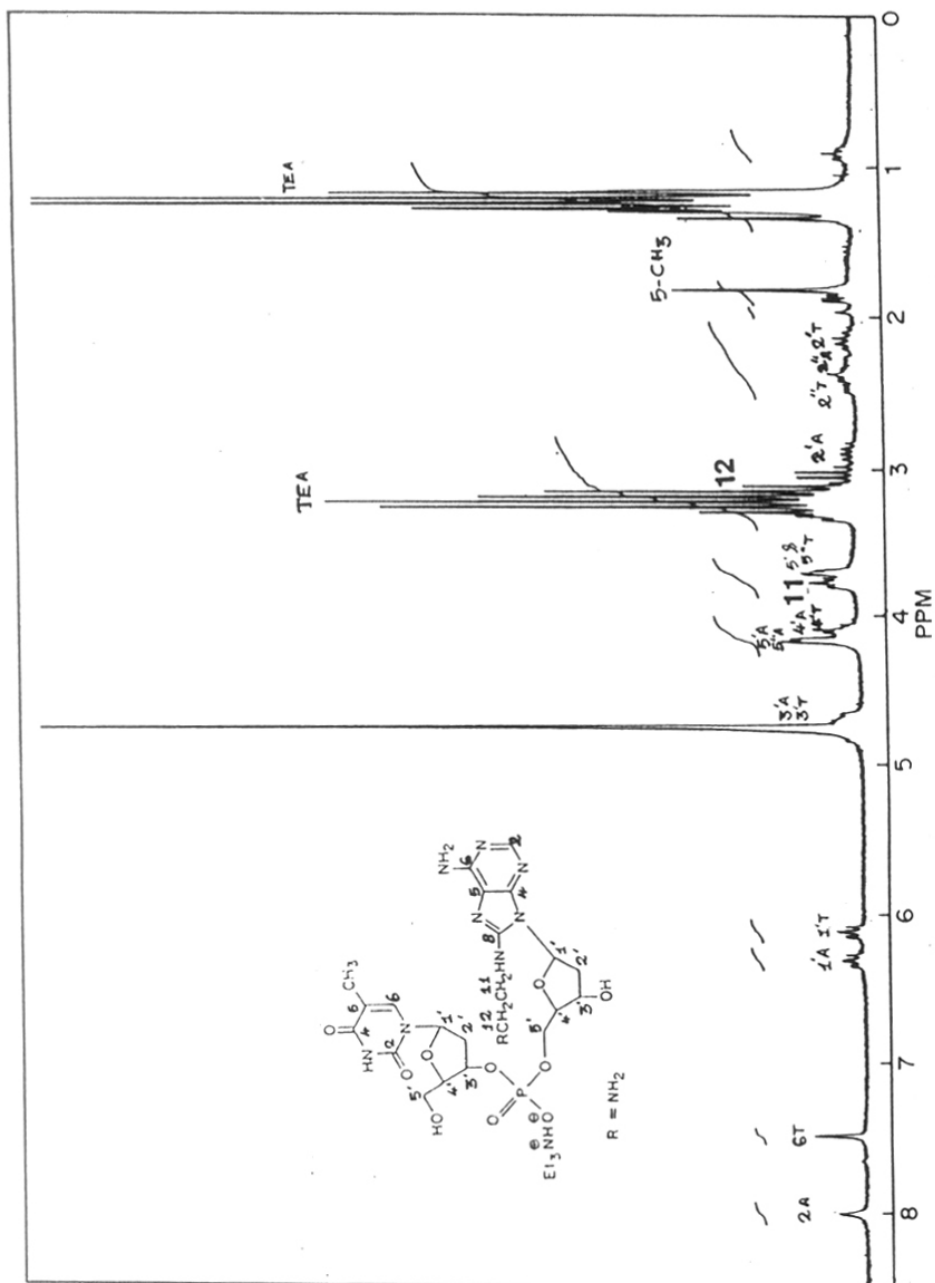


Fig. 5 300 MHz <sup>1</sup>H NMR spectrum of compound 5 in D<sub>2</sub>O.



Fig. 6 500 MHz spectrum of **24** in  $\text{D}_2\text{O}$ .

Fig. 7 200 MHz spectrum of 4 in D<sub>2</sub>O.

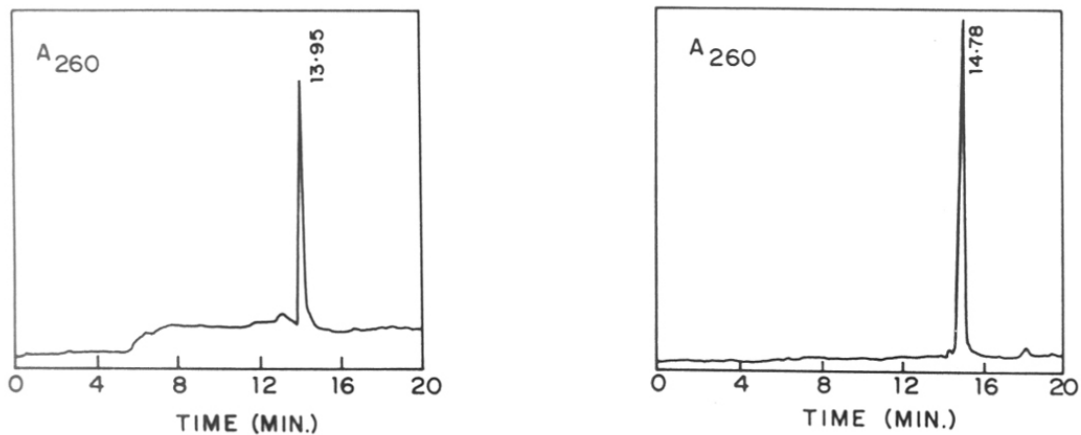


Fig. 8 Reverse phase HPLC of (a) **4**, (b) **5**.

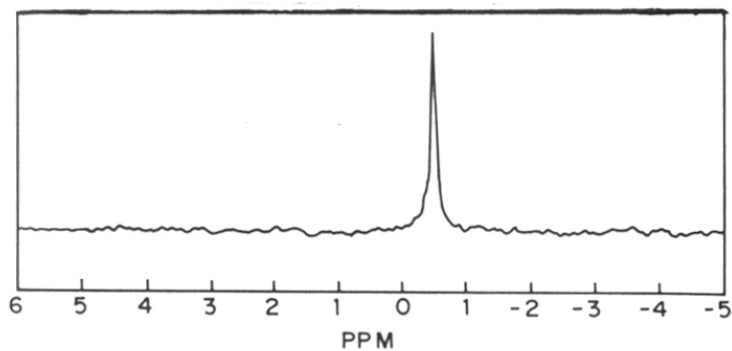


Fig. 9 <sup>31</sup>P NMR spectrum of **5** in D<sub>2</sub>O.

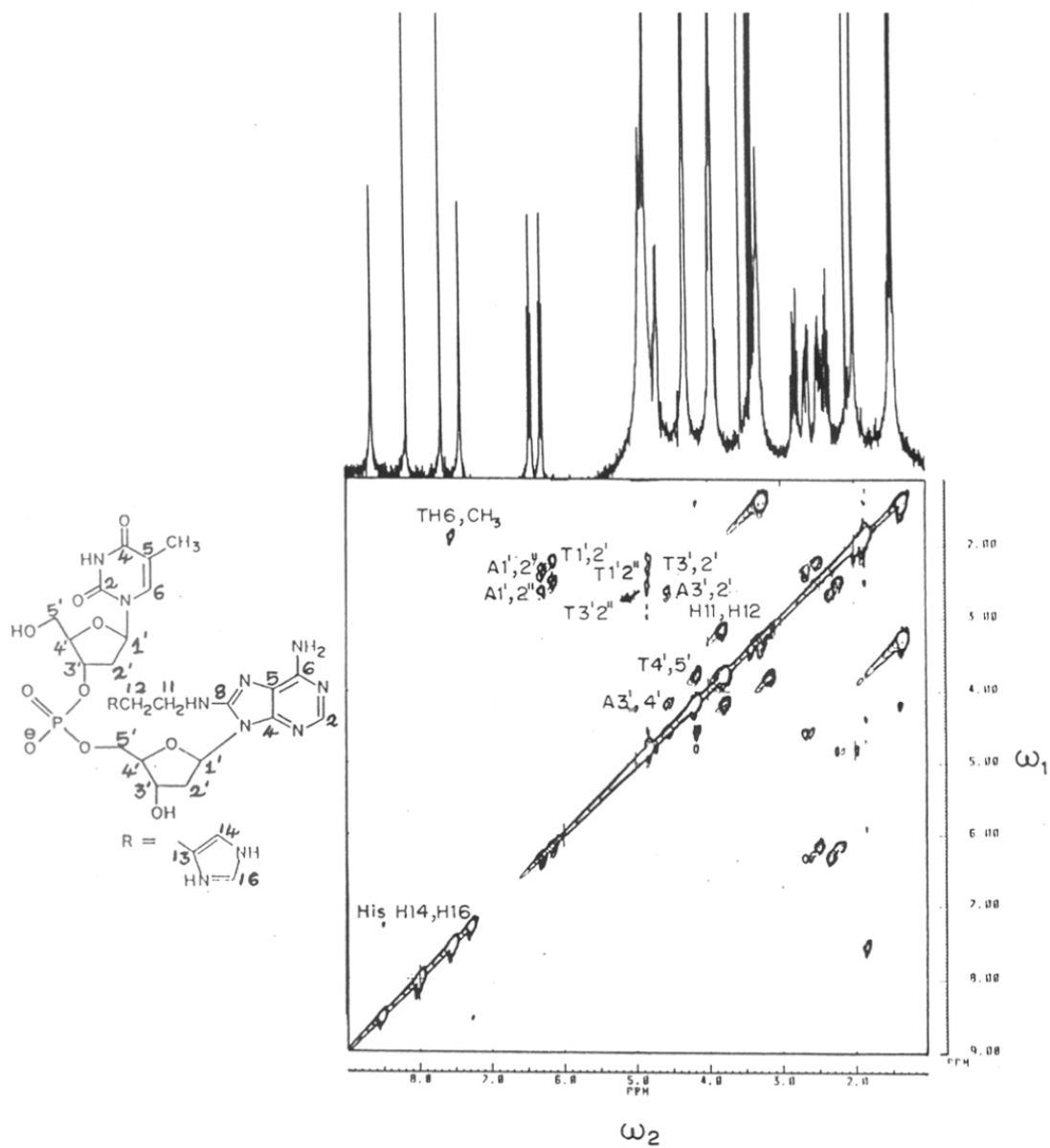


Fig. 10 2 D COSY spectrum of **5** in  $D_2O$ .

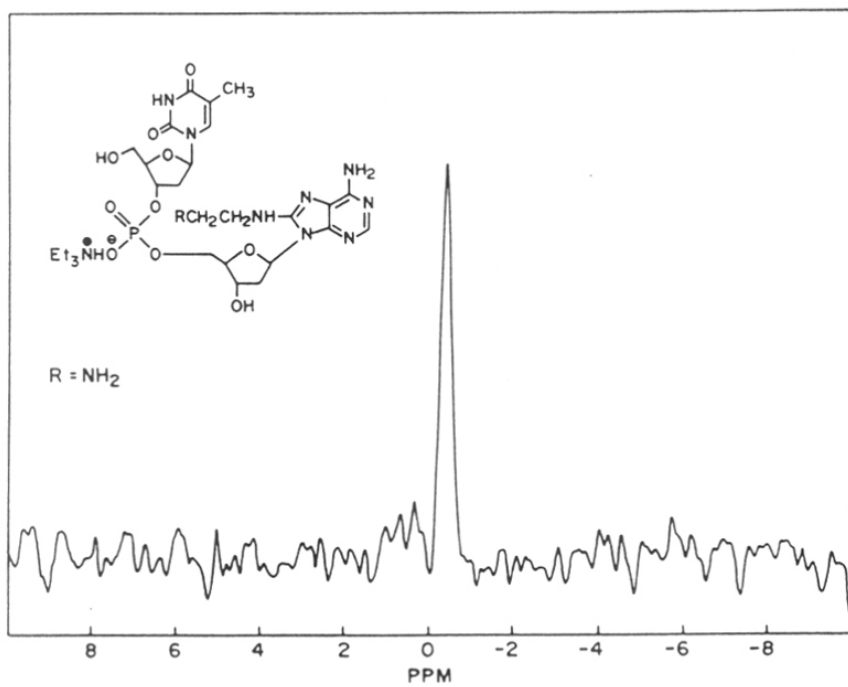


Fig. 11  $^{31}\text{P}$  NMR spectrum of 4 in  $\text{D}_2\text{O}$ .

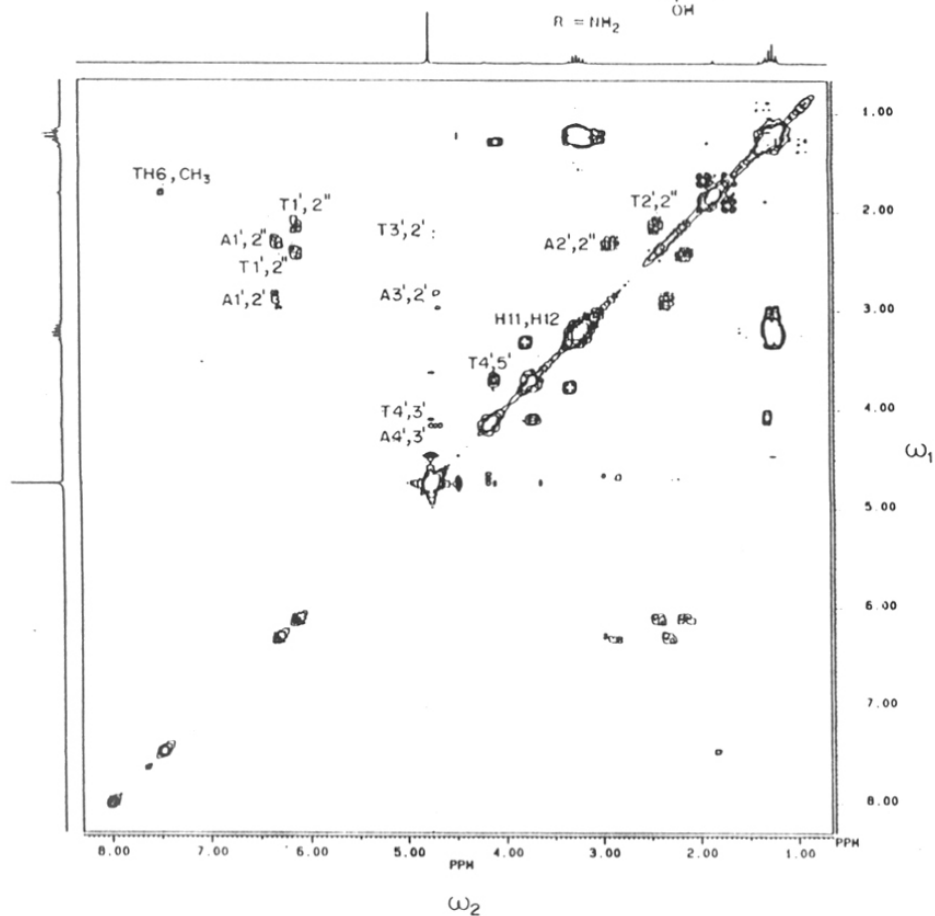
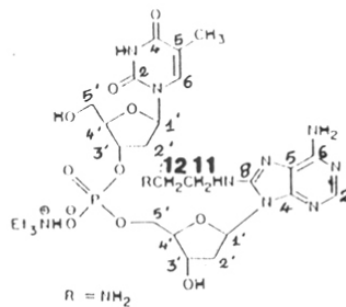
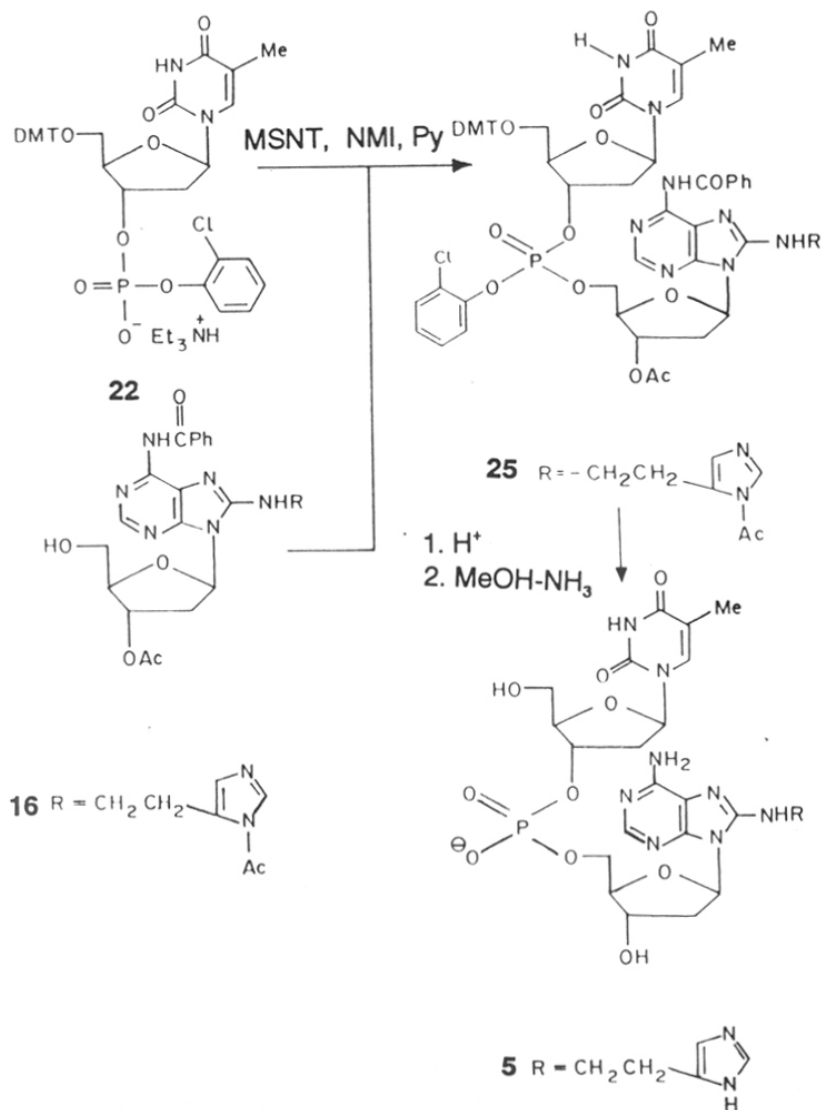


Fig. 12 2D COSY spectrum of 4 in D<sub>2</sub>O.

## SCHEME 6

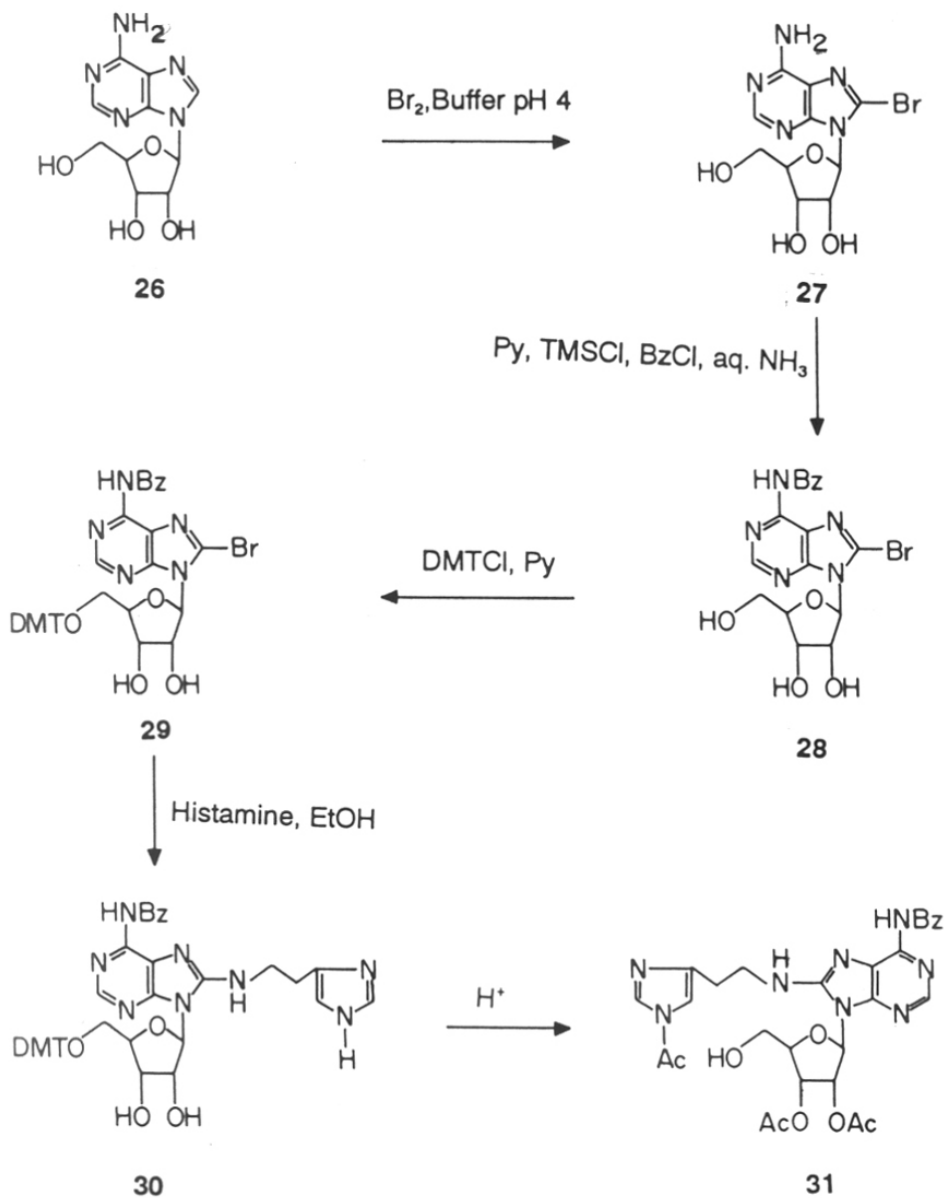


Although it is labile when present on the exocyclic amino function, it was found to have reasonable stability for protection of a side chain amino group.

The 5'-OH ribo component **31** required for synthesis of **6** was prepared starting from adenosine **26** (**Scheme 7**). It was first converted into its 8-bromo derivative **27** by treatment with bromine-water. This was followed by protection of exocyclic amino function by benzoyl group<sup>17</sup> (transient protection) to get **28**. 5'-Hydroxyl group of **28** was then selectively protected with 4,4'-dimethoxytrityl group to get **29**. This compound was then treated with excess of histamine to afford 8-histamino-rA **30**. The secondary 3'-hydroxyl and N-H of the imidazole in **30** were acetylated followed by treatment with mild acid to deprotect the 5'-O-DMT group to obtain **31** and was characterized by spectroscopic methods (**Fig. 13 and 14**).

The 3'-phosphate component **36** was synthesized from thymidine **32** (**Scheme 8**). Selective tosylation of 5'-hydroxyl group with pyridine and p-TsCl at 0°C give **33** which was transformed into 5'-deoxy-5'-(2-aminoethyl)amino derivative **34** (**Fig. 15, 16 and 17**) by treatment with 1,2-diaminoethane. This was converted into the corresponding N,N'-bistrifluoroacetyl derivative **35** with trifluoroacetic anhydride in presence of trimethylsilylchloride and pyridine. During this reaction, the 3'-OH remained unaltered and it was conveniently converted into the desired 3'-phosphodiester **36** by standard procedure.<sup>18</sup> The TFA group was stable to the phosphorylating conditions and no N-phosphorylation was noticed during this step (**Fig. 18**). The phosphodiester **36** was condensed with 5'-hydroxyl component **31** (**Scheme 9**) in presence of MSNT and NMI to obtain the dinucleotide **37** in 60% yield. This was then deprotected by aq. NH<sub>3</sub> to yield the target dinucleotide **6**. This was purified by ion-exchange chromatography over Sephadex DEAE A25 anion exchange resin and characterized by spectroscopic methods (**Fig. 19, 20, 21, 22**).



**SCHEME 7**

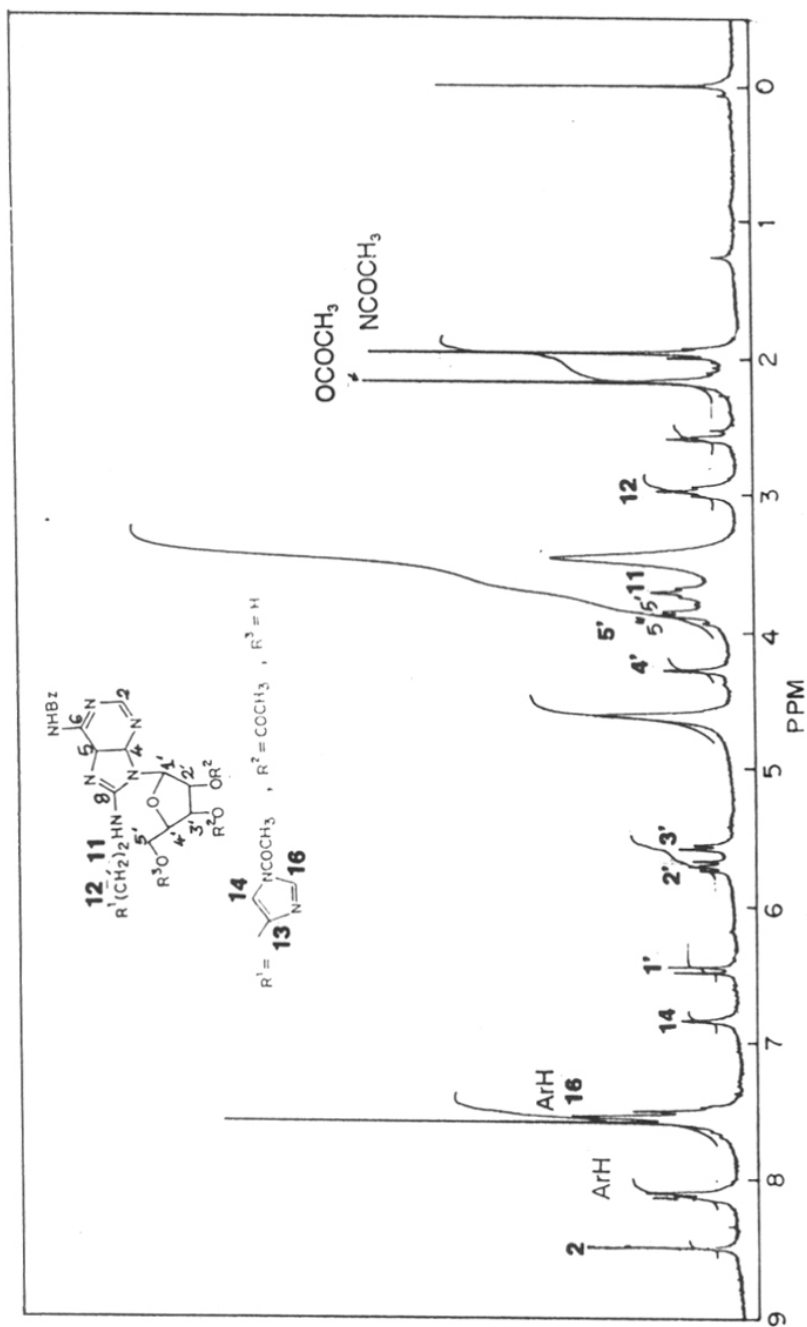


**Fig. 13** 200 MHz  $^1\text{H}$  NMR spectrum of **31** in  $\text{CDCl}_3 + \text{DMSO-d}_6$  (5:3)

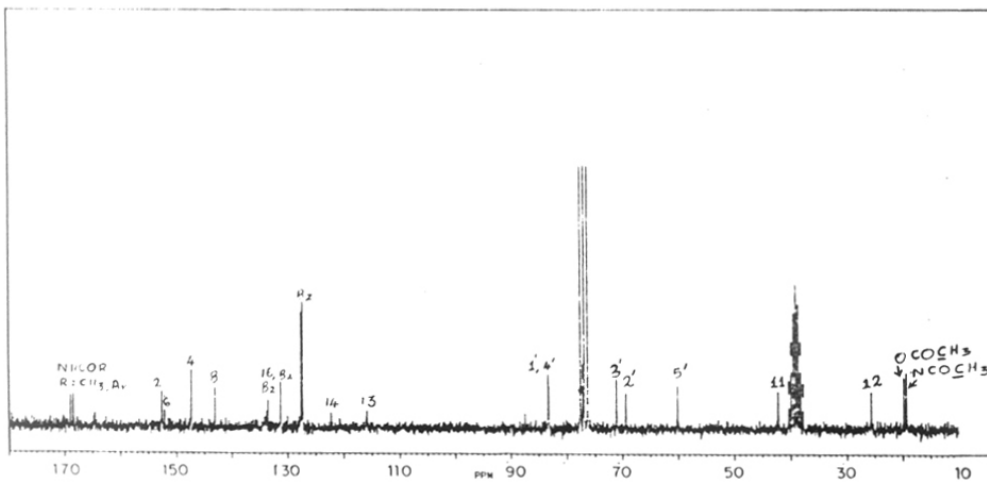


Fig. 14a  $^{13}\text{C}$  NMR spectrum of **31** in  $\text{CDCl}_3 + \text{DMSO-d}_6$  (5:3).

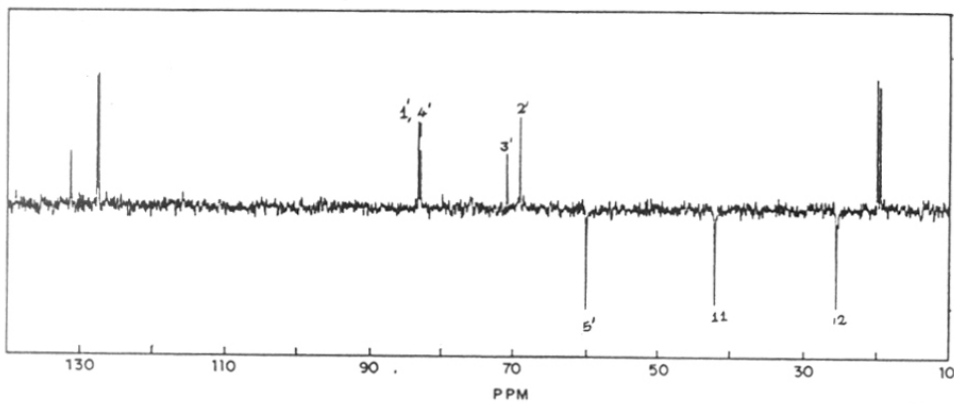
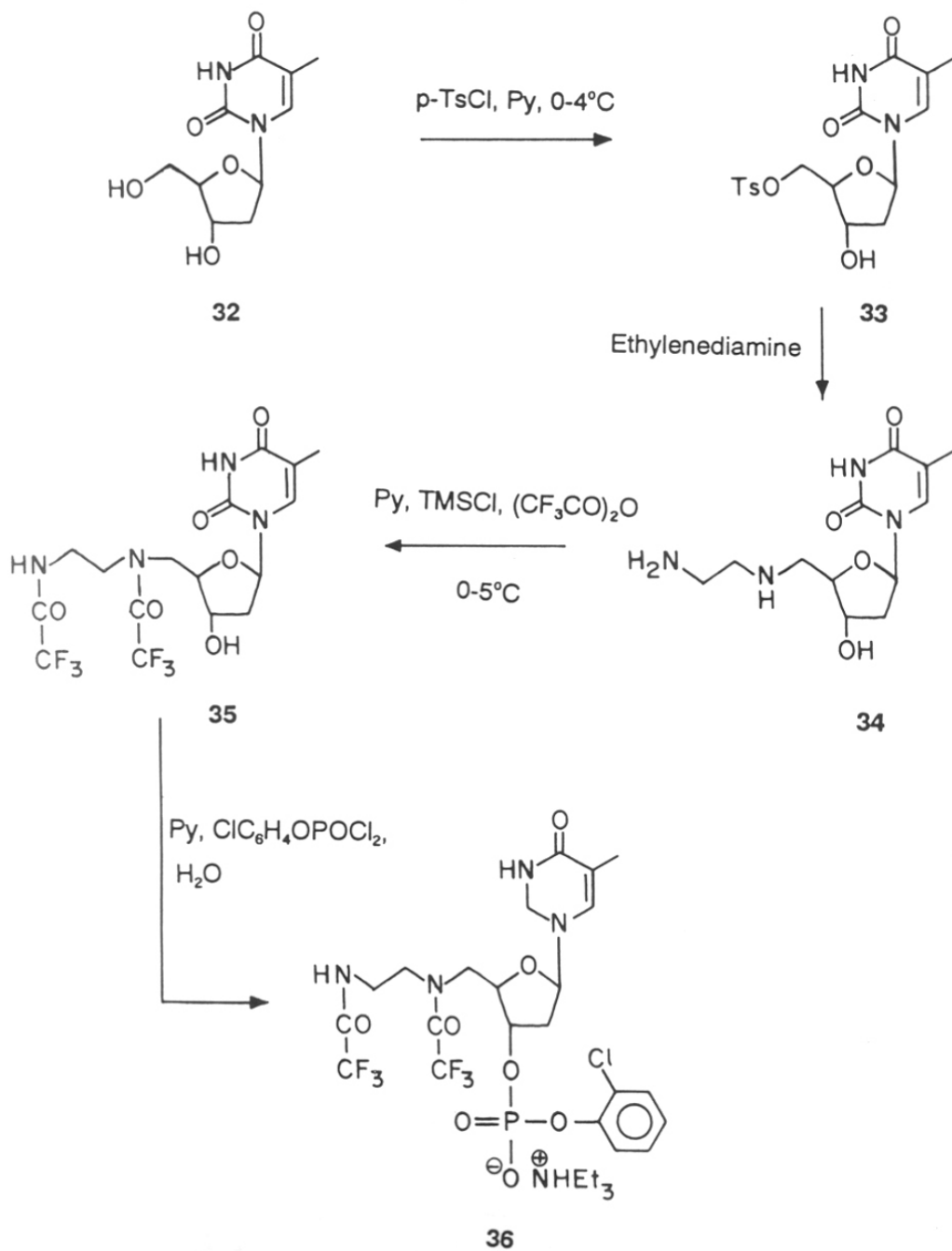
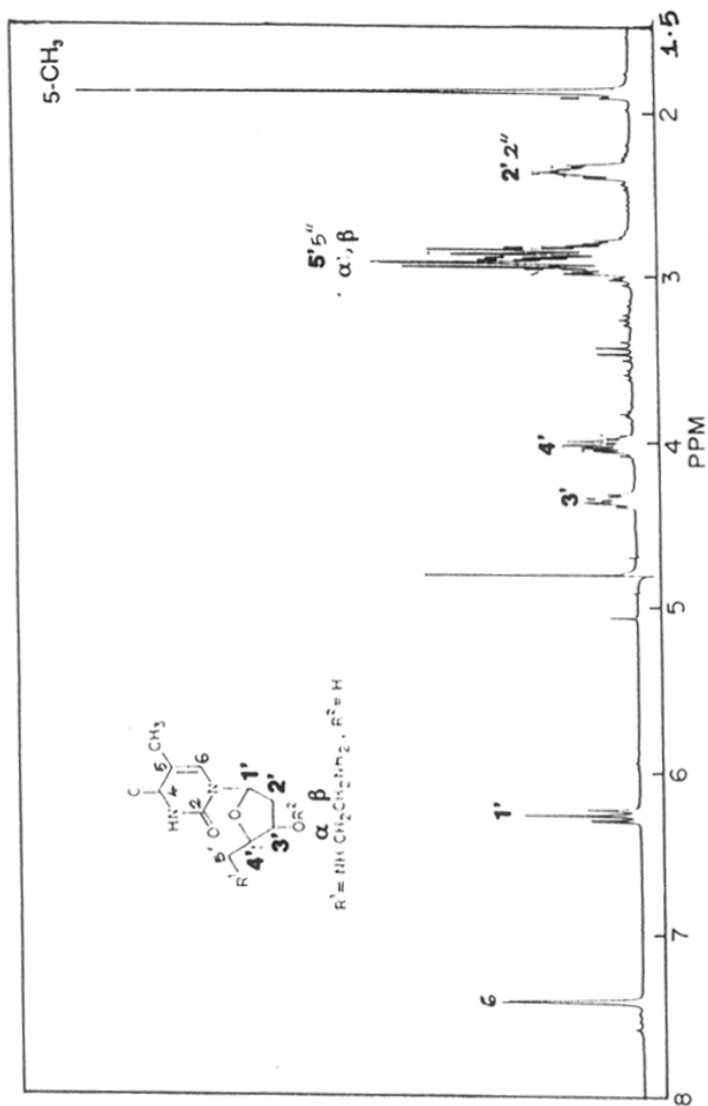


Fig. 14:b INEPT spectrum of **31** in  $\text{CDCl}_3 + \text{DMSO-d}_6$  (5:3).

## SCHEME 8





**Fig. 15** 200 MHz  $^1H$  NMR spectrum of **34** in  $D_2O$

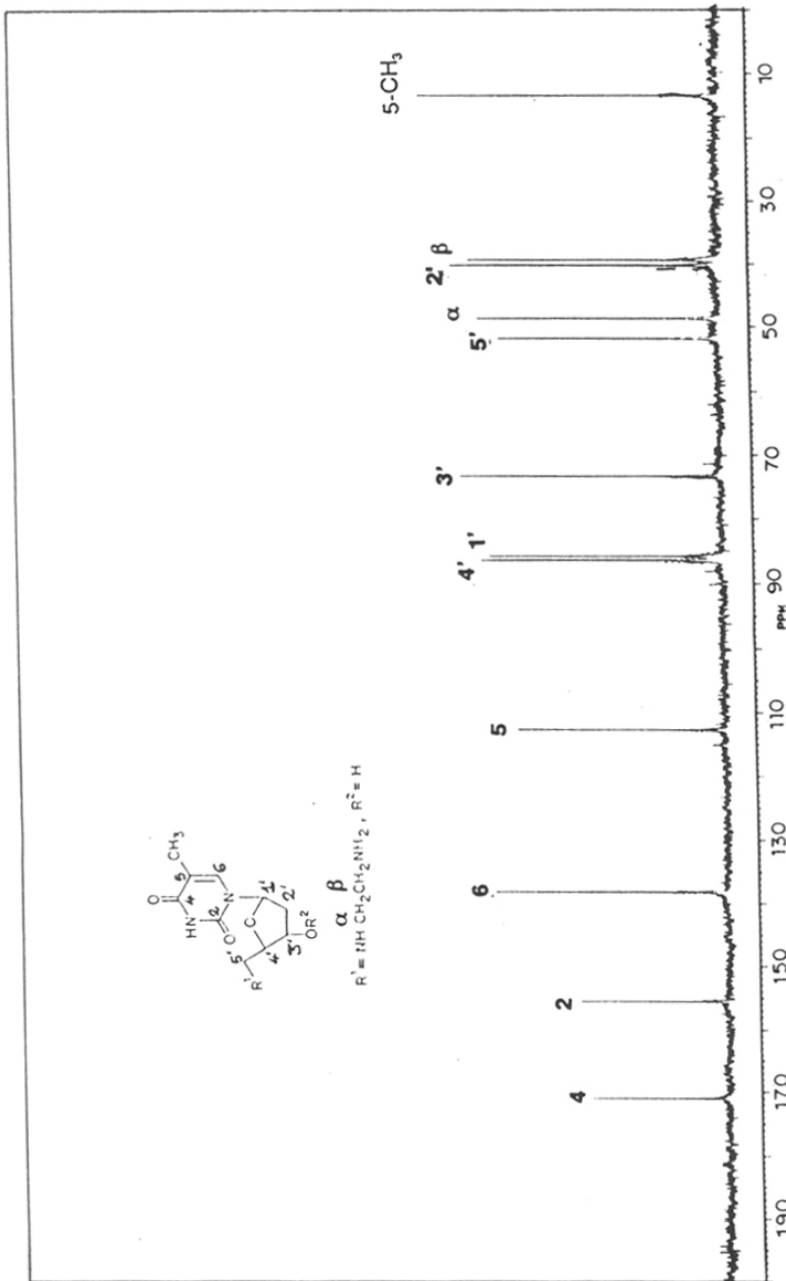
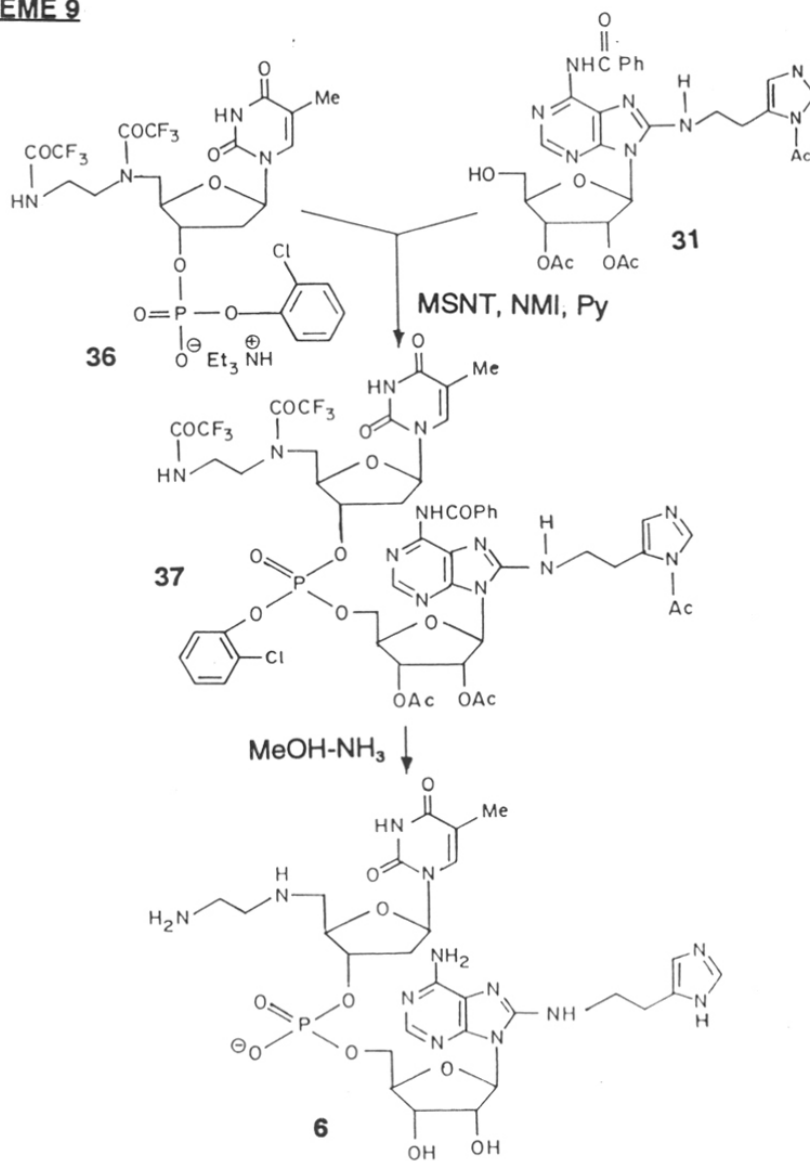


Fig. 16  $^{13}C$  NMR spectrum of 34 in  $D_2O$ .



**SCHEME 9**



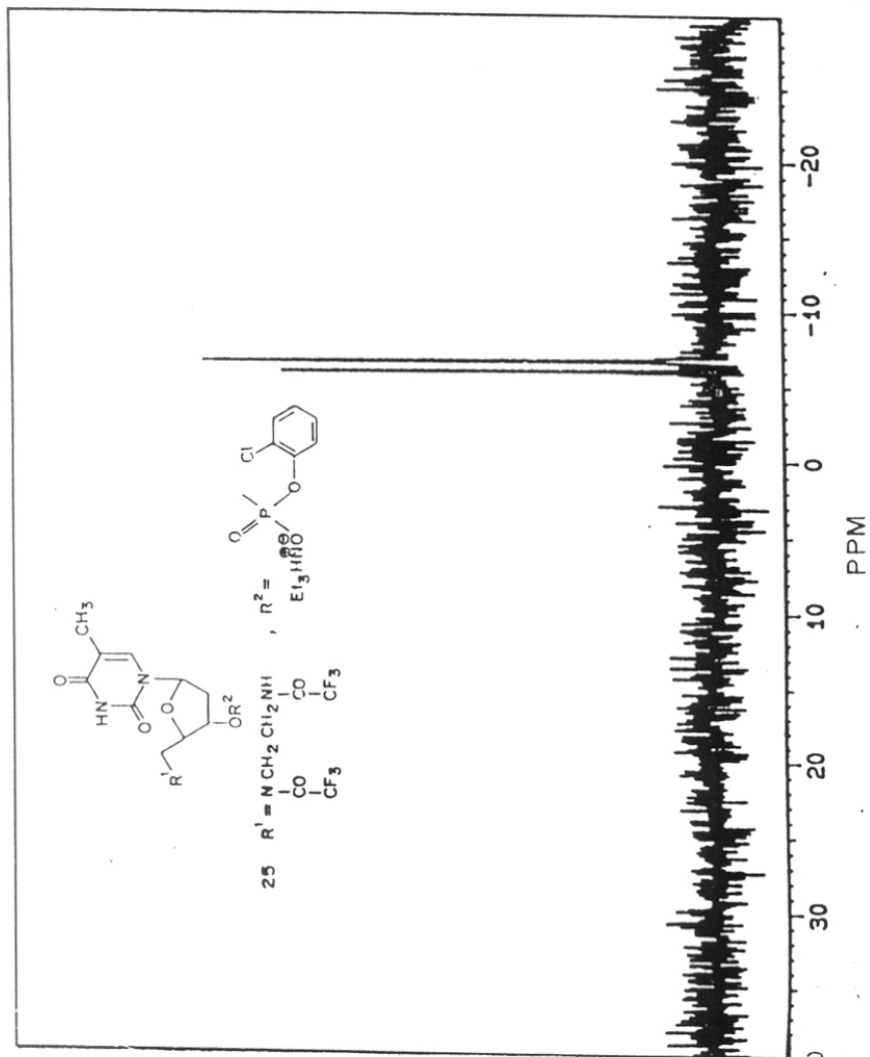


Fig. 18  $^3\text{P}$  NMR spectrum (81 MHz) of compound **36** in  $\text{CDCl}_3$ .

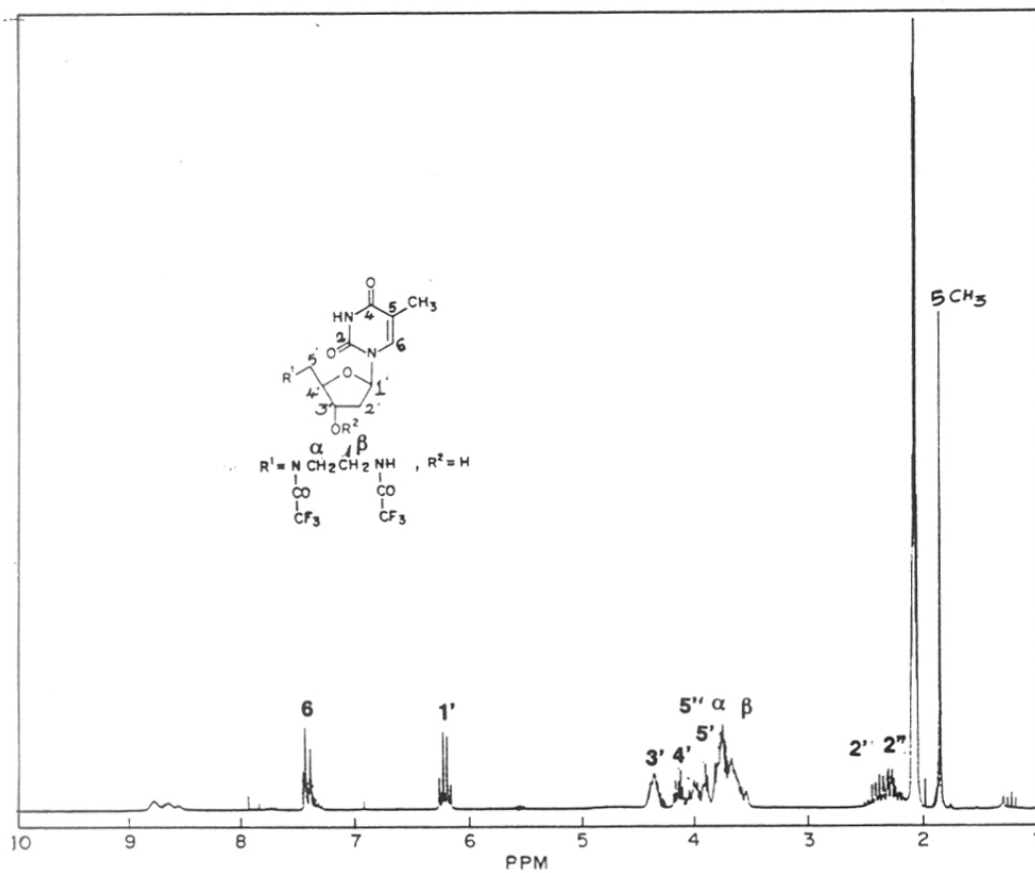


Fig. 19 200 MHz <sup>1</sup>H NMR spectrum of 35 in (CD<sub>3</sub>COCD<sub>3</sub>).

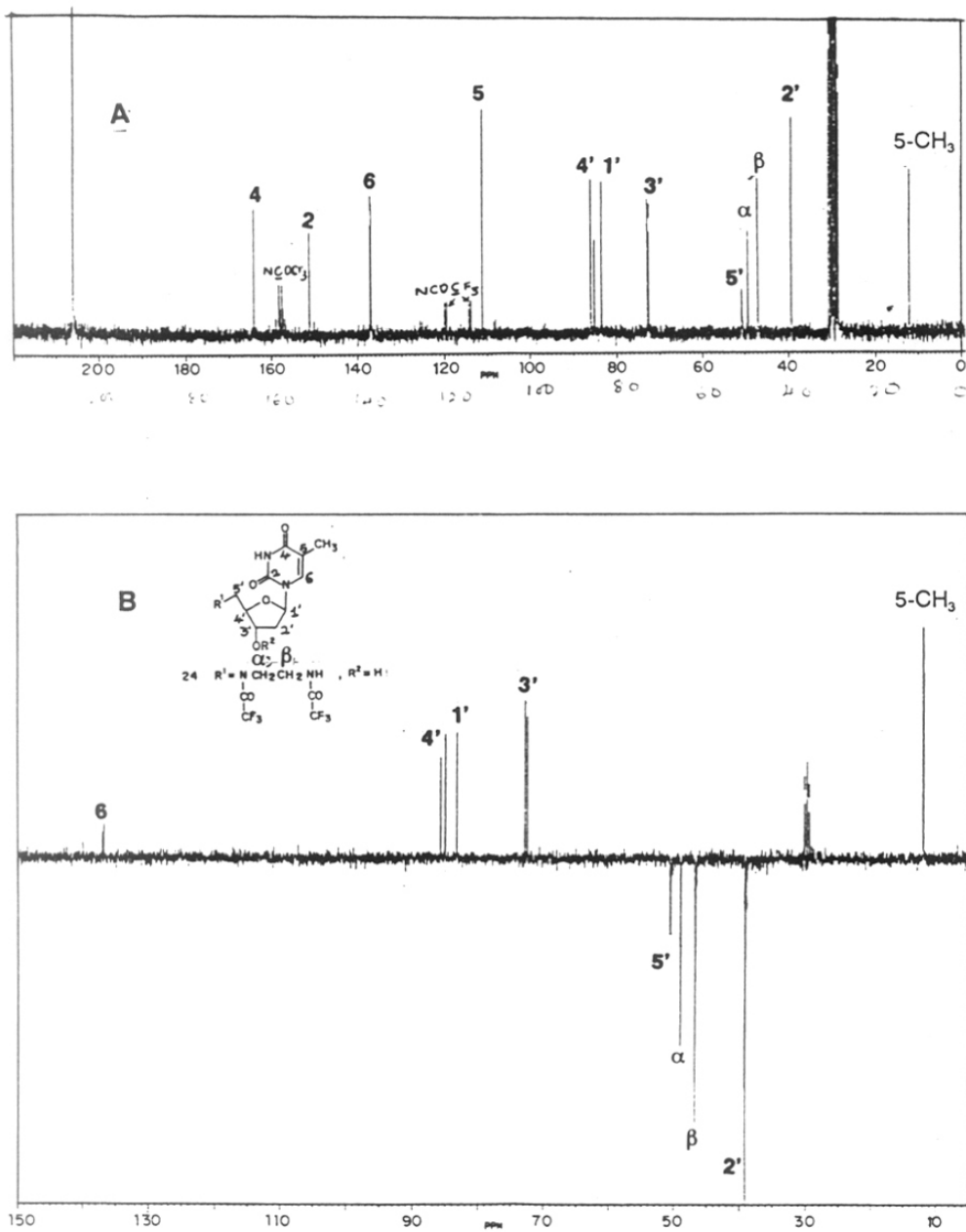


Fig. 20 A  $^{13}C$  NMR spectrum of **35** in  $(CD_3COCD_3)$ .

B INEPT spectrum of **35** in  $(CD_3COCD_3)$ .

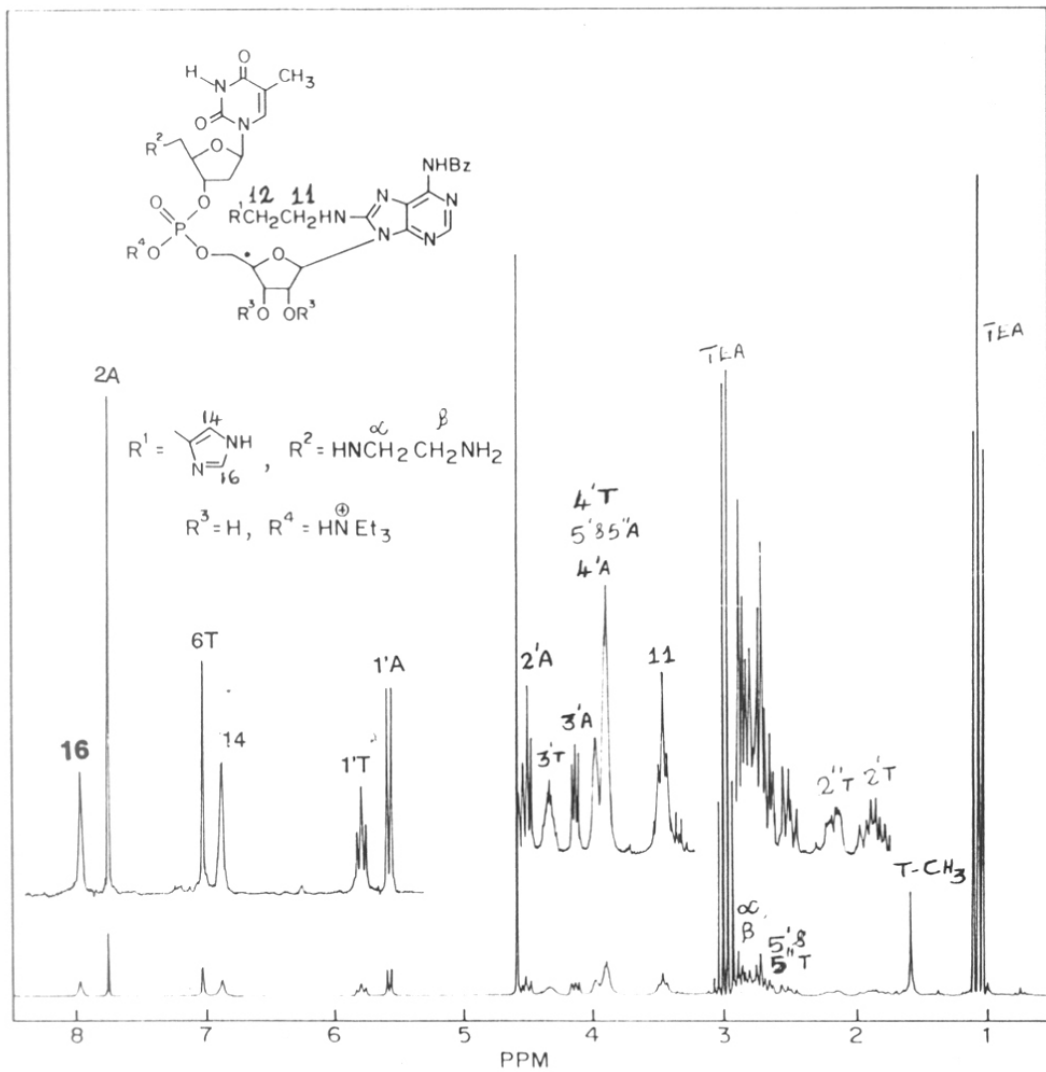


Fig. 21 A 200 MHz spectrum of compound **6** in  $\text{D}_2\text{O}$ .

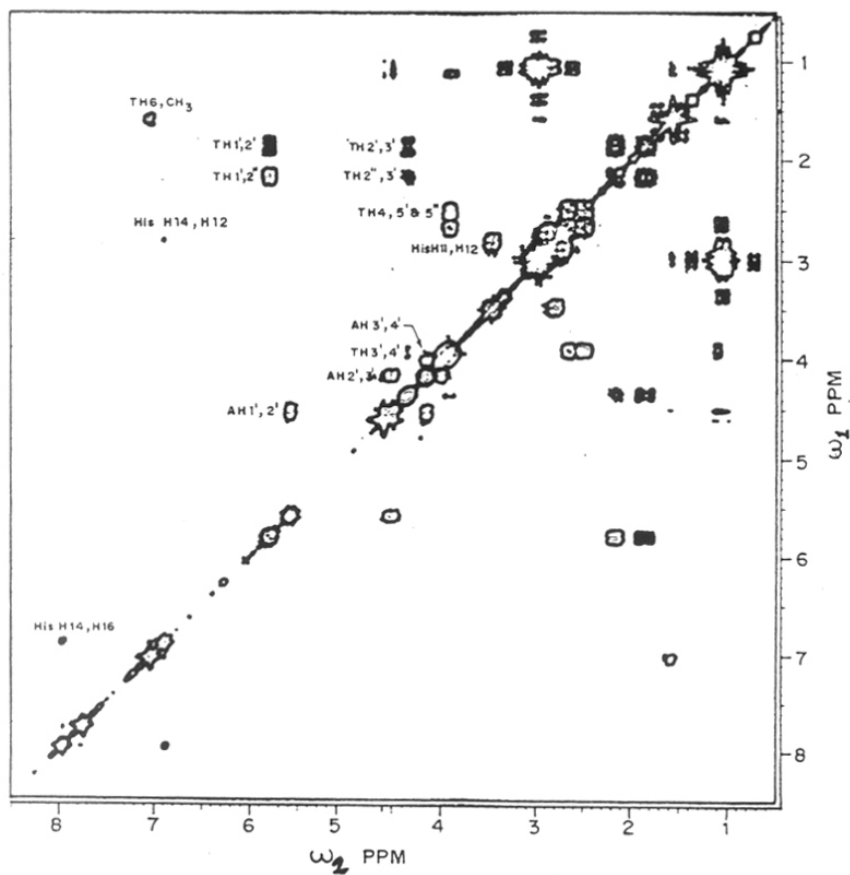


Fig. 21 B 2D COSY spectrum of 6.

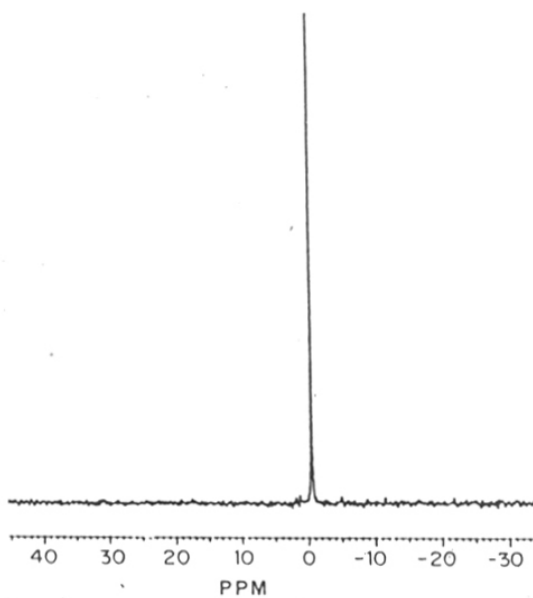


Fig. 22 A  $^{31}\text{P}$  NMR spectrum (81 MHz) of compound 6.

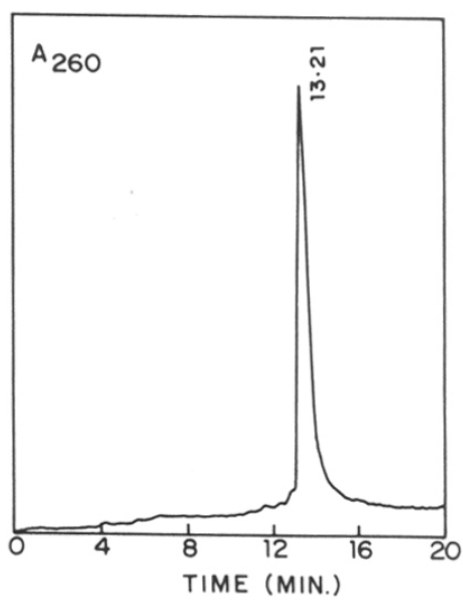


Fig. 22 B Reverse phase HPLC of 6 For conditions see experimental.

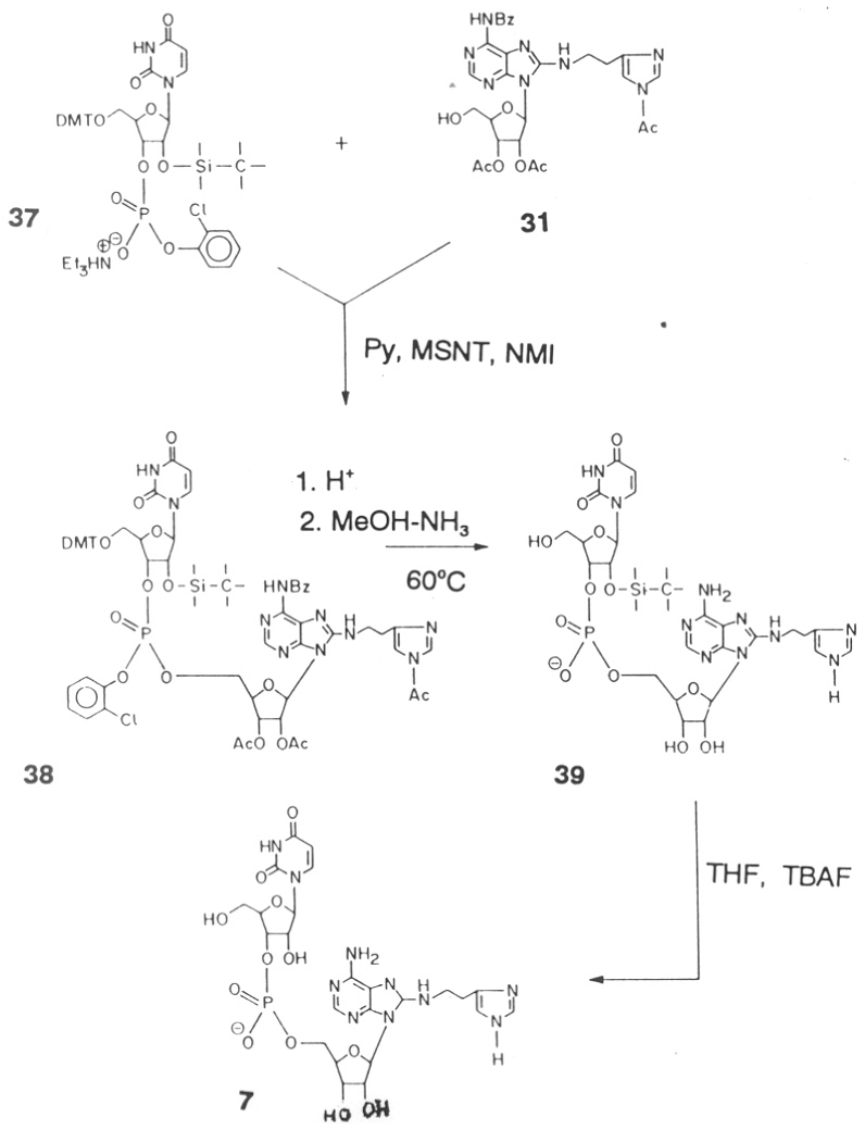
### 3.4.6 Synthesis of ribodinucleotide **7**

The model ribodinucleotide **7** was synthesised by condensation of the 5'-OH compound **31** with the ribo 3'-phosphodiester **37** (**Scheme 10**) possessing TBDMS as a 2'-OH protector. The compound **37** was synthesised according to the procedure reported in the literature by V. Gopalakrishnan et al.<sup>21</sup> The condensation product **38** was first 5'-deprotected by reaction with 2% DCA-DCM, followed by treatment with sat. MeOH-NH<sub>3</sub> to effect removal of phosphate and amino protecting groups gave **39**. Final reaction with tetrabutylammoniumfluoride (TBAF), resulted in the cleavage of 2'-O-silyl group without affecting the internucleotide linkage. The completely deprotected ribodinucleotide **7** was purified by ion-exchange chromatography and characterized by spectroscopy (**Fig. 23, 24, 25, 26**).

### 3.4.7 Synthesis of dinucleotide d(TpA) **8**

The unmodified dinucleotide d(TpA) was synthesised by solution phase phosphotriester chemistry according to **Scheme 11**. The N<sup>6</sup>-benzoyl-3'-O-Ac-5'-OH-2'-deoxyadenosine **42** was synthesised starting from 2'-deoxyadenosine **10** in four steps (**Scheme 12**). Exocyclic amino group was selectively protected by transient protection method and later the 5'-hydroxyl with DMT to obtain **41**. This was 3'-acetylated followed by delblocking of 5'-O-DMT group to obtain required 2'-deoxy adenosine derivative **42**.

**42** was condensed with 3'-phosphodiester **22** (**Scheme 11**) using MsCl and NMI to obtain the dinucleotide **43**. This was 5'-deprotected with 2 % DCA in DCM followed by treatment with MeOH-NH<sub>3</sub> to obtain the target dinucleotide **8**.

**SCHEME 10**



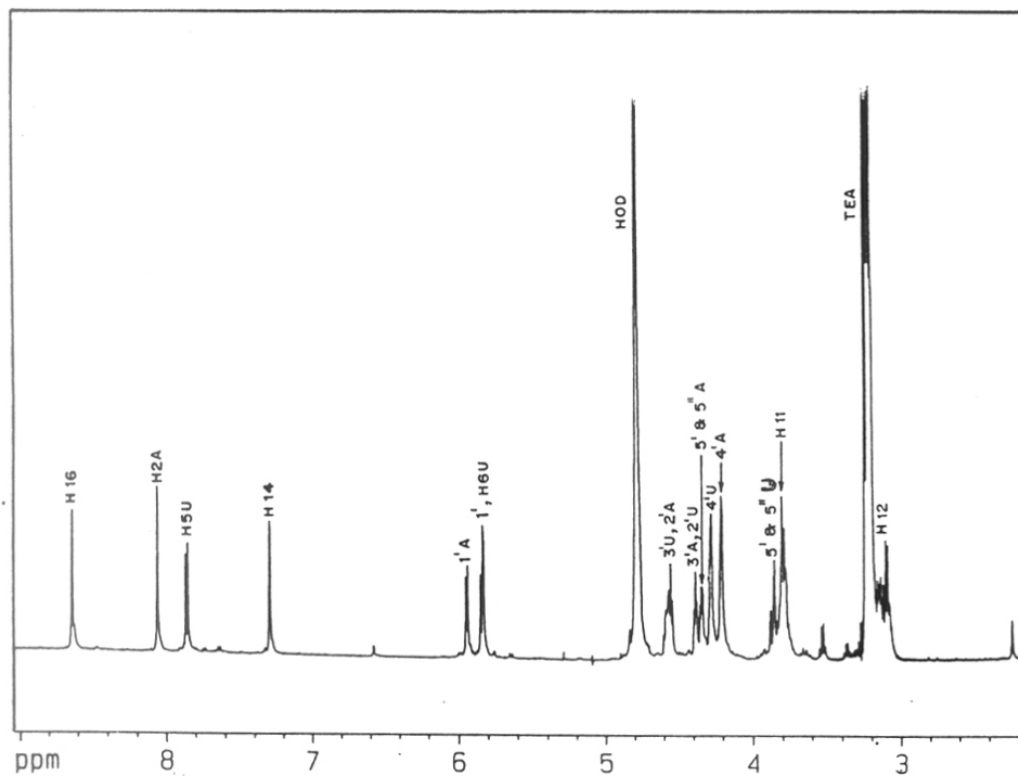


Fig. 23 500 MHz spectrum 7 in D<sub>2</sub>O.

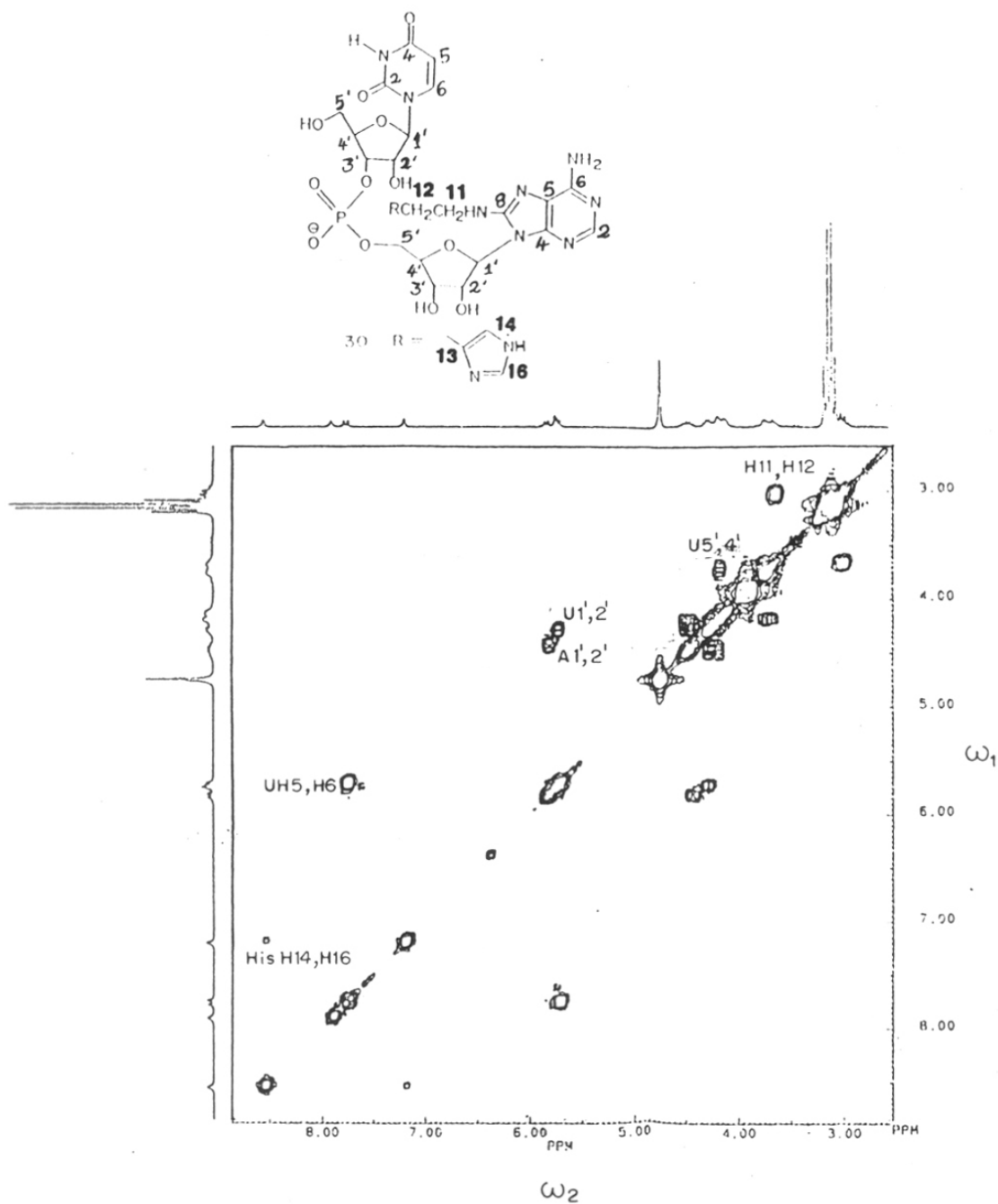


Fig. 24 2D COSY spectrum of 7 in D<sub>2</sub>O.

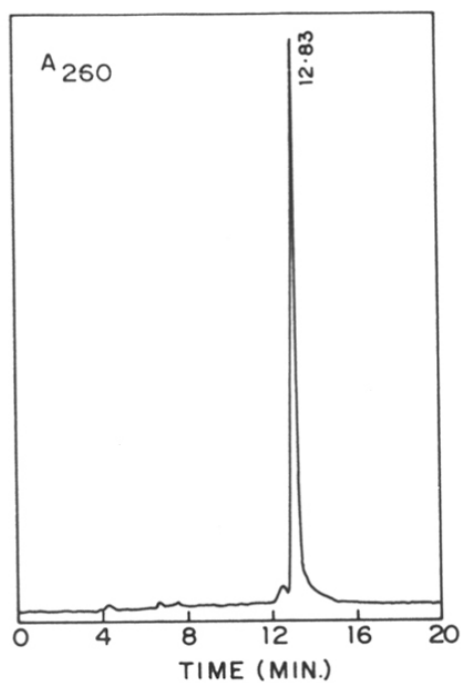


Fig. 25 Reverse phase HPLC of 7 For conditions see experimental.

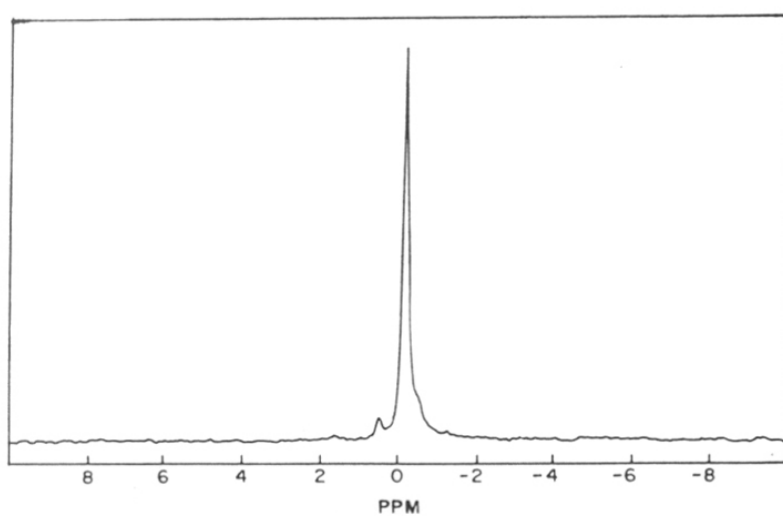
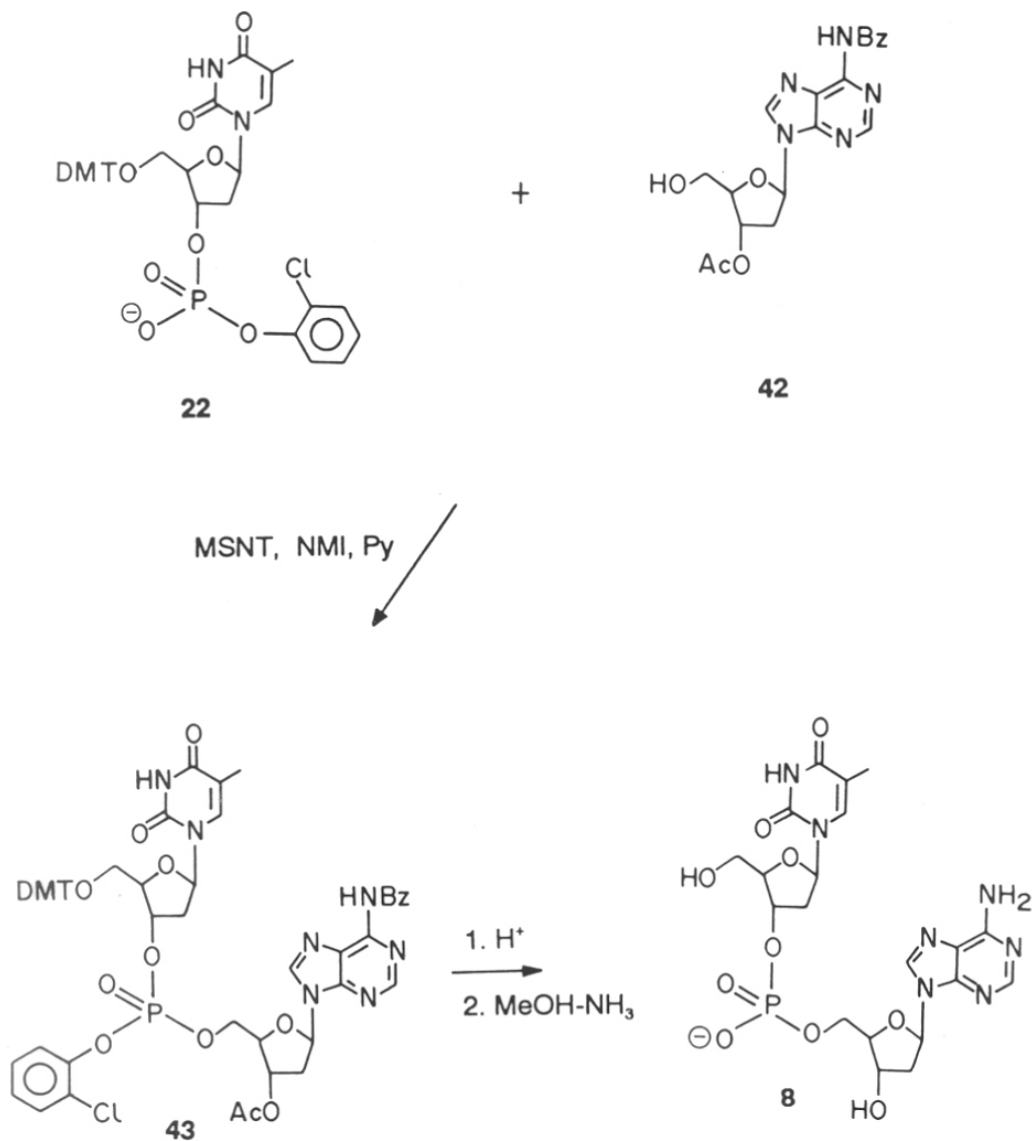
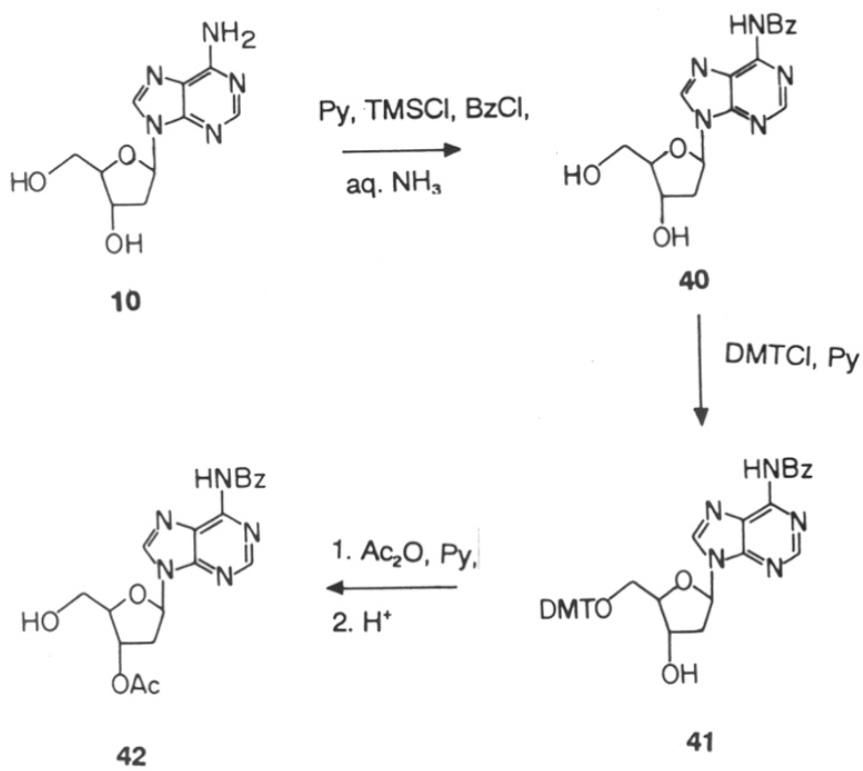


Fig. 26 <sup>31</sup>P NMR spectrum (81 MHz) of compound 7 in D<sub>2</sub>O Ref. 85% H<sub>3</sub>PO<sub>4</sub>.

**SCHEME 11**

**SCHEME 12**

### 3.4.8 Synthesis of ribodinucleotide UpA 9

The ribodinucleotide **9** was synthesised by similarly by following solution phase chemistry. The 3'-phosphodiester component **37** and 5'-hydroxyl component **44** (Scheme 13) were condensed in presence of MSNT and NMI to obtain the protected dinucleotide **45**. This was first 5'-detritylated by treatment with acid followed by deprotection of benzoyl and 2-chlorophenyl groups by reaction with MeOH-NH<sub>3</sub> to afford **46**. The 2'-O-silyl protecting group in **46** was removed with TBAF to obtain **9** which was purified by ion-exchange column chromatography (Sephadex DEAE-A25, Pharmacia) and characterised by spectroscopic methods.

## 3.5 CONFORMATIONAL STUDIES OF DINUCLEOTIDES BY <sup>1</sup>H NMR SPECTROSCOPY

One of the main pre-requisites for successful intramolecular interaction of internucleotide phosphate group with the C8-conjugated ligand in dinucleotides (**4-7**) is their relative spatial predisposition. This is indirectly related to the nucleoside sugar pucker (Fig. 27), the glycosyl torsion and phosphate conformation. In order to understand the possible variations in the above parameters, we have analysed the <sup>1</sup>H NMR spectra of the five dinucleotides (**4-6**, **8**, **24**). This also allows extraction of useful structural information from various <sup>1</sup>H-<sup>1</sup>H coupling constants.

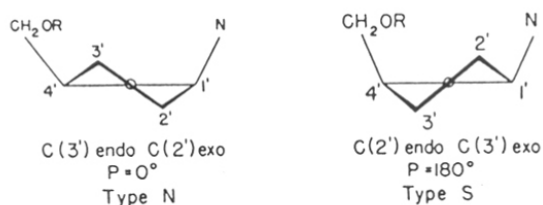
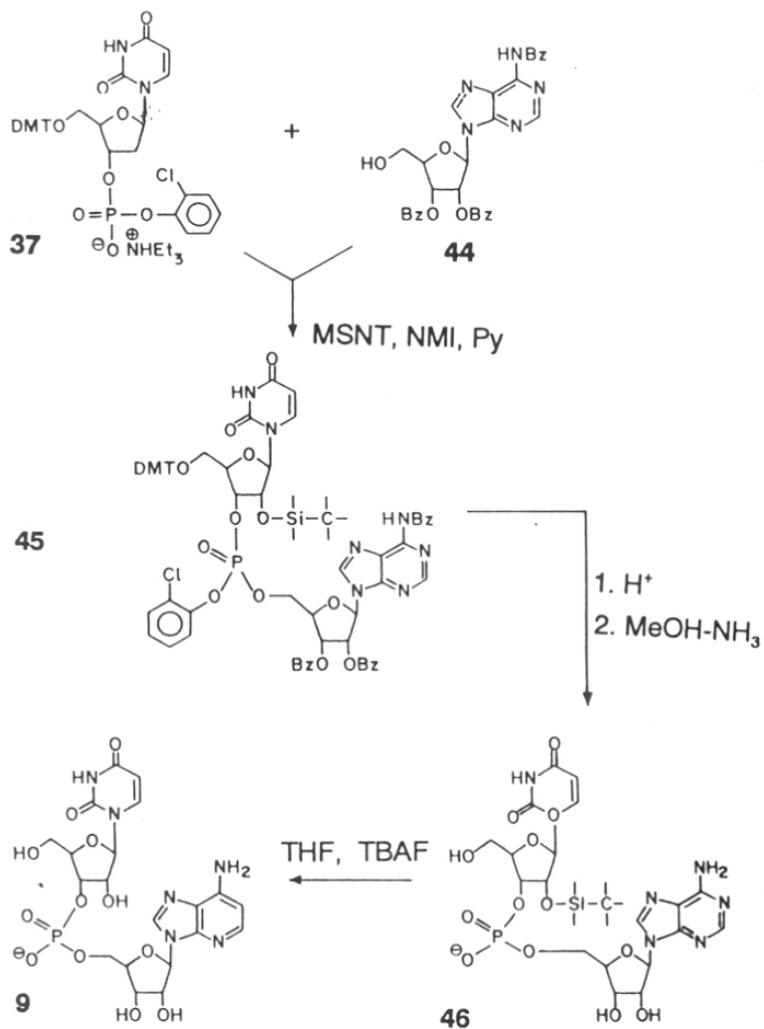


Fig. 27 Diagrammatic projections of the furanose ring in two twist conformations.

## SCHEME 13



Rinkel and Altona<sup>22</sup> have previously demonstrated that the conformational analysis of the sugar ring in nucleic acids can be performed by using sums of coupling constants viz.,  $\Sigma 1'$  ( $J_{1'2'} + J_{1'2''}$ ),  $\Sigma 2'$  ( $J_{1'2'} + J_{2'2''} + J_{2'3'}$ )  $\Sigma 2''$  ( $J_{1'2'} + J_{2'3'} + J_{2'2''}$ ) and  $\Sigma 3'$  ( $J_{2'3'} + J_{2'3''} + J_{3'4'}$ ). A  $\Sigma 1'$  value of 13.3 Hz or more was shown to arise by a predominant S-type conformation (2'-endo, >60%) wherein  $J_{1'2'} > J_{1'2''}$  and  $\Sigma 2' > \Sigma 2''$ . In case of ribose sugars the  $J_{1'2'}$  and  $J_{3'4'}$  can be used to estimate population of N-type conformer. Crucial to the success of this empirical method is the unambiguous assignment of all the protons of different sugar residues to obtain  $^1\text{H}$ - $^1\text{H}$  vicinal coupling constants of different sugar residues.

Rinkel and Altona<sup>22</sup> have derived empirical rules by examining the calculated coupling constants and sums of couplings for each sugar geometry of the deoxyribose ring along the pseudorotational cycle

- i) a  $\Sigma 1'$  value of 13.3 Hz or more indicates a predominant S-type conformer (pS > 60 %); the larger of the two couplings constituting the H1' multiplet is assigned as  $J_{1'2'}$ .
- ii) for a given residue, a predominant S type sugar conformation means that  $\Sigma 2' > \Sigma 2''$ . This rule allows an unambiguous discrimination between the H2' and H2'' resonances.
- iii) the value of  $\Sigma 2''$  is mainly influenced by the relative populations of S and N conformer and is an excellent marker to determine the fraction S-type conformers pS

$$pS = \frac{(31.5 - \Sigma 2'')}{10.9} \quad 1$$

Equation 1 is valid for the normal range of pseudorotation values pS -9° to +18°, pS 126° to 180° and  $\Phi_m$  35° to 40° where pS is the percentage of S conformer and  $\Phi_m$  is the angle of pseudorotation.



- iv)  $\Sigma 1'$  and  $\Sigma 3'$  are quite sensitive towards changes in pN and pS respectively and a knowledge of these two sums allows a valid estimate of phase angle of pseudorotation, the major conformers once pS is known from  $\delta 2''$  from equation 1.
- v)  $J_{1'2'}$  and  $J_{1'2''}$  are good markers for  $\Phi_S$  and for  $\Phi_N$  and are used together with the other coupling data in an overall fit of the experimental coupling to the calculated ones.

In the case of (near) isochronous H2' and H2'' resonances, only the following couplings are important:  $\Sigma 1'$ ,  $\Sigma 3'$  and the sum of  $J2'3'$  and  $J2''3'$  (not  $J1'2'$ ,  $J1'2''$ ,  $\Sigma 2'$  or  $\Sigma 2''$ ). The analysis of such a set of couplings is carried out in analogously to the procedure described above. In these cases however,  $\Sigma 1'$  and  $\Sigma 3'$  are the markers for pN (percentage of N conformer) and pS (percentage of S conformer) respectively and  $J1'3' + J2''3'$  is the marker for pS. Since  $\Sigma 2''$  is not available, the fraction S type conformer is roughly computed from equation 2 or from equation 3 as opposed to equation 1

$$pS = \frac{(16.9 - J2'3' - J2''3')}{8.9} \quad 2$$

$$pS = \frac{(\Sigma 1' - 9.8)}{5.9} \quad 3$$

In case of ribose sugar percentage of N conformer was calculated<sup>23</sup> by using the equation 4.

$$\%N = \frac{J3'4'}{J1'2' + J3'4'} \quad 4$$

$$\%S = 100 - N$$

### 3.5.1 Assignment of H1', H2', H3'

The complete proton chemical shift assignments of both sugar residues in 5 dinucleotides (**4-6**, **8**, **24**) was achieved by a combination of 1D and 2D NMR spectroscopy. The 2D NMR spectra were particularly needed for assignment of H3', H5' and H5'' which are normally masked in 1D spectra by the residual solvent HOD signal and the side chain methylene protons. 2D NMR was also helpful for assignment of H14 and H16 from imidazole moieties in **5** and **6**. Coupling constant values ( $J_{1'2'}$  and  $J_{2'3'}$ ) were computed by means of a first order analysis. For all the deoxyribose units, the H1' resonance appeared as a triplet and hence individual  $J_{1'2'}$  and  $J_{1'2''}$  couplings could not be obtained from this part of the spectrum. Alternatively, this information was sought from the total width of H2'' multiplet ( $=\Sigma 2''$ ) which explicitly showed all the eight lines arising from its simultaneous coupling to H2', H1' and H3' protons. The sole exception to this was the dinucleotide **4** in which an extensive overlap of resonances excluded a clear identification of H2'' signal. In the case of ribonucleotide r(UpA) **7** overlap of H2' and H3' signals prevented extraction of  $J_{1'2'}$  and  $J_{3'4'}$  coupling constants.

**Table I** summarizes the coupling constants and %S conformer calculated for various dinucleotides using the above empirical method. It is observed that in all dinucleotides, the sugar units in general show a clear preference to populate in S-type conformation (> 60%). The variation in S conformer population among the 5' nucleotidyl units of various dinucleotides was less than 15% (range 65 - 80%) compared to a variation of 35% (range 59 - 94%) among 3'-nucleotidyl units. In the unmodified dimer (dTpA), the 5'- sugar residue has a greater preference for the S-conformer population and is highest in case of C8-EDA modified dimer **4**. The computed data indicate that C8 modification does not change the sugar conformation, but instead increases the population of existing S-conformer. It is well known from previous observations<sup>23</sup> that

Table I: Coupling constants for estimation of %S conformers<sup>+</sup>

Dimers	J1'2'	J1'2''	Σ1'	Σ2'	Σ2''	%S	
8	dTp-	8.1	6.1	14.2	-	24.4	75
	-pdA	7.3	6.0	13.3	-	22.2	59
24	dTp-	7.6	6.1	13.7	28.9	23.3	66
	-pdA	7.9	6.7	14.6	29.5	25.1	81
4	dTp-	7.8	6.0	13.8	27.8	-	68
	-pdA	7.7	6.7	14.4	-	-	78
5	dTp-	7.4	6.2	13.6	28.1	23.8	64
	-pdA	8.0	6.6	14.6	29.6	23.8	81
6	dTp-	7.9	6.1	14.0	28.4	22.9	71
	-prA	6.4	-	-	12.7	-	60

$$+ \%S = \frac{\Sigma 1' - 9.8}{5.9},$$

$$* \%N = \frac{J3'4'}{J1'2' + J3'4'}$$

%S = 100-%N (see ref 17 and 18)

in unmodified dinucleotides, irrespective of the nature of base and sequence, the pentose ring shows a clear preference to exist in S-conformation. Our present data extends the above rule to the effect that purine C8 modification leads to a greater increase in S-conformer population. Interestingly, in contrast to this, the 5'-modification has negligible effect on sugar conformation.

Inspection of the relative proton chemical shifts reveals a consistent trend in C8 modification induced shifts of H1', H2" and H2' protons. A modification of base in 3'-nucleotidyl unit (-pdA) imparts a through-space deshielding effect on H1' and H2' of neighbouring 5'-nucleotidyl unit (dTp-) resulting in a downfield shift of these protons by ~ 0.2 and 0.6 ppm respectively, as compared to the corresponding protons in unmodified d(TpA) (**8**). On the otherhand, H2" of dTp- residues in **5** and **6** is upfield shifted by 0.2 ppm compared to H2" of d(TpA). The H1' and H2' protons of 3'-nucleotidyl unit in modified dinucleotides show a reverse effect: upfield shifts of H1' and a downfield shift of H2" (0.1 -0.2 ppm). Although changes in shifts for <sup>1</sup>H of modified 3'-dA unit would originate partly from electronic changes at C1' and C2', the nature of shifts observed for <sup>1</sup>H of dTp- suggests an anti conformation for the modified nucleoside (dA). In this conformation the C8-conjugated ligand is spatially close to the protons of adjacent 5'-sugar unit and thus inducing shifts arising from through-space dipolar effects. This is substantiated by the generally larger induced shifts in histamine conjugates compared to EDA derivative. This may be attributed to histamine ring current effects. Thus C8 modification does not significantly affect the glycosyl torsion (anti disposition) found in natural nucleotides while the sugar residues exhibit enhanced population of S-conformers. 2D NOSEY spectra although gave the expected characteristic cross peaks from both nucleotidyl units, indicated no NOE's useful for internucleotidyl conformational assignment.

### 3.6 Conformational studies of dinucleotides by $^{31}\text{P}$ NMR spectroscopy

An intramolecular interaction between the conjugated ligand and the internucleotidic phosphate group, either through electrostatic or H-bonding is expected to alter both the phosphate geometry and the electronic density at phosphorus. Evidence for such induced effects was sought from  $^{31}\text{P}$  NMR spectral shifts of the synthesised dinucleotides.

$^{31}\text{P}$  chemical shifts can potentially provide a probe for the analysis of conformation of phosphate ester backbone in nucleic acids, since the predominant contribution to chemical shifts arises from stereoelectronic effects.<sup>24</sup> It has been generally observed that phosphodiester in stereoelectronically favored  $g^-g^-$  conformation exhibit upfield shifts compared to those in  $gt$  or  $tg$  forms. In addition, the intrinsic conformational features of phosphate group may also have considerable influence on  $^{31}\text{P}$  chemical shifts. **Table II** shows comparative  $^{31}\text{P}$  chemical shifts of various dinucleotides synthesised in the present work. It is clearly seen that the observed chemical shifts fall into two ranges: -0.44 to -0.50 ppm (**4**, **6** and **24**) and -0.21 ppm (**7**). Extension of the generalized  $^{31}\text{P}$  chemical shift principles indicates that in **4**, **5** and **24**, the phosphate conformation is the stereoelectronically favored  $g^-g^-$  form similar to that observed in the

**Table II:  $^{31}\text{P}$  chemical shifts of dinucleotides 4-8 and 24**

Dimer	<b>4</b>	<b>5</b>	<b>6</b>	<b>7</b>	<b>8 (d(TpA))</b>	<b>24</b>
ppm	-0.45	-0.50	-0.49	-0.21	-0.49	-0.47

normal unmodified nucleic acids. In **7**, the observed downfield shift may arise due to contribution from either trans conformers (g't or tt) or intramolecular environmental effects or due to a contribution of both. These effects may influence the overall conformation of the molecule, in which the phosphate assumes a less favored, non-gauche form and consequently induces a downfield shift. In **7**, where an electrostatic interaction involving C8 side chain is less likely the observed trans geometry for phosphate may be due to one of the following structural consequences: i) the histidine imidazole NH proton may hydrogen bond with phosphate oxygen or ii) the imidazole ring nitrogen may hydrogen bond with 2'-hydroxyl. If the former is the case, then one should expect such an effect even in the dimers **5** and **6**. Although it is difficult to distinguish among the two possibilities, the present overall results suggests that imidazole on C8 side chain is involved in same intramolecular interaction leading to a conformational change in the phosphate group.

### 3.7 CONCLUSIONS

This chapter demonstrated the synthetic possibility of conjugating amino and imidazole containing side chains to C8 of adenosine or C5 of nucleosugars. A number of dinucleotides having this modification have been synthesized and characterized by  $^1\text{H}$  and  $^{31}\text{P}$  NMR spectroscopy. Conformational analysis of modified dinucleotides by  $^1\text{H}$  NMR spectroscopy showed that due to sugar modification, S conformer population of sugar residue increases compared to sugar residue in unmodified dinucleotide. An analysis of spectroscopic data also suggests an intramolecular interaction of the conjugated ligands with internucleotidic phosphate, as manifested by alteration of the sugar and phosphate conformations. These dinucleotides are first<sup>25</sup> of a group of compounds designed to model electrostatic and hydrogen bonding interactions present in the active site of ribonucleases.

### 3.8 EXPERIMENTAL

2'-Deoxynucleosides and 1-(mesitylene-2-sulphonyl)-3-nitro-1,2,4-triazole (MSNT) were obtained from Aldrich, U.K. 1-Methylimidazole (Fluka), histamine (Sigma) and ethylenediamine (SRL, India) were used without further purification. 8-Bromo-2'-deoxyadenosine<sup>16</sup>, 8-bromo-5'-O-(4,4'-DMT)-2'-deoxyadenosine<sup>26,28</sup>, and the nucleotide monomers<sup>18,27</sup> **22**, **37** were synthesised by reported procedures. Pyridine was refluxed and distilled from ninhydrin followed by distillation over CaH<sub>2</sub>. Column chromatography was carried out on silica gel (100-200 mesh, Loba Chemie, India), and TLC was performed on precoated plates (silica gel GF254, Merck 5554) Solvent; A: DCM-MeOH, 9:1 (V/V), Solvent B: DCM-MeOH, 9.5:0.5(V/V). The spots were visualised under UV light and by spraying 60% perchloric acid-ethanol (3:1) followed by charring. UV spectra were recorded on Perkin-Elmer Lambda 15 spectrometer. HPLC: Buffer A, 0.1 M TEAA; Buffer B, 30% CH<sub>3</sub>CN in 0.1 M TEAA, gradient A to B 20 min., flow rate 2 ml/min., UV detector at 260 nm. The melting points reported are uncorrected. NMR spectra were recorded on Bruker MSL 300 or AC 200 spectrometers. All chemical shifts are expressed in ppm. <sup>1</sup>H NMR spectra are reported downfield from TMS in CDCl<sub>3</sub> and in the case of D<sub>2</sub>O downfield from DSS. <sup>31</sup>P NMR spectra are recorded at 81 MHz with 85% H<sub>3</sub>PO<sub>4</sub> as external reference. <sup>13</sup>C NMR spectra were recorded at 50 MHz in both <sup>1</sup>H decoupled and INEPT modes.

#### 3.8.1 8-Bromoadenosine **27**

Adenosine **26** (4 g, 15 mmol) was dissolved in NaOAc buffer (1.0 M, pH 4, 100 ml) at 50 °C. Then the solution was cooled to room temperature and Br<sub>2</sub>-water (115 ml) was added. After 3 hrs. at room temperature usual work-up gave **27** as a yellow solid (4.07 gm, 78%) (mp 234 °C, decomp). R<sub>f</sub> (solvent A) = 0.24, λ = 264 nm (MeOH,

$\epsilon$ ,  $4.8 \times 10^4$ ).  $^1\text{H NMR}$  ( $\text{DMSO-d}_6$ )  $\delta$  8.08 (s, 1H, H2), 7.41 (s, 2H, 6NH), 5.9 (d,  $J = 7.7$  Hz, 1H, H1'), 5.1 (t,  $J = 7.7$  Hz, 1H, H2'), 4.25 (brs, 1H, H3'), 4.03 (brs, 1H, H4'), 3.66 (d,  $J = 10.5$  Hz, 1H, H5"), 3.55 (d,  $J = 10.5$  Hz, 1H, H5'), 5.7, 5.5, 5.3 (brs, 3 x OH);  $^{13}\text{C NMR}$  ( $\text{DMSO-d}_6$ )  $\delta$  155.2 (C6), 152.4 (C2), 149.9 (C4), 127.1 (C8), 119.8 (C5), 90.6 (C1'), 86.8 (C4'), 71.4 (C2'), 71.0 (C3'), 62.2 (C5'). M/e, 213 (100%,  $\text{C}_5\text{N}_5\text{H}_3\text{Br}$ ).

### 3.8.2 N<sup>6</sup>-Benzoyl-8-bromoadenosine (28)

8-Bromoadenosine (27) (3.8 g, 11 mmol) was benzoylated using transient protection procedure<sup>17</sup> using pyridine (90 ml), TMSCl (14 ml, 165 mmol) and benzoyl chloride (6.4 ml, 55 mmol) the residue obtained after work-up was purified by column chromatography. Eluting with DCM containing incremental amounts of MeOH afforded **28** (2.50 g, 66%) as a light brown solid (m. p. 129°C). R<sub>f</sub> (solvent A) = 0.43;  $\lambda = 282.3$  nm (MeOH,  $\epsilon$ ,  $8.2 \times 10^4$ ).  $^1\text{H NMR}$  ( $\text{CDCl}_3 + \text{DMSO-d}_6$ , 5:3)  $\delta$  8.7 (s, 1H, H2), 8.10 (m, 2H, ArH), 7.2-7.7 (m, 3H, ArH), 6.1 (d,  $J = 7.0$  Hz, 1H, H1'), 5.06 (dd,  $J = 5.9$ , 1H, H2'), 4.47 (d,  $J = 5.9$  Hz, 1H, H3'), 4.36 (brs, 1H, H4'), 3.95 (d,  $J = 14.7$  Hz, 1H, H5"), 3.75 (d,  $J = 11.8$  Hz, 1H, H5');  $^{13}\text{C NMR}$  ( $\text{DMSO-d}_6$ )  $\delta$  90.6 (C1'), 69.8 (C2'), 70.8 (C3'), 89.4 (C4'), 63.6 (C5'), 152.6 (C2), 149.9 (C4), 119.4 (C5), 154.9 (C6), 136.9 (C8), 165.4, 133.1, 127.3, 127, 132.4 (all from Bz).

### 3.8.3 N<sup>6</sup>-Benzoyl-8-bromo-5'-O-(4,4'-dimethoxytrityl)adenosine (29)

Compound **28** (2.40 g, 5.4 mmol) was dried by co-evaporation with dry pyridine and was redissolved in anhydrous pyridine (20 ml) and DMTCl (2.2 g, 6.6 mmol) was added. The reaction mixture was stirred at 25°C for 18 hrs. after which water (20 ml) was added and extracted with DCM (3 x 15 ml). The organic layer upon concentration gave an oily residue which was purified by column chromatography using DCM:MeOH as eluent to obtain **29** (2.90 g, 72%), as a white solid (mp 124°C). R<sub>f</sub>



(solvent A) = 0.67;  $\lambda$  = 282.0 nm (MeOH,  $\epsilon$ ,  $10.9 \times 10^4$ );  $^1\text{H NMR}$  ( $\text{CDCl}_3$ )  $\delta$  8.32 (s, 1H, H2), 7.92 (d,  $J$  = 7.3 Hz, 2H, ArH), 7.52-7.08 (m, 12H, ArH), 6.64 (dd,  $J$  = 8.6 and 4 Hz, 4H, ArH), 5.99 (d,  $J$  = 4.8 Hz, 1H, H1'), 5.41 (m, 1H, H2'), 4.63 (m, 1H, H3'), 4.19 (m, 1H, H4'), 3.65 and 3.64 (2xs, 6H,  $\text{OCH}_3$ ), 3.32 (m, 2H, H5');  $^{13}\text{C NMR}$  ( $\text{CDCl}_3$ )  $\delta$  90.2 (C1'), 71.1 (C2'), 71.5 (C3'), 84.2 (C4'), 63.5 (C5'), 152.0 (C2 and C6), 147.9 (C4), 121.5 (C5), 132.7 (C8), 136, 133.3, 132.7, 128.7, 164.5 (all from Bz), 55 ( $\text{DMT-OCH}_3$ ), 112.9, 158.4, 128.1, 128.7, 129.1, 130, 133.7, 135.8, 158.3 (all from DMT);  $\text{MS}(\text{FAB}^+)$  calculated for  $\text{M}^+$  753.6279, found 753.

#### 3.8.4 $\text{N}^6$ -Benzoyl-5'-O-(4,4'-dimethoxytrityl)-8-histamino-2'-deoxyadenosine 14

$\text{N}^6$ -Benzoyl-8-bromo-5'-O-(4,4'-dimethoxytrityl)-2'-deoxyadenosine **13** (0.35 g, 0.48 mmol) was dissolved in dry ethanol (10 ml). Histamine (0.11 g, 0.95 mmol) was added into this and the reaction mixture was stirred at room temperature for 18 hrs. Evaporation of ethanol gave a residue which was purified by silica gel column chromatography. Elution with DCM containing incremental amounts of MeOH gave **14**, which eluted with 6% MeOH-DCM (0.29 g, 79%) as colourless solid (M.P.  $134^\circ\text{C}$ ).  $R_f(\text{solvent A})$  = 0.37;  $\lambda$  = 311 nm (MeOH,  $\epsilon$ ,  $4.6 \times 10^4$ );  $^1\text{H NMR}$  ( $\text{CDCl}_3$ )  $\delta$  8.4 (s, 1H, H2), 8.04 (d,  $J$  = 6.8 Hz, 2H, ArH), 7.52 (s, H16 overlapping with ArH), 7.58-7.22 (m, 12H, ArH), 6.77 (dd,  $J$  = 8.9 Hz, 4H, ArH) 6.61 (t,  $J$  = 7.2 Hz, 2H, H1', overlapping with H14), 4.7(m, 1H, H3'), 4.14 (d,  $J$  = 3Hz, H4'), 3.77 (s, 6H,  $2 \times \text{OCH}_3$ ), 3.60 (m, 2H, H11), 3.4 (dd,  $J$  = 2.8 Hz, 2H, H5' and 5"), 2.87 (m, 1H, H2'), 2.6 (m, 2H, H12), 2.36 (m, 1H, H2'');  $^{13}\text{C NMR}$  ( $\text{CDCl}_3$ )  $\delta$  85.9 (C1'), 42 (C2'), 71.3 (C3'), 86.3 (C4'), 63.2 (C5'), 153 (C2), 147.9 (C4), 117.8 (C5), 153.6 (C6), 143.9 (C8), 38.1 (C11), 26 (C12), 129.9 (C13), 122.8 (C14), 134.2 (C16);  $\text{MS}(\text{FAB}^+)$  calculated for  $\text{M}^+$  766.859, found 767.

### 3.8.5 N<sup>6</sup>-Benzoyl-5'-O-(4,4'-dimethoxytrityl)-8-histaminoadenosine (30)

Compound **29** (0.93 g, 1.24 mmol) was reacted with histamine (280 mg, 2.52 mmol) in dry ethanol (25 ml) as above. The product was purified by column chromatography to afford **30** (0.76 g, 79%) as a solid (m. p. 137°C). R<sub>f</sub> (solvent A) = 0.27; λ = 310 (MeOH, ε, 11.0 × 10<sup>4</sup>); <sup>1</sup>H NMR (CDCl<sub>3</sub>) δ 8.29 (s, 1H, H2), 7.88 (d, J = 7.9 Hz, 2H, ArH), 7.41 (s, H16, overlapping with Ar-H), 7.4-7.1 (m, 12H, ArH), 6.70 (dd, J = 8.6 Hz and 1.8 Hz, 4H, ArH), 6.4 (s, 1H, H14) 6.09 (d, J = 5.9 HZ, 1H, H1'), 4.92 (m, 1H, H2'), 4.45 (m, 1H, H3'), 4.18 (m, 1H, H4'), 3.68 (s, 6H, 2xOCH<sub>3</sub>), 3.54 (d, J = 9.9 Hz, 1H, H5"), 3.33 (d, J = 6.4 Hz, 1H, H5'), 3.15 (m, 2H, H11), 2.50 (m, 2H, H12); <sup>13</sup>C NMR (CDCl<sub>3</sub>) δ 153.4 (C2), 148.1 (C4), 118.9 (C5), 153.7 (C6), 144 (C8), 88.1 (C1'), 70.8 (C2'), 71.7 (C3'), 84.7 (C4'), 63.3 (C5'), 37.3 (C11), 26.2 (C12), 130.5 (C13), 122.9 (C14), 135.2 (C16), 165.7, 133.7, 127, 127.8, 132.3 ( all from Bz), 158.7, 135.2, 133.6, 130.5, 129.2, 128.4, 128.2, 113.2, (all from DMT), 55.1 (DMT-OCH<sub>3</sub>).

### 3.8.6 3'-O-Acetyl-N<sup>6</sup>-benzoyl-8-(1-N-acetylhistamino)-2'-deoxyadenosine 16

Compound **14** (0.36 g, 0.47 mmol) was co-evaporated with dry pyridine (5ml), followed by dissolution in same solvent (5 ml). Acetic anhydride (0.27 ml, 2.8 mmol) was added and stirred for 6 hrs. at room temperature. The reaction mixture on work-up afforded 3'O, N<sup>15</sup>-diacetate of **15** (0.33 g, 83%) as a white solid (m. p. 136-137°C). R<sub>f</sub> (solvent A) = 0.58. <sup>1</sup>H NMR (CDCl<sub>3</sub>) δ 8.4 (s, 1H, H2), 8.06 (d, J = 7 Hz, 2H, ArH), 7.53 (s, 1H, H16 overlapping with ArH), 7.57-7.24 (m, 12H, ArH), 6.81(m, 4H, ArH), 6.78 (s, 1H, overlapping with ArH, H14), 6.48 (dd, 1H, H1'), 5.52 (t, 1H, H3'), 4.17 (m, 1H, H4'), 3.78 (s, 6H, 2 x OCH<sub>3</sub>), 3.54 (m, 2H, H11), 3.43 (m, 2H, H5'), 2.89 (m, 2H, H12), 2.74 (m, 1H, H2'), 2.17 (m, 1H, H2"), 2.1 (s, 3H, OCO-CH<sub>3</sub>), 2.06 (s, 3H, NCOCH<sub>3</sub>); Ms (FAB<sup>+</sup>) calculated for M<sup>+</sup> 851.9418, found 852. This compound (160 mg, 0.19 mmol) was detritylated using 2% DCA in DCM as above to obtain **16** (90 mg,

87%) as a white solid (m. p. 146°C). Rf (solvent A) = 0.47  $\lambda$  = 312 nm (MeOH,  $\epsilon$ , 11.6 x 10<sup>4</sup>). <sup>1</sup>H NMR (CDCl<sub>3</sub>)  $\delta$  8.4 (s, 1H, H2), 7.95 (d, J = 7Hz, 2H, ArH), 7.64 (s, 1H, H16), 6.67 (s, 1H, H14), 6.58 (dd, J = 10.1 and 5.6 Hz, 1H, H1'), 5.37 (d, J = 6 Hz, 1H, H3'), 4.05 (brs, 1H, H4'), 3.95 (d, J = 9.6 Hz, 1H, H5''), 3.81 (d, J = 9.8 Hz, 1H, H5'), 3.61 (t, J = 10 Hz, 2H, H11), 2.9 (t, J = 10 Hz, 2H, H12), 2.64 (m, 1H, H2'), 2.16 (m, 1H, H2''), 2.08 (s, 3H, OCOCH<sub>3</sub>), 2.03 (s, 3H, NCOCH<sub>3</sub>); FAB MS 766 (M<sup>+</sup>+1).

### 3.8.7 N<sup>6</sup>-Benzoyl-5'-O-[4,4'dimethoxytrityl-8-amino(2-aminoethyl)]-2'-deoxyadenosine 17

Compound **13** (800 mg, 1.1 mmol) was taken in absolute ethanol (20 ml) into which ethylenediamine (0.52 ml, 7.8 mmol) was added. The reaction mixture was stirred at room temperature for 20 hrs. The excess solvent was removed under vacuum and the product purified by silica gel column chromatography. Elution with DCM:MeOH gave compound **17** (530 mg, 68%) as a white solid (m. p. 123°C). Rf (solvent A) = 0.18; Ninhydrin positive;  $\lambda$  = 308 nm (MeOH,  $\epsilon$ , 5.4 x 10<sup>4</sup>); <sup>1</sup>H NMR (CDCl<sub>3</sub>:DMSO-d<sub>6</sub>: D<sub>2</sub>O, 5:3:1)  $\delta$  8.28(s, 1H, H2), 7.98 (dd, J = 7.9 Hz, 2H, ArH), 7.53-7.11 (m, 12H, ArH), 6.70 (dd, J = 8.8 Hz, J = 3.5 Hz, 4H, ArH), 6.38 (t, J = 6.9 Hz, 1H, H1'), 4.56 (m, 1H, H3'), 4.03 (m, 1H, H4'), 3.69 (s, 6H, 2 x OCH<sub>3</sub>), 3.4 (dd, J = 10.7 and 4.9 Hz, 1H, H5''), 3.26 (dd, J = 10.7 and 4.5 Hz, 1H, H5'), 3.08 (t, J = 5 Hz, 2H, H11), 3.0 (m, 1H, H2', overlapping with H11), 2.73 (t, J = 5 Hz, 2H, H12), 2.25 (m, 1H, H2''); <sup>13</sup>C NMR (CDCl<sub>3</sub>:DMSO-d<sub>6</sub>, 5:3)  $\delta$  85.6 (C1'), 42.6 (C2'), 70.8 (C3'), 82.9 (C4'), 63.1 (C5'), 41 (C11), 36.9 (C12), 123.4 (C5), 153 (C2), 147.4 (C4), 153.7 (C6), 144 (C8), 165, 133.6, 127.7, 126.8, 131.5 (all from Bz).

### 3.8.8 3'-O-Acetyl-N<sup>6</sup>-benzoyl-8-amino(2-N-acetyl-aminoethyl)-2'-deoxyadenosine 19

Compound **17** (180 mg, 0.27 mmol) was acetylated as above using dry pyridine (2.6 ml) and acetic anhydride (150  $\mu$ l, 1.60 mmol) for 14 hrs. Aqueous work-up

afforded 3'O, N<sup>13</sup>-diacetate of **18** (182 mg, 86%). Rf (solvent A) = 0.56; Ninhydrin negative. This compound (180 mg, 0.23 mmol) was dissolved in DCM (1 ml) to which 2% DCA in DCM (10 ml) was added while cooling in an ice bath. The reaction was complete in 5 min. after which the mixture was extracted with DCM (30 ml) and washed with aq. sat. NaHCO<sub>3</sub>. On concentration, a white foam was obtained which was purified by column chromatography to afford **19** (96 mg, 83%) (m. p. 138°C). Rf (solvent A) = 0.42;  $\lambda = 308$  (MeOH,  $\epsilon$ ,  $5.4 \times 10^4$ ). <sup>1</sup>H NMR (CDCl<sub>3</sub>)  $\delta$  8.38 (s, 1H, H<sub>2</sub>), 7.9 (dd, J = 7.0 Hz and 2.0 Hz, 2H, ArH), 7.61-7.4 (m, 3H, ArH), 6.55 (dd, J = 10.0 and 5.4 Hz, 1H, H<sub>1'</sub>), 5.36 (d, J = 6.3 Hz, 1H, H<sub>3'</sub>), 4.09 (brs, 1H, H<sub>4'</sub>), 3.92 (d, J = 10.8 Hz, 1H, H<sub>5''</sub>), 3.83 (dd, J = 11.6 and 2.2 Hz, 1H, H<sub>5'</sub>), 3.56 (t, J = 5 Hz, 2H, H<sub>11</sub>), 3.34 (m, 2H, H<sub>12</sub>), 2.67 (m, 1H, 2'), 2.15 (m, 1H, H<sub>2''</sub>), 2.04 (s, 3H, OCOCH<sub>3</sub>), 1.89 (s, 3H, NCOCH<sub>3</sub>); <sup>13</sup>C NMR (CDCl<sub>3</sub>)  $\delta$  85.2 (C<sub>1'</sub>), 41.9 (C<sub>2'</sub>), 75.6 (C<sub>3'</sub>), 83.4 (C<sub>4'</sub>), 61.7 (C<sub>5'</sub>), 153.4 (C<sub>6</sub>), 147.8 (C<sub>4</sub>), 143.0 (C<sub>8</sub>), 153.1 (C<sub>2</sub>), 123.1 (C<sub>5</sub>), 39.9 (C<sub>11</sub>), 35.2 (C<sub>12</sub>), 171.6 (OCOCH<sub>3</sub>), 170.3 (NCOCH<sub>3</sub>), 22.7 (OCOCH<sub>3</sub>), 20.8 (NCOCH<sub>3</sub>), 165.3, 133.7, 132.1, 128.4, 127.6, (all from Bz).

### 3.8.9 Dimer **23**

The 3'-phosphodiester **22** (346 mg, 0.41 mmol) and the 5'-hydroxyl compound **19** (90 mg, 0.18 mmol) were dried by co-evaporation with dry pyridine (2 ml) and the residue dissolved in dry pyridine (1 ml). After the addition of 1-methylimidazole (350  $\mu$ l, 4.28 mmol) and MSNT (400 mg, 1.35 mmol) the reaction mixture was kept stirred at room temperature for 25 min. when TLC showed its completion. It was quenched with sat. aq. NaHCO<sub>3</sub> (3 ml) and extracted with DCM (2x10 ml). The dried organic layer was concentrated and the resultant residue was purified by column chromatography when the dimer **23** eluted with DCM/MeOH (120 mg, 55%). Rf (solvent A) = 0.53; <sup>31</sup>P NMR (CDCl<sub>3</sub>) ppm -6.7 and -7.6.

### 3.8.10 Dimer 25

This was synthesised by a similar condensation of **22** (142 mg, 0.17 mmol) and **16** (50 mg, 0.09 mmol) in dry pyridine (1 ml) containing 1-methylimidazole (130  $\mu$ l, 1.62 mmol) and MSNT (151 mg, 0.51 mmol). Yield 61% (70 mg). R<sub>f</sub> (solvent A) = 0.62; <sup>31</sup>P NMR (CDCl<sub>3</sub>) ppm -6.5 and -7.6.

### 3.8.11 Dimer 24

The dimer **23** (120 mg, 0.1 mmol) after 5'-detritylation with 2% DCA in DCM was dissolved in freshly prepared sat. MeOH-NH<sub>3</sub> (15 ml) and heated in a sealed tube at 60°C for 24 hrs. It was cooled and removal of excess of MeOH-NH<sub>3</sub> gave a residue which was purified on DEAE Sephadex A-25 column (2 cm x 12 cm). Elution was performed using TEAA buffer (pH 7.0) using a gradient from 0.01 M to 0.2 M (200 ml each) with a flow rate of 1 ml/min. The fractions containing desired product was pooled and lyophilised to obtain **24** as a white solid (50 mg, 76%). HPLC retention time 13.7 min.;  $\lambda = 272$  nm (H<sub>2</sub>O,  $\epsilon$ , 6.38 x 10<sup>4</sup>), <sup>31</sup>P NMR ppm -0.47; <sup>1</sup>H NMR (D<sub>2</sub>O)  $\delta$  6.11 (t, 1H, H1'T), 6.27 (t, 1H, H1'A), 2.14 (m, 1H, H2'T), 2.47 (m, 1H, H2" T), 2.79 (m, 1H, H2'A) 2.34 (m, 1H, H2"A), 4.73 (m, 1H, H3'T, overlapping with HOD signal) 4.65 (m, 1H, H3'A, overlapping with HOD signal), 4.12 (m, 1H, H4'T), 4.15 (brs, 1H, H4'A), 3.74 (m, 2H, H5'&5"T), 4.19 (m, 2H, H 5' and 5"A, overlapping with 4'A), 7.49 (s, 1H, H6), 1.87 (s, 3H, 5-CH<sub>3</sub>), 7.96 (s, 1H, H8), 3.59 (m, 2H, H11), 3.43 (m, 2H, H12), 1.99 (s, 3H, NCOCH<sub>3</sub>).

### 3.8.12 Dimer 4

The compound **24** (50 mg, 0.07 mmol) was dissolved in aq. NaOH (1 M, 2 ml) and heated over a water bath at 60°C for 6 hrs. The reaction was monitored by HPLC and after completion the reaction mixture was concentrated to 1 ml and loaded into a DEAE Sephadex A-25 column (2 cm x 12 cm). Elution was performed with TEAB

buffer (pH 7.3) using gradient from 0.01 M to 0.2 M (200 ml each) with a flow rate of 1 ml/min. The fractions containing desired products were pooled and lyophilised to get **4** (32 mg, 67%). HPLC retention time 13.95 min.;  $^{31}\text{P}$  NMR ppm -0.45;  $^1\text{H}$  NMR ( $\text{D}_2\text{O}$ )  $\delta$  8 (s, 1H, AH2), 7.48 (s, 1H, TH6), 6.31 (t, J = 6.8, 1H, H1'A), 6.12 (t, J = 7.4 Hz, 1H, H1'T), 4.8 (m, H3'T overlapping with HOD signals), 4.72 (m, H3'A overlapping with HOD signal), 4.15 (m, 3H, H5', 5" and 4' A), 4.1 (m, 1H, 4'T), 3.77 (t, J = 4.4 Hz, 2H, H11), 3.7(m, 2H, H5'T), 3.31(m, H12, overlapping with TEA signals), 2.89 (m, 1H, 2'A) 2.44(m, 1H, H2"T), 2.37 (m, 1H, H2"A), 2.13 (m, 1H, H 2'T), 1.84 (s, 3H, 5- $\text{CH}_3$ ).

### 3.8.13 Dimer 5

Dimer **25** (70 mg, 0.06 ml) was first 5'O-deprotected with 2% DCA followed by reaction with sat.  $\text{MeOH-NH}_3$  as above to obtain **5** (44 mg, 70%), as white solid. HPLC retention time 14.78 min.;  $\lambda = 271$  nm ( $\text{H}_2\text{O}$ ,  $\epsilon$ ,  $10.9 \times 10^4$ );  $^{31}\text{P}$  NMR ( $\text{D}_2\text{O}$ ) ppm -0.50;  $^1\text{H}$  NMR ( $\text{D}_2\text{O}$ )  $\delta$  6.04 (t, 1H, H1'T), 6.17 (t, 1H, H1'A), 2.13 (m, 1H, H2'T), 2.40 (m, 1H, H2"T), 2.53 (m, 1H, H2'A), 2.22 (m, 1H, H2"A), 4.8 (m, H3'T, overlapping with HOD signal), 4.46 (m, 1H, H3'A), 4.08 (m, 4H, H4'A, H4'T and H5' & 5"A), 3.69 (m, 4H, H5' & 5" T and H11), 3.05 (m, 2H, H12), 8.54 (s, 1H, H16), 7.23 (s, H, H14), 7.85 (s, 1H, H2A), 7.45 (s, 1H, H6T), 1.89 (s, 3H, 5- $\text{CH}_3$ ).

### 3.8.14 N<sup>6</sup>-Benzoyl-2',3'-O-diacetyl-8-(15N-acetyl)histaminoadenosine 31

Compound **30** (0.68 g, 0.87 mmol) was acetylated with pyridine (10 ml) and acetic anhydride (0.7 ml, 7 mmol) by usual procedure to obtain the peracetate (0.72 g, 91%). This was detritylated by 2% DCA in DCM to obtain **31** (0.28 g, 58%), as a white solid (m. p. 157°C). Rf (solvent A) = 0.26;  $\lambda = 311$  (MeOH,  $\epsilon$ ,  $10.7 \times 10^4$ ).  $^1\text{H}$  NMR ( $\text{CDCl}_3 + \text{DMSO-d}_6$ , 5:3)  $\delta$  8.5 (s, 1H, H2), 8.07 (d, J = 6.5 Hz, 2H, ArH), 7.6-7.4 (m, 4H, H16, ArH overlapping with H16), 6.83 (s, 1H, H14), 6.46 (d, J = 8.4 Hz, 1H, H1'), 5.69 (dd, J = 5.9 Hz and 5.8 Hz, 1H, H2'), 5.55 (d, J = 5.9 Hz, 1H, H3'), 4.28

(brs, 1H, H4'), 3.90 (d, J = 11.5 Hz, 1H, H5\*), 3.82 (d, J = 11.5, 1H, H5'), 3.66 (t, J = 6.3 Hz, 2H, H11), 2.97 (t, J = 6.5 Hz, H12), 2.18 (s, 6H, 2 x OCOCH<sub>3</sub>), 1.96 (s, 3H, NHCOCH<sub>3</sub>); <sup>13</sup>C NMR (CDCl<sub>3</sub>+DMSO-d<sub>6</sub>, 5:3) δ 168.9 and 168.4 (NHCO<sub>2</sub>R, R = CH<sub>3</sub>, Ar), 152.6 (C6), 147.3 (C4), 129.2 (C5), 152.1 (C2), 143.0 (C8), 83.3 (C1'), 71.1 (C3'), 69.4 (C2'), 83.0 (C4'), 60.1 (C5'), 19.3, 19.8 (2',3'-OCOCH<sub>3</sub>), 25.6 (NHCOCH<sub>3</sub>), 42.2 (C11), 25.5 (C12), 115.9 (C13), 122.2 (C14), 133.8 (C16), 133.5, 127.3, 131.2, 127.6 (all from Bz) M/e 564 ( M<sup>+</sup>-CH<sub>3</sub>CO).

### 3.8.15 Dimer 38

The 3'-phosphodiester **37** (205 mg, 0.22 mmol) and 5' hydroxyl component **31** (100 mg, 0.17 mmol) were condensed together in presence of MSNT (190 mg, 0.65 mmol) and 1-methylimidazole (100 μl, 1.29 mmol) in pyridine (1.6 ml) as above to afford **38**. <sup>31</sup>P NMR (CDCl<sub>3</sub>) ppm -5.46 and -5.86.

### 3.8.16 Dimer 7

The dimer **38** was 5'-detritylated with 2% DCA in DCM as described before. This was followed by treatment with sat. MeOH-NH<sub>3</sub> (15 ml) at 50°C in a sealed tube for 18-20 hrs. Removal of excess MeOH-NH<sub>3</sub> followed by co-evaporation with dry THF (2 x 2 ml) gave a residue (**39**) which was treated with 1 M TBAF in dry THF (0.9 ml), at room temperature for 4 hrs. The reaction was quenched with autoclaved TEAA buffer (2ml, 0.05 M, pH 7), evaporated and the residue was loaded on a column of DEAE sephadex A-25 (2cm x 12 cm). Elution was performed with TEAA buffer using gradient from 0.01 M TEAA to 0.2 M TEAA (200 ml each, pH 7.0). The fractions corresponding to major peak were pooled and lyophilised to afford **7** (47 mg, 36% overall yield). HPLC retention time 12.83 min.; λ = 271 nm (H<sub>2</sub>O, ε, 5.5 x 10<sup>4</sup>); <sup>31</sup>P NMR (D<sub>2</sub>O) ppm -0.21; <sup>1</sup>H NMR (D<sub>2</sub>O, 500 MHz) δ 5.95 (d, 1H, H1'A), 5.84 (d, 1H, H1'U, overlapping with H5), 4.57 (m, 2H, H2'A and H3'U), 4.39 (t, 2H, H2'U and H3'A),

4.35 (q, 2H, H5' and H5" A), 4.29 (brs, 1H, 4'U), 4.22 (brs, 1H, 4'A), 3.84 (dd, 2H, H5' and H5" U), 8.64 (s, 1H, H16), 8.07 (s, 1H, H2A), 7.86 (d, 1H, H6U), 7.3 (s, 1H, H14), 5.86 (d, H5U, overlapping with H1'U), 3.79 (t, 2H, H11), 3.2 (m, H12, overlapping with TEA).

### 3.8.17 5'-(2-aminoethyl)amino-5'-deoxythymidine **34**

5'-Tosylthymidine **33** (4.86 g, 12.3 mmol) was treated with ethylene diamine (15 ml) at room temperature for 22 hrs. Excess ethylenediamine was removed under reduced pressure and the residue was purified by column chromatography. Elution with isopropanol-aq.NH<sub>3</sub> (9/1, V/V) gave **34** as a hygroscopic solid (m. p. 86°C). Rf (isopropanol:aq.NH<sub>3</sub>:H<sub>2</sub>O, 6:1:1) = 0.33;  $\lambda = 266$  nm (MeOH,  $\epsilon$ ,  $3.0 \times 10^4$ ); <sup>1</sup>H NMR (D<sub>2</sub>O)  $\delta$  7.4 (s, 1H, H6), 6.26 (t, J = 6.9 Hz, 1H, H1'), 4.34 (m, 1H, H3'), 4.01 (m, 1H, H4'), 3.02-2.75 (m, 6H, H5', H $\alpha$  and H $\beta$ ), 2.35 (m, 2H, H2' and H2''), 1.87 (s, 3H, 5-CH<sub>3</sub>); <sup>13</sup>C NMR (D<sub>2</sub>O)  $\delta$  155.5 (C2), 171 (C4), 138 (C6), 112.6 (C5), 13.3 (5-CH<sub>3</sub>), 86.4 (C1'), 40.1 (C2'), 73.2 (C3'), 85.8 (C4'), 51.8 (C5'), 48.6 (C $\alpha$ ), 39.2 (C $\beta$ ). M/e, 254 (M<sup>+</sup>-CH<sub>2</sub>NH<sub>2</sub>), 225 (M<sup>+</sup>-NHCH<sub>2</sub>CH<sub>2</sub>NH<sub>2</sub>), 159 (C<sub>7</sub>H<sub>15</sub>N<sub>2</sub>O<sub>2</sub>).

### 3.8.18 5'-(2-N-trifluoroacetyl aminoethyl)-N-trifluoroacetyl amino-5'-deoxythymidine **35**

Compound **34** (2.22 g, 5 mmol) was dried by co-evaporation with anhydrous pyridine and dissolved in pyridine (50 ml). To this, TMSCl (4.4 ml, 50 mmol) was added while cooling (0°C) and stirred for 1h. This was followed by addition of trifluoroacetic anhydride (4.3 ml, 30 mmol) and stirred for further 2 hrs., at 0-5°C. The reaction was quenched with water (20 ml) the product was extracted with DCM (3 x 25 ml). The organic layer was concentrated to a residue which on purification by column chromatography (DCM:MeOH) gave **35** (2.23 g, 60%) as a solid (m. p. 97°C). Rf (solvent A) = 0.45;  $\lambda = 264$  nm (MeOH,  $\epsilon$ ,  $5.1 \times 10^4$ ); <sup>1</sup>H NMR (CD<sub>3</sub>COCD<sub>3</sub>)  $\delta$  7.45 (s, 1H,



H6), 6.2 (q,  $J = 6.5$  Hz, 1H, H1'), 4.34 (m, 1H, H3') 4.15 (m, 1H, H4'), 3.95 (dd,  $J = 4.7$  Hz, 1H, H5'), 3.85 (dd,  $J = 4.7$  Hz 1H, H5'), 2.30 (m, 2H, H2'), 1.84 (s, 3H, CH<sub>3</sub>), 3.57-3.79 (m, 4H, H $\alpha$  and H $\beta$ ). <sup>13</sup>C NMR (CD<sub>3</sub>COCD<sub>3</sub>)  $\delta$  164.2 (C4), 158.2 and 157.5 (NCOCF<sub>3</sub>), 151 (C2), 137 (C6), 119.9 and 114.2 (NCOCF<sub>3</sub>), 111.1 (C5), 83.5 (C1'), 39.3 (C2'), 73 (C3'), 86 (C4'), 50.7 (C5'), 12.0 (5-CH<sub>3</sub>), 49.2 (C $\alpha$ ), 46.9 (C $\beta$ ). M/e 476 (M<sup>+</sup>).

### 3.8.19 Triethylammonium[5'-(2N-trifluoroacetylaminoethyl)-N-trifluoroacetylamino-5'-deoxythymidine-3'-O-(2-chlorophenylphosphate)] 36

Compound **35** (0.47 g, 0.9 mmol) was dried by co-evaporation with anhydrous pyridine (10 ml). In a separate flask (2-chlorophenyl)dichloro phosphate (1.6 ml, 9.1 mmol) was dissolved in dry pyridine (10ml) to which water (0.16 ml) was added slowly while cooling. The mixture was allowed to reach room temperature during 10 min. The precipitated pyridinium chloride was removed by filtration and the clear filtrate was added to the dry deoxynucleoside **35**. The mixture was concentrated to half of its volume and kept for 30 min. at room temperature. The reaction was quenched by the addition of TEAA (1 M, 20 ml, pH 6.3), it was then extracted with DCM (30 ml), washed with TEAA (0.1 M, 2x15 ml) and the organic phase was concentrated. The residue was purified by column chromatography, (DCM-MeOH) to yield **36** (0.46 g, 61%). R<sub>f</sub> (solvent A) = 0.21; <sup>31</sup>P NMR (CDCl<sub>3</sub>) ppm -6.14 and -6.86.

### 3.8.20 Dimer 37

The dinucleotide **37** was obtained by condensation of the monomer **36** (200 mg, 0.26 mmol) with 5'-hydroxyl nucleoside **31** (120 mg, 0.2 mmol) in dry pyridine (2.6 ml) in presence of MSNT (232 mg, 0.78 mmol) and NMI (125  $\mu$ l, 1.60 mmol). The reaction product was purified by column chromatography (DCM:MeOH) to yield **37**

(150 mg, 60%) as a white solid.  $R_f$  (solvent A) = 0.61.  $^{31}\text{P}$  NMR ( $\text{CDCl}_3$ )  $\delta$  -6.71 and -7.55.

### 3.8.21 Dimer 6

The above dimer (**37**) (150 mg, 0.12 mmol) was treated with sat.  $\text{MeOH-NH}_3$  (10 ml) in a sealed tube at  $60^\circ\text{C}$  for 24 hrs. Removal of excess reagents and purification of residue by ion-exchange column chromatography (DEAE Sephadex A25, 2 cm x 10 cm) and eluted with TEAB buffer (pH 7.30) and gradient 0.01 M, to 0.2 M (200 ml each) to give **6** (52 mg, 53%). HPLC retention time 13.21 min.;  $\lambda = 271$  nm ( $\text{H}_2\text{O}$ ),  $\epsilon$ ,  $7.8 \times 10^4$ ;  $^{31}\text{P}$  NMR ( $\text{D}_2\text{O}$ )  $\delta$  -0.49;  $^1\text{H}$  NMR ( $\text{D}_2\text{O}$ )  $\delta$  8.17 (s, 1H, H16), 7.95 (s, 1H, H2A), 7.23 (s, 1H, H6T), 7.09 (s, 1H, H14), 5.99 (t, 1H, H1'T), 5.78 (d, 1H, H1'A), 4.72 (t, 1H, H2'A), 4.56 (m, 1H, H3'T), 4.36 (t, 1H, H3'A), 4.20 (brs, 1H, H4'A), 4.13 (brs, H5' & 5'A, overlapping with H4'A), 4.11 (brs, 1H, 4'T, overlapping with 5'A), 2.85 (m, 1H, 5"T), 2.71 (dd, 1H, 5'T), 2.39 (m, 1H, 2"T), 2.05 (m, 1H, 2'T), 3.68 (t, 2H, H11), 2.95 (t, 2H, H12), 3.1 (m, 2H,  $\alpha\text{H}$ ), 2.86 (m, 2H,  $\beta\text{H}$ ), 1.79 (s, 3H, 5- $\text{CH}_3$ ).

### 3.8.22 8-Bromo-2'-deoxyadenosine<sup>16</sup> 11

2'-Deoxy adenosine **10** (8 gm, 31.5 mmol) was dissolved in 260 ml of sodium acetate buffer (pH 5, added 0.5 M NaOH to 0.5 M acetic acid) by heating at  $50^\circ\text{C}$  on a water bath. To this saturated  $\text{Br}_2$  water (140 ml) was added drop by drop and stirred the reaction mixture overnight. The precipitate obtained was filtered. Filtrate concentrated under vacuum to half the volume and kept at  $4^\circ\text{C}$  overnight. The precipitate was filtered and washed with acetone. Precipitate was pooled together to obtain a brown solid (4.92 g, 47%). M. P. =  $240^\circ\text{C}$  (decompose),  $R_f$  (ethyl acetate:Acetone: $\text{H}_2\text{O}$ , 5:10:1) = 0.76,  $\lambda = 264$  nm ( $\text{MeOH}$ ,  $\epsilon$ ,  $9.4 \times 10^4$ ),  $^1\text{H}$  NMR ( $\text{DMSO-d}_6$ )  $\delta$  8.12 (s, 1H, H2), 7.53 (s, 1H, NH), 6.30 (q,  $J = 6.5$  Hz, 1H, H1'), 4.49 (t,  $J = 2.6$  Hz, 1H, H3'), 3.90 (d,  $J = 2.4$  Hz, 1H, H4'), 3.78 (dd,  $J = 5.33$  Hz, 1H, H5"), 3.63 (dd,  $J = 5.33$  Hz, 1H, H5'), 3.14 (m, 1H, H2"), 2.2

(m, 1H, H2'),  $^{13}\text{C}$  NMR ( $\text{DMSO-d}_6$ )  $\delta$  152.8 (C2), 155.24 (C6), 150.44 (C4), 127.4 (C8), 120.27 (C5), 87.3 (C1'), 38.1 (C2'), 71.88 (C3'), 88.71 (C4'), 62.77 (C5').

### 3.8.23 N<sup>6</sup>-Benzoyl-8-bromo-2'-deoxyadenosine 12

Compound **11** (6 g, 18.18 mmol) was desiccated overnight and suspended in dry pyridine (182 ml) in a 1 litre round bottom flask. The reaction mixture was protected from moisture (drying tube) and cooled it in an ice bath. Trimethylchlorosilane (23.1 ml, 182 mmol) was added drop wise using an addition funnel at 0°C. After 30 minutes while stirring benzoyl chloride (10.6 ml, 91 mmol) was added drop wise. Reaction mixture was allowed to reach at room temperature over 2 hrs. The reaction was quenched by slow addition of cold water (36 ml) followed by hydrolysis with concentrated ammonia (36 ml, 30%). After 15 minutes TLC indicated a single spot due to benzoyl derivative. Prolonged reaction time gave back the starting material. The reaction mixture was concentrated to an oil. Wash the oil with diethyl ether (4 x 50 ml). Residue was purified by silica gel column chromatography (100-200 mesh) and eluted with MeOH:CH<sub>2</sub>Cl<sub>2</sub>, 1:9 to afford **12** as a solid (4.9 g, 62%). M. P. 132°C, R<sub>f</sub> (solvent A) = 0.5,  $\lambda$  = 284.6 nm (MeOH,  $\epsilon$ , 11.34 x 10<sup>4</sup>).  $^1\text{H}$  NMR ( $\text{DMSO-d}_6$ )  $\delta$  8.73 (s, 1H, H2), 8.25 (d, J = 8.8 Hz, 2H, Ar-H), 7.53 (m, J = 8.8 Hz, 3H, Ar-H), 6.43 (t, J = 8.8 Hz, 1H, H1'), 4.57 (t, J = 5.9 Hz, 1H, H3'), 3.9 (q, J = 5.9 Hz, 1H, H4'), 3.73 (dd, J = 5.9 Hz, 1H, H5'), 3.56 (dd, J = 5.9 Hz, 1H, H5'), 3.37 (m, 1H, H2''), 2.33 (m, 1H, H2')  $^{13}\text{C}$  ( $\text{DMSO-d}_6$ )  $\delta$  153 (C6), 151.7 (C2), 149.4 (C4), 132.2 (C8) 126.1 (C5), 86.8 (C1'), 37.29 (C2'), 71.34 (C3'), 88.4 (C4'), 62.4 (C5'), 133.4, 128.7, 132.3, 128.9, 166.2 (all from BzC).

### 3.8.24 N<sup>6</sup>-Benzoyl-8-bromo-5'-O-(4,4'-dimethoxytrityl)-2'-deoxyadenosine <sup>26</sup> 13

Compound **12** (4.5 g, 10.4 mmol) was dried by co-evaporation with dry pyridine (2 x 30 ml). The residue was then dissolved in dry pyridine (51 ml). 4,4'-Dimethoxytrityl chloride (4.2 g, 12.4 mmol) was added and stirred at room temperature for 20 hrs.

during which time pyridine hydrochloride was separated out. Methanol was added and extracted with  $\text{CH}_2\text{Cl}_2$  (3 x 30 ml).  $\text{CH}_2\text{Cl}_2$  layer was pooled together and dried over  $\text{Na}_2\text{SO}_4$ . On evaporation of  $\text{CH}_2\text{Cl}_2$  yielded the crude product which was purified by column chromatography and eluted with  $\text{CH}_2\text{Cl}_2$ /pyridine, 99:1 containing increasing amount of methanol to obtain **13** (4.9 g, 64%). M. P. = 126°C,  $R_f$  (solvent A) = 0.73,  $\lambda = 282.2$  nm (MeOH,  $\epsilon$ ,  $8.96 \times 10^4$ ),  $^1\text{H}$  NMR ( $\text{CDCl}_3$ )  $\delta$  8.56 (s, 1H, H2), 7.98 (d,  $J = 1.6$  Hz, 2H, Ar-H), 7.65-7.17 (m, 12H, Ar-H), 6.65 (m, 4H, Ar-H), 6.45 (dd,  $J = 2.7$  and 6.1 Hz, 1H, H1'), 4.14 (q,  $J = 5.9$  Hz, H4'), 3.77 (s, 3H,  $\text{OCH}_3$ ), 3.76 (s, 3H,  $\text{OCH}_3$ ), 3.55 (m, 1H, H2''), 3.39 (d,  $J = 5.9$  Hz, 2H, H5' & H5''), 2.41 (m, 1H, H2')  $^{13}\text{C}$  ( $\text{CDCl}_3$ )  $\delta$  36.82 (C2'), 63.8 (C5'), 72.61 (C3'), 86.4, 85.27 (C1' & C4'), 152.5 (C6), 148.3 (C2), 145 (C4), 127 (C5), 132.6 (C8), 55.13, 96.1, 113.1 (DMT-C), 158.5 (CO).

### 3.8.25 Triethylammonium[5'-O-dimethoxytritylthymidine-3'-O-(2-chlorophenyl phosphate)]<sup>27</sup> **22**

5'-O-4,4'-dimethoxytrityl thymidine **21** (1g, 1.84 mmol) was co-evaporated with anhydrous pyridine. In a separate flask 2-chlorophenyl phosphorodichloridate (3 ml, 18 mmol) was dissolved in dry pyridine (20 ml). Water (0.32 ml, 18 mmol) was added (by a syringe) to this solution under cooling and the mixture was left at room temperature for 10 minutes. After removing pyridinium chloride precipitate by filtration was mixed with the 5'-O-4,4'-dimethoxytrityl thymidine. the mixture was concentrated to half the volume and allowed to react for 30 minutes. Completion of the reaction was monitored by TLC. The reaction was stopped by the addition of 1m TEAB (46 ml). After 10 minutes  $\text{CHCl}_3$  was added for extraction and the mixture was washed with 0.1 M TEAB. The organic phase was evaporated to an oil, then co-evaporated with toluene and dried in vacuum. Purified by column chromatography and eluted with  $\text{CH}_2\text{Cl}_2$ /TEA (99:1) containing increasing amount of methanol to get a white solid M. P. = 105°C,  $R_f$  (solvent A) = 0.35,  $^{31}\text{P}$  NMR ( $\text{CDCl}_3$ )  $\delta$  -5.77 and -6.13,  $^1\text{H}$  NMR ( $\text{CDCl}_3$ )  $\delta$  11.59, 9.15 (NH), 7.59 (s, 1H,

H6), 7.5-6.7 (m, 17H, Ar-H), 6.15 (t,  $J = 6.4$  Hz, H1'), 5.03 (brs, 1H, H3'), 4.05 (m, 1H, H4'), 3.74 (m, 6H, 3 x NCH<sub>2</sub>-), 3.33 (m, 2H, H5' & H5"), 2.95 (s, 6H, 2 x OCH<sub>3</sub>), 2.35 (m, 1H, H2'), 2.17 (m, 1H, H2"), 1.81 (s, 3H, 5CH<sub>3</sub>), 1.2 (t,  $J = 3.6$  Hz, 9H, 3 x CH<sub>3</sub>) <sup>13</sup>C NMR (CDCl<sub>3</sub>)  $\delta$  163.7 (C4), 150.4 (C2), 136.2 (C6), 110.7 (C5), 86.9 (C4'), 84.6 (C1'), 75.4 (C3'), 63.9 (C5'), 39.1 (C2'), 12.4 (5-CH<sub>3</sub>), 55.1, 96.1 (DMT-C), 45.8 (N-CH<sub>2</sub>-), 8.4 (N-CH<sub>2</sub>-CH<sub>3</sub>).

### 3.8.26 5'-O-(p-toluenesulphonyl)thymidine 33

A solution of p-toluenesulfonyl chloride (5 g, 26 mmol) in dry pyridine (20 ml) was added to the solution of thymidine (32) (4.48 g, 20 mmol) in dry pyridine (5 ml) at 0°C. Reaction mixture was stirred at 0°C for 1 hr. and kept at 4°C for 2-3 days. Reaction was monitored by TLC. Pyridine was removed under vacuum and the residue obtained was triturated with diethyl ether, to obtain a white solid which was further crystallized from EtOH to get 33 (4.96 g, 63%) M. P. = 177°C (decomp), R<sub>f</sub> (solvent A) = 0.6,  $\lambda = 265$  nm (MeOH,  $\epsilon$ ,  $5.28 \times 10^4$ ), <sup>1</sup>H NMR (CD<sub>3</sub>COCD<sub>3</sub>) 10.13 (brs, 1H, NH), 7.87 (d,  $J = 8.3$  Hz, 2H, Ar-H), 7.53 (d,  $J = 8.3$  Hz, 2H, Ar-H), 6.35 (t,  $J = 6.7$  Hz, 1H, H1'), 4.9 (d,  $J = 3.33$  Hz, 1H, OH), 4.43 (m, 1H, H3') 4.32 (m, 2H, H5' & H5"), 4.08 (m, 1H, H4'), 2.5 (s, 3H, ArMe), 2.3 (t,  $J = 9.2$  Hz, 2H, H2' & H2"), 1.87 (s, 3H, 5-CH<sub>3</sub>), IR (nujol) cm<sup>-1</sup> 1370 and 1190 (O=S=O), m/e 155 (CH<sub>3</sub>-C<sub>6</sub>H<sub>4</sub>-SO<sub>2</sub>), 126 (C<sub>5</sub>H<sub>6</sub>O<sub>2</sub>N<sub>2</sub>).

### 3.8.27 N<sup>6</sup>-Benzoyl-2'-deoxy adenosine 40

2'-Deoxyadenosine (10) (1.5 g, 6 mmol) dried by co-evaporation with pyridine and was suspended in dry pyridine (30 ml). Trimethylchlorosilane (3.8 ml, 30 mmol) was added at 0°C. The mixture was stirred for 15 minutes and to this was added benzoyl chloride (3.6 ml, 30 mmol). The reaction mixture was allowed to come to room temperature and stirred for 2 hrs. after which it was cooled in an ice bath and quenched with water (12 ml). After 5 minutes it was treated with aqueous ammonia (12 ml, 29%) at

room temperature for 30 minutes. The mixture evaporated to dryness. The residue was dissolved in water (110 ml). It was washed with diethyl ether and the aqueous layer on cooling yielded **40** (1.73 g, 82%).

### 3.8.28 N<sup>6</sup>-Benzoyl-5'-O-(4,4'-dimethoxytrityl)-2'-deoxy adenosine **41**

N<sup>6</sup>-benzoyl-2'-deoxyadenosine **40** (1.4 g, 3.9 mmol) was dissolved in anhydrous pyridine (12 ml) and the solution evaporated to dryness. The solid was dissolved in pyridine (8 ml) and treated with 4,4'-dimethoxytrityl chloride (1.33 g, 4.7 mmol). The reaction mixture was stirred at room temperature for 4 hrs. Methanol (1 ml) was added to the reaction mixture to quench the reaction and extracted with CH<sub>2</sub>Cl<sub>2</sub> (3 x 30 ml). The organic layer was washed with 1 M aqueous bicarbonate (20 ml) and evaporated to dryness, resulting in a gummy mass. This was chromatographed by the short column method on a silica gel column and eluted with dichloromethane containing 1% triethylamine and increasing amounts of methanol to obtain **41** (1.72 g, 66%)

### 3.8.29 3'-O-Acetyl-N<sup>6</sup>-benzoyl-2'-deoxy adenosine **42**

Compound **41** (0.54 g, 0.76 mmol) was co-evaporated with dry pyridine. Residue was dissolved in anhydrous pyridine (8 ml) and acetic anhydride (0.6 ml, 0.91 mmol) was added and extracted with CH<sub>2</sub>Cl<sub>2</sub>. Organic layer was dried over anhydrous sodium sulphate and evaporated to dryness to get 3'-O-acetyl-N<sup>6</sup>-benzoyl-2'-deoxyadenosine. R<sub>f</sub> (solvent B) 0.83. This was then dissolved in CH<sub>2</sub>Cl<sub>2</sub> (1ml) and cooled by immersing in an ice bath. To this 2 % dichloroacetic acid in dichloromethane was added till the reaction was completed. Progress of the reaction was monitored by TLC. Dilute The reaction mixture with CH<sub>2</sub>Cl<sub>2</sub> (25 ml) and washed with saturated NaHCO<sub>3</sub> solution (2 x 10 ml) and saturated NaCl solution (10 ml). Organic layer was dried over anhydrous Na<sub>2</sub>SO<sub>4</sub> and concentrated to get a gum which was purified by silica gel column chromatography and eluted with CH<sub>2</sub>Cl<sub>2</sub>/MeOH to get **42** (290 mg, 88% yield). <sup>1</sup>H NMR (CDCl<sub>3</sub>)

$\delta$  9.35 (s, 1H, NH), 8.75 (s, 1H, H8), 8.15 (s, 1H, H2), 8 (d, J = 8.8 Hz, 2H, ArH), 7.55 (m, 3H, ArH), 6.35 (q, J = 5.9 Hz), 5.55 (d, J = 5.9 Hz, 1H, H3'), 4.25 (brs, 1H, H4'), 3.9 (m, 2H, H5' & H5"), 3.15 (m, 1H, H2'), 2.45 (m, 1H, H2"), 2.1 (s, 3H, OCH<sub>3</sub>).

### 3.8.30 Dimer 43

The 3'-phosphodiester **22** (249 mg, 0.25 mmol) and the 5'-hydroxyl compound **42** (60 mg, 0.15 mmol) were dried by co-evaporation with pyridine (1.5 ml) and the residue dissolved in dry pyridine (0.9 ml). 1-Methylimidazole (292 mg, 3.56 mmol) and MsCl (486 mg, 2.22 mmol) were added and the reaction mixture was kept stirred at room temperature for 20 minutes when TLC showed its completion. The reaction was quenched with NaHCO<sub>3</sub> (2.5 ml) and extracted with DCM (2 x 10 ml). The dried organic layer was concentrated and the resultant residue was purified by column chromatography when the dimer **43** eluted with CH<sub>2</sub>Cl<sub>2</sub>/MeOH (110 mg, 72%)

### 3.8.31 Dimer 8

Dimer **43** (110 mg, 0.1 mmol) detritylated with 2% dichloroacetic acid in dichloromethane. This was then dissolved in freshly prepared sat. MeOH-NH<sub>3</sub> (15 ml) and heated in a sealed tube at 60°C for 18 hrs. It was cooled and removal of excess of MeOH-NH<sub>3</sub> gave a residue which was purified on DEAE Sephadex A-25 column (2 cm x 12 cm). Elution was performed using TEAA buffer (pH 7.0) using a gradient from 0.01 M (200 ml) to 0.2 M (200 ml) with a flow rate of 1 ml/minute. The fractions containing desired product were pooled and lyophilised to obtain **8** as white solid (40 mg, 58%). Further purity was established by HPLC (retention time 11.6 minute, solvent A 5% acetonitrile in 0.1 M TEAA, solvent B 30% acetonitrile in 0.1 M TEAA, A to B in 20 minutes, at B 10 minutes, UV at 254 nm).  $\lambda = 260.1$  nm (H<sub>2</sub>O,  $\epsilon$ , 11.6 x 10<sup>4</sup>), <sup>31</sup>P NMR (D<sub>2</sub>O)  $\delta$  -0.49, <sup>1</sup>H NMR (D<sub>2</sub>O)  $\delta$  6.30 (t, 1H, H1'A), 5.9 (t, 1H, H1'T), 2.81 (m, 1H, H2'A), 1.59 (m, 1H, H2'T). 2.13 (m, 1H, H2"A), 2.54 (m, 1H, H2" T), 4.54 (brs, 1H, H3'A), 4.72

(m, 1H, H3'T), 4.00 (brs, 1H, H4'T), 4.17 (m, 1H, H4'A), 3.59 (m, 2H, H5' & H5" T), 3.96 (m, 2H, H5' & H5" A), 1.75 (s, 3H, 5-MeT), 8.02 (s, 1H, H2A), 8.31 (s, 1H, H8A), 7.29 (s, 1H, H6T).

### 3.8.32 Dimer 45

N<sup>6</sup>,2',3'-Tribenzoyl adenosine **44** (50 mg, 0.09 mmol) was co-evaporated in pyridine (0.5 ml) along with DMT-r(Up) **37** (110 mg, 0.12 mmol). This was then dissolved in pyridine (1 ml) to which MSNT (103 mg, 0.35 mmol) and NMI (55  $\mu$ l, 0.69 mmol) was added. After 15 minutes the reaction was quenched with aq. NaHCO<sub>3</sub> and extracted into CH<sub>2</sub>Cl<sub>2</sub> (3 x 10 ml). The organic layer was washed with saturated brine, dried and concentrated to a foam. This was chromatographed on a short column (1 cm x 6 cm) of silic gel (5 gm) using CH<sub>2</sub>Cl<sub>2</sub> containing 0.5 % TEA as eluent and monitored by TLC. The appropriate fractions were pooled and concentrated to yield **45** a white foam (108 mg, 87%). <sup>31</sup>P NMR (CDCl<sub>3</sub>)  $\delta$  -6.87 and -7.35.

### 3.8.33 Dimer 46

Dimer **45** (108 mg, 0.08 mmol) dissolved in dichloromethane (1 ml) and detritylated with dichloroacetic acid in dichloromethane (3%) at 0°C. An orange colouration was obtained immediately. After 10 minutes the product was diluted with CH<sub>2</sub>Cl<sub>2</sub> (5 ml) and extracted with aq. NaHCO<sub>3</sub> solution (10 ml). The orange red colour disappeared at this point. The organic layer was then dried and concentrated. This material was then chromatographed over silica gel (10 g) by the short column method. The column was initially eluted with dichloromethane (75 ml) and then with anhydrous THF/pyridine (3:1, v/v, 70 ml) to elute the desired product which was then concentrated under reduced pressure. The residue was dissolved in freshly prepared sat. MeOH-NH<sub>3</sub> (10 ml) and heated at 50°C in a sealed flask for 16 hrs. The solution was cooled and the excess



$\text{NH}_3$  was allowed to evaporate and the methanol was removed under reduced pressure to get the dimer **46** (46 mg, 89%)

### 3.8.34 Dimer 9.

Dimer **46** (46 mg, 0.07 mmol) was co-evaporated with THF (2 x 1 ml) and then dissolved in 1 M TBAF in THF (0.5 ml) to remove TBDMS group. After 2 hrs. the reaction was quenched with an equal volume of sterile TEAA (0.05 M, 1 ml, pH = 6.8) and loaded on to the DEAE Sephadex column (2 x 20 cm) and eluted with buffer A (0.01 M TEAA, 200 ml), B (0.2 M, TEAA, 200 ml). The fractions containing the major peak were pooled and lyophilised to get the dimer **9** (32 mg, 85%) as white solid.  $^{31}\text{P}$  NMR ( $\text{D}_2\text{O}$ )  $\delta$  -0.95,  $^1\text{H}$  NMR ( $\text{D}_2\text{O}$ )  $\delta$  6.1 (d, 1H, H1'A), 5.75 (d, 1H, H1'U overlapping with H5), 4.5 (m, 2H, H2'A and H3'U), 4.35 (brs, 2H, H5' and H5'A), 4.25 (m, 1H, 4'U), 4.2 (m, 1H, 4'A), 3.8 (m, 2H, H5' & H5'U), 8.43 (s, 1H, H8A), 8.2 (s, 1H, H2A), 7.78 (d, 1H, H6U), 5.74 (d, 1H, H5U, overlapping with H1'U).

## 3. 9. REFERENCES

1. (a) Hosseini, M. W.; Lehn, J. M.; Maggiora, L.; Mertes, K. B.; Mertes, M. P. *J. Am. Chem. Soc.* **1987**, *109*, 537. (b) Hengge, A. C.; Cleland, W. W. *J. Org. Chem.* **1991** *56*, 1972. (c) Morrow, J. R.; Trogler, W. C. *Inorg. Chem.* **1988** *27*, 3387. (d) Chin, J. *Acc. Chem. Res.* **1991**, *24*, 145.
2. (a) Breslow, R.; Anslyn, E.; Huany, D. L. *Tetrahedron* **1991**, *47*, 2365. and references cited therein (b) Barbier, B.; Brack, A. *J. Am. Chem. Soc.* **1988**, *110*, 6880. (c) Basile, L. A.; Raphel, A. L.; Barton, J. K. *J. Am. Chem. Soc.* **1987**, *109*, 7550.
3. (a) Richards, F. M.; Wyckoff, H. W. *The Enzymes* **1971**, *4*, 647. (b) Blackburn, P.; Moore, S. *The Enzymes* **1982**, *15*, 317. (c) Pace, V. C. N.; Heinemann, U.; Hahn, U.; Saenger, W. *Angew. Chem. Int. Ed. Engl.* **1991**, *30*, 343.

4. (a) Freemont, P. S.; Friedman, J. M.; Beese, L. S.; Anderson, M. R.; Steitz, T. A. *Proc. Natl. Acad. Sci., USA* **1988**, *85*, 8924. (b) Beese, L. S.; Steitz, T. A. *EMBO. J.* **1991**, *10*, 25.
5. Kim, E. E.; Wyckoff, H. W. *J. Mol. Biol.* **1991**, *218*, 449.
6. De Rosch, M. A.; Trogler, W. C. *Inorg. Chem.* **1990**, *29*, 2409.
7. (a) Uhlman, E.; Peyman, A. *Chem. Rev.* **1990**, *90*, 544. (b) Bischofberger, N.; Shea, R. G. in *Nucleic Acids Targeted Drug Design* C. L. Propst and T. J. Perun (eds), Marcel and Dekker: New York, **1992**, p 571. (c) Cook, P. D. *Anti Cancer Drug Design* **1991**, *6*, 585. (d) Zon, G. *Pharmaceutical Research* **1988**, *5*, 539. (e) Cohen, J. S. (ed) *Topics in Molecular Structural Biology* Macmillan Press, **1989**, *12*, p 79. (f) Matteucci, M.; Kuei-Ying, L.; Butcher, S.; Moulds, C. *J. Am. Chem. Soc.* **1991**, *113*, 7767.
8. Stein, C. A.; Cohen, J. S. *Cancer Res.* **1988**, *48*, 2659.
9. (a) Shelton, V. M.; Morrow, J. R. *Inorg. Chem.* **1991**, *30*, 4295. (b) Hendry, P.; Sargeson, A. M. *J. Am. Chem. Soc.* **1989**, *111*, 2521. (c) Herschlag, D.; Jencks, W. P. *J. Am. Chem. Soc.* **1990**, *112*, 1942. (d) Koike, T.; Kimura, E. *J. Am. Chem. Soc.* **1991**, *113* 8935.
10. Morrow, J. R.; Buttrely, L. A.; Shelton, V. M.; Berback, K. A. *J. Am. Chem. Soc.* **1992**, *114*, 1903.
11. (a) Breslow, R. *Acc. Chem. Res.* **1991**, *24*, 317. (b) Breslow, R.; Zhang, B. *J. Am. Chem. Soc.* **1992**, *114*, 5882. (c) Rebeck, J. Jr. *Angew. Chem. Int. Ed. Engl.*, **1992**, *29*, 245. (d) Cram, D. *Angew. Chem. Int. Ed. Engl.* **1988**, *27*, 1009. (e) Lehn, J. M. *Angew. Chem. Int. Ed. Engl.* **1988**, *27*, 89.
12. Smith, J.; Ariga, K.; Anslyn, E. V. *J. Am. Chem. Soc.* **1993**, *115*, 362.
13. Modak, S. M.; Janice, K. G.; Merriman, M. C.; Winkler, K. A.; Bashkin, K.; Stern, M. K. *J. Am. Chem. Soc.* **113**, 283.
14. (a) Bashkin, J. K.; Gard, J. K.; Modak, S. A. *J. Org. Chem.* **1990**, *55*, 5125. (b)

- Bashkin, J. K.; McBeath, R. J.; Modak, A. S.; Sample, K. R.; Wise, W. B. *J. Org. Chem.* **1991**, *56*, 5125-5132. (c) Wang, G.; Bergstrom, D. E. *Tetrahedron Lett.* **1993**, *34*, 6725. (d) Wang, G.; Bergstrom, D. E. *Tetrahedron Lett.* **1993**, *34*, 6721.
15. Kim, J. H.; Chin, J. *J. Am. Chem. Soc.* **1992**, *114*, 9792.
16. (a) Ikehara, M.; Kaneko, M. *Tetrahedron* **1970**, *26*, 4251. (b) Ikehara, M.; Uesugi, S.; Uesugi, M. *Chem. Commun.* **1967**, 17.
17. Ti G, S.; Gaffney, B. L.; Jones, R. A. *J. Am. Chem. Soc.* **1982**, *104*, 1316.
18. RajendraKumar, G. V.; Sivakamisundari, N.; Ganesh, K. N. *Proc. Ind. Acad. Sci. (Chem. Sci.)* **1985**, *95*, 357.
19. Strazewski, P.; Tamm, C. *Angew. Chem. Int. Ed. Eng.* **1990**, *29*, 36.
20. Takeda, T.; Ikeda, K.; Mizuno, Y.; Ueda, T. *Chem. Pharm. Bull.* **1987**, *35*, 3558.
21. Gopalakrishnan, V.; Ganesh, K. N.; Gunjal, A.; Likhite, S. M. *Tetrahedron* **1991**, *47*, 1075.
22. Rinkel, L. J.; Altona, C. J. *Biomolec. Struct. Dyn.* **1987**, *4*, 621.
23. (a) Altona, C.; Sundaralingam, M. *J. Am. Chem. Soc.* **1972**, *94*, 8205. b) Altona, C.; Sundaralingam, M. *J. Am. Chem. Soc.* **1973**, *95*, 2333.
24. Gorenstein, G. (ed) *<sup>31</sup>P NMR, Principles and Applications* Academic Press, NY, **1984**.
25. Prakash, T. P.; Kumar R. K.; Ganesh, K. N. *Tetrahedron* **1993**, *49*, 4035. (b) Prakash, T. P.; Kumar, R. K.; Ganesh, K. N. *Nucleosides & Nucleotides* **1993**, *12*, 713.
26. Gait, M. J. (ed.) *"Oligonucleotide synthesis a practical approach"* IRL Press, Oxford, **1985**.
27. Efimov, V. A.; Reverdatto, S. V.; Chakhmakhcheva, O. V. *Nucleic Acid Res.* **1982**, *10*, 6675.
28. Singh, D.; Kumar, V.; Ganesh, K. N. *Nucleic Acids Res.* **1990**, *18*, 3339.

**CHAPTER 4**  
**STUDIES ON METAL ION MEDIATED HYDROLYSIS OF**  
**MODIFIED DINUCLEOTIDES**

#### 4.1 INTRODUCTION

Metal ions are well known to promote substantial acceleration of reactions in homogeneous solution.<sup>1</sup> Catalysis occurs because the metal ions have an ability to coordinate with a substrate or reactant and stabilize the transition state. In enzymatic processes involving metal ion catalysis, the enzyme provides specificity towards substrate and is involved in specific complexation of metal ion to enhance the reactivity. Metal ions can either act as "super acids," as if it were a proton of magnified charge<sup>2</sup> even at neutral pH (where  $[H^+]$  is  $10^{-7}$  M) or serve as carriers of electrons in red-ox reactions.

Metal ions, including transition metals and rare earths are well known to catalyze the hydrolysis of a variety of esters and amides.<sup>3</sup> They are also known to catalyze many biologically important substitution reactions at phosphorous (V).<sup>1</sup> Hydrolysis of phosphates is one type of substitution reaction that has been widely studied and includes hydrolysis of ATP,<sup>4</sup> phosphate diester and monoester.<sup>6</sup> In these reactions, bifunctional species containing both nucleophilic ( $OH^-$ ) and an electrophilic (metal ion) centers are probably more effective. Although hydroxy metallic ions are considerably weaker bases<sup>7</sup> than hydroxide itself, they are catalytically more active by a factor of 10.

A second type of substitution reaction at phosphorus (V) promoted by metal ions is that of transesterification.<sup>8</sup> Among this class, cleavage of RNA is the most prominent example. This reaction proceeds by attack of 2'-hydroxyl group of a ribose on internucleotide phosphate to produce 2',3'-cyclic phosphate ester with concomitant cleavage of RNA strand. In hydrolysis or transesterification reactions, the metal ion may bind to the phosphate ester to activate the phosphorus center or may bind to the leaving alkoxide group to assist its departure.<sup>1</sup> The difference between hydrolysis and transesterification lies in the nature of the attacking nucleophile.

Many divalent and trivalent metal ions promote transesterification of RNA including those of  $\text{La}^{3+}$ ,<sup>9</sup>  $\text{Eu}^{3+}$ ,<sup>10</sup>  $\text{Bi}^{3+}$ ,<sup>8</sup>  $\text{Al}^{3+}$ ,<sup>8</sup>  $\text{Cd}^{2+}$ ,<sup>8</sup>  $\text{Ce}^{3+}$ ,<sup>8</sup>  $\text{Pb}^{2+}$ ,<sup>11</sup>  $\text{Zn}^{2+}$ ,<sup>12</sup>  $\text{Cu}^{2+}$ ,<sup>12a,d,e</sup>  $\text{Ni}^{2+}$ ,<sup>12a,d,e</sup>  $\text{Co}^{2+}$ ,<sup>12d,e</sup>  $\text{Mn}^{2+}$ ,<sup>13</sup> and  $\text{Mg}^{2+}$ .<sup>14</sup> Recently, metal complexes of polydentate ligands have attracted focus for RNA transesterification. The macrocyclic complexes modulate the efficiency of cleavage by keeping the metal ion in solution, without leading to formation of the metal hydroxide or metal-nucleotide complexes. Metal-ion promoted cleavage is slow at 37°C and attempts to accelerate depends on use of bifunctional catalysis<sup>15</sup> by zinc complexes containing a pendant general base. It has been demonstrated by Breslow et al.<sup>16</sup> that imidazole and zinc together effect higher rate of dinucleotide cleavage than either reagent alone.

Although ribonuclease A does not use metal ions for catalysis,<sup>1d</sup> imidazole groups from two histidines located in the active site, act as a general acid-base system. The positively charged component of this system- the imidazolium ion, conceptually, behaves like a metal-ion in electrophilic catalysis. RNA cleavage with  $\text{Zn}^{2+}$ -imidazole is not an exact mimic of RNase since imidazole is not an integral part of the molecule. However, studies on this system has led to a deeper understanding of the mechanism of RNA hydrolytic reaction, in particular, the nature of the first step.<sup>16</sup> Chapter I gives a more detailed introduction to the use of other metal-complexes in phosphate hydrolysis.

In light of the above facts, it was thought worthwhile to investigate metal ion promoted cleavage of dinucleotides conjugated with histamine **1**, **2** and **3** and ethylenediamine **4** and the unmodified dinucleotide r(UpA) **5**, that were synthesized as in Chapter III. It was envisaged that the covalently linked catalytic imidazole, in proximity to the phosphate, may bring acceleration of the hydrolysis or transesterification reaction compared to the unmodified dinucleotide. It was indeed found that in presence of  $\text{Zn}^{2+}$ ,

the hydrolysis of C8-histamino ribodinucleotide **3** was 10-15 times faster than that of unmodified ribodinucleotide **5**. Further, mechanistically, the reaction was a true enzyme mimic since it went through 2',3 cyclic-UMP as an intermediate, generated in first step by an intramolecular attack of 2'-OH on phosphodiester bond, as in ribonucleases.

## 4.2 RESULTS AND DISCUSSION

### 4.2.1 Hydrolysis of **1-5** with $ZnCl_2$

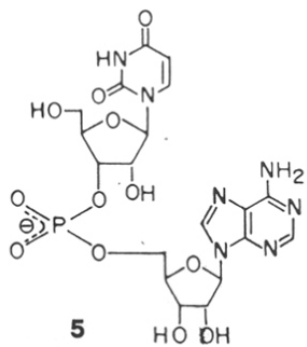
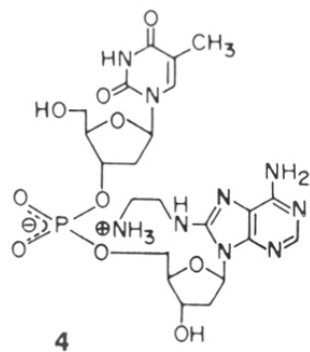
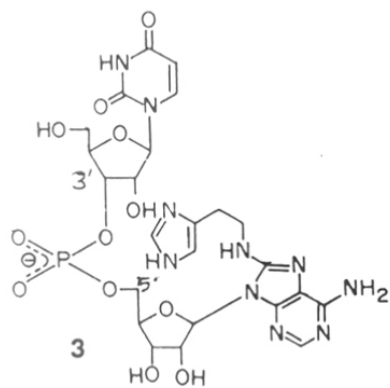
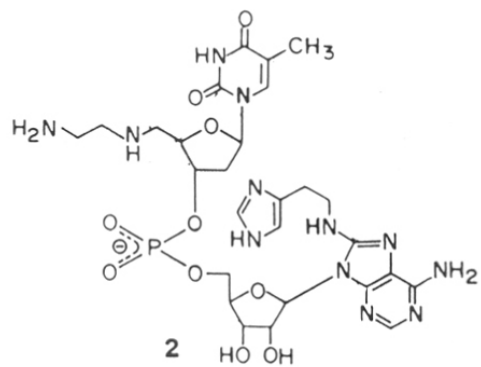
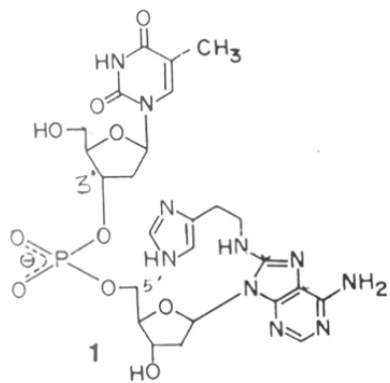
The dinucleotides **1-5** were subjected to reactions with  $CuCl_2$ ,  $NiCl_2$ ,  $CoCl_2$ ,  $MgCl_2$  and  $ZnCl_2$  without addition of any imidazole. The substrates were incubated individually with the above salts at pH 7.0 at different concentrations of  $ZnCl_2$ , at different temperatures (30-80°C) for 24-72 hrs. and the reactions were monitored by HPLC. Except **3** and **5** all other dinucleotides showed complete absence of reaction under above conditions even at elevated temperatures of 70 °C (Table I). Compounds **3** and **5**

Table I: Cleavage reactions of dinucleotides **1-5** in presence of metal ions.

Metal salt	<b>1</b>	<b>2</b>	<b>3</b>	<b>4</b>	<b>5</b>
$CuCl_2$	-	-	-	-	-
$NiCl_2$	-	-	-	-	-
$CoCl_2$	-	-	-	-	-
$MgCl_2$	-	-	-	-	-
$ZnCl_2$	-	-	+	-	+

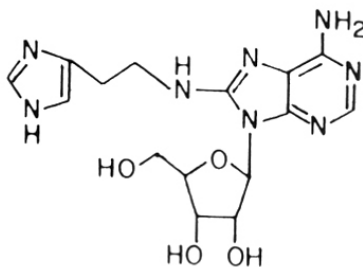
+ Hydrolysis

- No hydrolysis





cleaved in presence of  $ZnCl_2$  whereas in presence of other metal ions it did not show any cleavage. Reactions of **3** and **5** with  $ZnCl_2$  showed formation of cleavage products even at  $40^\circ C$ . In case of **3**, the reaction was completed within 10-12 hr. at  $70^\circ C$  and led to appearance of 2 products (**Fig. 1**). The peak eluting at 23.8 min was identified as the 5'-OH nucleoside (**6**) by comparison and coinjection with an authentic sample of **6** available by prior work (Chapter III). This meant that the only other product of reaction eluting at 15.1 min must correspond to the phosphate component which could be one or all of the following: 2',3'-cUMP, 3'-UMP or 2'-UMP. These have very close retention times in HPLC and their analysis and identification is discussed later.

**6**

Irrespective of the actual nature of the peak at 15.1 min., it is apparent that the cleavage was taking place at P-O5' bond rather than O3'-P bond. This is similar to the enzymatic cleavage of RNA which leads to the formation of 5'-OH component and 3'-phosphate residue. The well known alkaline hydrolysis too proceeds by cleavage at P-O5' bond to generate 5'-hydroxy component and a mixture of 2' and 3'-phosphates.

The unmodified ribodinucleotide **5** also behaved similarly in  $ZnCl_2$  reactions with and without addition of stoichiometric amount of imidazole (**Fig. 2**). It yielded the corresponding 5'-OH **7** and 3'-phosphate **8** components with elution times of 15 min

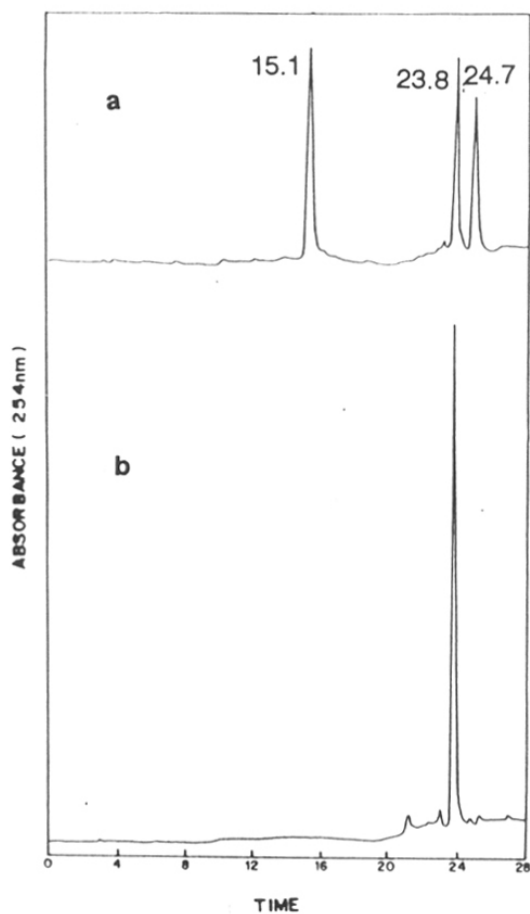


Fig. 1 a) Reverse phase HPLC of the product of the cleavage reaction of **3** Reaction conditions : r-UpA-Hist. **3** ( $1.7 \times 10^{-5}$  M) with  $\text{ZnCl}_2$  ( $1 \times 10^{-3}$  M) in HEPES Buffer (pH 7) incubated at  $55^\circ\text{C}$ . HPLC conditions, programme 3 (See exptl.).  
b) HPLC of compound **6**, HPLC conditions, programme 3 (See exptl.).

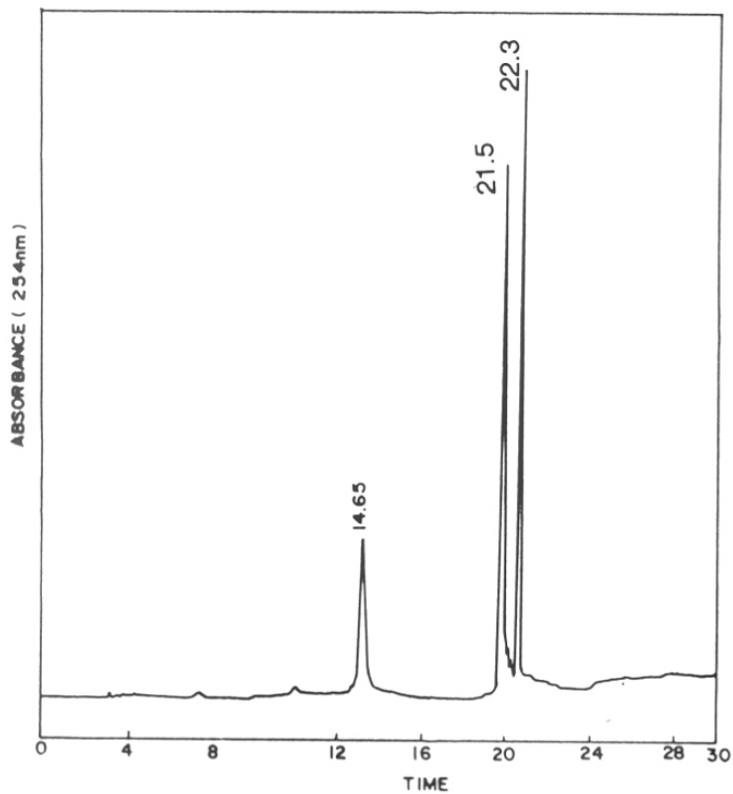
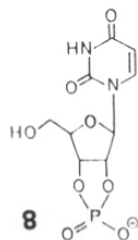
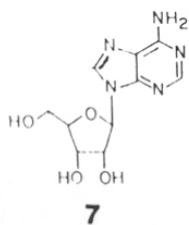


Fig. 2 Reverse phase HPLC of the product of the cleavage of **5** Reaction Conditions : rUpA **5** ( $1.7 \times 10^{-5}$  M)  $\text{ZnCl}_2$  ( $1 \times 10^{-3}$  M) Imidazole ( $0.5 \times 10^{-3}$  M) HEPES buffer (pH 7),  $55^\circ\text{C}$  HPLC condition: programme 3 (see experimental)



and 21.5 min respectively. The formation of above products indicate that C8 modification does not lead to any change in the cleavage pattern in  $\text{ZnCl}_2$  reaction and the hydrolysis occurs with cleavage at P-O5' site.

The reaction was not seen with metal-ions other than  $\text{Zn}^{2+}$ , and this means a specific involvement of  $\text{Zn}^{2+}$ , probably as an electrophilic catalyst or by complexing with substrate in some way to bring about phosphate scission. The non observance of this reaction with 2'-deoxy analogues **1** and **2** suggested the prime requirement of the 2'-hydroxyl group for the reaction. This suggests an intramolecular attack of 2'-OH to generate 2'3'-cyclic phosphate accompanied by cleavage of P-O5' bond to form 5'-hydroxy component **6**. It was also observed that hydrolysis of **3** was independent of  $\text{ZnCl}_2$  concentration with no significant change in reaction progress observed upon varying the concentration from 1 mM to 10 mM. In contrast to this, the unmodified dinucleotide **5** showed a decrease in reaction rate at higher  $\text{ZnCl}_2$  concentrations (10 mM).

#### 4.2.2 Reaction kinetics

In order to evaluate the catalytic efficiency imparted by the anchored imidazole, the kinetics of  $\text{ZnCl}_2$  reactions with **3** and **5** were investigated. The starting dinucleotides and the scission products could be clearly resolved on reverse phase HPLC and this provided a nice handle to follow the reaction kinetics. The samples taken out as aliquots at various intervals were injected onto HPLC system for peak/product analysis. The peaks were detected at 254 nm and this puts a limit on following the kinetics by quantification of product development. The two liberated products have different extinction coefficients and hence show unequal integral values. Therefore, kinetic constants were obtained by following the disappearance of starting dinucleotides as computed from HPLC peak integration. The rate constants were calculated from a plot of  $\log [A]$  (where  $[A]$  is the area percentage of the starting dinucleotide) vs time (Fig. 3) with linear re-

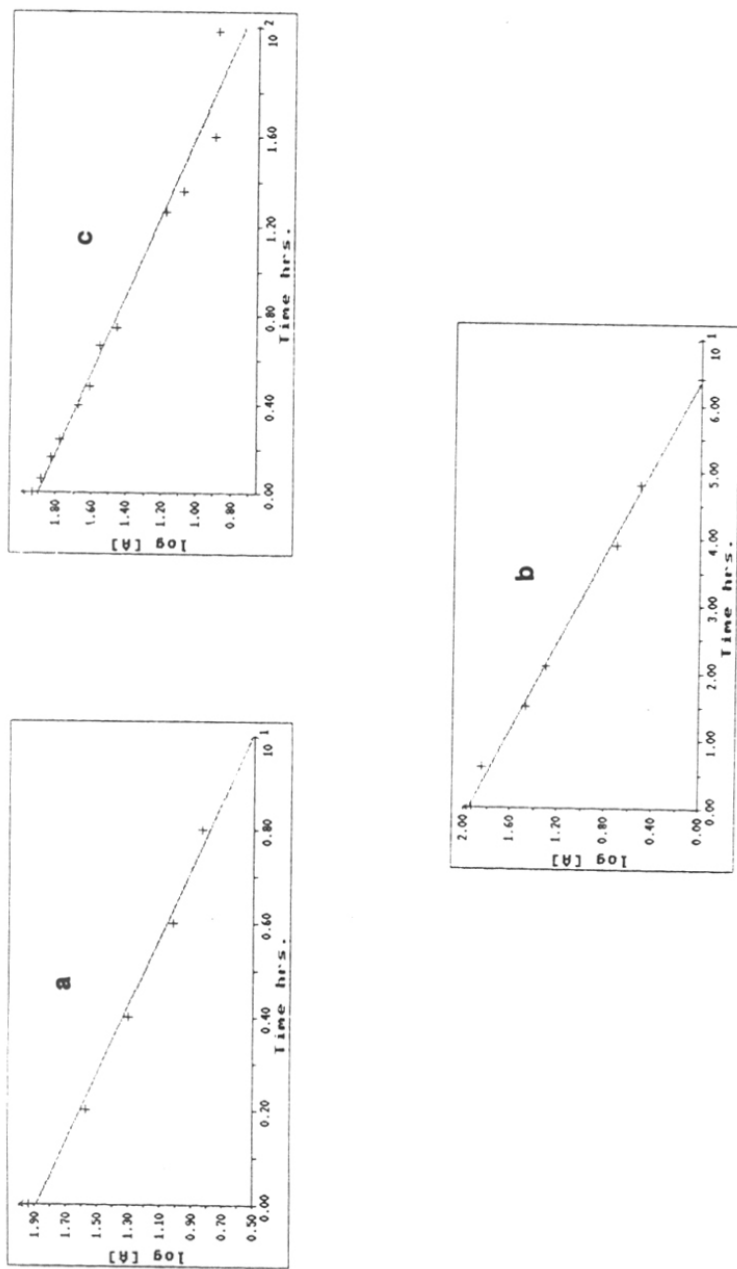


Fig. 3 Plot of logarithm of area percentage of **3** Vs time (hrs.) at 70°C, 55°C, 40°C pH 7 (HEPES buffer) in presence of 1 mM ZnCl<sub>2</sub> a) 70°C b) 55°C c) 40°C

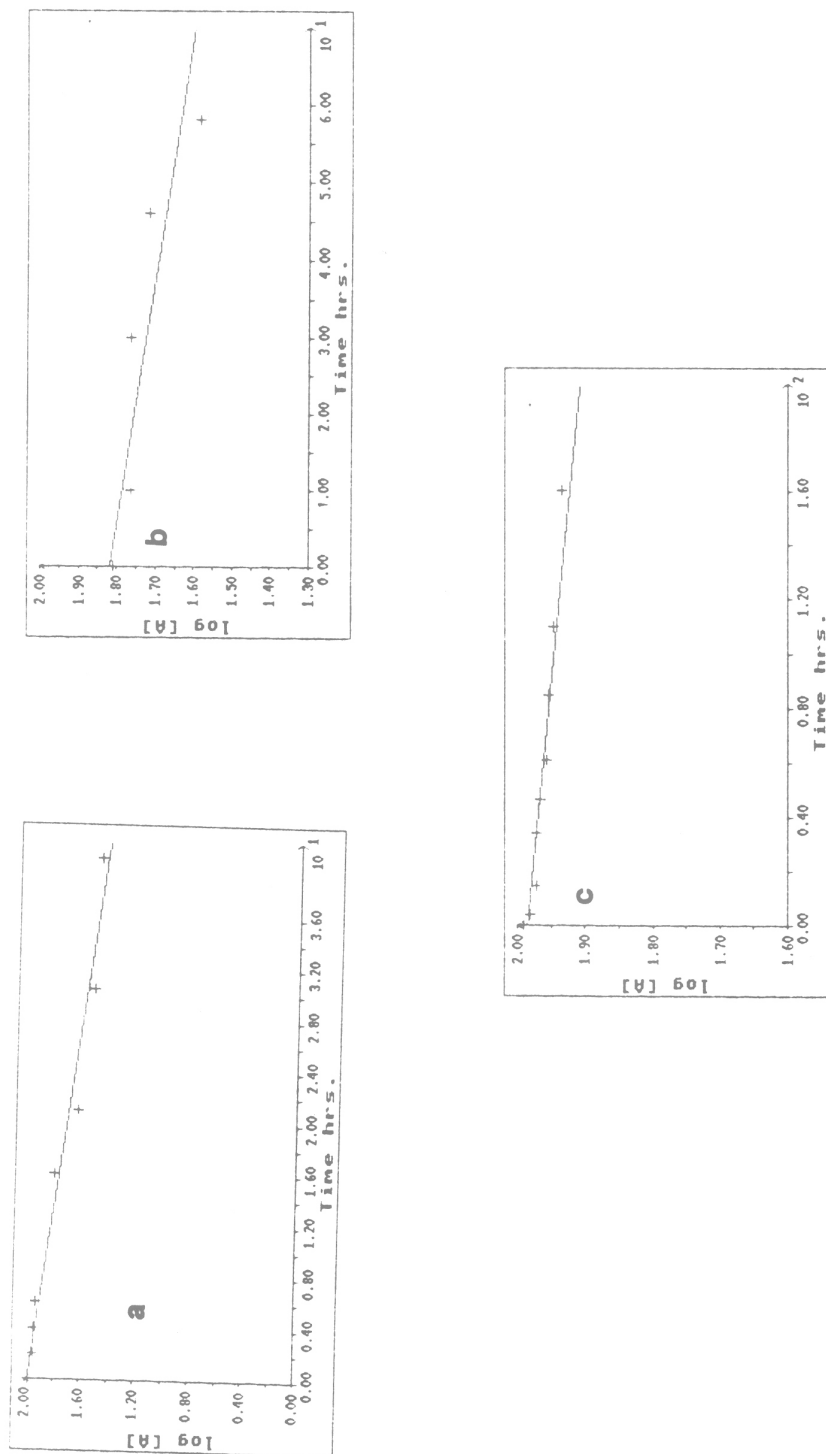


Fig. 4 Plot of logarithm of area percentage of 5 Vs time (hrs.) at 70°C, 55°C, 40°C pH 7 (HEPES buffer) in presence of 1 mM ZnCl<sub>2</sub> a) 70°C b) 55°C c) 40°C

gression analysis carried by using Enzfitter software. The reaction obeyed pseudo first order kinetics as seen from the linearity of this plot and a good fit to the first order kinetic equation.

The reactions were monitored for at least three half lives ( $3 \times t_{1/2}$ ) in case of **3**. Identical values for successive  $t_{1/2}$ 's also confirmed the first order of the reaction. The rate constants were derived from the observed slopes. The experiment was repeated for both **3** and **5** at three different temperatures 40°, 55°, and 70° C (Fig. 3, 4). Both compounds showed increase in rates at higher temperatures and Table II shows these results.

Table II: Pseudo first order rate constant for the hydrolysis reaction of **3** ( $1.7 \times 10^{-5}$  M) and **5** ( $1.7 \times 10^{-5}$  M) in presence of  $\text{ZnCl}_2$  ( $1 \times 10^{-3}$  M).

Temperature °C	K(obs.) ( <b>3</b> ) $\text{h}^{-1} \times 10^3$	K(obs.) ( <b>5</b> ) $\text{h}^{-1} \times 10^3$	$\frac{\text{K(obs.) (3)}}{\text{K(obs.) (5)}}$
40	12.9	0.8912	14.5
55	70.6	7.24	9.6
70	316.6	30.37	10.1

It is seen from above Table that hydrolysis of r(UpA)-His **3** is 10-15 times faster than that of r(UpA) **5** at the range of temperatures investigated. On the face of it, this was a gratifying result since ribodinucleotide **3** was designed with the rationale that proximity of imidazole may accelerate the hydrolysis of phosphate by intramolecular

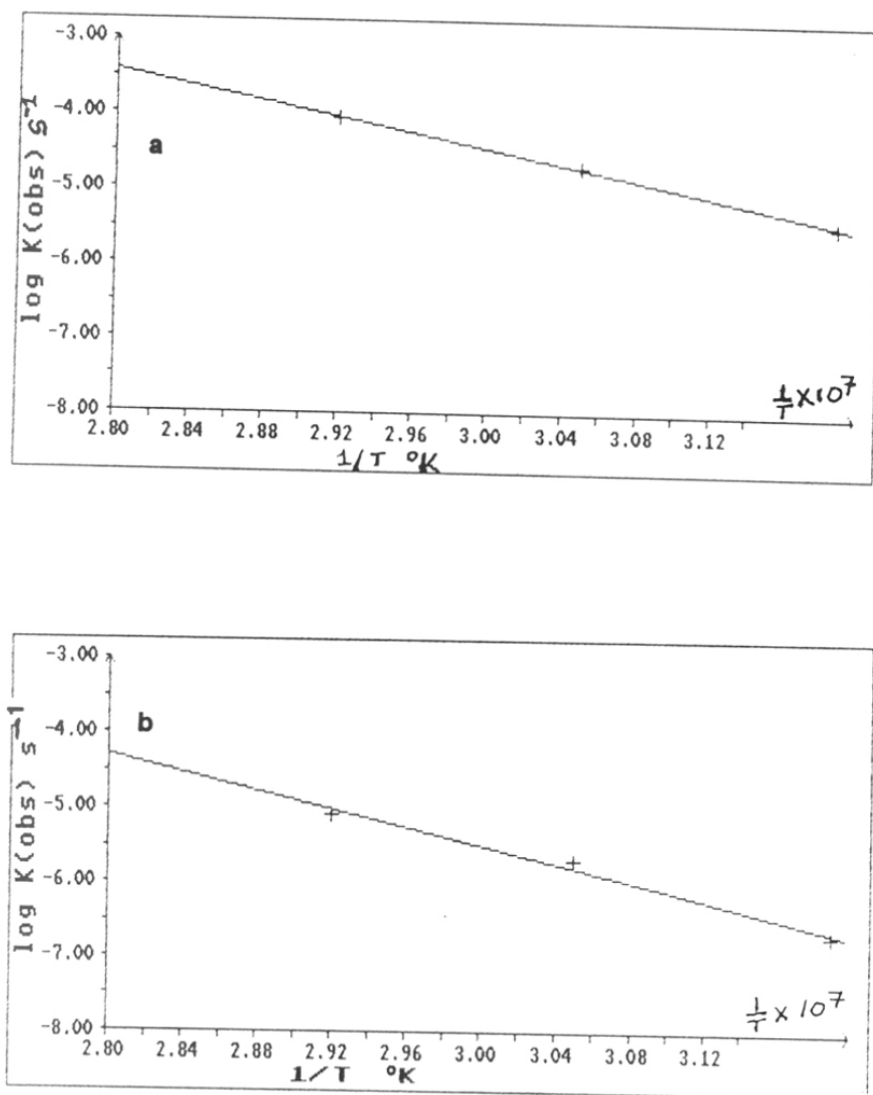


Fig. 5 Effect of temperature on  $K(\text{obs})$  for the hydrolysis of **3** (a) and **5** (b) in presence of  $\text{ZnCl}_2$  ( $1 \times 10^{-3}$ ), pH 7, HEPES buffer.



Table III: Dependence of K on ZnCl<sub>2</sub> concentration at 55°C.

ZnCl <sub>2</sub> mM	K(obs.) (3) h <sup>-1</sup> x 10 <sup>3</sup>	K(obs.) (5) h <sup>-1</sup> x 10 <sup>3</sup>	$\frac{K(\text{obs}) (3)}{K(\text{obs}) (5)}$
10	74	1.2	61.7
1	70.6	7.2	9.6

effects. The reaction rates were also measured at higher concentration of ZnCl<sub>2</sub> (10 mM), for both **3** and **5** and the enhancement in rates for **3** over **5** under these conditions was about 61 (**Table III**).

#### 4.2.3 Evaluation of thermodynamic parameters

The measurements of reaction rate at different temperatures permit evaluation of Arrhenius parameters, energy of activation ( $E_a$ ), enthalpy ( $\Delta H$ ) and entropy ( $\Delta S$ ) of activation and the associated free energy change ( $\Delta G$ ), from appropriate equations. A plot of  $\log K$  vs  $1/T$  gave a straight line for both **3** and **5** and from the slope of this line the energy of activation  $E_a$  (**Fig. 5**) could be obtained. From a knowledge of  $E_a$ , the enthalpy of activation ( $\Delta H$ ) could be calculated. The rate constant also permits evaluation of  $\Delta G$  by standard method which also allows computation of  $\Delta S$ . **Table IV** shows the values of various activation parameters evaluated for **3** and **5**. It is noticed that the energy of activation for unmodified dinucleotide **5** is about 4 kcal/mole higher than that of imidazole linked dinucleotide **3**. This is as expected for catalytic reactions. The free energies of activation differed only marginally ( $\delta\Delta G = 1.5$  kcal/mole). Notable differences were in  $\Delta H$  and  $\Delta S$  values. The C8 histamino r(UpA) has a catalytically favorable

Table IV: Thermodynamic activation parameters for the hydrolysis of **3** ( $1.7 \times 10^{-5}$  M) and **5** ( $1.7 \times 10^{-5}$  M) at 70°C,  $\text{ZnCl}_2$  ( $1 \times 10^{-3}$  M). Standard error in all calculations were + 0.025 - + 0.04 kcal mol<sup>-1</sup>.

Compound	$E_a$ kcal mol <sup>-1</sup>	$\Delta H^*$ kcal mol <sup>-1</sup>	$\Delta G^*$ kcal mol <sup>-1</sup>	$\Delta S^*$ e.u
<b>5</b>	27.1	26.4	28.1	-5.1
<b>3</b>	23.6	22.9	26.5	-10.6

lower enthalpy of activation ( $\delta \Delta H = 4$  kcal/mole) but an unfavorable large negative entropy of activation ( $\delta \Delta S = -5$  eu). The implication of these are discussed later.

#### 4.2.4 pH Dependence of $\text{ZnCl}_2$ reaction

As pointed out earlier,<sup>7</sup> although hydroxy metallic ions are considerably weaker bases than hydroxide itself, they are catalytically more active at least by a factor of 10. The observed catalysis in  $\text{ZnCl}_2$  reaction, in principle can also arise due to such metal bound hydroxide which may have a direct nucleophilic attack on the phosphate or deprotonate the 2'-OH to initiate this process. To distinguish this process from that involving the imidazole of histidine, the effect of pH on  $\text{ZnCl}_2$  reaction was studied. This was also essential since an aqueous solution of  $\text{ZnCl}_2$  is acidic and was brought to neutral pH 7.0 by addition of aqueous NaOH which may possibly give rise to some metallic hydroxide.

The reaction of **3** dissolved in buffers at various pH's (6.2, 6.52, 7.0, 7.42 and 7.9) containing 1 mM  $\text{ZnCl}_2$  was followed by HPLC analysis (see exptl.). A control containing **3** in above buffer but without any  $\text{ZnCl}_2$  was the background reaction used for analysis and it was found that hydrolysis of **3** was negligible in the absence of  $\text{ZnCl}_2$ . The pH-rate profile obtained from these experiments is shown in Fig. 6. It is seen that the profile is bell shaped, with a maximum reaction rate at pH 7.0. This is typical of acid base catalysis without any pH dependent background water reaction. This also suggested that the imidazole of C8-side chain is the active species involved in catalysis rather than metal-bound hydroxide. In the latter case, the pH rate profile would show a plateau on the basic side due to the catalytic hydroxide which remains prevalent in the basic pH regime. On the contrary, the observed results indicate that the reaction rate falls off at both acidic and basic pH region, with a maximum at neutral pH. This experiment confirms the catalytic role of imidazole from the C8 side chain of **3** in hydrolysis reaction.

#### 4.2.5 Identification of reaction products

So far, discussion is centered mainly on reaction rates calculated by the disappearance of the substrate. The identification of products, particularly the phosphate carrying component of dU and dA-His. is relevant to the mechanistic analysis. An important clue came from HPLC analysis of the kinetic experiments. Fig. 7 shows HPLC analysis of r(UpA)-His- $\text{ZnCl}_2$  reaction at 40° C done at various intervals. It is noticed that the sharp peak at 1.99 min, develops with time and stays stable even at the end of 207 hr. However, around 126 hr. a small broad peak at 2.65 min. starts appearing and grows slowly to about 10 % of the total peak at 1.99 min, by the time reaction is completed (207 hrs.)

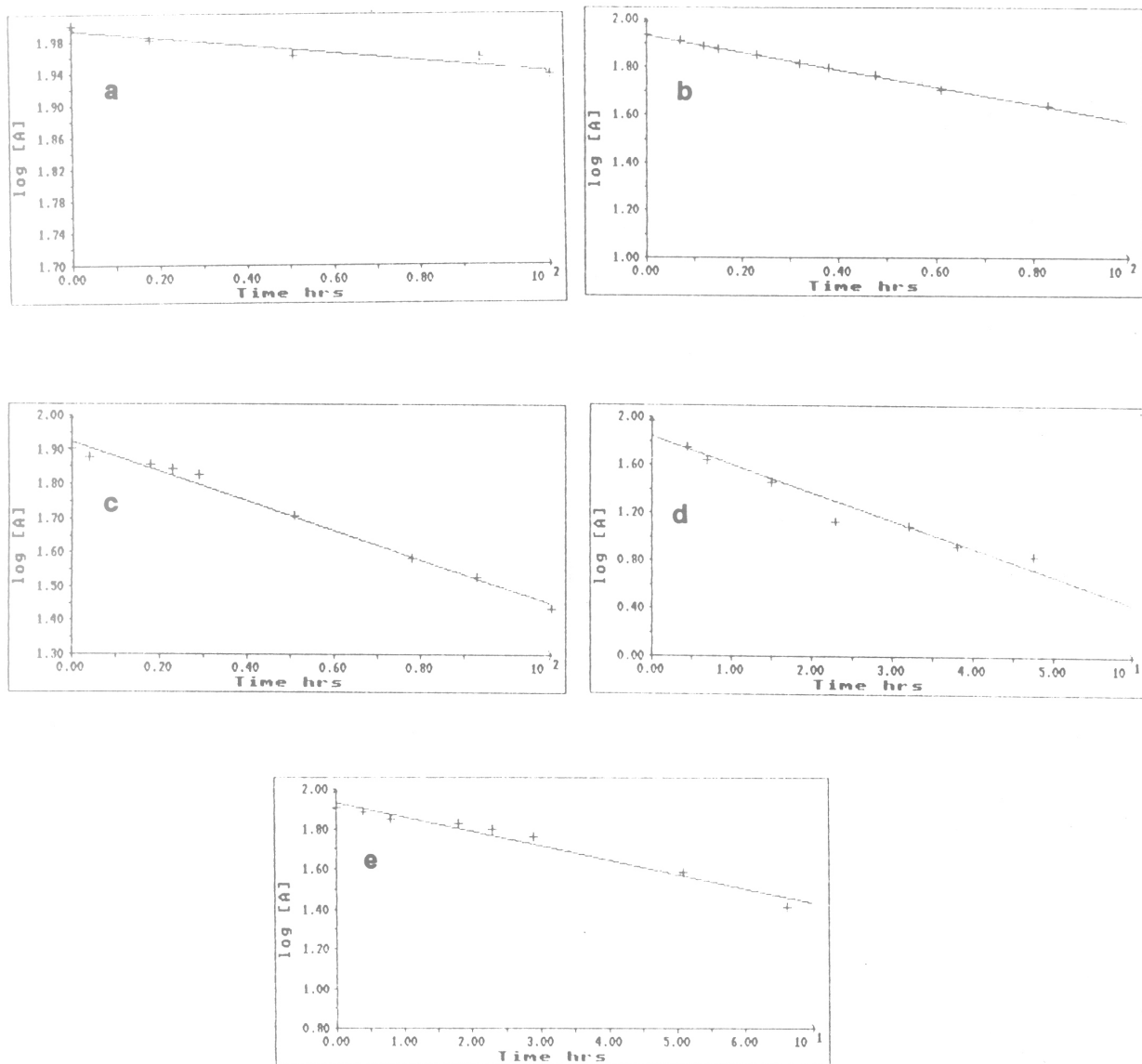


Fig. 6 a) Plot of logarithm of area percentage of 3 Vs time (hrs) at different pH's (a) 6.2 (b) 6.5 (c) 9 (d) 7.4 and (e) 7.9 at 55°C in presence of  $\text{ZnCl}_2$  ( $1 \times 10^{-3}$  M), pH 7.

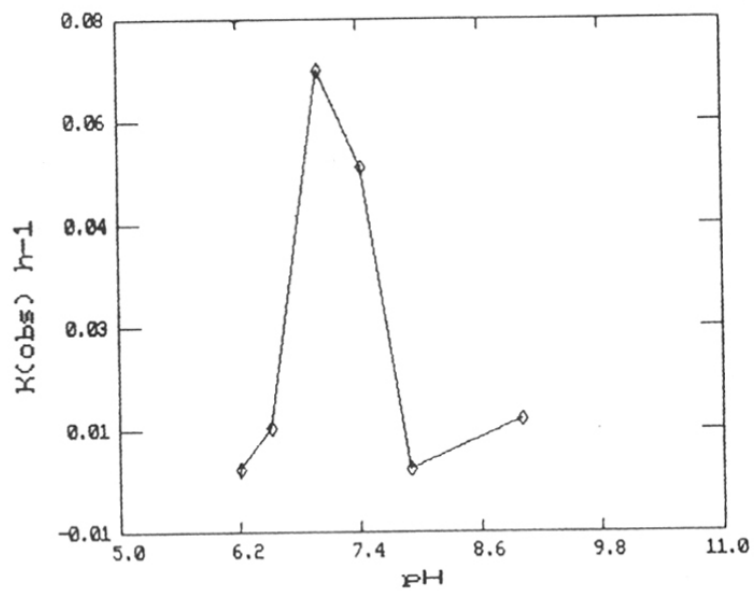


Fig. 6b Dependence of  $K(\text{obs})$  on pH for the transesterification of rUpA-Histamine 3 ( $1.7 \times 10^{-5} \text{ M}$ ) by  $\text{ZnCl}_2$  ( $1 \times 10^{-3} \text{ M}$ ) at  $55^\circ\text{C}$

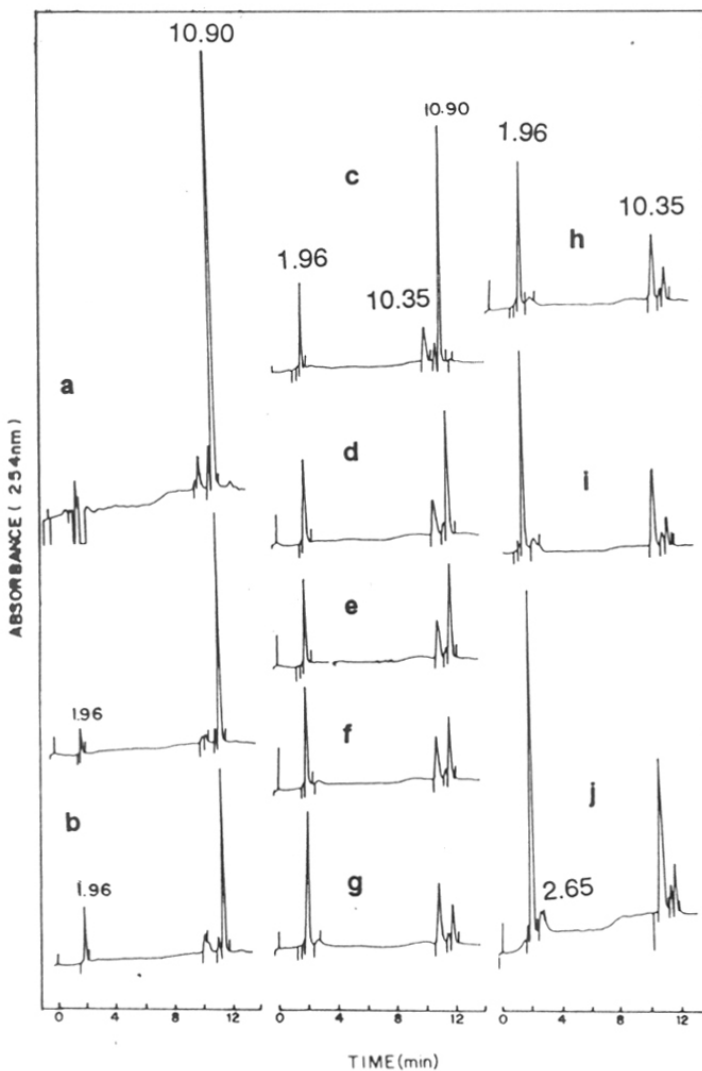


Fig. 7 HPLC of the hydrolysis product of **3** at 40°C HEPES buffer, pH 7, (a) 0 hrs. (b) 16 hrs. (c) 24 hrs. (d) 39.5 hrs. (e) 48 hrs. (f) 74.5 hrs. (g) 126.5 hrs. (h) 135.5 hrs. (i) 160 hrs. (j) 207.5 hrs. HPLC condition: programme 1 (see experimental).

**Fig. 8** depicts similar results of a hydrolysis experiment on **3** done in presence of  $\text{ZnCl}_2$  at  $70^\circ\text{C}$ . The results are much more dramatic here. The reaction is almost complete by 13 hr as seen from disappearance of **3** at 10.92 min. By 17 hrs. the minor peak appeared at 2.64 min and started growing rapidly, at the expense of peak at 1.99 min, and reaching full height by 49 hrs. At the end of 49 hrs., this initially formed sharp peak was totally transformed into a broad peak at 2.64 min. Thus the final product (phosphate, 2.64 min) observed at  $70^\circ\text{C}$  arises from an intermediate (1.99 min). A rational analysis would indicate that this intermediate is probably cyclic 2',3'-UMP which would subsequently hydrolyse to a mixture of 2' & 3'-monophosphates. The 2' and 3'-monophosphates have very close retention times in HPLC and proved to be quite difficult to resolve. We therefore sought to compare the product profile of  $\text{ZnCl}_2$  reaction with those of alkali and enzymatic hydrolytic reactions.

**Fig 9** shows such a comparison of products from hydrolysis of **3** and **5** under three conditions:  $\text{ZnCl}_2$ , alkali and enzyme. It is well known that the enzymatic hydrolysis of RNA leads to formation of only 3'-monophosphate while alkali hydrolysis would lead to a mixture of 2' and 3'-phosphates. In both cases, it is difficult to detect the intermediate 2',3'-cUMP. Although 2' and 3' phosphates proved difficult to resolve, the alkali hydrolyzed product clearly showed a doublet feature in both cases (in **3**, resolution is less and only a shoulder is seen). In contrast, the enzyme product in both cases showed a fairly sharp peak from the reaction. The  $\text{ZnCl}_2$  reaction indicated a broad peak whose shape suggests that the product is a mixture of 2' and 3'-phosphates.

Thus,  $\text{ZnCl}_2$  reaction of **3** and **5** led to formation of the corresponding 5'-hydroxyl components and at  $40^\circ\text{C}$ , 2',3'-cUMP is formed while at  $70^\circ\text{C}$ , the hydrolyzed products 2' and 3'-phosphates are obtained. The HPLC peak analysis gives a clear cut profile in support of above sequence of reactions.

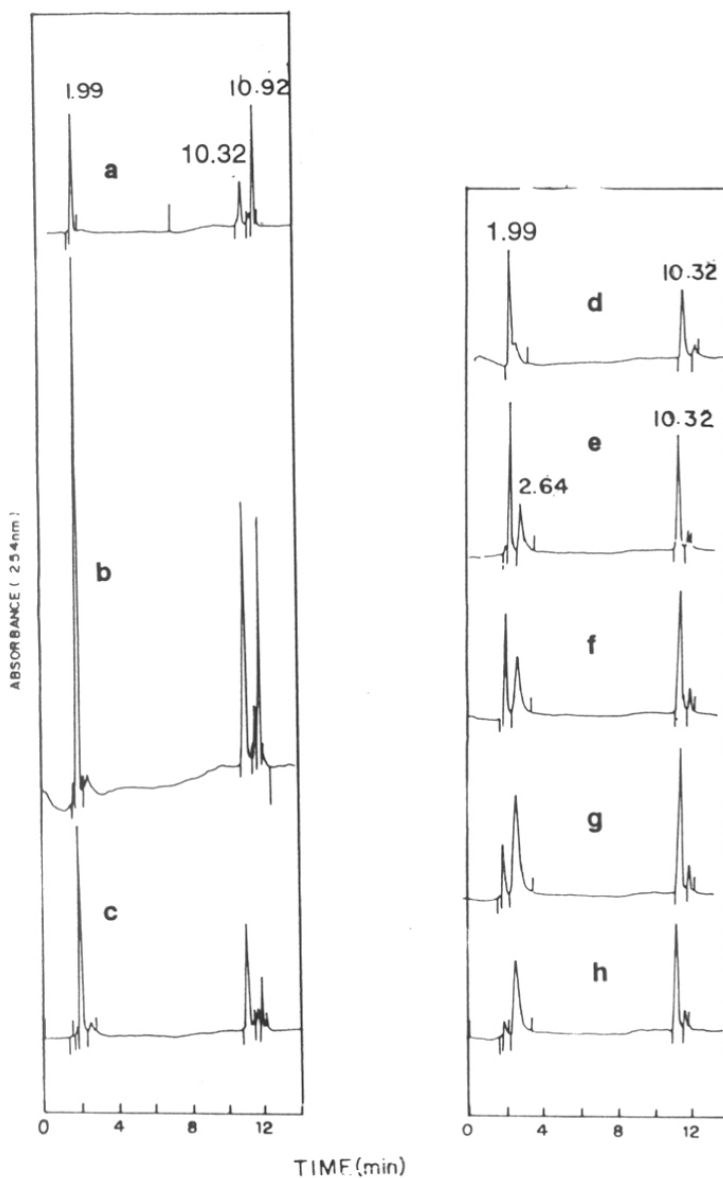


Fig. 8 HPLC of the hydrolysis product of **3** at 70°C HEPES buffer, pH 7 (a) 2 hrs. (b) 4 hrs. (c) 6 hrs. (d) 13 hrs. (e) 17 hrs. (f) 29 hrs. (g) 39.5 hrs. (h) 49 hrs. HPLC condition: programme 1 (see experimental).



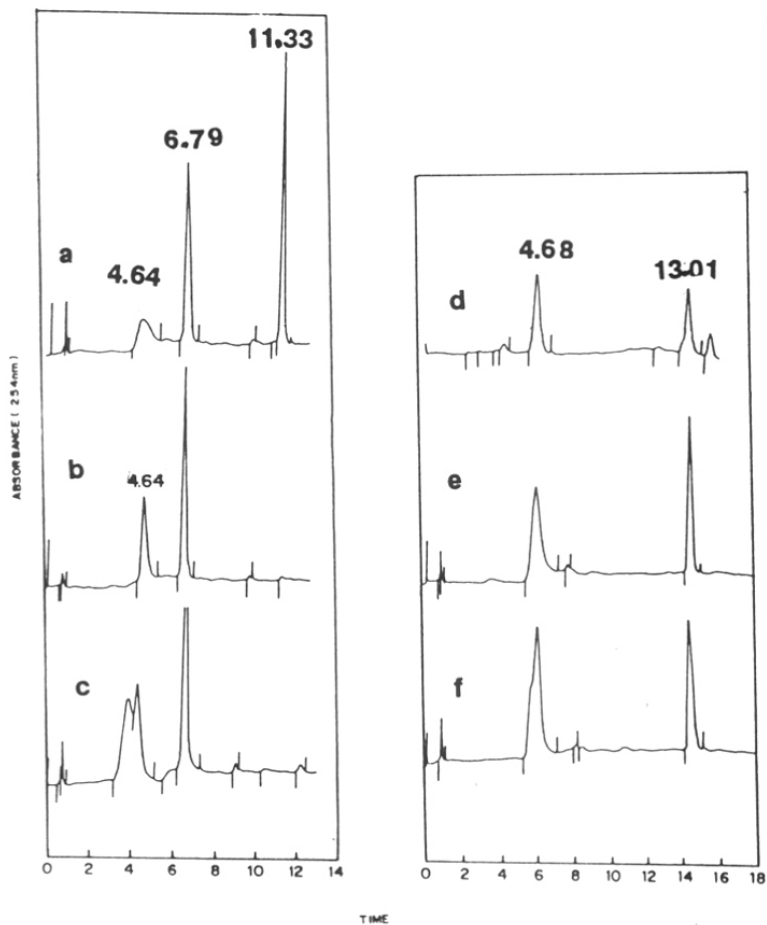


Fig. 9 HPLC chromatogram of hydrolysis product of **5** with (a) ZnCl<sub>2</sub> (1 mM) (b) ECo R1 (c) NaOH (1 M) and **3** with (d) ZnCl<sub>2</sub> (e) ECo R1 (f) NaOH (1 M). HPLC condition: programme 2 (see experimental).

#### 4.2.6 Mechanistic discussion of the reactions

**Role of Imidazole:** In biological systems, enzymes achieve the high rates for reactions by pre-organization of functional groups catalytically involved in a particular reaction.<sup>1d</sup> To mimic the enzymatic action of ribonuclease, the dinucleotide r(UpA) (**3**) containing histamino side chain at C8 was designed. It was thought that the spatial proximity of imidazole would accelerate the self-hydrolysis of **3**. The kinetic data clearly indicated a rate enhancement of 10-15 in the hydrolysis of **3** with ZnCl<sub>2</sub> as compared to that of **5** under similar conditions. This corresponds to a 10 M to 15 M effective molar concentration<sup>17</sup> of imidazole in **3**. This is a very reasonable value for local concentration effects in intramolecular nucleophilic attack of 2'-O<sup>-</sup> to generate cyclic phosphate. This is also truly akin to the mechanism used by enzymes. The rate enhancement is not that dramatic as seen in intramolecular reactions involving a direct attack of nucleophile on phosphates.

The proximity of the catalytic groups to the reaction center usually leads to a predominance of intramolecular nucleophilic over intramolecular general basic catalysis. The observed pH-rate profile and the requirement of 2'-OH, clearly rules out a direct intramolecular nucleophilic attack of Zn-bound hydroxide on phosphate residue. Imidazole with a pK<sub>a</sub> of 7 is most effective in general base catalysis under neutral conditions. It is therefore most likely that the anchored imidazole is directly involved in the catalytic cleavage by intramolecular general base catalysis.

**Role of Zn<sup>2+</sup>:** The most important characteristic of a metal ion promoted or catalysed reaction is its positive charge. For maximal effects, the metal ion should be directly associated with a substrate molecule and electronically linked to the reactive bond of substrate to be broken. A metal ion acts like a superproton<sup>17</sup> and has advantages in electrophilic catalysis: (i) it can introduce multiple positive charges whereas, a proton

introduces only a single positive charge (ii) metal ions can operate in neutral solutions where protons are ineffective and (iii) metal ion co-ordinates several donor atoms whereas a proton can co-ordinate only one. In addition, metal-bound hydroxyl ions are potent nucleophiles at neutral pH; for e.g. water bound to zinc ionizes with a  $pK_a$  of 7 in contrast to free water with a  $pK_a$  of 14. The combination of metal-bound hydroxyl and intramolecular reaction provides some of the largest rate enhancements found in strain free systems.

The observed pH-rate profile with a maximum at pH 7 (bell-shaped) in  $ZnCl_2$  promoted hydrolysis of **3** and **5** rules out any role for metal-bound hydroxide as the rate is expected to increase or stay constant at alkaline pH (plateau beyond 7.0). How else does  $Zn^{2+}$  catalyze the present reaction? It may be involved in either one or a combination of the following effects: (i) it can act as an electrophilic catalyst by neutralization of anionic charge ( $P-O^-$ ) of phosphate and thereby enhance the intramolecular nucleophilic attack of  $2'-O^-$  (ii) it may enhance the leaving group tendency of  $5'-O^-$  by stabilization via co-ordination and (iii) it may simultaneously complex with phosphate and imidazole to activate phosphate for receiving a nucleophilic attack. Although (i) is a more reasonable explanation, (ii) and (iii) cannot be completely ruled out. It has been reported earlier that  $ZnCl_2$  suppresses the  $3'-5' \rightarrow 2'-5'$  isomerization which is prevalent in imidazole catalysis.<sup>16</sup>

The data obtained from the **Fig. 8** also leads to calculations of kinetic rate constant for hydrolysis of  $2',3'$ -cUMP, following the rate of disappearance of peak at 1.99 min (**Fig. 10**). The  $K_1$  thus obtained was 12.5 times (**Table V**) slower than  $K_1$  for the first step (transphosphorylation step). The implication of this are discussed later (4.2.8).

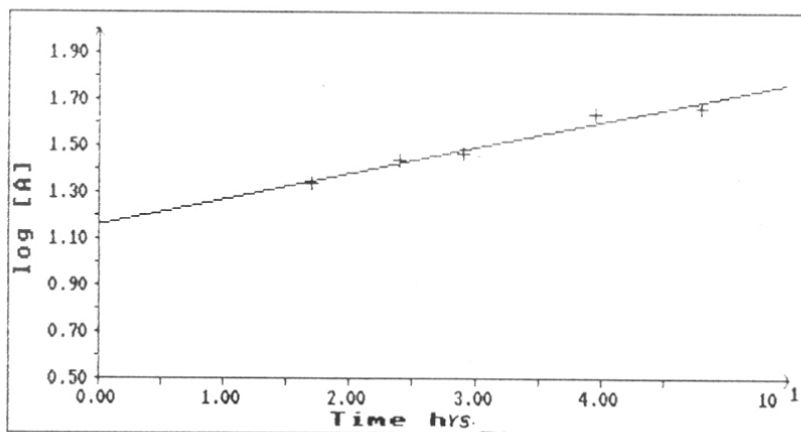


Fig. 10 Plot of logarithm of area percentage of the 2',3'-cUMP Vs time (hrs.) in the hydrolysis of **3** ( $1.7 \times 10^{-5}$  M) with  $\text{ZnCl}_2$  ( $1.7 \times 10^{-3}$  M) at  $70^\circ\text{C}$ , pH 7, HEPES buffer.

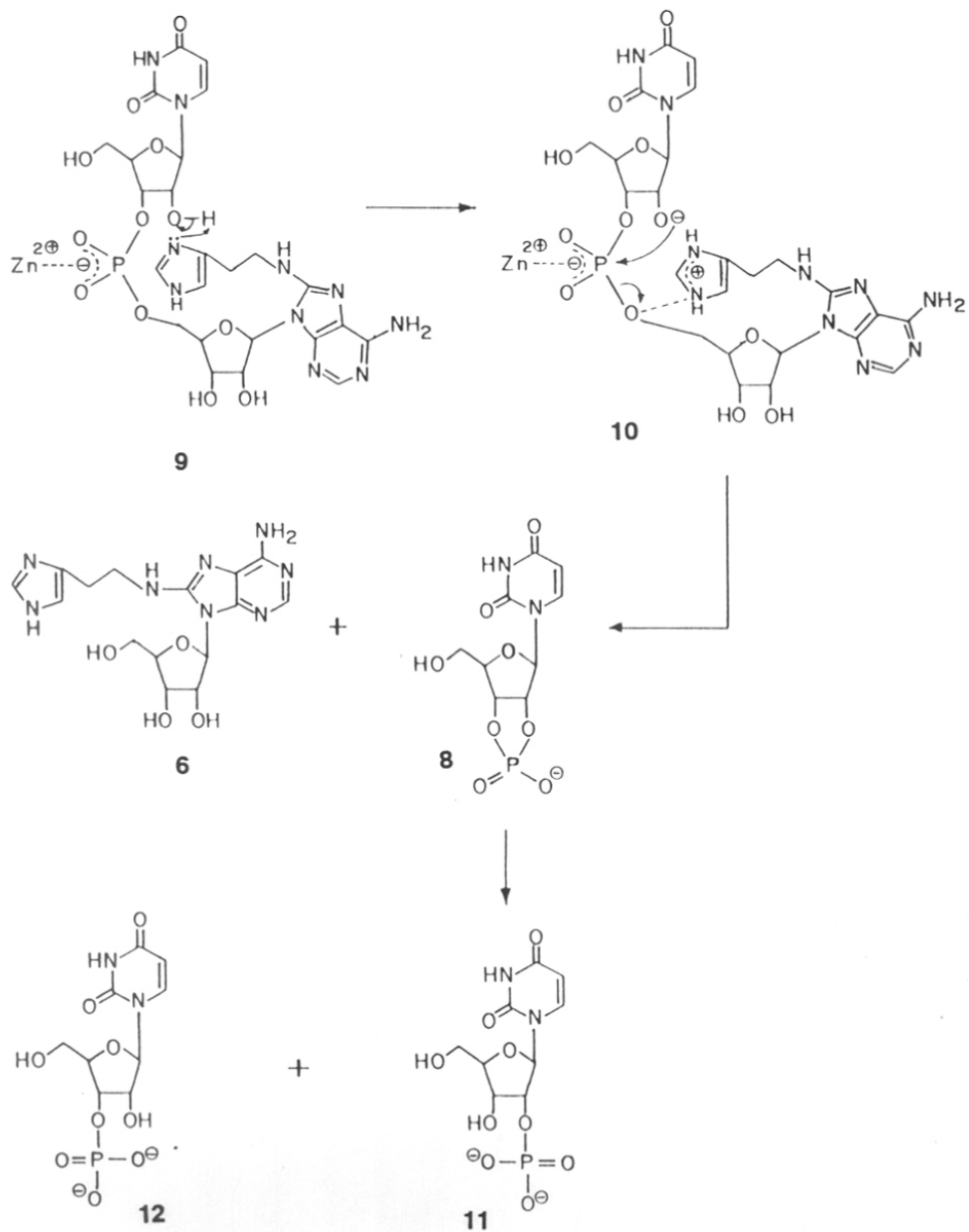
Table V: Comparison of K for transphosphorylation and hydrolysis of 2',3'-cUMP which is formed in the hydrolysis of **3**, at  $70^\circ\text{C}$ , 1 mM  $\text{ZnCl}_2$ .

Transphosphorylation	Hydrolysis of 2',3'-cUMP	$\frac{K(\text{obs.}) (\text{T})}{K(\text{obs.}) (\text{H})}$
K(obs.) (T)	K(obs.) (H)	
$\text{h}^{-1} \times 10^3$	$\text{h}^{-1} \times 10^3$	
316.6	25.4	12.5

#### 4.2.7 Kinetics and thermodynamics: Chemical and mechanistic implications

Based on the above discussion the probable chemical steps involved in  $\text{ZnCl}_2$ -promoted hydrolysis of **5** may be summarized as follows (**Scheme 1**). The first step involves electrophilic binding of phosphate by  $\text{Zn}^{2+}$ , accompanied by a rapid deprotonation of 2'-OH by the basic N of imidazole **9**. Intramolecular attack by 2'-O<sup>-</sup> on phosphate is simultaneously followed by cleavage of P-O5' bond **10**. Alcoholate anions are poor

## SCHEME 1



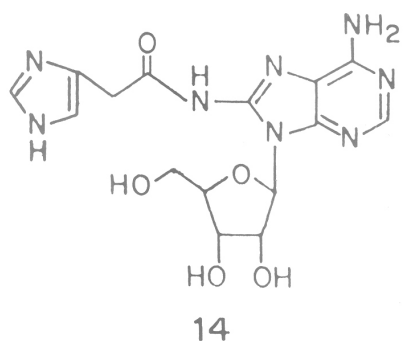
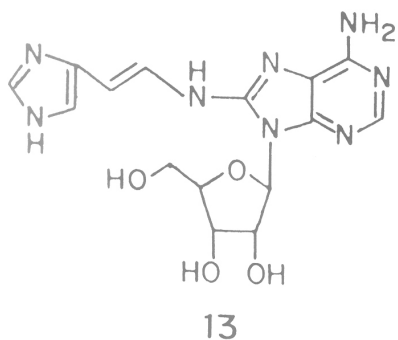
leaving groups and being strongly basic are difficult to expel. Under neutral conditions, expulsion of alcohols is aided by general acid catalysis. Highly basic groups can be activated for expulsion by complexation with metal ions. The scission of P-O5' bond with alcoholate as a leaving group is perhaps aided by either  $Zn^{2+}$  complexation or by intramolecular protonation with acidic nitrogen of C8 anchored imidazole.

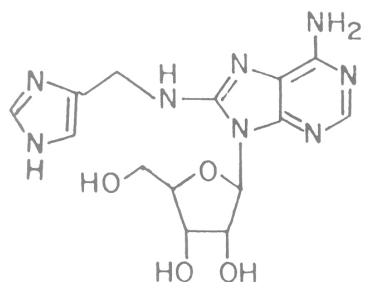
While thermodynamics describes relative tendencies of reactions to occur, kinetics is concerned with the rates at which they occur. Derivation of thermodynamic parameters involves measurement of kinetics of the reaction as a function of temperature. The fact that the acceleration observed in  $ZnCl_2$  promoted hydrolysis of **3** compared to **5** is about to 10-15 fold higher agrees with the main contributions to the acceleration coming from increased effective local concentration of imidazole in **3**. In general, intramolecular reactions may be superior either because the ground state is raised (destabilized) or the transition state is lowered. The activation parameters clearly point out a lower energy of activation (23.6 kcal/mole) for reactions involving internal imidazole in **3**, and also accompanied by a decreased enthalpy of activation. Both these effects are favorable components for catalysis. However, the more negative  $\Delta S$  observed with **3** is an unfavorable component for catalysis.

In practice, the enthalpic and entropic contributions to catalysis are not separable, since tight binding required for a reacting group simultaneously decreases both entropy and enthalpy required for the transition state formation. Normally, the rate enhancement of intramolecular reactions is associated with entropic advantage compared to a bimolecular reaction.<sup>1a</sup> Thus although proximity of a group is of overriding importance, the requirement of correct orientation for facile catalysis should also be considered. The catalyst must not only have large effective concentrations, but also possess a correct stereochemical orientation.<sup>11c</sup> This is important since intramolecular

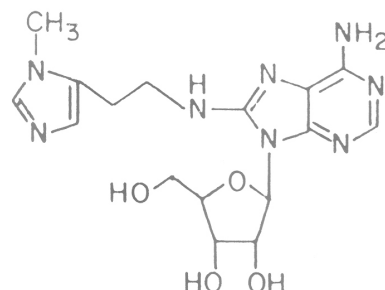
processes do not lose translational degree of freedom while rotational degree of freedom is lost compared to intermolecular reactions. The observed unfavorable  $\Delta S$  in the present reaction may be attributed to this factor. The imidazole attached to C8, though nearby, to effect higher local concentration may not have a proper orientation to enhance the catalysis dramatically. The spatial pre-disposition of side chain in **3** is also perhaps influenced by the rigid dinucleotide structure with preferred sugar conformation and glycosyl distortions.

The conformation of a molecule undergoing intramolecular catalysis can have a large effect on the catalytic rate constants and the use of derivatives having a more favorable conformation for larger intramolecular catalysis may be considered. In case of **3** such improvements may probably be achieved by introduction of double bond into the C8 side chain as in **13** or by linking via a peptide group at C8 instead of alkylamino linkage as in **14** or even by shortening it through removal of one C-atom as in **15**. All these induce conformational rigidity of spacer chain. However to be effective these modifications should not have any deleterious effects on acid-base property of imidazole ring involved in catalysis. The basicity of imidazole may also be increased by use of N-methyl imidazole in side chain **16**.





15



16

#### 4.3 Relevance to RNA mechanism

The sequence of events taking place in the depolymerization- hydrolysis of RNA by RNase<sup>18,19</sup> is represented as shown in Fig. 11. First step involves transphosphorylation reaction from the 5'-position of one nucleotide to the 2'-position of the adjacent nucleotide leading to formation of a 2',3'-cyclic phosphodiester. During the second step, the 2',3'-cyclic phosphodiester is hydrolyzed to a 3'-nucleotide. It is widely accepted<sup>19</sup> that the catalytic mechanism involves general acid-base catalysis: in the first step His 119 acts as an acid and His-12 as a base whereas in the second, the role of histidines are reversed.

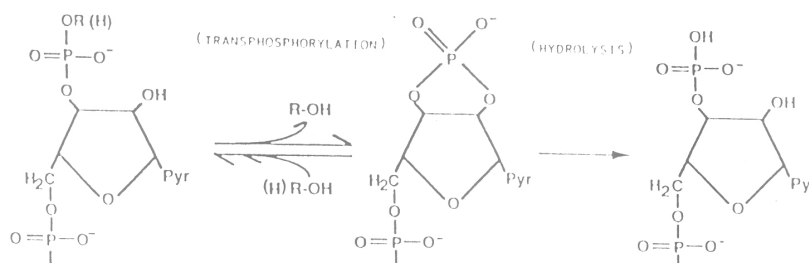


Fig. 11 Sequence of events that takes place in the depolymerization of RNA by RNase<sup>18,19</sup>.



Although formation of 2',3'-cyclic phosphate is mandatory<sup>20</sup> to the reaction mechanism, considerable ambiguity exists as to whether the reaction is taking place sequentially on the enzyme or the cyclic phosphates are actually released to the medium as true products. In the latter case, no hydrolysis takes place until all susceptible 3',5'-phosphodiester bonds have been cyclised. A recent<sup>21</sup> report has given evidence for a time lag in the formation of 3'-mononucleotide. With simple substrates, the hydrolytic reaction has been transformed to true 2',3'-cyclic nucleotide. The kinetic parameters have indicated<sup>22</sup> that the ratio of rate of transphosphorylation to the rate of hydrolysis of cyclic phosphodiester at pH 7.0 and 25°C is about 1800. The transphosphorylation rate also depends on the nature of the leaving nucleoside in both RNase A and RNase T<sub>1</sub>.

In light of the above facts on ribonuclease enzyme, the ZnCl<sub>2</sub> catalysed self cleavage of **3** can be termed as a true mechanistic mimic of ribonuclease enzymatic reaction. As discussed in the previous sections, it goes through same steps as the enzyme till the formation of cyclic phosphodiester. The only difference is that Zn<sup>2+</sup> performs the role of imidazolium (His 119) species while the C-8 linked imidazole is like His 12. The primary product of the chemical reaction has been unambiguously identified as the cyclic phosphodiester just as in case of ribonuclease. The next step of hydrolysis is slower than the first step. In the chemical reaction at 70°C, it was found that the hydrolysis of 2',3'-cUMP by ZnCl<sub>2</sub> is about 12 times slower than the first transphosphorylation step. Qualitatively, such a phenomenon has been noticed in the enzymes<sup>22</sup> as well, though the slowness is of a much larger magnitude. This difference can be attributed to the absence of catalytic imidazole in the second step in the self cleavage reaction, while such is not the case with enzymes.

In conclusion, the catalysis of self cleavage of **3** in presence of  $\text{ZnCl}_2$  mirrors same mechanistic principles as in case of enzymes and hence is a true enzyme mimic. Some possibilities for improvement in the chemical system have already been discussed.

#### 4.4 CONCLUSIONS

Metal ion mediated hydrolytic cleavage of modified dinucleotides were carried out. It was observed that the modified dinucleotide **3** was hydrolyzed in presence of  $\text{ZnCl}_2$  whereas other modified dinucleotides **1**, **2** and **4** did not react. The rate of hydrolysis of **3** in presence of  $\text{ZnCl}_2$  was 10-15 times higher than the unmodified dinucleotide **5**. The thermodynamic activation energy computed from kinetic parameters for the reaction of **3** was less than that of **5** by 4 kcal/mole. The product analysis by HPLC suggested that the reaction involves cleavage of P-O5' bond with the formation of C8-histamino dA and 2'3'-cUMP in the first step. The later subsequently got hydrolysed by a slower reaction to a mixture of 2' and 3' uridine monophosphates. Thus the designed model compound **3** is a true mechanistic mimic of the first step of the hydrolysis of RNA by RNase A.

#### 4.5 EXPERIMENTAL

##### 4.5.1 Materials

The metal salts  $\text{ZnCl}_2$ ,  $\text{CoCl}_2$ ,  $\text{NiCl}_2$  and  $\text{CuCl}_2$  were of highest purity available and obtained from S.D. Fine Chemicals (India), Imidazole was purchased from Loba Chemicals (India). Reagent grade HEPES (N-(2-hydroxyethyl)piperazine-N'-ethanesulphonic acid), MOPS (4-Morpholinepropanesulphonic acid), ACES {2-[(2-amino-2-oxoethyl)-amino]ethanesulphonic acid} and Tris {2-amino-2-(hydroxymethyl)-1,3-propanediol} were procured from Sigma (USA). The concentration of Zinc (II) was determined by titration against EDTA with Eriochrom black T as indicator. All solutions were

made with Milli-Q purified water after autoclaving. All glasswares were acid washed and oven-dried at 200°C prior to use, to avoid contamination by ribonucleases. Plasticwares (Sigma, USA) were used without special treatment and gloves were worn in all stages of preparation of solutions.

#### 4.5.2 Instrumentation

HPLC system (Waters) equipped with M440 absorbance UV detector set at 254 nm, M 6000A dual pumps, U6K injector and HP3380 integrator was used for the analysis of the reaction products. All kinetic analysis were done on Novapak C18 column (3.9 mm x 15 cm). A digital ion analyzer (Contorl Dynamics) equipped with temperature selector probe was used for all pH adjustments. The following buffers (10 mM) were used for reactions at different pH's.

pH	Buffer
6.2	ACES
6.5 and 7	HEPES
7.4 and 7.9	MOPS
9	Tris.

The concentration of dinucleotides **2**, **3**, **4** and **5** were  $1.7 \times 10^{-5}$  M as determined by UV absorption spectroscopy using following extinction coefficient (**2**,  $\epsilon = 6.07 \times 10^4 \text{ M}^{-1}\text{cm}^{-1}$ , **3**  $\epsilon = 10.89 \times 10^4 \text{ M}^{-1}\text{cm}^{-1}$ , **4**  $\epsilon = 7.82 \times 10^4 \text{ M}^{-1}\text{cm}^{-1}$ , **5**  $\epsilon = 5.52 \times 10^4 \text{ M}^{-1}\text{cm}^{-1}$ ). The concentration of metal chlorides were varied over the range 1-10 mM for the hydrolysis reaction and the temperature varied from 50-80 °C.

Following buffers and programmes were used for HPLC analysis

##### Programme 1

Buffer A = 0.1 M TEAA containing 0 % acetonitrile

Buffer B = 0.1 M TEAA containing 30 % acetonitrile

A to B in 20 min at B 10 min

Flow rate 2 ml/ min, UV at 254 nm

Programme 2

Buffer A = 0.1 M TEAA containing 0 % acetonitrile

Buffer B = 0.1 M TEAA containing 30 % acetonitrile

10 min 20 % B (linear gradient)

20 min 20 % B

50 min 50 %B

51 min 100 % B

Flow rate 2 ml/min, UV at 254 nm

Programme 3

Buffer A = 0.1% TEAA containing 0% acetonitrile

Buffer B = 0.1% TEAA containing 5% acetonitrile

Buffer C = 0.1% TEAA containing 30% acetonitrile

Time min.	%A	%B	%C
0	100	0	0
5	0	100	0
10	0	100	0
20	0	0	100
30	0	0	100

#### 4.5.3 Evaluation of thermodynamic activation parameters

The effect of temperature on the reaction was examined by determining the pseudo first order rate constant at different temperatures. Relation between energy of activation and rate constants is depicted in the equation 1.<sup>23</sup>

$$\log K = \log A - \frac{2.303 E_a}{R} \frac{1}{T} \quad 1$$

where  $K$  is pseudo first order rate constant,  $A$  is Arrhenius parameter,  $R$  is the gas constant,  $T$  is the temperature,  $E_a$  is the activation energy, which is interpreted as the amount of energy the molecule must have in order to be able to react. A plot of  $\log K$  vs  $1/T$  will give a straight line, and the slope gives the Arrhenius energy of activation. Other thermodynamic parameters were calculated by using the following equations<sup>23</sup>

$$\Delta H^* = E_a - RT \quad 2$$

$$\Delta G^* = -RT \ln \frac{K h}{T K_b} \quad 3$$

where  $K$  is the observed rate constant  $S^{-1}$  for the reaction at given temperature  $T$ ,  $K_b$  is Boltzmann's constant,  $h$  is the Planck's constant.

$$\Delta G^* = \Delta H^* - T\Delta S^* \quad 4$$

$$-\Delta S^* = \frac{(\Delta G^* - \Delta H^*)}{T} \quad 5$$

$\Delta S^*$  and  $\Delta H^*$  are the standard entropy and enthalpy of activation for the formation of the activated complex from the reactants. The results obtained are given in the **Table IV**.

#### 4.5.4 Kinetic analysis

Compound **3** ( $1.7 \times 10^{-5}$  M, 440  $\mu$ l) in HEPES buffer (pH 7, 10 mM) containing 1 mM  $ZnCl_2$  in an eppendorf heated at 55°C in a temperature controlled Julabo water bath. At different intervals of time aliquots of 40  $\mu$ l were drawn out and quenched either by keeping at 0°C (deep freeze) or by adding EDTA (1 mM). Each sample of constant volume was injected into HPLC for analysis. The peak area from HPLC data was used

for kinetic analysis. The logarithm of the area percentage was plotted against time and gave a straight line. A linear regression analysis of the data was done by using Enzfitter programme. From the slope of the line pseudo first order rate constants were calculated. A control experiment in which all the components except  $\text{ZnCl}_2$  was also carried out to check the stability of compounds for prolonged times at  $55^\circ\text{C}$ . The reactions were repeated at  $40^\circ\text{C}$  and  $70^\circ\text{C}$ . Analysis at each temperature was repeated 3 times to obtain consistent rate constants.

Kinetic analysis of hydrolysis of **5** ( $1.7 \times 10^{-5}$  M) was also done similarly with 1 mM  $\text{ZnCl}_2$  in 10 mM HEPES buffer containing 0.5 mM imidazole at pH 7. The reactions done at  $55^\circ\text{C}$  as described above. The rate constant was calculated from the semilog plot. The reaction was repeated by using 10 mM  $\text{ZnCl}_2$  in HEPES buffer containing 0.5 mM  $\text{ZnCl}_2$  and following the same procedure described above. The reaction was also repeated with the compound **5** at different temperatures  $40^\circ\text{C}$  and  $70^\circ\text{C}$  under identical conditions.

#### 4.5.5 pH Profile

The pseudo first order rate constants for hydrolysis of compound **3** was determined at different pH at  $55^\circ\text{C}$ . Solutions of different buffers (10 mM) at different pH (6.2, 6.52, 7, 7.42, 7.9, 9) containing 1 mM  $\text{ZnCl}_2$  were used for the reactions. In all experiments, corresponding controls were done only with buffer (without  $\text{ZnCl}_2$ ) at same concentrations of **3**. The reaction kinetics was followed by HPLC. A plot of rate constant against pH gave a bell shaped graph, with maximum rate constant at pH 7.

#### 4.5.6 RNase A digestion of 3 and 5

Compounds **3** and **5** (1  $\mu$ l = 0.1 OD) were treated separately with RNase A (10  $\mu$ l, 10 mg/ml) in Tris HCl (pH 7.5, 10 mM) and NaCl (15 mM). The mixture was incubated at 37°C for 1 hr and the product was analyzed by HPLC.

#### 4.5.7 Alkali digestion of compounds 3 and 5

Compounds **3** and **5** (1  $\mu$ l, 0.1 OD) were dissolved individually in 1 M NaOH (20  $\mu$ l) and heated at 37 °C for 22 hrs. The products were analyzed by HPLC.

#### 4.6 REFERENCES

1. (a) Fersht, A. (ed.) *Enzyme Structure and Mechanism* W. H. Freeman: New York, **1977**. (b) Walsh, C. (ed.) *Enzymatic Reaction Mechanisms* W. H. Freeman: New York, **1979**. (c) Jencks, W. P. (ed.) *Catalysis in Chemistry and enzymology* Dover Publications, Inc.: New York, **1969**. (d) Dugas, H.; Penney, C. (eds.) *Bioorganic Chemistry* Springer Verlag, **1981**. (e) Bruice, T. C.; Benkovic, S. J. (eds.) *Bioorganic Mechanisms* Benjamin, **1966**.
2. Westheimer, F. H. *Spec. Publ. Chem. Soc.*, **1957**, *8*, 1.
3. (a) Breslow, R.; McAllister, C. *J. Am. Chem. Soc.*, **1971**, *93*, 7096. (b) Sigman, D. S.; Jorgensen, C. T. *J. Am. Chem. Soc.*, **1972**, *94*, 1724. (c) Buckingham, D. A.; Collman, J. P.; Happer, D. A. R.; Marzilli, L. G. *J. Am. Chem. Soc.*, **1967**, *89*, 1082. (d) Kimura, E. *Inorg. Chem.*, **1974**, *13*, 951.
4. (a) Sigel, H.; Hofstetter, F.; Martin, R. B.; Milburn, R. M.; Scheller-Krattiger, V.; Scheller, K. H. *J. Am. Chem. Soc.*, **1984**, *106*, 7935. (b) Sigel, H.; Amsler, P. E. *J. Am. Chem. Soc.*, **1976**, *98*, 7390. (c) Hediger, M.; Milburn, R. M. *J. Inorg. Biochem.*, **1982**, *16*, 165.
5. (a) Morrow, J. R.; Trogler, W. C. *Inorg. Chem.*, **1988**, *27*, 3387. (b) Hendry, P.; Sargeson, A. M. *J. Am. Chem. Soc.*, **1989**, *111*, 2521. (c) Chin, J.; Banaszczyk, M.;

- Jubian, V.; Zou, X. *J. Am. Chem. Soc.*, **1989**, *111*, 186. (d) Chin, J.; Zou, X. *Can. J. Chem.*, **1987**, *65*, 1882. (f) Basile, L. A.; Raphael, A. L.; Barton, J. K. *J. Am. Chem. Soc.*, **1987**, *109*, 7550.
6. (a) Jones, D. R.; Lindoy, L. F.; Sargeson, A. M. *J. Am. Chem. Soc.*, **1983**, *105*, 7327. (b) Farrell, F. J.; Kjellstrom, W. A.; Spiro, T. G. *Science*, **1969**, *164*, 320. (c) Chin, J.; Banaszczyk, M. *J. Am. Chem. Soc.*, **1989**, *111*, 4103.
7. (a) Chaffe, E.; Dasgupta, T. P.; Harris, G. M. *J. Am. Chem. Soc.*, **1973**, *95*, 4169. (b) Palmer, D. A.; Harris, G. M. *Inorg. Chem.*, **1974**, *13*, 965. (c) Buckingham, D. A.; Engelhardt, L. M. *J. Am. Chem. Soc.*, **1975**, *97*, 5915.
8. Shelton, V. M.; Morrow, J. R. *Inorg. Chem.*, **1991**, *30*, 4295.
9. Eichhorn, G. L.; Butzow, J. J. *Biopolymers*, **1965**, *3*, 79.
10. Rordorf, B. F.; Kearns, D. R. *Biopolymers*, **1976**, 1491.
11. (a) Werner, C.; Krebs, B.; Keith, G.; Dirheimer, G. *Biochim. Biophys. Acta.*, **1976**, *432*, 161. (b) Brown, R. S.; Hingerty, B. E.; Dewan, J. C.; Klug, A. *Nature*, **1983**, *303*, 543. (c) Brown, R. S.; Dewan, J. C.; Klug, A. *Biochemistry*, **1985**, *24*, 4785. (d) Farkas, W. R. *Biochim. Biophys. Acta*, **1967**, *155*, 401.
12. (a) Stern, M. K.; Bashkin, J. K.; Sall, E. D. *J. Am. Chem. Soc.*, **1990**, *112*, 5357. (b) Eichhorn, G. L.; Tarien, E.; Butzow, J. J. *Biochemistry*, **1971**, *10*, 2014. (c) Butzow, J. J.; Eichhorn, G. L. *Biochemistry*, **1971**, *10*, 2019. (d) Butzow, J. J.; Eichhorn, G. L. *Biopolymers*, **1965**, *3*, 95. (e) Ikenaga, H.; Inoue, Y. *Biochemistry*, **1974**, *13*, 577.
13. Dange, V.; Van Atta, R. B.; Hecht, S. M. *Science*, **1990**, *248*, 585.
14. (a) Wintermeyer, W.; Zachau, H. G. *Biochim. Biophys. Acta.*, **1973**, *299*, 82. (b) Cech, T. R. *Science*, **1987**, *236*, 1532.
15. Breslow, R.; Huang, D. -L. *Proc. Natl. Acad. Sci. U. S. A*, **1991**, *88*, 4080.
16. Breslow, R.; Huang, D. -L.; Anslyn, E. *Proc. Natl. Acad. Sci. U. S. A.*, **1989**, *86*, 1746.
17. Bender, M. I.; Bergeron, R. J.; Komiyama, M. Eds. *The Bioorganic Chemistry of*



*Enzymatic Catalysis*, John Wiley and Sons. Inc.: Canada, 1984.

18. Richards, F. M.; Wyckoff, H. A. in *The Enzymes* Academic Press: New York, 1971, 4, pp 647.
19. Eftink, M. R.; Biltonen, R. L. in *Hydrolytic Enzymes* Elsevier Amsterdam, 1987, pp. 333.
20. (a) Markham, R.; Smith, J. D. *Biochem. J.*, 1952, 52, 558. (b) Brocklehurst, K.; Crook, E. M.; Wharton, C. W. *Chem. Comm.*, 1967, 63.
21. Guasch, A.; Barman, T.; Travers, F.; Cuchillo, C. M. *J. Chromatogr.* 1989, 473, 281.
22. Cuchillo, C. M.; Pares, X.; Guasch, A.; Barman, T.; Travers, F.; Nogues, V. M. *FEBS Letters* 1993, 333, 207.
23. Hosseini, M. W.; Lehn, J. M.; Maggiora, L.; Mertes, K. B.; Mertes, M. P.; *J. Am. Chem. Soc.*, 1987, 109, 537.

**CHAPTER 5**  
**AMINE TETHERED OLIGONUCLEOTIDES:- SYNTHESIS AND**  
**BIOPHYSICAL STUDIES**

## 5.1 INTRODUCTION

The previous chapter demonstrates the successful incorporation of amine moieties in dinucleotides for potential intramolecular interactions. It was also observed that appropriately positioned amine (imidazole) functionality can accelerate intramolecular phosphate ester hydrolysis. Since aliphatic amines are protonated at physiological pH, the amine tethered oligonucleotides will have diminished net charge compared to their unmodified analogs. Their inherent positive charge and chain conformational mobility may allow electrostatic interaction with anionic phosphate group of polynucleotide and induce specific structural changes in DNA.<sup>1</sup> Oligonucleotides with reduced net charge and enhanced resistance to nucleases are of current interest as antisense drugs that target mRNA.<sup>2</sup> It is known that bacteriophages use a variety of different hypermodified bases to protect their DNA from attack by phosphodiesterase present in their hosts.<sup>3,4</sup> Bacteriophage  $\phi$ w-14 is known to replace approximately half of the thymines present in its DNA with positively charged,  $\bar{\alpha}$ -putrescinythymine to achieve such protection, resulting in one hypermodified base, on an average, for every eight nucleotides.<sup>4</sup> These observations inspired us to synthesize higher homologues of amine tethered dinucleotides to study their structural properties. Polyamines are also capable of forming metal complexes that cleave DNA and oligonucleotides with tethered polyamines may have utility in site-directed scission of DNA.

Synthetic oligonucleotides are able to bind complementary nucleic acid sequences with high affinity and specificity. Yet these small DNA molecules are inherently ill-equipped to report binding or to effect chemical modification of target sequences.<sup>5</sup> In order to overcome this limitation, a number of synthetic methods have been devised for the attachment of non natural ligands to synthetic DNA<sup>6,7</sup> and these routes have furnished hybrid DNA molecules containing a wide array of ligands for use as nucleases<sup>8</sup>,

detection probes<sup>9</sup> and photoaffinity reagents<sup>10</sup> and artificial repressors.<sup>11</sup> The polyamine tethered oligonucleotides may have potential applications in such areas.

There are three synthetic approaches<sup>5b</sup> to functionally tethered oligonucleotides (FTO):

- (i) the dedicated monomer strategy
- (ii) the convertible nucleoside strategy and
- (iii) post-synthetic modifications

The first two methods are ideally suited for introduction of tethers at internal positions of an oligonucleotide and third method is normally employed for modifications at 5'-end. However, method (iii) can also be employed in combination with (i) and (ii) to introduce appropriate labels at internal base sites.

Dedicated monomer strategy: A modified monomer (amidite/H-phosphonate) is synthesized so as to contain a tethered functional group in a protected form (**Fig. 1**). This modified monomer, when supplied to the automated synthesizer along with standard amidite/phosphonates, gets incorporated at the desired position during the oligonucleotide synthesis. The resin bound fully protected FTO thus obtained is deprotected to yield the final product FTO.

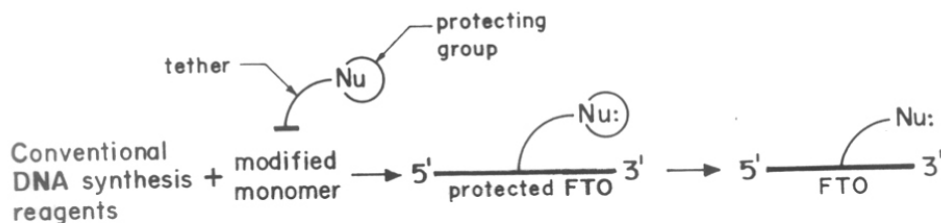


Fig. 1 Dedicated monomer strategy.

Convertible nucleoside strategy: This method also employs a modified monomer, in conjugation with conventional nucleotides and the modified monomer contains a leaving group "Y" that can be displaced by nucleophiles (Fig. 2). Use of this "convertible nucleoside" monomer in an automated synthesiser yields a convertible oligonucleotide, which can be reacted with nucleophiles to yield FTOs.

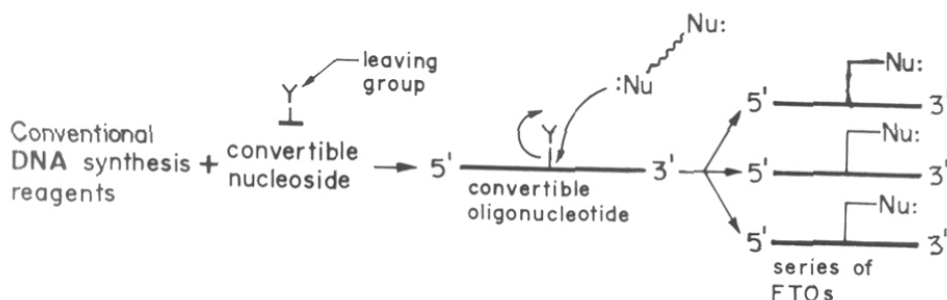
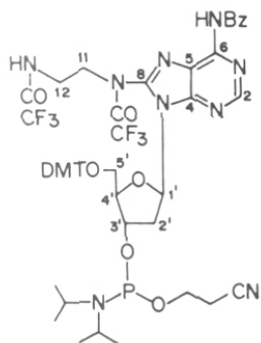
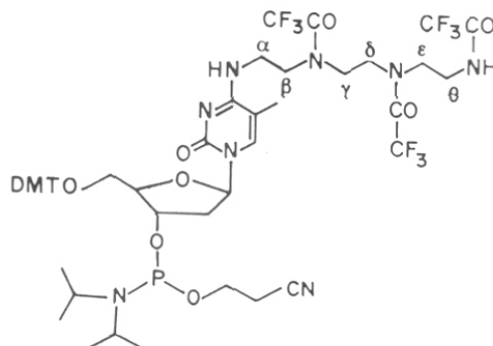


Fig. 2 Convertible nucleoside strategy.

## 5.2 PRESENT OBJECTIVES

This chapter reports synthesis of di and polyamine tethered oligonucleotides and studies on structural variations induced by these modifications. For unambiguous synthesis of such modified oligonucleotides, dedicated monomer strategy was used whereby the modified monomer was introduced at the desired position in the oligonucleotide sequence. In addition to the diamine conjugated oligonucleotides, those with polyamine conjugates were also synthesized in view of the importance of polyamines such as spermine, spermidine etc. in influencing DNA structure. For this purpose the

protected phosphoramidite monomers **1** and **2** containing tethered polyamines were chemically synthesised. These modified monomers were incorporated at the specific positions on DNA chain during the oligonucleotide synthesis using an automated synthesizer. Trifluoroacetyl group was used for N-protection of the side chain amino groups. Successful incorporation of the modified monomer into the sequence was unambiguously established by synthesis of a trinucleotide containing this modified monomer in milligram quantity for its characterization by  $^1\text{H}$  NMR spectroscopy. The stability of modified oligonucleotides were investigated by UV melting experiments. The ability of modified nucleoside monomers in base pairing with complementary nucleoside were also studied by  $^1\text{H}$  NMR titrations to evaluate binding constants.

**1****2**

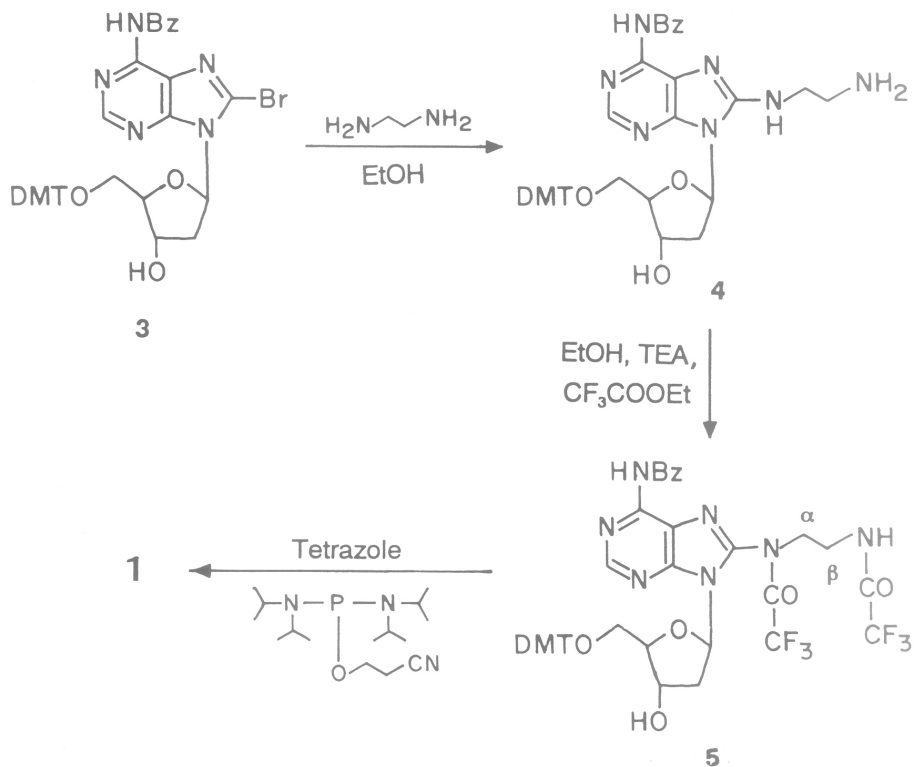
## 5.3 RESULTS AND DISCUSSION

### 5.3.1 Synthesis of modified monomers **1** and **2** and its incorporation into oligonucleotide sequences

The monomers **1** and **2** were prepared according to the **Scheme 1** and **Scheme 2** respectively. The target monomer **1** was prepared in 3 steps from the 5'-O',N<sup>6</sup>-pro-

tected-8-bromo-2'-deoxyadenosine **3** ( for synthesis, refer Chapter III, section 3.8.24). Aminoalkylation at C8 was achieved by reaction of 1,2-diaminoethane with **3** in ethanol (**Scheme 1**) to obtain **4** in 70% yield. The N<sup>6</sup>-benzoyl group was stable to these reaction conditions. Acetyl and benzoyl groups as protectors for C8-EDA group proved to be too stable for final deblocking with aq.NH<sub>3</sub> and could only be deprotected by 1M NaOH. The trifluoroacetyl group as a protector for C8-side chain amino functions had stability to solid phase DNA synthesis by phosphoramidite chemistry. Unlike acetyl & benzoyl groups it was also found to be labile for final deprotecting reagent (ammonia). The N,N'-bis(trifluoroacetyl) derivative **5** was synthesised from **4** by reacting with CF<sub>3</sub>COOEt in

### SCHEME-1



MeOH/TEA.<sup>12</sup> The 3'-hydroxyl group remained unaltered during this reaction. **5** was then transformed into the required  $\beta$ -cyanoethylphosphoramidite **1** by standard method<sup>13</sup> using tetrazole and 2-cyanoethyl-N,N,N'-tetraisopropylphosphorodiamidite in dry DCE. No N-phosphonylation was observed as seen by <sup>31</sup>P NMR of **1** which gave signals (149.9 and 149.5 ppm) characteristic of O-amidites. All compounds were purified by chromatography and characterized by <sup>1</sup>H and <sup>13</sup>C NMR (Fig. 3).

Phosphoramidite **1** was incorporated into the well studied Dickerson's dodecamer sequence at defined sites (**6**, **7**) by using an automated DNA synthesiser (Pharmacia, GA Plus). The coupling efficiencies of modified amidite **1** was similar to the commercial phosphoramidite of normal nucleosides. This indicated no significant effect of base modifications on the coupling reaction. The stability of the TFA group towards the capping/oxidation reagents used for solid phase DNA synthesis was established by treating the compound **5** with reagents for longer times (3 hrs.). **5** remained unaffected as seen by <sup>1</sup>H NMR spectroscopy. After completion of synthesis, final on-column detritylation was followed by aq. NH<sub>3</sub> treatment to yield fully deprotected oligonucleotides **6** and **7**. These were desalted on NAP-25 gel filtration column and followed by purification by FPLC (Pharmacia) over reverse phase column. HPLC analysis was carried out to establish the purity of the oligonucleotides **6** and **7** (Fig. 4).

**6**, d(CGCGAA\*<sup>T</sup>TCGCG)

**7**, d(CGCGA\*A\*<sup>T</sup>TCGCG)

The successful incorporation of **1** and retention of C8 modified dA in oligonucleotide sequences was proved by solid phase synthesis of a trinucleotide **8** on 10  $\mu$ mole scale for unambiguous characterization by <sup>1</sup>H NMR spectrum (Fig. 5, 6). The diagnostic signals due to H2 (7.95 ppm) and the two methylenes from C8-amino(2-aminoethyl)side



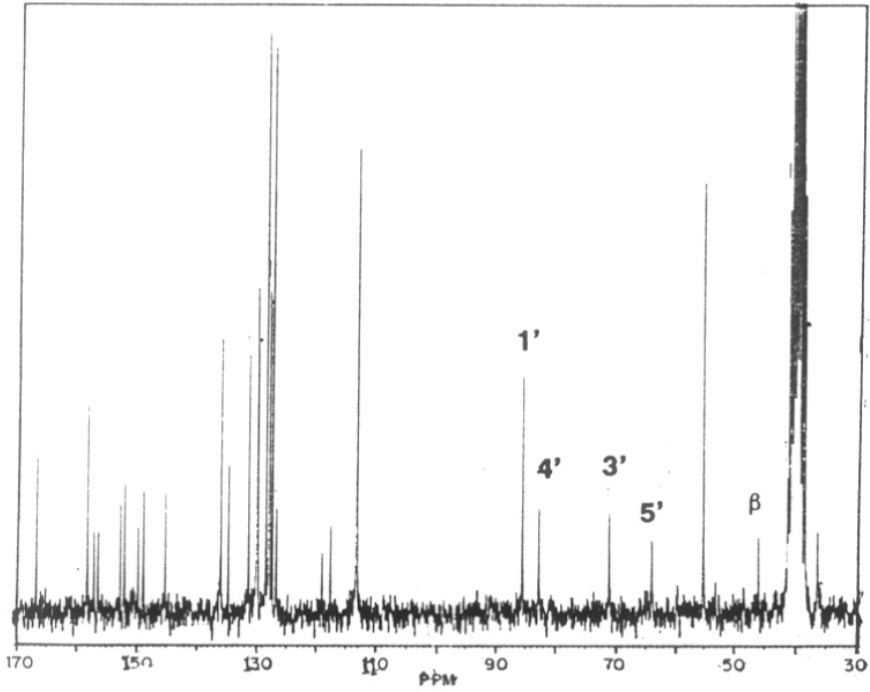


Fig. 3(a)  $^{13}\text{C}$  spectrum of 5 in  $\text{DMSO-d}_6$ .

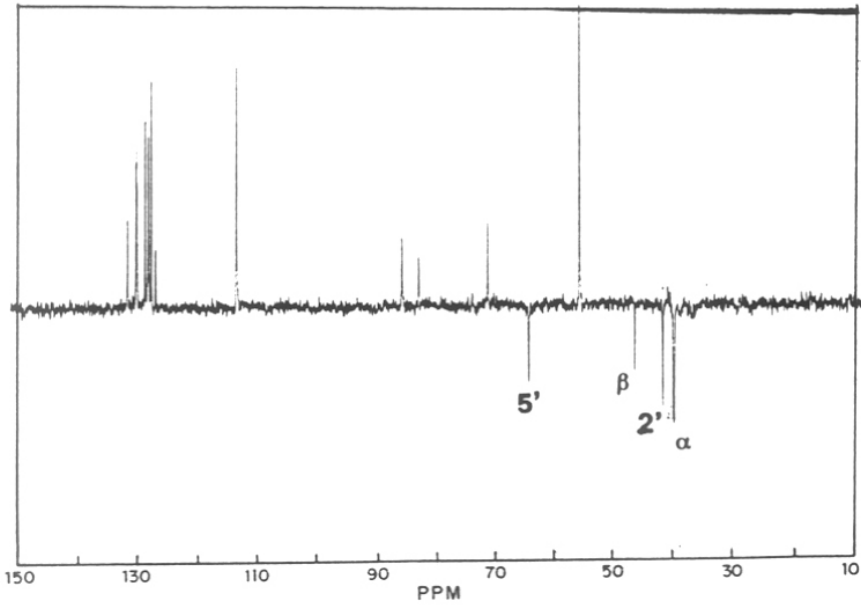


Fig. 3(b) INEPT spectrum of 5 in  $\text{DMSO-d}_6$ .

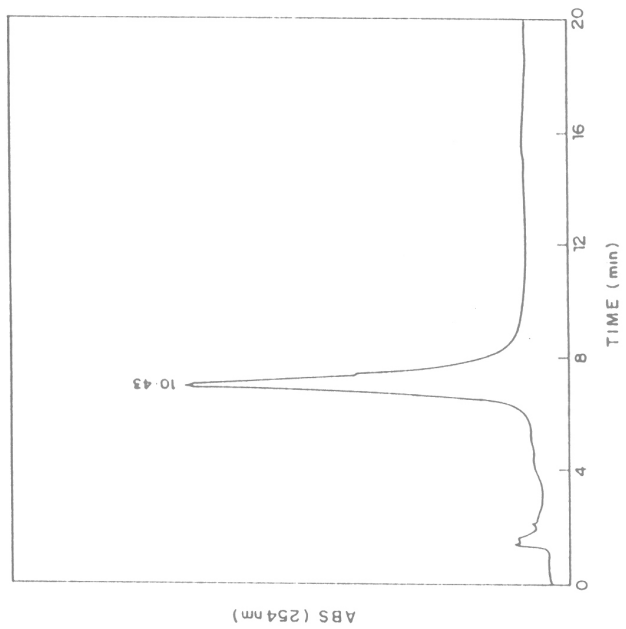


Fig. 4(b) Reverse phase HPLC of 7.

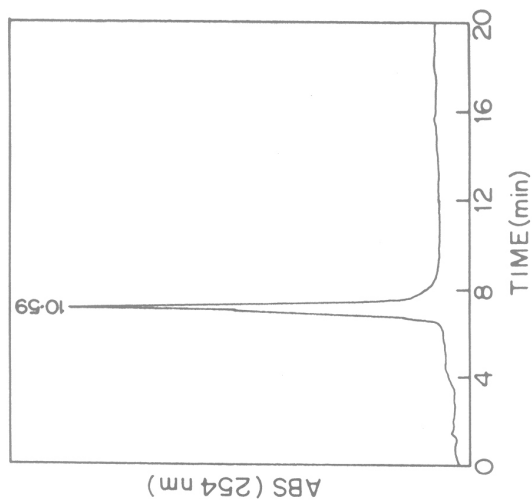


Fig. 4(a) Reverse phase HPLC of 6.

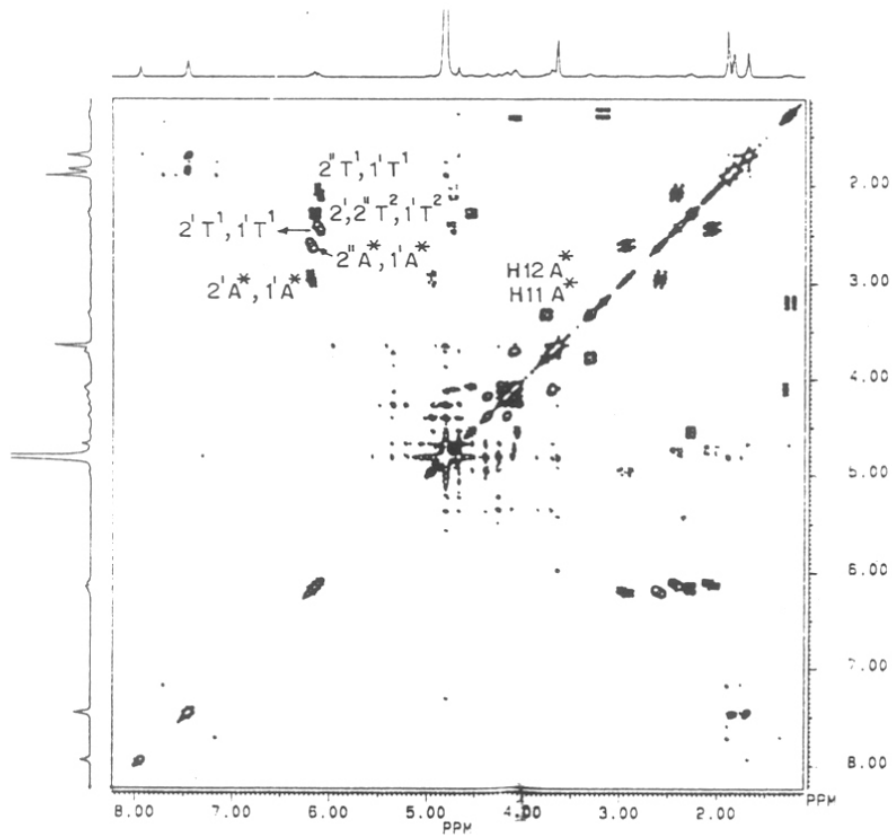


Fig. 6 2D COSY spectrum of **8** in  $D_2O$ .

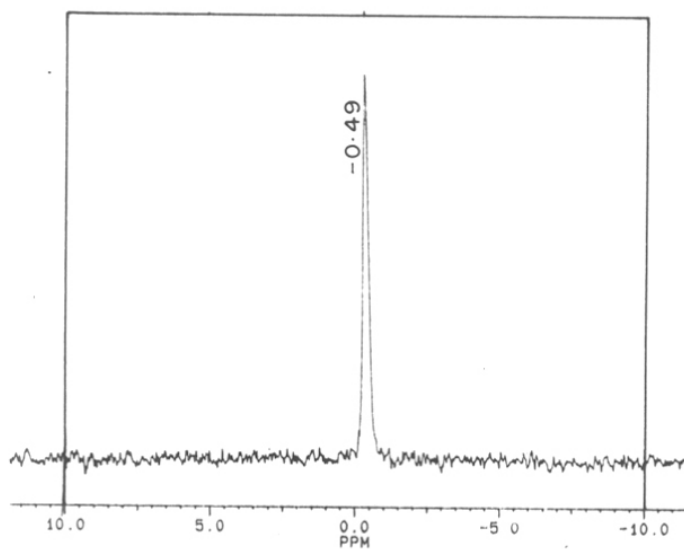
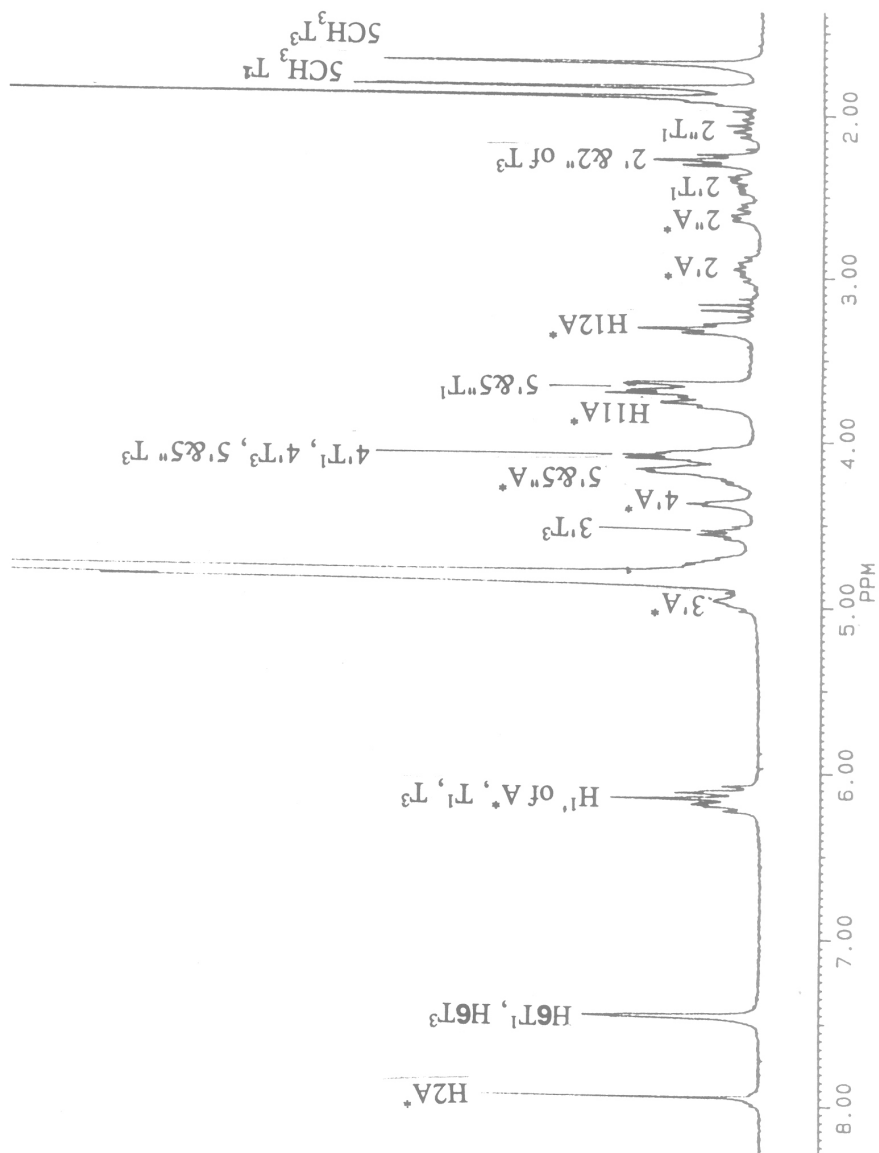
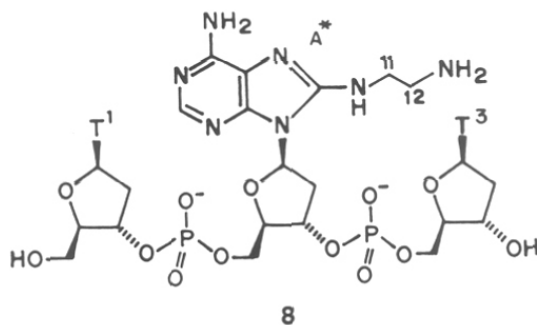


Fig. 7  $^{31}P$  NMR spectrum of **8**.

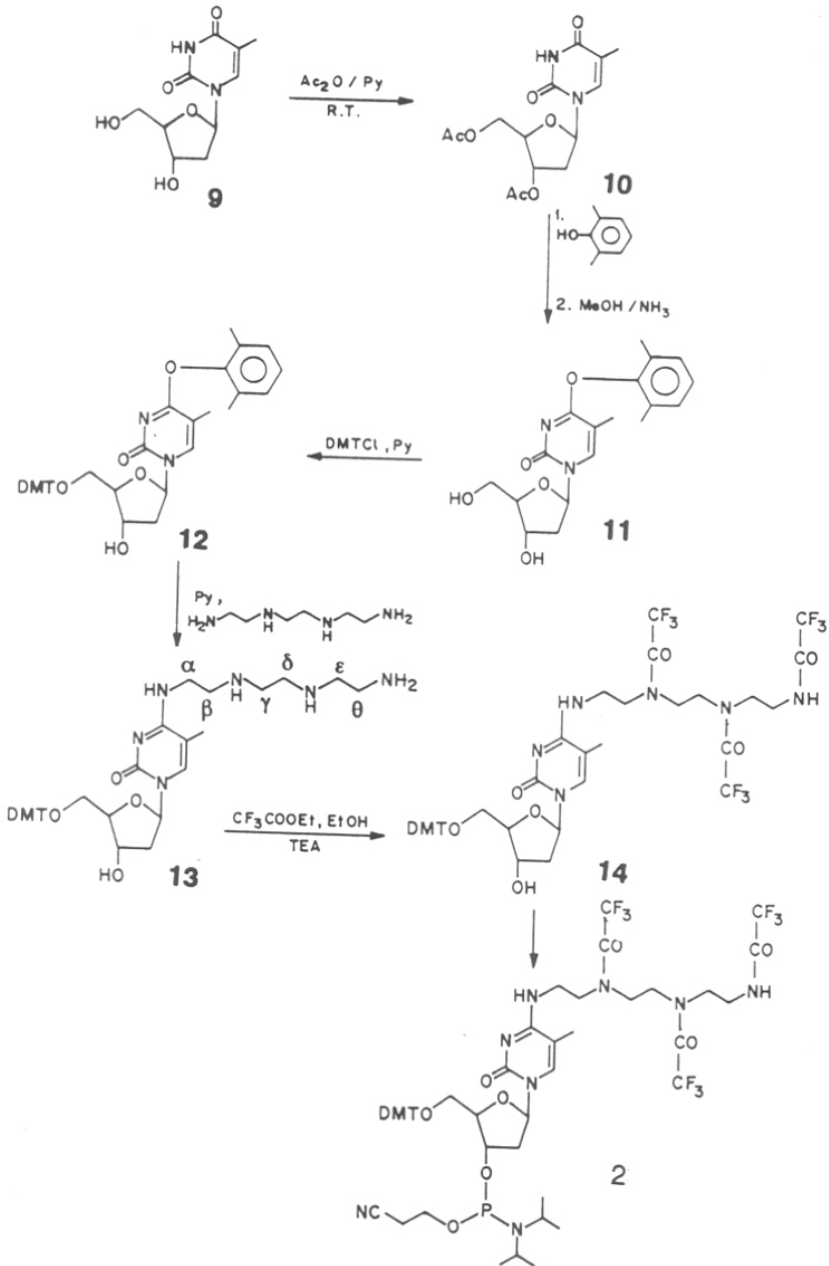
Fig. 5 200 MHz NMR spectrum of **8** in  $D_2O$ .



chains of dA (H11, 3.8 & H12, 3.3 ppm) and H6 (7.45 ppm, overlapping) and 5-CH<sub>3</sub> (1.88 & 1.68 ppm) of T1 and T3 could be clearly assigned in <sup>1</sup>H NMR. **8** gave a single <sup>31</sup>P NMR signal at -0.49 ppm (**Fig. 7**) characteristic of phosphodiester and indicating no N-phosphonylations.

The synthesis of modified amidite **2** containing the polyamine tether at N<sup>4</sup> position of dC was achieved by convertible nucleoside method following the synthetic methodology described in the **Scheme 2**. Thymidine was first acetylated by Ac<sub>2</sub>O/Py to get 2',3'-bis-O-acetylthymidine **10**. This was converted into 4-O-(2,6-dimethylphenyl)thymidine (**11**) by treatment with 2,6-dimethylphenol in presence of TPSCI, TEA and DABCO,<sup>13</sup> followed by deprotection of 2',3'-O-acetyl group using methanolic NH<sub>3</sub> to obtain **11**. Selective protection of 5'-hydroxyl group was achieved by treatment with DMTCI/Py to afford **12**. Reaction of **12** with triethylene tetramine in pyridine yielded the polyamine tethered nucleoside **13**. The presence of proton signals (multiplet) due to N-CH<sub>2</sub>CH<sub>2</sub>-N- (2.09-2.95 ppm) and a characteristic signal at 3.6 ppm due to dC-N<sup>4</sup>-α CH<sub>2</sub> group are confirmatory evidences for the incorporation of the amine on the nucleoside (**Fig. 8**). Further proof came from <sup>13</sup>C NMR where signals of all methylenes adjacent to NH appeared at 41 to 49 ppm (**Fig. 9**). The possibility of secondary amine displacing

## SCHEME 2



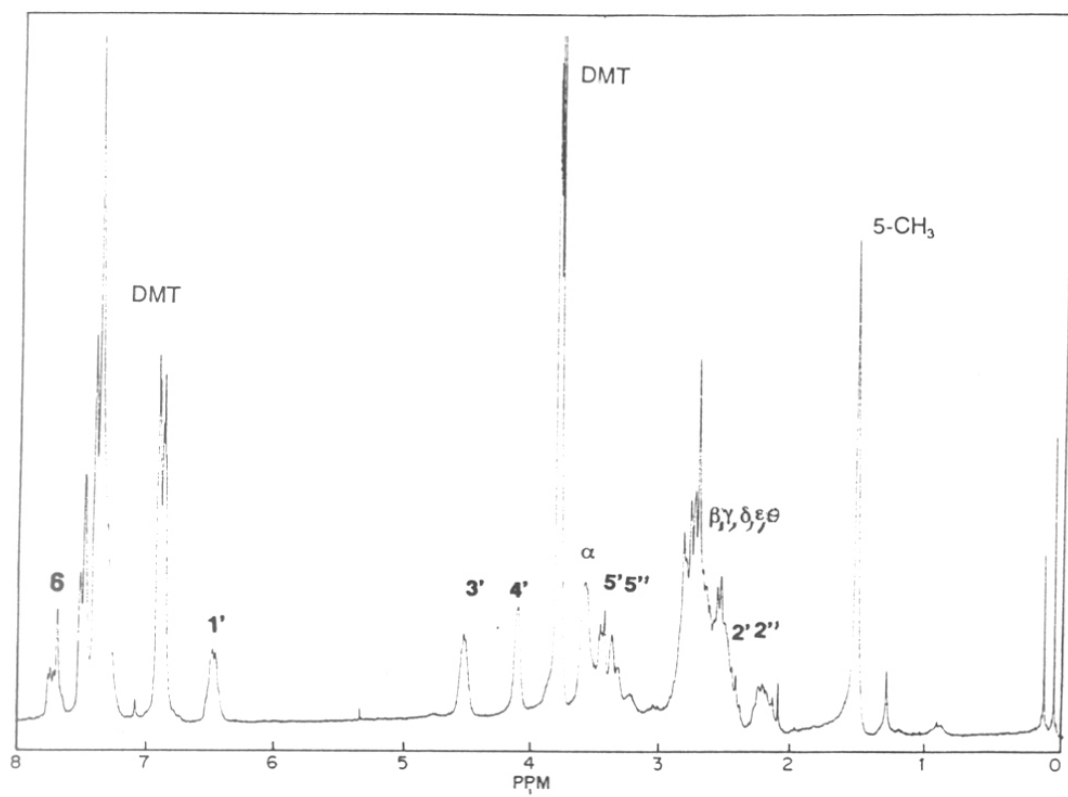


Fig. 8 200 MHz  $^1\text{H}$  NMR spectrum of **13** in  $\text{CDCl}_3$ .

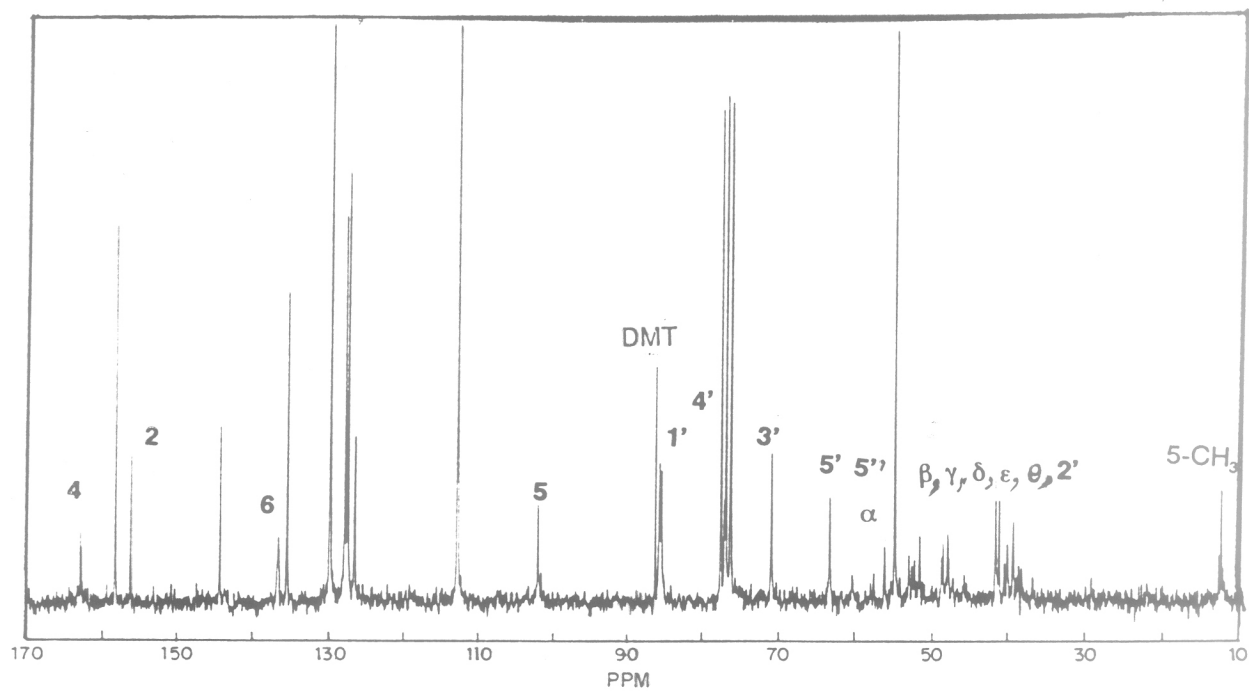


Fig. 9a  $^{13}\text{C}$  NMR spectrum of **13** in  $\text{CDCl}_3$ .

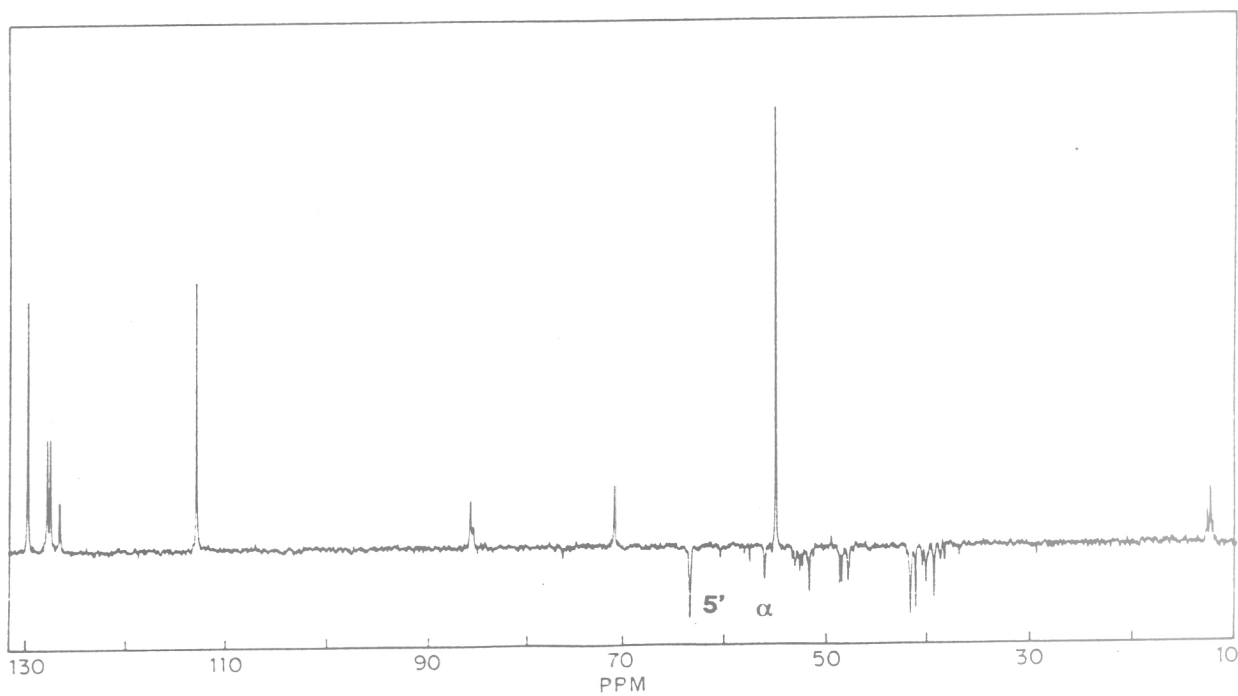
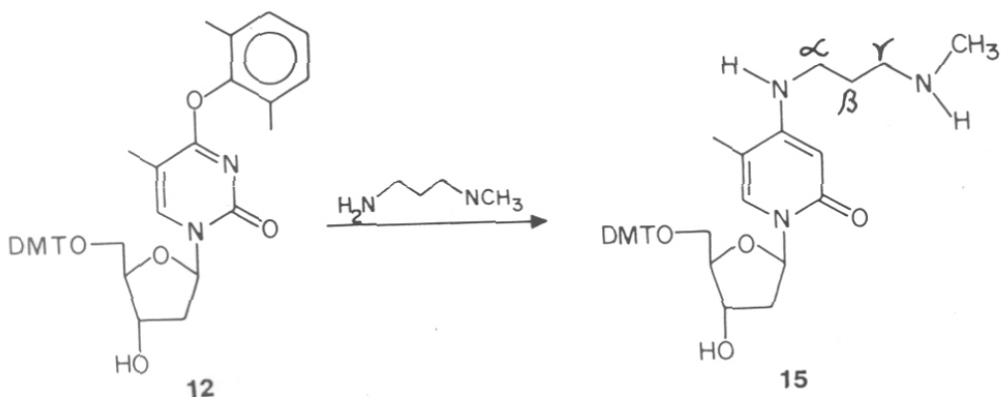


Fig. 9b INEPT spectrum of **13** in  $\text{CDCl}_3$ .



2,6-dimethylphenol was ruled out by carrying out a model displacement reaction with N-methyl-1,4-diaminoethane (Scheme 3) and characterizing the product **15**. Attack of secondary amine at C-4 of **12** would lead to a compound having N-CH<sub>3</sub> attached directly to nucleobase. <sup>13</sup>C chemical shift of such N-CH<sub>3</sub> is reported<sup>15</sup> to be 48.7 ppm, whereas the chemical shifts observed in the compound **15** is 33.3 ppm corresponding to an aliphatic N-CH<sub>3</sub> group (Fig. 10). This observation was also supported by <sup>1</sup>H NMR spectrum (Fig. 11) where N-CH<sub>3</sub> chemical shift appeared at 2.65 ppm as against 2.9-3 ppm expected for aromatic N-CH<sub>3</sub>. This shows that the product obtained was due to the reaction of primary amine. **13** was conveniently converted into N,N'-tristrifluoroacetyl derivative **14** by treatment with CF<sub>3</sub>COOEt in EtOH. FAB MS showed molecular ion peak corresponding to tristrifluoroacetyl derivative (984, M<sup>+</sup>+Na<sup>+</sup>, Fig. 12). It has been reported in the literature<sup>16</sup> that trifluoroacetyl group on the aromatic N is unstable. The three trifluoroacetyl groups are therefore present on the three aliphatic amino groups. 3'-OH function which remained unaffected during this reaction was then phosphitylated to **2** as described previously. No N-phosphonylation was observed as seen by <sup>31</sup>P NMR spectrum (Fig. 13) of the compound **2** which contained only two signals (149.5 and 149.1 ppm) characteristic of O-amidite. All other compounds were well characterized by <sup>1</sup>H & <sup>13</sup>C NMR (Fig. 14, 15) and FAB MS (Fig. 16).

### SCHEME 3



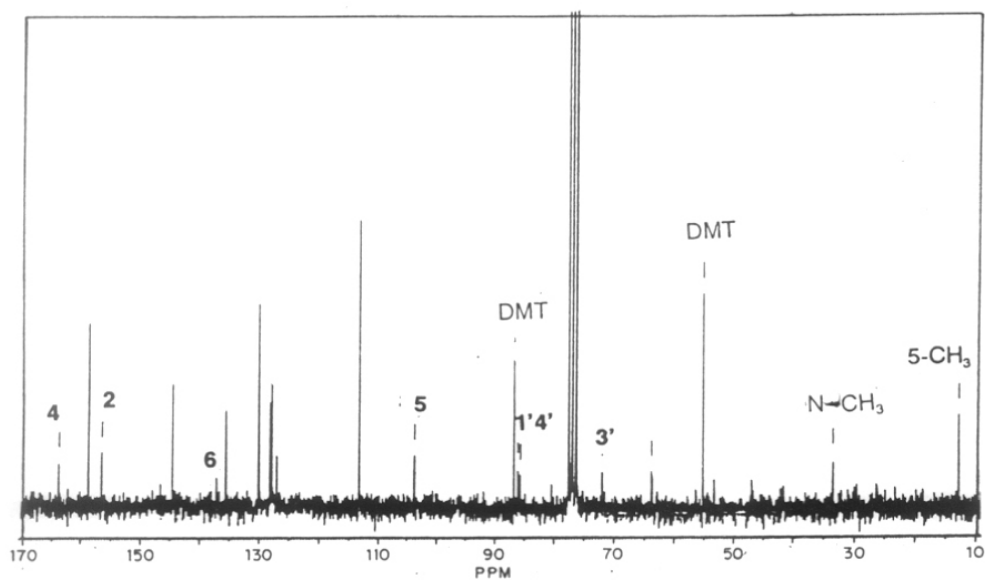


Fig. 10a  $^{13}\text{C}$  NMR spectrum of **15** in  $\text{CDCl}_3$ .

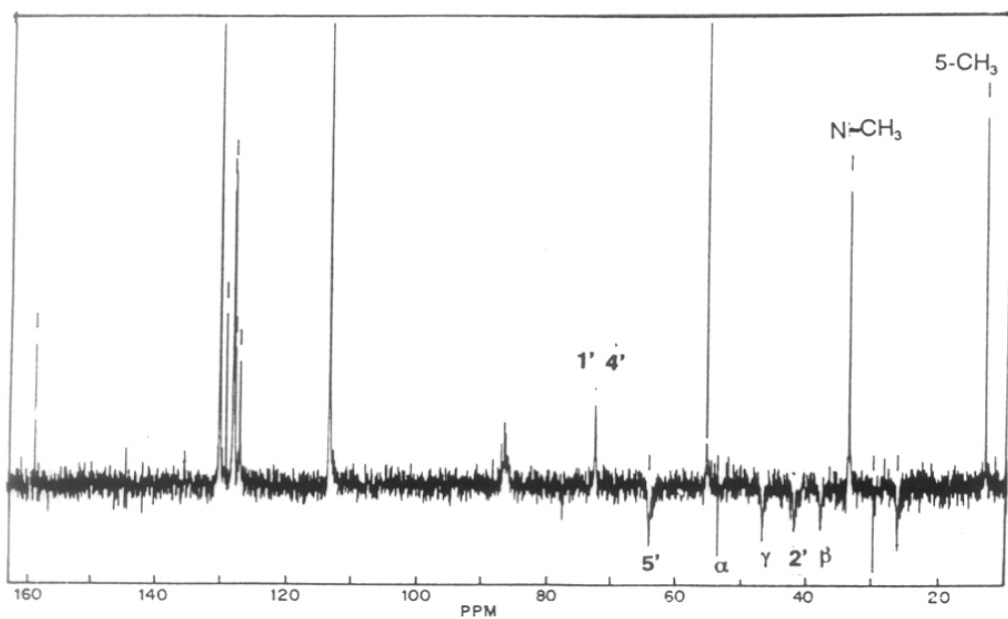


Fig. 10b INEPT spectrum of **15** in  $\text{CDCl}_3$ .

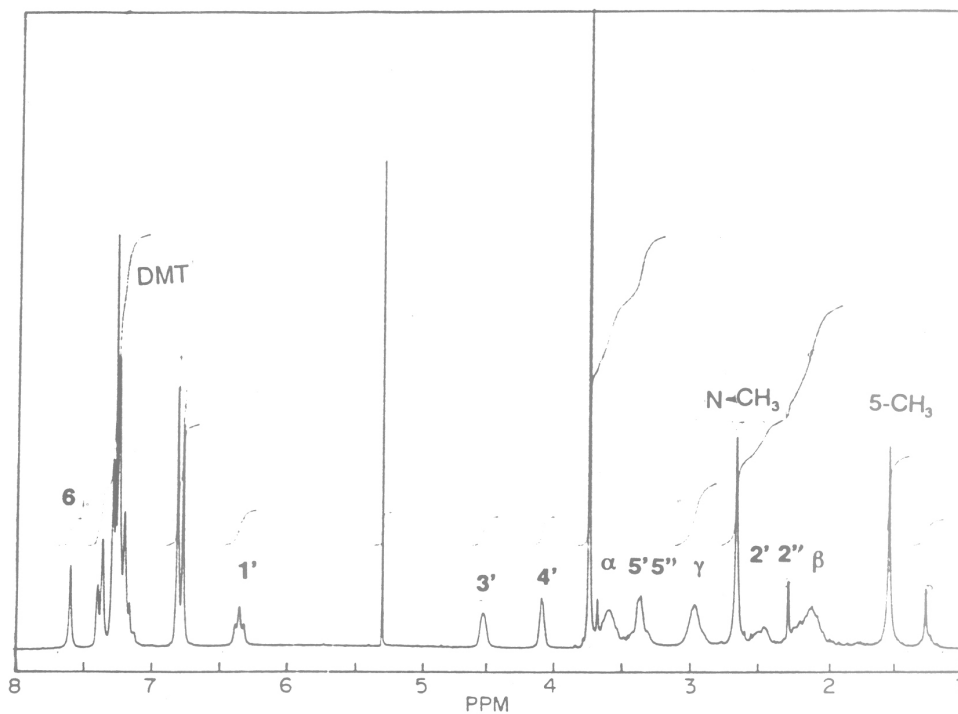


Fig. 11 200 MHz  $^1\text{H}$  NMR spectrum of **15** in  $\text{CDCl}_3$ .

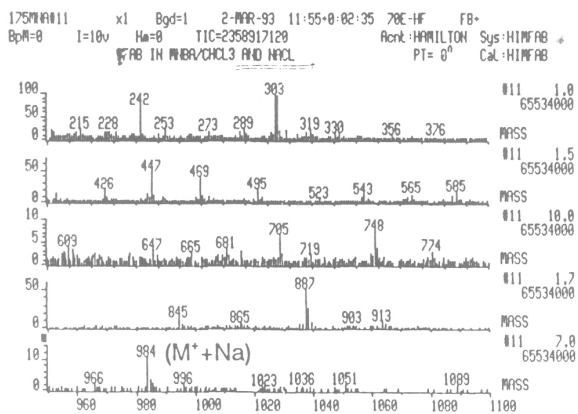


Fig. 12 Mass spectrum (FAB<sup>+</sup>) of **14**.

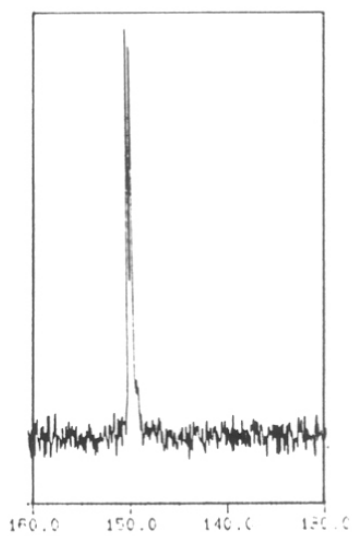


Fig. 13  $^{31}\text{P}$  NMR spectrum of **2** in  $\text{CDCl}_3$ .

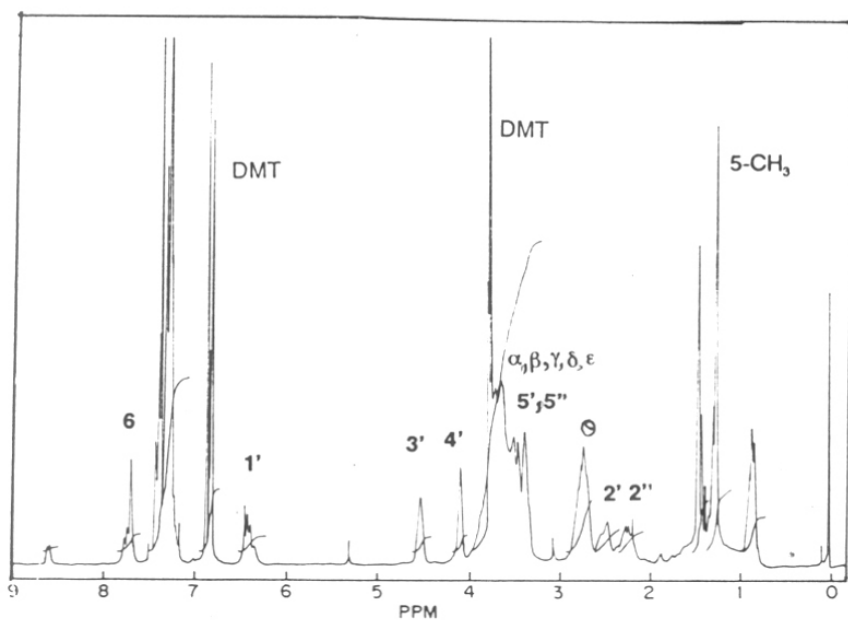


Fig. 14 200 MHz  $^1\text{H}$  NMR spectrum of **14** in  $\text{CDCl}_3$ .

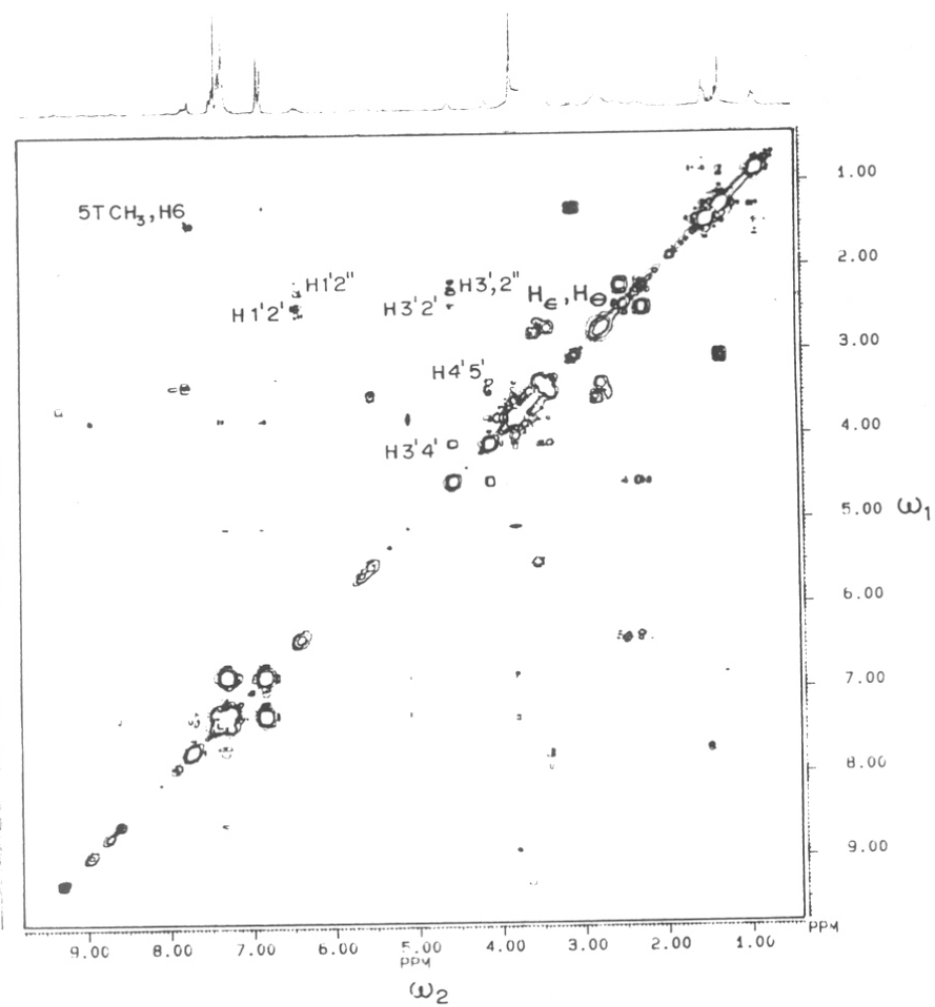


Fig. 15 2D COSY spectrum of **14** in CDCl<sub>3</sub>, cross peaks are assigned according to the coupling pattern.

The compound **2** was incorporated into the oligonucleotide sequences **16**, **17**, **18** at defined sites on an automated DNA synthesizer by using procedures described before. The stability of compound **14** towards the reagents used for the solid phase synthesis was established by treating compound **14** with reagents for times longer than the coupling time (3 hrs) and checking the structure of product by  $^1\text{H}$  NMR spectroscopy. No modifications were seen. As in the case of the amidite **1**, coupling efficiencies of modified amidite **2** was similar to the commercial phosphoramidites of the normal nucleotides (Table I). The unmodified oligonucleotides complementary to **17**, **18** and Dickerson's dodecamer **19** were synthesized by standard procedure.

**16**, d(CGC\*GAATTCGCG)

**17**, d(CAC\*TGCTAAGCT)

**18**, d(CACTGC\*TAAGCT)

**19**, d(CGCGAATTCGCG)

**20**, d(CACTGCTAAGCT)

**21**, d(AGCTTAGCAGTG)

The desalted oligonucleotides (NAP Column) were then further purified by reverse phase chromatography (C18) (FPLC, Pharmacia RPC HR (5/5)) and purity was further established by HPLC (Fig. 17).

### 5.3.2 Enzyme digestion

Oligonucleotides **6**, **7**, and **19** were 5'-end labeled with  $\gamma$ - $^{32}\text{P}$  ATP and subjected to Eco R1 restriction enzyme digestion. It was observed that modified oligonucleotides **6** and **7** were not cleaved whereas **19** was susceptible to cleavage (Figure 18). The stability of **6** and **7** to digestion by restriction enzymes EcoRI confirmed modification

TABLE I

## Gene Assembler Plus

Date : 5.03.1993  
 Sequence : TPP12  
 Synthesis : TPP12  
 Scale : 1.3 micromole  
 Sequence Length : 12  
 Column : 1  
 Final Detritylation : Yes  
 Coupling Efficiency Threshold : 90 %

Pos	Base	Retention mins	Duration mins	Peak ht %FS	Acc Area %min	Last eff %	Ave eff %
12	G	0.39	1.00	447	58.33	-	-
11	C	0.42	1.00	3002	354.66	-	-
10	G	0.39	1.00	3002	263.72	-	-
9	C	0.43	1.00	3001	351.32	99.5	99.5
8	T	0.43	1.00	2862	361.58	-	99.5
7	T	0.44	1.00	2676	371.44	102.7	100.0
6	A	0.42	1.00	3002	327.45	-	100.0
5	A	0.42	1.00	3002	321.57	98.2	100.0
4	G	0.42	1.00	3002	260.85	99.8	100.0
3	Y	0.45	1.00	1805	270.73	-	-
2	G	0.40	1.00	2799	213.52	90.5	98.2
1	C	0.44	1.70	2245	280.83	97.2	98.0

Total synthesis yield from start = 80.1 %

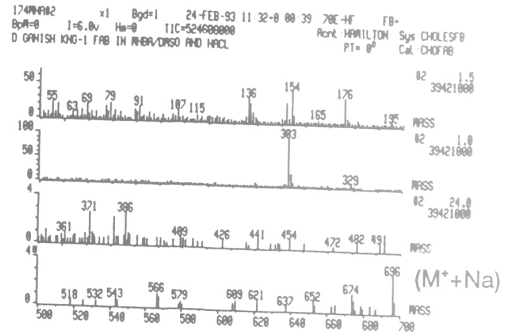
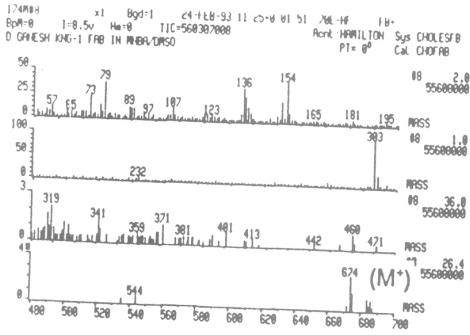


Fig. 16 Mass spectrum of (FAB<sup>+</sup>) of 14.

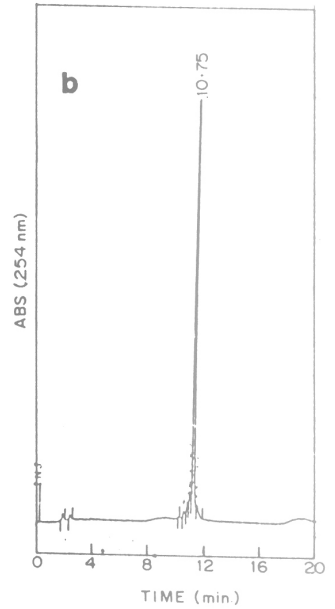
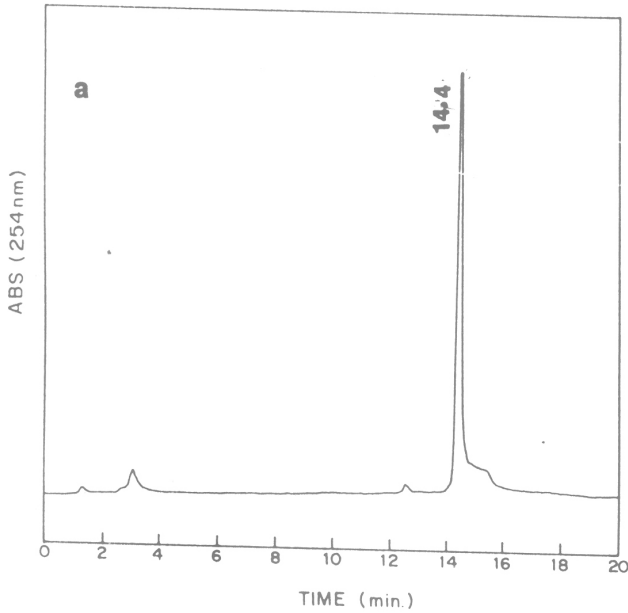


Fig. 17 Reverse phase HPLC of (a) 16, (b) 18.



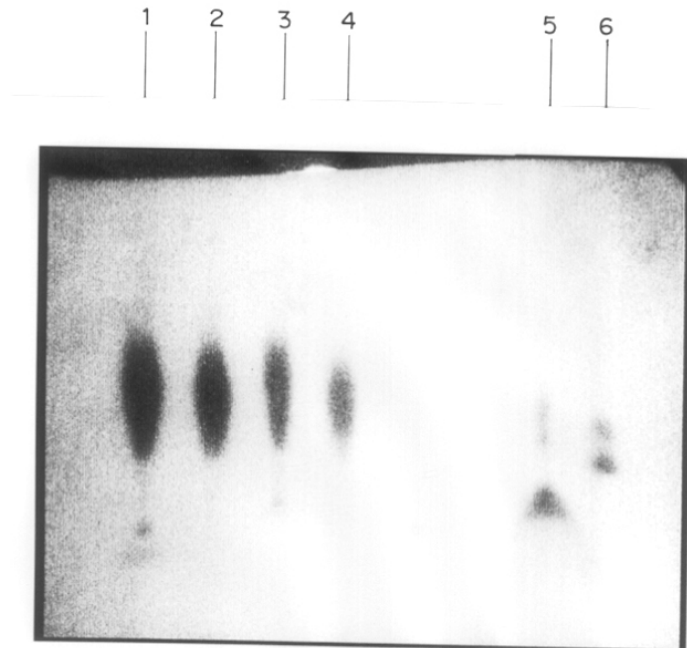


Fig. 18 Digestion of **6,7,19** with restriction enzyme Eco R1. For conditions see experimental. Lane 1, **6** + Eco R1, Lane 2, **6**; Lane 3, **7** + Eco R1; Lane 4, **7**; Lane 5, **19** + Eco R1; Lane 6, **19**.

within the recognition site (GA\*ATTC). This observation gave additional proof for the incorporation of EDA side chain in the oligonucleotides **6** and **7**.

### 5.3.3 UV Melting experiments of oligonucleotides

The transition between an ordered, duplex structure and a single stranded random state in a nucleic acid can be conveniently monitored using ultraviolet (UV) absorbance.<sup>17</sup> As the ordered stacks of base pairs are disrupted, the UV absorbance increases due to hypochromicity; the amount of hypochromicity is a measure of the base pairing and stacking of the secondary structure. The absorbance in the disordered state approaches the sum of the absorbances of the constituent nucleotides. The easiest way to denature a nucleic acid is by heating. The resulting profile of absorbance versus temperature is called a melting curve which is normally sigmoid in form. The mid-point of this transition, defined as the melting temperature " $T_m$ ", is characteristic of base composition, sequence and the structure of DNA. The dependence of  $T_m$  on DNA concentration yields information on the molecularity and quantitative thermodynamic data for the melting transition.<sup>17</sup>

The melting experiments of purified self complementary oligonucleotides **6**, **7** and **16** (0.3 to 0.6 OD units) were done in buffer A (see experimental). The change in absorbance at 260 nm was recorded at 0.5°C intervals (Fig. 19). As compared to Dickersons' dodecamer **19**, the modified oligonucleotides **6** and **16** showed a lower  $T_m$  (Table II) whereas **7** did not form any stable duplex structure. The C8 side chain in modified dA protrude into the major groove of DNA helix. In sequences containing modifications in the middle (**6**, **7**) a repulsion of two positively charged  $\omega\text{-NH}_3^+$  groups situated spatially close to each other (one from each strand) in the self complementary duplex DNA may be responsible for the observed destabilization. Thus the modifications on C base (**17** and **18**) were tried on non-self complementary sequences. Therefore

sequences with modifications at internal position (18) and that towards 5' end (17) were synthesised and duplexes were generated from hybridization corresponding to unmodified complementary sequence 21.

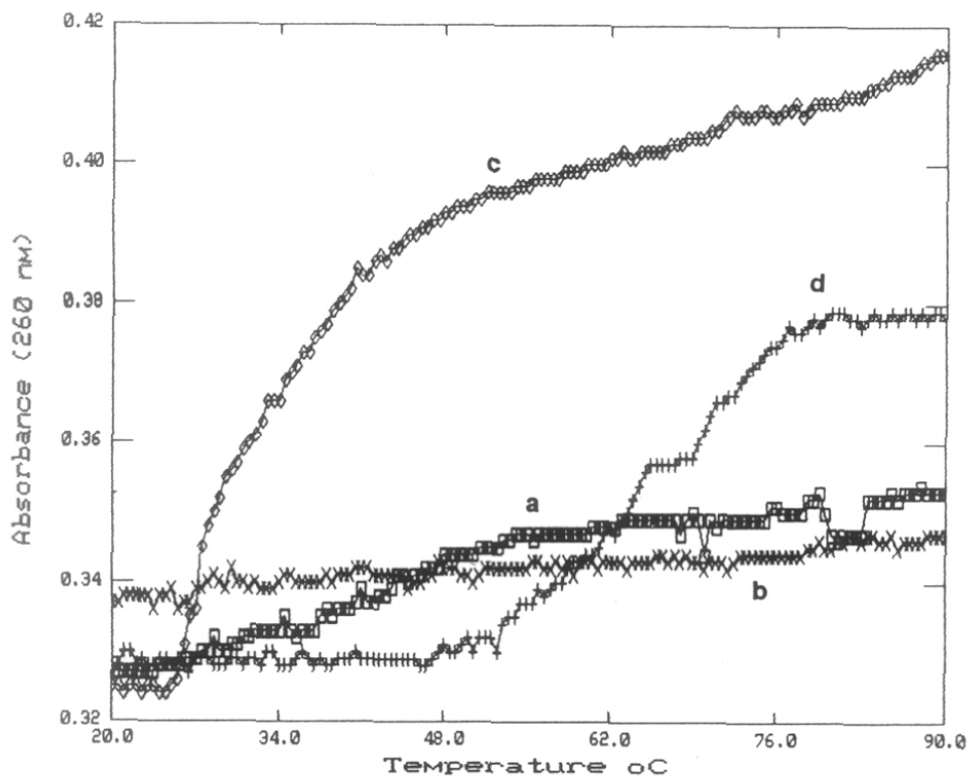


Fig. 19 Temperature Vs Absorbance ( $\lambda = 260$  nm) plot for (a) 6, (b) 7, (c) 16 and (d) 19

Table II:  $T_m$  of C8 modified oligonucleotides.

No.	Sequences	$T_m$ °C
19	5' d(CGCGAATTCGCG) 3'	61
6	5' d(CGCGAA <sup>*</sup> TTCGCG) 3'	42.2
7	5' d(CGCGA <sup>*</sup> A <sup>*</sup> TTCGCG) 3'	<20

The  $t_m$  of the duplex DNA derived from **17** and **18** showed much lower  $T_m$  (Fig. 20) compared to unmodified duplex DNA **20:21** (Table III). In all sequences, the base modification considerably destabilized the duplex formation.

Table III:  $T_m$  of C4 modified oligonucleotides.

No	Sequences	$T_m$ °C
16	5' d(CGC <sup>*</sup> GAATTCGCG) 3'	31.7
17:21	5' d(CAC <sup>*</sup> TGCTAAGCT) 3' 3' d(GTGACGATTCGA) 5'	26
18:21	5' d(CACTGC <sup>*</sup> TAAGCT) 3' 3' d(GTGACGATTCGA) 5'	14
20:21	5' d(CACTGCTAAGCT) 3' 3' d(GTGACGATTCGA) 5'	41

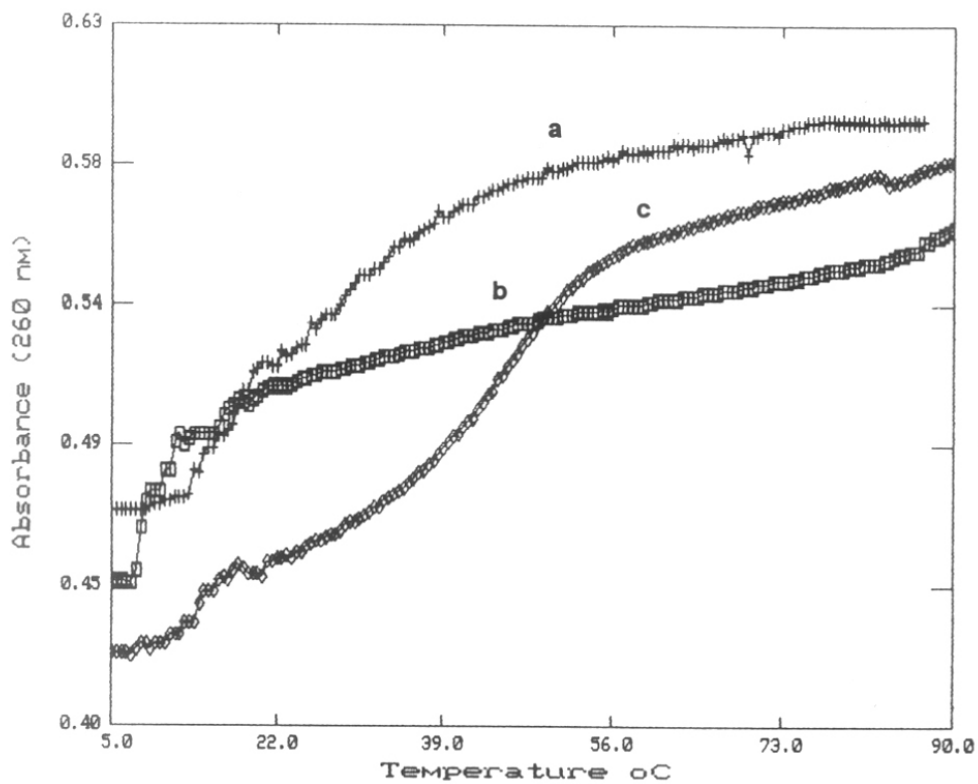


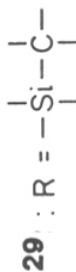
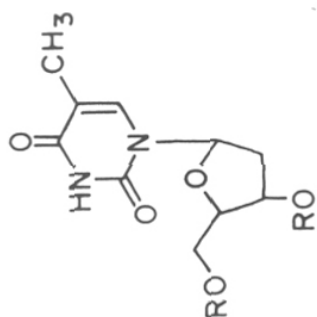
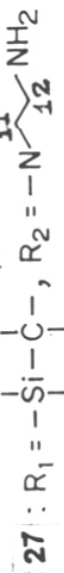
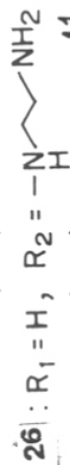
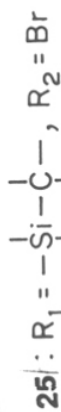
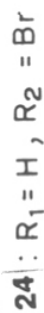
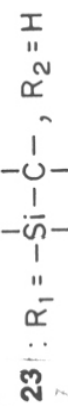
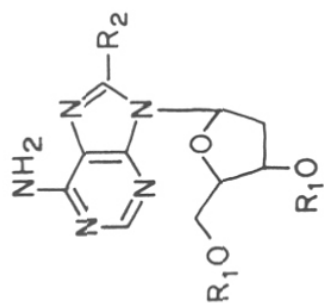
Fig. 20 Temperature Vs Absorbance ( $\lambda = 260$  nm) plot for duplexes of (a) 17:21 (b) 18:21 and (c) 20:21

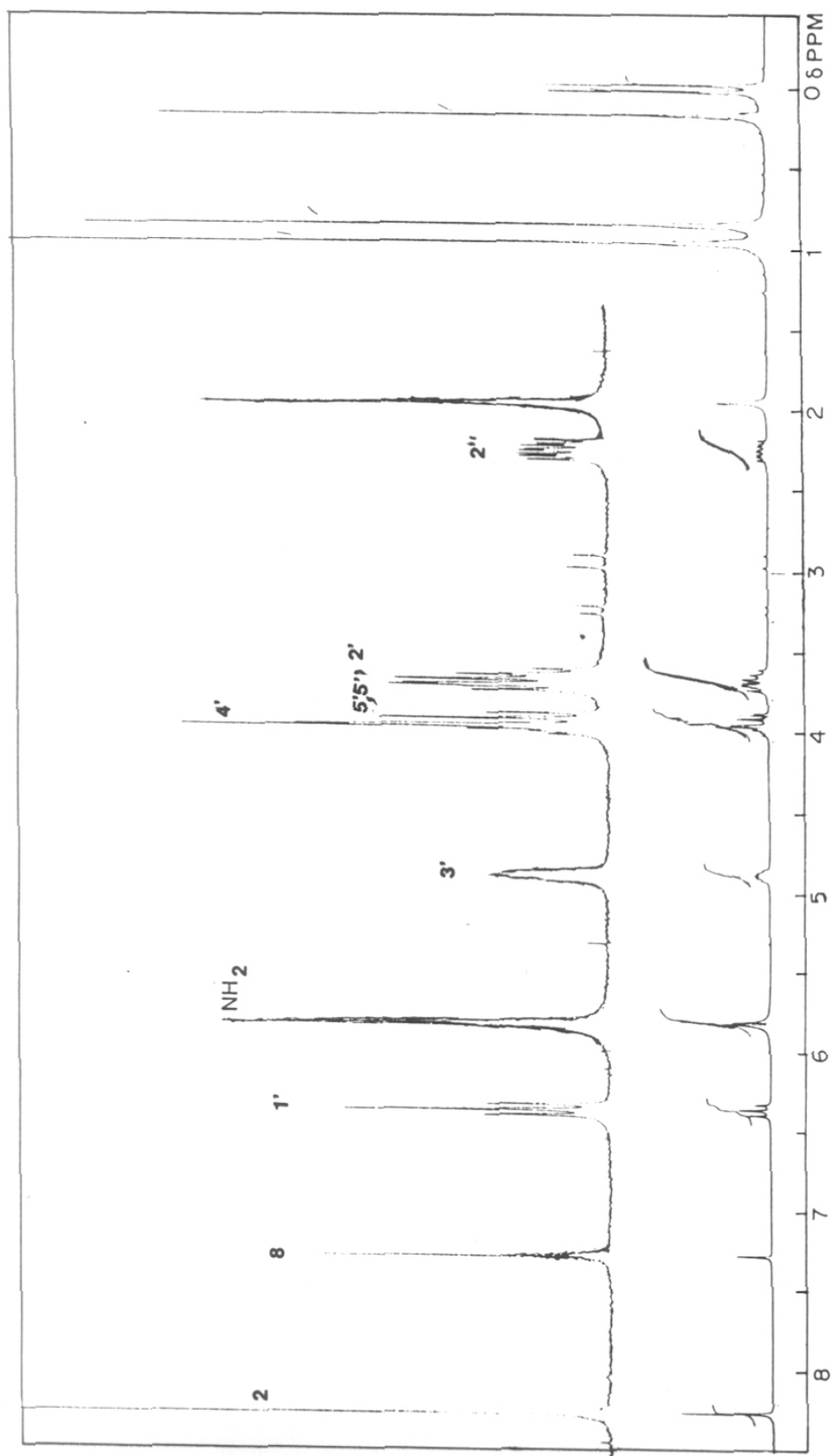
The duplex with modification in the middle (18:21) showed much larger destabilization ( $\Delta t_m$  27 °C) compared with the duplex with modification towards 5' end (16:21) ( $\Delta t_m$  15°C). Comparison of  $t_m$  data of all sequences clearly indicated that (i) modification at C8 of dA are more tolerable (less destabilizing) than dC-modification at N<sup>4</sup>(6 vs 16), (ii) modifications towards 5' end destabilize less than modification in the middle of the sequence, (iii) double modification (7) causes large destabilization of duplex and (iv) single modification seen in non-self complementary sequences destabilizes the duplex to a less extent.

#### 5.3.4 Base pairing studies of monomers

In order to understand the effect of base modification at the monomeric level base pairing studies were carried out by <sup>1</sup>H NMR spectroscopy. It has been demonstrated earlier that by use of soluble monomers and base derivatives, the complexation can be studied at low dielectric solvents such as CDCl<sub>3</sub><sup>18</sup> and DMSO-d<sub>6</sub><sup>19</sup>. It was also reported in the literature that substitution on nucleobase affects the hydrogen bonding affinity of monomer complementary pairs.<sup>18</sup> To understand the effect of EDA at C8 position of dA at monomer level, base pairing studies of modified nucleosides with complementary bases were carried out.

The nucleosides were converted into their corresponding 3',5'-bis (TBDMS) derivatives according to the literature<sup>20</sup> and purified by chromatography to spectroscopic purity (Fig. 21, 22). The association constants between the complementary pairs dA:dT (23:29), dA-Br:dT (25:29) and dA-EDA:dT (27:29) were determined by titrimetry involving incremental, stoichiometric addition of dA (23), dA-EDA (27) or dA-Br (25) to the pyrimidine component (29) in chloroform-d. The titrations were monitored by <sup>1</sup>H NMR spectral changes after each addition. In all experiments, the imino N3 proton (N3-H) of



Fig. 21 200 MHz  $^1\text{H}$  NMR spectrum of 25.



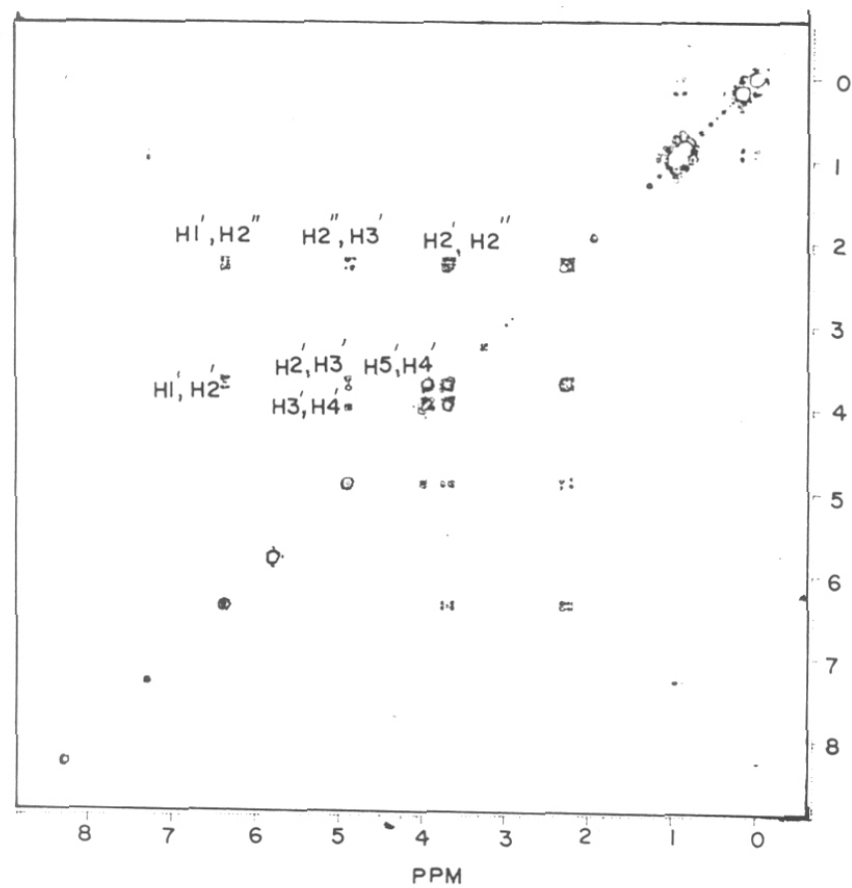


Fig. 22 2D COSY spectrum of **25**. Cross peaks corresponding to H 1', 2' and H2', H2'' was used for the assignment of 2' protons

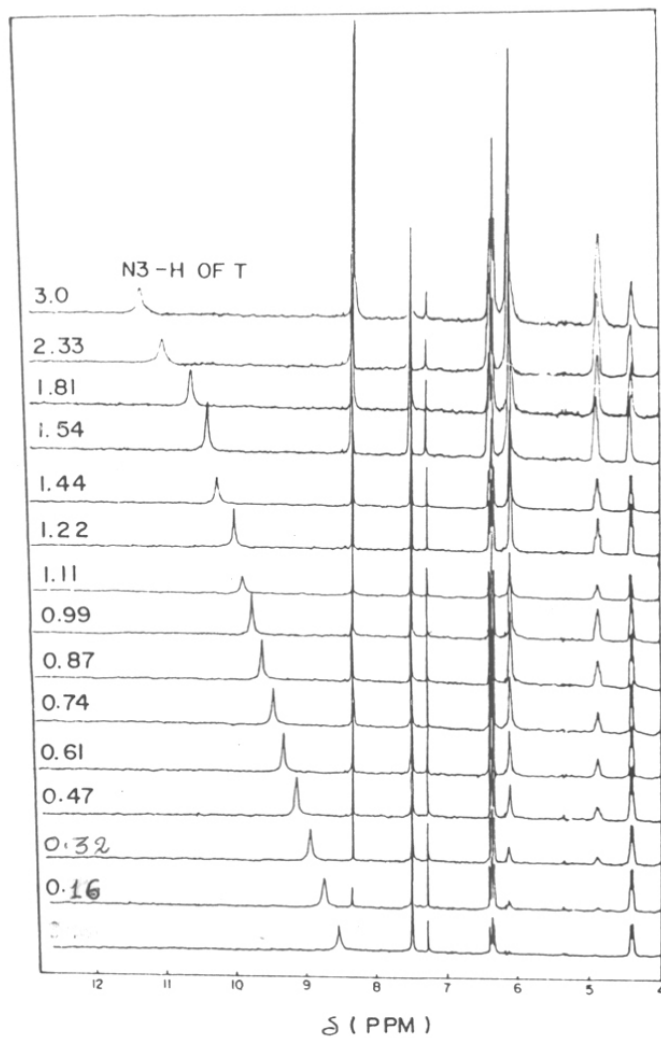


Fig. 23  $^1\text{H}$  NMR spectrum (200 MHz) of dT (**29**) upon addition of dA-Br (**25**). Conditions: 0.03 M **29** (0.4 ml),  $\text{CDCl}_3$ ,  $21^\circ\text{C}$ , dT-dA-Br quotients [dT/dA-Br] are indicated on the left side.

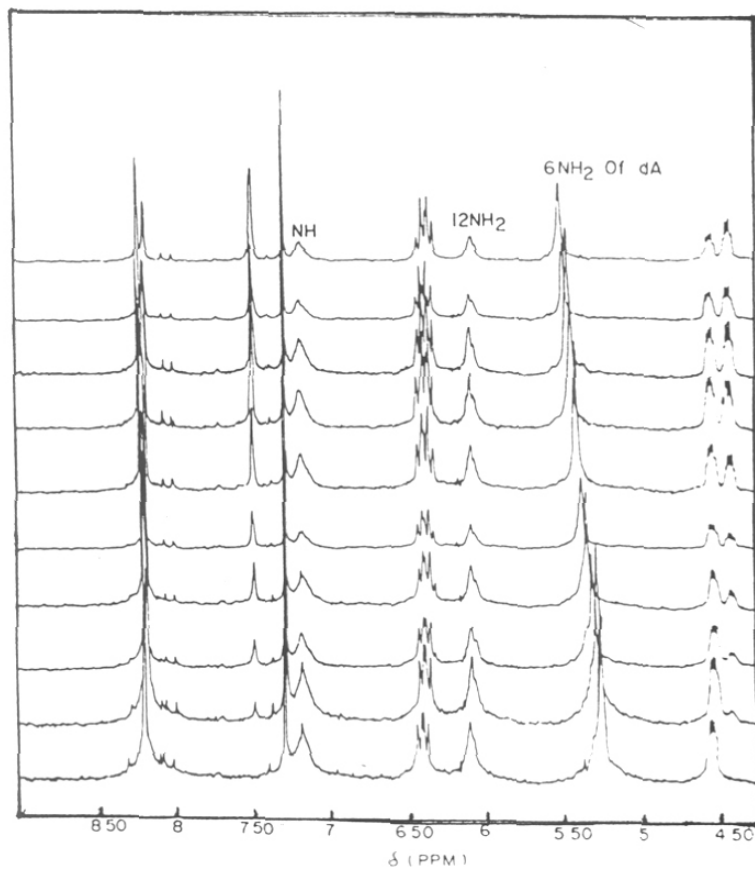


Fig. 24  $^1\text{H}$  NMR Spectrum (200 MHz) of 27 upon addition of 29. Exocyclic amino (6-NH<sub>2</sub>) and aliphatic amino (12 NH<sub>2</sub>) and imino (NH) protons are indicated in the tip of the peaks. Conditions same as *fig.23*

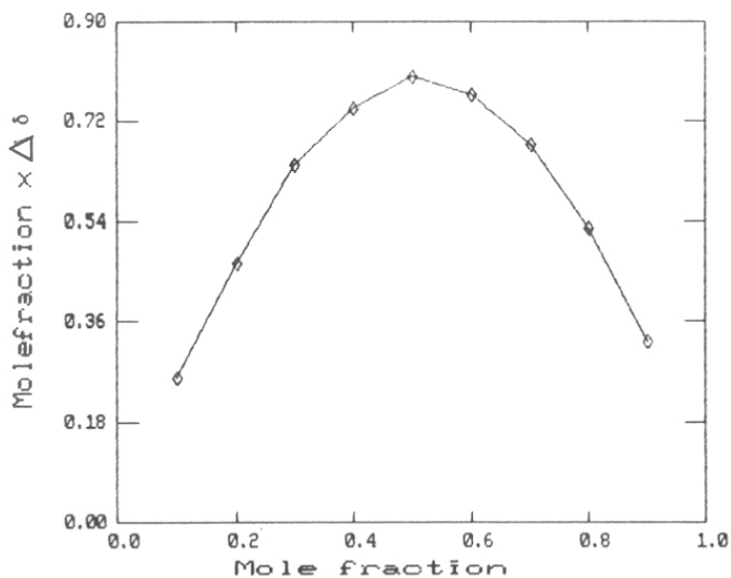


Fig. 25 Jobs plot for the complexation of dA (**23**) with dT (**29**). Complexation was followed by  $^1\text{H}$  NMR spectroscopy (200 MHz). Shift in the N3-H protons of dT upon addition of dA was monitored,  $\text{CDCl}_3$ ,  $21^\circ\text{C}$

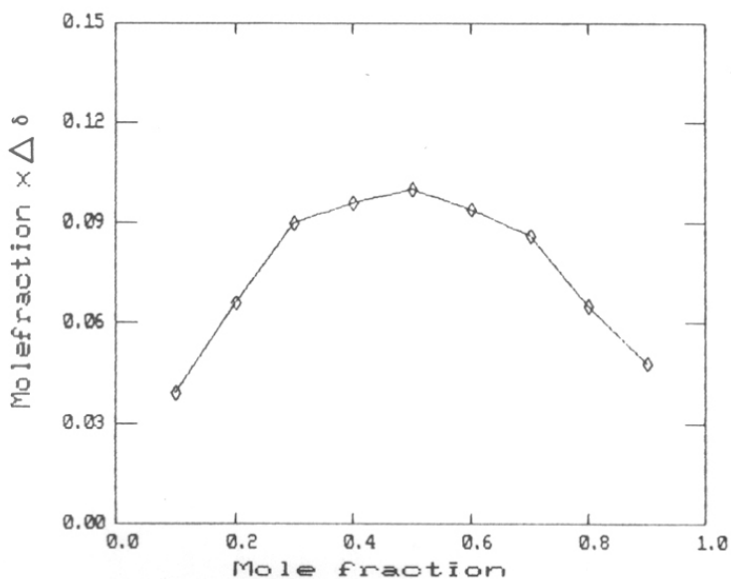


Fig. 26 Job's plot for the complexation of dT (**29**) with dA-EDA (**27**). Conditions same as Fig. 25.

pyrimidine exhibited significant downfield shifts, whose magnitude varied as a function of purine concentration (Fig. 23). The protons of the exocyclic 6-NH<sub>2</sub> group of dA also shifted downfield compared to free dA as expected for a Watson-Crick base pairing (Fig. 24). Other signals did not show any shifts during the titration experiments. Stoichiometry of complexation was established by Job's method of continuous variance<sup>21</sup> (Fig. 25, 26) which showed a clear 1:1 complexation in all cases. The binding constants were computed for 1:1 complexation using Hostest II program<sup>22</sup> (Table IV).

Table IV Association constants for nucleoside base pairs, K M<sup>-1</sup>. Computed by using HOSTEST II programme<sup>21</sup>

Base pairs	dA:dT (23:29)	dA-Br:dT (24:29)	dA-EDA:dT (27:29)
Association Constants	50	12.4	95.7

The values indicate that base modifications introduced by substitution of C8-H with amine tether slightly stabilize normal Watson-Crick base pairing while C8-Br substitutions destabilize the WC base pairing. C8-Br substitution induces considerable anti- $\rightarrow$ syn conversion<sup>23</sup> of purine base in nucleosides. However, in case of C8-EDA, the C8-NH proton may H-bond intramolecularly either with C5'-O or C4'-O to promote WC base pairing stereoelectronically. But it must be cautioned that, the effects seen on base pairing at monomer level in organic solvent (CDCl<sub>3</sub>) may not have much implication to those at oligonucleotide/DNA level since additional factors such as base stacking etc. become operative in duplex formation in aqueous media.

#### 5.4 CONCLUSIONS

The convenient synthetic approaches described in this chapter show the possibility of incorporating intelligent functional groups into the oligonucleotide sequences. The

successful incorporation and retention of modified amidite (1) was unambiguously showed by  $^1\text{H}$  NMR spectrum. The purity of the amine tethered oligonucleotides were established by HPLC. Stability of modified Dickerson's sequences 6, 7 & 19 towards restriction enzyme EcoR1 tendered further proof for successful incorporation of the amine into the oligonucleotide sequence. Biophysical studies (melting) also showed the structural variability of the modified sequences compared to the unmodified oligonucleotides. Such modified oligos may have various applications in the field of chemical nucleases, detection probes, photoaffinity reagents, artificial repressors and antisense drugs that target mRNA.

## 5.5 EXPERIMENTAL

N,N-Dimethylamino pyridine (Sigma, USA), mesitylene sulphonyl chloride, dimethyl phenol, DABCO, dimethoxytrityl chloride, nucleosides, TBDMSCI (all from Aldrich, USA) were used without purification. Ethyl trifluoroacetate was prepared from trifluoroacetic anhydride and ethanol by following reported procedure.<sup>12</sup> All melting points were uncorrected. Column chromatography was carried out on silica gel (100-200 mesh, Loba Chemie, India) and TLC were performed on precoated plates (silica gel GF<sub>254</sub>, Merck 5554), Solvent A, DCM-MeOH, 9:1, V/V, Solvent B: DCM-MeOH, 9.5:0.5, V/V; The spots were visualised under UV light and by spraying with 60% perchloric acid-ethanol (3:1) followed by charring. NMR spectra were recorded on Bruker AC200 spectrometer. All chemical shifts are expressed in ppm and reported downfield from TMS in  $\text{CDCl}_3$ .  $^{31}\text{P}$  NMR spectra are recorded at 81 MHz with 85%  $\text{H}_3\text{PO}_4$  as external reference  $^{13}\text{C}$  NMR were recorded at 50 MHz in both  $^1\text{H}$  decoupled and INEPT modes.

All standard normal phosphoramidites (A, G, C and T) used for solid phase synthesis (GA plus Pharmacia) were purchased from Pharmacia (Sweden). Acetonitrile for HPLC and FPLC was obtained from E. Merck. Solvents for solid phase DNA synthe-

sis were distilled and dried. Acetonitrile was refluxed and distilled over  $P_2O_5$  and calcium hydride, and stored over molecular sieves. Dichloroethane was passed through a column of basic alumina and distilled over  $P_2O_5$ . Purification of the oligonucleotides were carried out on a Pharmacia LCC-500 liquid chromatograph equipped with a gradient mixing system, uv detector (254 nm) and a photometer out put recorder. All HPLC analysis were carried out on Waters Associates HPLC consisting of M440 absorbance UV detector set at 254 nm, M 6000 A dual pump, U6K injector, HP3380 integrator. Column used for the analysis was Nova Pak C18 reverse phase column. Radioactive [ $\gamma$ - $^{32}P$ ]ATP was obtained from BARC (INDIA). Restriction enzymes EcoR1 and T4 kinase were procured from New England Biolabs. Electrophoresis chemicals polyacrylamide, urea, TEMED etc. were purchased from Sigma, USA. Electrophoresis power pack (Macrodrive 5000) was from Pharmacia-LKB and apparatus from Biotech India.

All temperature dependent UV spectra were recorded on a  $\lambda$  15-Perkin Elmer spectrophotometer fitted with an automatic 5 cell changer, peltier heating and a digital temperature controller. The temperature was varied with  $0.5^\circ\text{C}$  per minute and controlled by a the temperature programmer. Samples were kept stirred during the melting experiment with help of a tiny magnetic stirrer which is attached to the cell holders. The melting experiment was done over the temperature  $5$ - $90^\circ\text{C}$ . The cell component was purged with nitrogen at temperature below  $15^\circ\text{C}$  to avoid condensation of water on the walls of the cuvette. Melting temperature was found out by a plot of temperature ( $^\circ\text{C}$ ) Vs absorbance at 260 nm.

#### 5.5.1 $N^6$ -Benzoyl-10N,13N'-ditrifluoroacetyl- 5'-O-(4,4'-dimethoxy trityl-8-amino(2-aminoethyl)-2'-deoxyadenosine 5.

$N^6$ -Benzoyl-5'-O-(4,4'-dimethoxytrityl-8-amino(2-aminoethyl)-2'-deoxyadenosine 4 (0.41 g, 0.6 mmol) was dissolved in dry ethanol (7 ml). Dry triethylamine (1.3 ml, 9

mmol) and ethyltrifluoroacetate (1 ml, 9 mmol) were added successively and stirred at ambient temperature for 18 hrs. The reaction was monitored by TLC, showed complete conversion of starting material (ninhydrin spray, positive) to product (ninhydrin spray negative, faster moving). Ethanol was removed under vacuum and the residue was dissolved in dichloromethane (20 ml) and washed with water (3 x 15 ml). Organic layer was dried over anhydrous  $\text{Na}_2\text{SO}_4$  and evaporated to yield white solid **5** (0.41 g, 79%),  $R_f$  (MeOH: $\text{CH}_2\text{Cl}_2$ , 1:9 v/v) = 0.6,  $\lambda = 307.5$  nm (MeOH,  $\epsilon$ ,  $4.8 \times 10^4$ ).  $^1\text{H}$  NMR ( $\text{DMSO-d}_6$ )  $\delta$  9.5 (brs, 2H, NH), 6.1 (t,  $J = 6.3$  Hz, 1H, H1'), 4.6 (m, 1H, H3'), 3.9 (m, 1H, H4'), 3.7 (s, 6H, 2 x  $\text{OCH}_3$ ), 3.4 (m, 4H, H11 and H12), 3.2 (dd,  $J = 4.2$  and 3.8 Hz, H5'), 3.1 (dd,  $J = 5.9$  and 6.6 Hz, H5''), 3.0 (m, 1H, H2'), 2.1 (m, 1H, H2''),  $^{13}\text{C}$  NMR ( $\text{DMSO-d}_6$ )  $\delta$  157.4 ( $\text{NHCOCF}_3$ ), 156.7 ( $\text{NHCOCF}_3$ ), 152.9 (C6), 152.3 (C2), 149.1 (C8), 127 (C5), 119.3 ( $\text{NCOCF}_3$ ), 117.8 ( $\text{NHCOCF}_3$ ), 85.8 (C1'), 83.0 (C4'), 71.2 (C3'), 64.2 (C5'), 55.4 ( $\text{OCH}_3$ ), 46.3 (C11), 41.5 (C2'), 39.7 (C12).

#### 5.5.2 **N<sup>6</sup>-Benzoyl-3'-O-(2-cyanoethyl-N,N-diisopropylphosphoramido)-10N,13N'-di trifluoroacetyl-5'-O-(4,4'-dimethoxytrityl)-8-amino(2-aminoethyl)-2'-deoxyadenosine 1.**

Compound **5** (0.36 g, 0.4 mmol) and tetrazole (0.028 g, 0.4 mmol) were co-evaporated with dry 1,2-dichloroethane (2 x 2 ml). The residue was then dissolved in dry 1,2-dichloroethane (4 ml) and 2-cyanoethyl-N,N,N',N'-tetraisopropyl phosphorodiamidite (0.2 ml, 0.6 mmol) was added and stirred at room temperature for 3 hrs. The progress of reaction was indicated by a faster moving spot on TLC (ethylacetate:acetone, 1:1). The reaction mixture was diluted with  $\text{CH}_2\text{Cl}_2$  (15 ml), washed with 10 % aq.  $\text{NaHCO}_3$  (10 ml), the organic layer was dried over anhydrous  $\text{Na}_2\text{SO}_4$  and evaporated under vacuum to get **1** as a foam (0.43 g, 98%),  $R_f$  (EtOAc:acetone 1:1, v/v) = 0.43.  $^{31}\text{P}$  NMR ( $\text{CDCl}_3$ )  $\delta$  149.9 and 149 ppm;  $^1\text{H}$  NMR ( $\text{CDCl}_3$ )  $\delta$  8.2 (s, 1H, H2), 7.7 (m, 2H, ArH), 7.1-7.6 (m, 12H, ArH), 6.78 (m, 4H, ArH), 6.2 (d, 1H,  $J = 5.6$  Hz, H1'), 4.85 (m,



1H, H3'), 4.15 (m, 1H, H4'), 3.8 (s, 6H, 2 x OCH<sub>3</sub>), 3.25-3.8 (m, 6H, 11H, 12H, O-CH<sub>2</sub>-), 2.75 (m, 3H, H2' and CH<sub>2</sub>CN) 2.1 (m, 1H, H2''), 1.25 (d, 12H, 2 x NC(CH<sub>3</sub>)<sub>2</sub>).

### 5.5.3 Trimer d(TpA\**p*T) 8.

The trimer d(TpA\**p*T) was synthesized on a Pharmacia GA plus automated DNA synthesizer on dT resin (10 μmol). The modified monomer (dA\*, 0.1 M in CH<sub>3</sub>CN) was used in the synthesis and the overall coupling efficiency was 98%. After the completion of synthesis the cassette was treated with aqueous NH<sub>3</sub> (5 ml, 29%) in a sealed tube at 60°C overnight. The tube was cooled, excess ammonia was boiled off and then centrifuged. The supernatant was then concentrated to 1 ml. This was loaded on a column (2 cm x 12 cm) of DEAE Sephadex (A-25). Elution was performed with ammonium bicarbonate (buffer A = 0.01 M, buffer B = 0.2 M), with a flow rate of 1 ml/min. and fractions each of 5 ml were collected. All fractions corresponding to major peak were pooled together and lyophilised. The residue was then co-evaporated 2-3 times with D<sub>2</sub>O on a speed vac concentrator. Further purity was established by HPLC. Yield 6 mg. <sup>31</sup>P NMR (D<sub>2</sub>O) -0.49 ppm, <sup>1</sup>H NMR (D<sub>2</sub>O) δ 7.95 (s, 1H, H2A\*), 7.45 (s, 2H, H2T1, H2T2), 6.15 (m, 3H, H1'A\*, H1'T1, H1'T2), 4.95 (brs, 1H, H3'A\*), 4.55 (m, 1H, H3'T3), 4.35 (m, 1H, H4'A\*), 4.18 (m, 2H, H5' & H5" A), 4.1 (m, 4H, H4'T1, H4'T3, H5' & 5"T3), 3.75 (t, 2H, H11A\* overlapping with H5' & H5" T1), 3.68 (m, 2H, H5' & H5" T1), 3.3 (t, 2H, H12A\*), 2.85 (t, 2H, H2'A\*), 2.6 (m, 1H, H2"A\*), 2.4 (m, 1H, H2'T1), 2.25 (t, 2H, 2' & 2" T3), 2.08 (m, 1H, 2"T1), 1.83 (s, 3H, 5CH<sub>3</sub>T1), 1.7 (s, 3H, 5CH<sub>3</sub>T3).

### 5.5.4 5',3'-O-Diacetylthymidine 10.

Thymidine (4 g, 16.5 mmol) was dissolved in dry pyridine (15 ml) to which this acetic anhydride (5 ml, 45.3 mmol) was added drop wise and stirred at room temperature overnight. Pyridine was removed under reduced pressure and the residue obtained was dissolved in CH<sub>2</sub>Cl<sub>2</sub> (30 ml) and washed with aq. NaHCO<sub>3</sub> (20 ml). Organic layer

was dried over anhydrous  $\text{Na}_2\text{SO}_4$  and concentrated under reduced pressure to get **10** as a white solid. (4.26 g, 79 %), M. P. = 135°C,  $R_f$  (MeOH:CH<sub>2</sub>Cl<sub>2</sub> 1:9) = 0.6,  $\lambda = 264.3$  (MeOH,  $\epsilon = 9.2 \times 10^4$ ). <sup>1</sup>H NMR (CDCl<sub>3</sub>)  $\delta$  9.5 (s, 1H, NH), 7.28 (s, 1H, H6), 6.33 (dd, J = 5.4 and 8.1 Hz, 1H, H1'), 5.2 (m, 1H, H3'), 4.35 (m, 2H, H5' & H5''), 4.24 (m, 1H, H4'), 2.5 (m, 1H, H2'), 2.2 (m, overlapping with OCOCH<sub>3</sub> peaks, 1H, H2''), 2.14 (s, 6H, 2 x OCOCH<sub>3</sub>), 1.85 (s, 3H, 5CH<sub>3</sub>).

#### 5.5.5 4-O-(2,6-Dimethylphenyl)-thymidine **11**.

5',3'-O-Diacetylthymidine (3.26 g, 10 mmol) was dissolved in dry CH<sub>2</sub>Cl<sub>2</sub> (40 ml) to which mesitylenesulphonyl chloride (5.4 g, 24.7 mmol) was added. The reaction mixture was cooled by immersing in an ice bath (0-5°C), and triethylamine was added dropwise (3.6 g, 35.6 mmol) followed by addition of dimethylaminopyridine (0.24 g, 2 mmol). The reaction mixture was allowed to attain room temperature and stirring continued for 3 hrs, after which the TLC showed a faster moving spot (MeOH:CH<sub>2</sub>Cl<sub>2</sub>, 1:9). To this 2,6-dimethyl phenol (10.0 g, 81.9 mmol), triethylamine (10.0 g, 98.8 mmol) and DABCO (0.2 g, 1.8 mmol) were added and stirred overnight. The reaction mixture was diluted with CH<sub>2</sub>Cl<sub>2</sub> and washed with 5% NaOH solution to remove excess of phenol. The organic phase was dried over anhydrous  $\text{Na}_2\text{SO}_4$  and concentrated. The crude product was purified by silica gel (100-200 mesh) column chromatography and eluted with hexane/CH<sub>2</sub>Cl<sub>2</sub>.

This was treated with sat. MeOH-NH<sub>3</sub> at room temperature for 2 hrs. after which the TLC showed the reaction to be completed. The excess solvent was removed under reduced pressure and the product was purified by column chromatography to obtain **11** (2.8 g, 80%) as a white foam.  $R_f$  (MeOH:CH<sub>2</sub>Cl<sub>2</sub>, 1:9) = 0.5,  $\lambda = 288.5$  (MeOH,  $\epsilon = 6.8 \times 10^4$ ). <sup>1</sup>H NMR (CDCl<sub>3</sub>:DMSO-d<sub>6</sub>, 7:3) 8.2 (s, 1H, H6), 7 (s, 3H, ArH), 6.15 (t, J = 6.1 Hz, 1H, H1'), 4.48 (s, 2H, OH), 4.3 (m, 1H, H3'), 3.9 (m, 1H, H4'), 3.7 (m, 2H, H5' & H5''), 2.35 (m, 1H, H2'), 2.15 (m, 10H, 2 x ArCH<sub>3</sub>, 5CH<sub>3</sub>, H2'').

### 5.5.6 5'-O-(4,4'-Dimethoxytrityl)-4-O-(2,6-dimethylphenyl) thymidine 12.

Compound **11** (2.4 g, 7.2 mmol) was dried over  $P_2O_5$  and co-evaporated with dry pyridine (2 x 15 ml). It was then redissolved in required amount of dry pyridine (35 ml) and 4,4'-dimethoxytrityl chloride (2.94 g, 8.68 mmol) and stirred at room temperature for 4 hrs. The reaction was quenched with methanol (2 ml) and excess pyridine was removed under reduced pressure. The residue was dissolved in  $CH_2Cl_2$  (25 ml) and washed with sat.  $NaHCO_3$  solution (2 x 20 ml) the organic layer was dried over anhydrous  $Na_2SO_4$  and evaporated to dryness. It was then purified by silica gel column chromatography and eluted with  $CH_2Cl_2$  containing 0.5 % triethylamine with incremental amount of methanol. Yield 62% (2.86 g),  $R_f$  ( $CH_3OH:CH_2Cl_2$ , 1:9) = 0.57,  $\lambda = 282.7$  nm (MeOH,  $\epsilon$   $9.4 \times 10^4$ ),  $^1H$  NMR ( $CDCl_3$ ) 8.0 (s, 1H, H6), 7.5-7.2 (m, 9H, ArH), 7 (s, 3H, ArH), 6.82 (d, J = 9.3 Hz, 4H, ArH), 6.3 (t, J = 7.1 Hz, 1H, H1'), 4.5 (brs, 1H, H3'), 4.08 (m, 1H, H4'), 3.8 (s, 6H, 2 x  $OCH_3$ ), 3.4 (m, 2H, H5' & H5''), 2.6 (m, 1H, H2'), 2.2 (m, 1H, H2''), 2.1 (s, 3H, Ar- $CH_3$ ), 2.02 (s, 3H, Ar- $CH_3$ ), 1.7 (s, 3H, 5- $CH_3$ ).

### 5.5.7 5'-O-(4,4'-Dimethoxytrityl)-5-methyl-4-N-(triethylenetriamine)-2'-deoxycytidine 13.

Compound **12** was dissolved (2.56 g, 4 mmol) in dry pyridine (10 ml) to which excess triethylene tetraamine (4 ml) was added and heated at 60°C over a water bath for 10-12 hrs. The reaction mixture was diluted with  $CH_2Cl_2$  (25 ml) and washed with water (2 x 20 ml). The organic layer was dried over anhydrous  $Na_2SO_4$  and evaporated. The crude product obtained was purified by column chromatography and eluted with  $CH_2Cl_2/CH_3OH$  to afford **13** as solid (1.6 g, 59 %),  $\lambda = 276$  nm (MeOH,  $\epsilon$   $11 \times 10^4$ ), M. P. = 114°C,  $^1H$  NMR ( $CDCl_3$ )  $\delta$  7.65 (s, 1H, H6), 7.1-7.5 (m, 9H, Ar-H), 6.83 (d, J = 9.3 Hz, 4H, ArH), 6.46 (t, J = 6.98 Hz, 1H, H1'), 4.55 (brs, 1H, H3'), 4.1 (brs, 1H, H4'), 3.8 (s, 6H, 2 x  $OCH_3$ ), 3.6 (brs, 2H,  $\alpha$  H), 3.45 (m, 1H, H5'), 3.3 (m, 1H, H5''), 2.05-2.95 (m, 12H,  $\beta$ ,  $\gamma$ ,  $\delta$ ,  $\epsilon$ ,  $\theta$  H, H2', H2''), 1.5 (s, 3H, 5- $CH_3$ ),  $^{13}C$  NMR ( $CDCl_3$ )  $\delta$  162.9 (C4),

156.1(C2), 136.6 (C6), 102.1 (C5), 85.7, 85.4 (C1', C4'), 71 (C3'), 63.4 (C5'), 39.3 (C2'), 12.2 (5-CH<sub>3</sub>), 54.8 (DMT-OCH<sub>3</sub>), 158.2, 156.1, 144.3, 135.4, 129.7, 127.9, 127.5, 126.5, 112.9, 86.2 (all from DMT), 56.1, 51.6, 48.4, 47.8, 41.5, 41.1 (C $\alpha$ , C $\beta$ , C $\gamma$ , C $\delta$ , C $\epsilon$ , C $\theta$ ), MS(FAB<sup>+</sup>) calculated for M<sup>+</sup>+Na<sup>+</sup> 695.8126, found 696.

#### 5.5.8 5'-O-(4,4'-Dimethoxytrityl)-5-methyl-4N-(N',N''N''')-tristrifluoroacetyltriethylenetriamine)-2'-deoxycytidine **14**.

Compound **13** (1.2 g, 1.78 mmol) was dissolved in dry ethanol (24 ml), to which dry triethylamine (8 ml) and ethyltrifluoroacetate (6.8 ml) were added. The reaction mixture was stirred at room temperature for 24 hrs. after which ethanol was removed under reduced pressure. The residue was dissolved in dichloromethane (25 ml) and washed with water (3 x 15 ml). The organic phase was dried over anhydrous Na<sub>2</sub>SO<sub>4</sub> and evaporated to get a residue which was purified by silica gel column chromatography to get **14** as a solid (1.24 g, 73 %), M. P. = 103°C, R<sub>f</sub> (MeOH:CH<sub>2</sub>Cl<sub>2</sub>, 1:9) = 0.52,  $\lambda$  = 276.5 nm (MeOH,  $\epsilon$  11 X 10<sup>4</sup>). <sup>1</sup>H NMR (CDCl<sub>3</sub>)  $\delta$  7.75 (s, 1H, H6), 7.1-7.5 (m, 9H, ArH), 6.85 (d, J = 8.4 Hz, 4H, ArH), 6.45 (t, J = 6.5 Hz, 1H, H1'), 5.55 (brs, 1H, NH), 4.55 (brs, 1H, H3'), 4.1 (brs, 1H, H4'), 3.8 (s, 6H, 2 x OCH<sub>3</sub>), 3.15-3.7 (m, 12H,  $\alpha$ ,  $\beta$ ,  $\gamma$ ,  $\delta$ ,  $\epsilon$ , H5' and H5''), 2.8 (m, 2H,  $\theta$  H), 2.43 (m, 1H, H2'), 2.2 (m, 1H, H2''), 1.45 (s, 3H, 5-CH<sub>3</sub>). MS(FAB<sup>+</sup>) calculated for (M<sup>+</sup>+Na<sup>+</sup>) 983.8387, found 984.

#### 5.5.9 3'-O-(2-cyanoethyl-N,N-diisopropylphosphoramido)-5'-O-(4,4'-Dimethoxytrityl)-5-methyl-4N-(N',N''N''')-tristrifluoroacetyltriethylenetriamine)-2'-deoxycytidine **2**.

A mixture of compound **14** (0.42 g, 0.46 mmol) and tetrazole (0.03 g, 0.46 mmol) was co-evaporated with dry dichloroethane (2 x 3 ml). The residue was then dissolved in dry dichloroethane (4.6 ml) 2-cyanoethyl-N,N,N',N'-tetraisopropylphosphorodiamidite (0.214 g, 0.71 mmol, 230  $\mu$ l) was added and stirred at room temperature for 4 hrs.

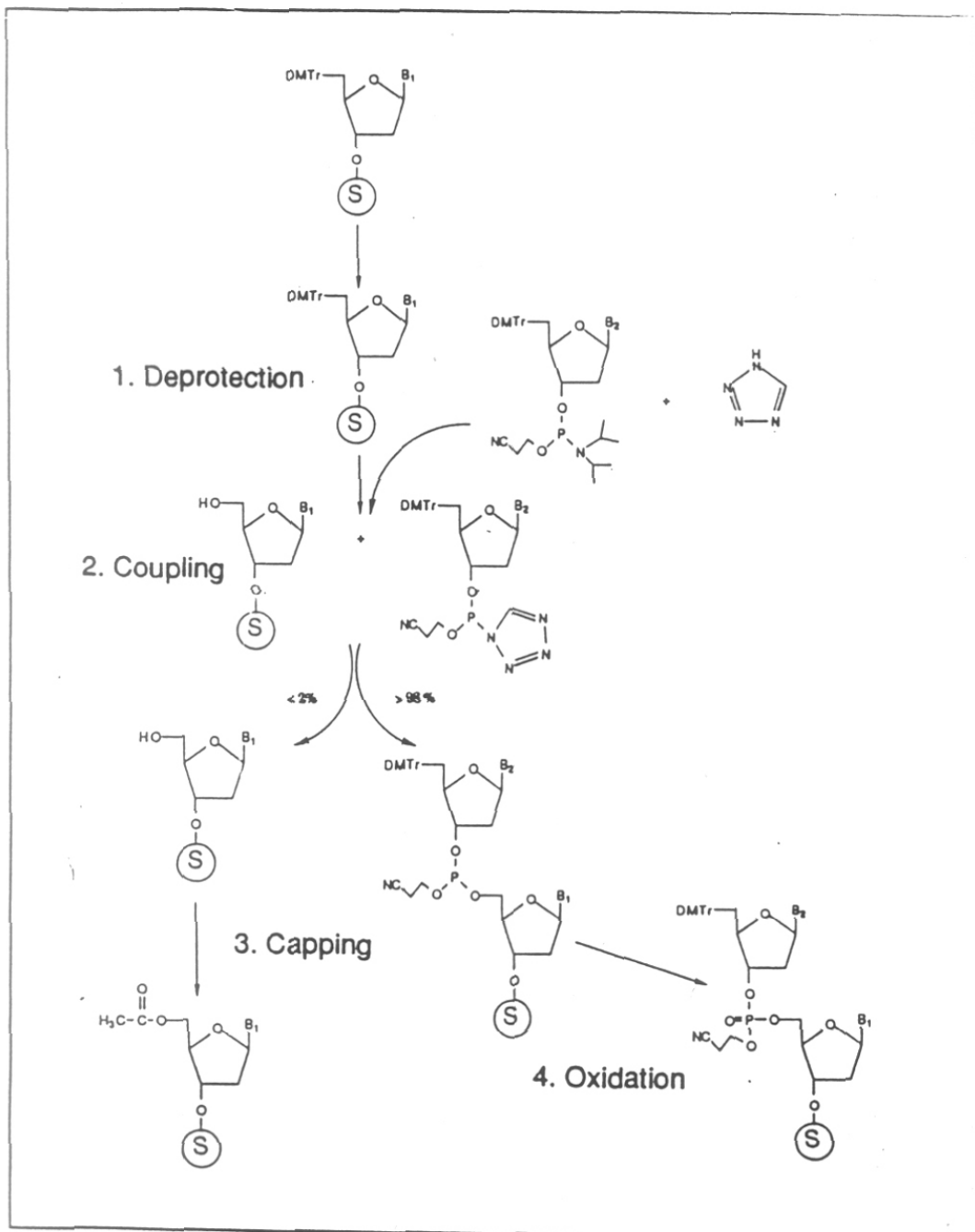
Dichloroethane was removed under reduced pressure and dissolved in dry  $\text{CH}_2\text{Cl}_2$  (10 ml) and washed with 10 % aq.  $\text{NaHCO}_3$  solution (5 ml). The organic layer was dried over anhydrous  $\text{Na}_2\text{SO}_4$  and evaporated under vacuum to obtain **2** as a foam.  $R_f$  ( $\text{MeOH}:\text{CH}_2\text{Cl}_2$ , 0.5:9.5) = 0.32,  $^{31}\text{P}$  NMR ( $\text{CDCl}_3$ )  $\delta$  149.5 and 149.1

#### 5.5.10 Solid phase synthesis of oligonucleotides and purification

Oligonucleotides were synthesized on Pharmacia Gene Assembler (GA Plus) by phosphoramidite chemistry.<sup>23</sup> The steps involved in the assembly of oligonucleotides consisted of (i) condensation (ii) capping (iii) oxidation and (iv) 5' deprotection. **Scheme 4** shows the reaction cycle for each coupling which was repeated for every other coupling. Each step was followed by washing with solvent to remove excess reagents. The cycle time used for each coupling is indicated in the **Table v**. To achieve successful synthesis, following precautions were taken during the synthesis: (i) use of absolutely dry solvents (acetonitrile and dichloroethane) is essential since the internucleotide bond formation in phosphoramidite is inhibited by even trace amounts of water and (ii) high purity reagents (monomers, oxidation and capping solutions).

After the coupling and oxidation reactions but prior to acid treatment for deprotection in each step, 5'-end capping was done to arrest the growth of the unreacted chains and to remove trace amounts of water and keep the reaction medium dry. The coupling efficiency as monitored by trityl assay (UV detector) was over 90% at each step. The **Table I** shows an example of the synthesis report obtained after synthesis.

At the end of the synthesis, deprotections of exocyclic amino and internucleotide phosphate group were achieved by treatment with aqueous ammonia at 60°C for 24 hrs. The oligonucleotide sequences were passed through NAP (Pharmacia) columns, containing Sephadex G-25, to achieve desalting.



SCHEME-IV

**TABLE-V: Reagent/Solvent delivery timings in solid phase synthesis**

Reagent	Time	Flow ml/min
1. Ethylenedichloride wash	1.3	2.5
2. Detritylation 3% DCA/EDC	2.0	2.5
3. Acetonitrile wash	1	2.5
4. Tetrazole	0.1	1.0
5. Amidite (0.1 M soln.)	0.1	0.5
6. Tetrazole (0.5 M)	0.1	1.0
7. Acetonitrile	0.2	2.0
8. Recycle during coupling	3	2.5
9. Acetonitrile wash	0.3	2.5
10. Capping A	0.1 X 2	0.5
11. Capping B	0.1 X 2	0.5
12. Acetonitrile wash	0.3	2.5
13. Oxidation	0.1	2.5
14. Acetonitrile	1.0	2.5

Oxidation solution: 0.01 M Iodine in collidine/water/acetonitrile. (260ml dry acetonitrile + 1.03g iodine + 24ml collidine + 120 ml distilled water)

Capping A: 6% Dimethylamino pyridine (DMAP) in acetonitrile.

Capping B: 50ml dry acetonitrile + 20ml acetic anhydride + 30ml collidine.

Detritylation: 1% trichloroacetic acid in ethylene dichloride.

The purification of the synthesized oligonucleotides was performed using reverse phase FPLC RPC HR (5/5) (Pharmacia). Buffer A: 5% acetonitrile in 0.1 M TEAA; Buffer B: 20% acetonitrile in 0.1 M TEAA, Programme- 0 to 5 minutes 0% B, 5 to 50 minutes 70% B, 50-55 minutes 100% B, 55 to 60 minutes 100 % B, 60 to 62 minutes 0 % B, 62 to 67 minutes 0 % B. The appropriate peaks were collected and lyophilised to remove the triethylammonium acetate salt. The fractions were monitored for absorbance at 260 nm and the relevant fractions were pooled and concentrated. The amount of oligonucleotides were estimated using UV spectra and following extinction coefficients: T,  $\epsilon = 8.8$ ; C,  $\epsilon = 7.3$ ; G,  $\epsilon = 11.7$ ; A,  $\epsilon = 15.4$  in  $\text{cm}^2/\mu\text{mol}$ .

The oligonucleotides were checked for their purity by HPLC, using a reverse phase column (C18) and following buffers were used for the analysis: Buffer A:5% acetonitrile in 0.1% TEAA, Buffer B:30% acetonitrile in 0.1% TEAA. Gradient A to B in 20 minutes with a flow rate of 2 ml/min. Following normal oligonucleotides were synthesized for the study **19**, **20** and **21**.

#### **Dickerson's dodecamer 6 & 7.**

0.1 M solution of the compound **1** in dry acetonitrile was used for the solid phase synthesis of oligonucleotide sequences **6** and **7**. The synthesis was carried out according to the procedure discussed above on a 1.3  $\mu\text{mol}$  scale. Pre packed cassettes with G resin were used (Pharmacia). Crude oligos were purified by FPLC and purity was further established by HPLC.

#### **Oligonucleotide 16, 17 and 18**

0.1 M solution of the compound **2** in dry acetonitrile was used for the solid phase synthesis of oligonucleotides. The synthesis was carried out on a Pharmacia GA Plus



on 1.3  $\mu\text{mol}$  scale as described above. The crude oligos obtained were purified by FPLC to obtain the pure sequences **16**, **17** and **18**. Further purity was established by HPLC.

#### 5.5.11 3',5'-Bis-(t-butyldimethylsilyl)-8-bromo-2'-deoxyadenosine **25**

8-Bromo-2'-deoxyadenosine (0.4 g, 1.2 mmol) was dissolved in dry DMF to which t-BDMSCl (0.73 g, 4.8 mmol) and imidazole (0.71g, 10.5 mmol) were added and stirred at room temperature for 9 hrs. The reaction was monitored by TLC and after completion (9 hrs.) DMF was removed under reduced pressure. The residue was dissolved in  $\text{CH}_2\text{Cl}_2$  and washed with water. The organic layer was concentrated on a rotavapor under reduced pressure. It was then purified by silica gel column chromatography and eluted with  $\text{CH}_2\text{Cl}_2$ -Hexane. Major side product was trisilyl compound which was separated from the required product **25** by column chromatography. The product **24** obtained in 39% yield (0.297 g).  $^1\text{H}$  NMR ( $\text{CDCl}_3$ )  $\delta$  8.25 (s, 1H, H2), 6.35 (t, J = 7.3 Hz, 1H, H1'), 5.8 (s, 2H, 6-NH<sub>2</sub>), 4.9 (m, 1H, H3'), 3.95 (m, 1H, H4'), 3.9 (d, J = 6.8 Hz, 1H, H5"), 3.68 (m, 2H, H2' and H5'), 2.5 (m, 1H, H2"), 0.95 (s, 9H, 3 x CH<sub>3</sub>), 0.85 (s, 9H, 3 x CH<sub>3</sub>), 0.18 (s, 6H, 2 x CH<sub>3</sub>), 0 (d, 6H, 2 x CH<sub>3</sub>).

#### 5.5.12 8-Amino(2-aminoethyl)-2'-deoxyadenosine **26**

8-Bromo-2'-deoxyadenosine **24** (0.43 g, 1.3 mmol) was dissolved in 1,2-diaminoethane (0.5 ml) and stirred at room temperature for 8 hrs after which TLC showed completion of the reaction. The excess ethylenediamine was removed under reduced pressure, to obtain a residue which was thoroughly washed with  $\text{CHCl}_3$  to get pure product in quantitative yield.  $^1\text{H}$  NMR ( $\text{D}_2\text{O}$ )  $\delta$  8.46 (s, 1H, H2), 6.38 (dd, J = 6.1 Hz, 1H, H1'), 4.65 (m, 1H, H3'), 4.2 (m, 1H, H4'), 3.93 (brs, 2H, H5' & H5"), 3.75 (m, 2H,  $\alpha$  H), 3.4 (t, J = 7.3 Hz, 2H,  $\beta$  H), 2.81 (m, 1H, H2'), 2.35 (m, 1H, H2").

### 5.5.13 3',5'-Bis(t-butyldimethylsilyl)-8-amino(2-aminoethyl)-2'-deoxyadenosine 27

Compound **26** (0.46 g, 1.5 mmol) was dissolved in dry DMF (1.5 ml) to which t-BDMSCl (0.87 g, 5.8 mmol) and imidazole (0.8 g, 11.8 mmol) were added and stirred at room temperature for 9 hrs. After completion of reaction, DMF was removed under reduced pressure. The residue was dissolved in CH<sub>2</sub>Cl<sub>2</sub> (20 ml) and washed with water (3 x 10 ml). Organic layer was evaporated under reduced pressure and the residue obtained was purified by silica gel column chromatography and eluted with CH<sub>2</sub>Cl<sub>2</sub>/MeOH to get **27** (0.27 g, 27 %) as white solid. <sup>1</sup>H NMR (CDCl<sub>3</sub>) δ 8.23 (s, 1H, H2), 7.2 (s, Overlapping with CHCl<sub>3</sub> peak, 2H, NH<sub>2</sub>), 6.38 (dd, J = 8.2 & 6.8 Hz, 1H, H1'), 6.2 (brs, 1H, NH), 5.45 (brs, 2H, 6-NH<sub>2</sub>), 4.55 (m, 1H, H3'), 3.98 (m, 1H, H4'), 3.9 (d, J = 2.7 Hz, 1H, H5"), 3.83 (d, J = 2.7 Hz, 1H, H5'), 3.58 (m, 4H, α H and β H), 2.78 (m, 1H, H2'), 2.2 (m, 1H, H2"), 0.93 (s, 18H, 6 X CH<sub>3</sub>), 0.13 (s, 12H, 4 X CH<sub>3</sub>)

### 5.5.14 3',5'-di-O-(t-butyldimethylsilyl)-2'-deoxythymidine 29

Thymidine **28** (0.5 g, 2.06 mmol) was dissolved in dry DMF (2 ml) into which imidazole (0.84 g, 6.18 mmol) and TBDMSCl (0.93 g, 6.18 mmol) were added. The reaction mixture was stirred at room temperature for 8 hrs. DMF was removed under reduced pressure and the residue dissolved in CH<sub>2</sub>Cl<sub>2</sub> (20 ml) and washed with water (2 x 15 ml). The organic layer was concentrated on a rotavapor and the residue obtained was purified by silica gel column. CH<sub>2</sub>Cl<sub>2</sub>/hexane was used as eluent to elute **29** (1 g, 97 %). <sup>1</sup>H NMR (CDCl<sub>3</sub>) δ 8.85 (s, 1H, N3-H), 7.4 (s, 1H, H6), 6.33 (dd, J = 5.9 and 7.8 Hz 1H, H1'), 4.41 (m, J = 2.7 Hz, 1H, H3'), 3.92 (m, 1H, H4'), 3.8 and 3.7 (ddd, 2H, H5' and 5"), 2.0 and 2.2 (ddd, J = 2.7 and 5.9 Hz, H2' and H2"), 1.9 (s, 3H, 5-CH<sub>3</sub>), 0.9 (2 x s, 18H, 2 x C(CH<sub>3</sub>)), 0.06 and 0.13 (2 x s, 12H, 2 x Si(CH<sub>3</sub>)<sub>2</sub>). <sup>13</sup>C NMR (CDCl<sub>3</sub>) δ 163.5 (C4), 150.1 (C2), 134.5 (C6), 110.7 (C5), 87.8 (C4'), 84.8 (C1'), 72.2 (C3'), 62.9 (C5'), 41.3 (C2'). Analysis, Cal. C<sub>22</sub>H<sub>42</sub>O<sub>5</sub>N<sub>2</sub>Si<sub>2</sub>: C, 56.13; H, 8.98; N, 5.95. Found: C, 55.94; H, 9.5; N, 5.75.

### 5.5.15 3',5'-di-O-(t-butylidimethylsilyl)-2'-deoxyadenosine **23**

To 2'-Deoxyadenosine **22** (0.4 g, 1.6 mmol) in dry DMF (1.8 ml) TBDMSCI (0.72 g, 4.8 mmol) and imidazole (0.65 g, 9.6 mmol) were added. By following the same procedure as described above the product **23** was obtained in 62% yield (0.47 g).  $^1\text{H}$  NMR ( $\text{CDCl}_3$ )  $\delta$  8.35 (s, 1H, H8), 8.15 (s, 1H, H2), 6.45 (t,  $J = 6.4$  Hz, 1H, H1'), 5.9 (s, 2H,  $6\text{NH}_2$ ), 4.61 (m, 1H, H3'), 4.01 (m, 1H, H4'), 3.7 and 3.8 (ddd, 2H, H5' and H5''), 2.4 and 2.5 (ddd,  $J = 6.4, 4.1$  and  $13.0$  Hz, 2H, H2' and H2''), 0.93 (s, 18H,  $2 \times \text{C}(\text{CH}_3)_3$ ), 0.15 (s, 12 H,  $2 \times \text{Si}(\text{CH}_3)_2$ ).  $^{13}\text{C}$  NMR ( $\text{CDCl}_3$ )  $\delta$  155.3 (C6), 149.6 (C4), 139.1 (C8), 120.1 (C5), 87.9 (C4'), 84.3 (C1'), 71.9 (C3'), 62.8 (C5'), 41.2 (C2'). Analysis, Calc.  $\text{C}_{22}\text{H}_{41}\text{O}_3\text{N}_5\text{Si}_2$ : C, 55.08; H, 8.60; N, 14.59. Found: C, 55; H, 8.5; N, 14.36.

### 5.5.16 5'-O-(4,4'-dimethoxytrityl-4N-(N-methyl-3-aminopropyl)-5-methyl-2'-deoxycytidine **15**

Compound **12** (0.33 g, 0.5 mmol) was dissolved in dry pyridine (1.5 ml) and N-methyl-1,3-diaminopropane (0.5 ml) was added and heated at  $60^\circ\text{C}$  for 12 hrs. Pyridine was removed under vacuum and the residue was dissolved in  $\text{CH}_2\text{Cl}_2$  (10 ml) and washed with water ( $2 \times 5$  ml). The organic layer was evaporated and the gum obtained was purified by silica gel column chromatography to get **15** (0.24 g, 75 %).  $R_f = 0.4$  (15 %  $\text{MeOH}-\text{CH}_2\text{Cl}_2$ ),  $^1\text{H}$  NMR  $\delta$  7.6 (s, 1H, H6), 7.1-7.45 (m, 9H, ArH), 6.8 (d,  $J = 7.6$  Hz, 4H, ArH), 6.35 (t,  $J = 6.3$  Hz, 1H, H1'), 4.5 (brs, 1H, H3'), 4.1 (brs, 1H, H4'), 3.75 (s, 6H,  $2 \times \text{OCH}_3$ ), 3.6 (m, 2H,  $\alpha$  H), 3 (m, 2H,  $\gamma$  H), 3.38 (m, 2H, 5' & H5''), 2.65 (s, 3H, N- $\text{CH}_3$ ), 2.45 (m, 1H, H2'), 2.13 (m, 3H,  $\beta$  H, H2''), 1.53 (s, 3H, 5- $\text{CH}_3$ );  $^{13}\text{C}$  NMR ( $\text{CDCl}_3$ )  $\delta$  163.7 (C4), 156.4 (C2), 137 (C6), 103.7 (C5), 86, 85.6 (C1', C4'), 71.9 (C3'), 63.7 (C5'), 41.7 (C2'), 53.6 ( $\text{C}\alpha$ ), 37.6 ( $\text{C}\beta$ ), 46.7 ( $\text{C}\gamma$ ). 33.4 (N- $\text{CH}_3$ ), 12.8 (5- $\text{CH}_3$ ).

### 5.5.17 5'-End labeling of oligonucleotides 6, 7 and 19

The oligonucleotides **6**, **7** and **19** were 5'-end labeled by using T4 polynucleotide kinase (10 units/200 pmol) and [ $\gamma$ - $^{32}$ P]ATP (spec. act. 3000  $\mu$ Ci/mm)<sup>24</sup> as follows. Oligonucleotides **6**, **7** and **19** (15  $\mu$ l, 0.2 OD) were taken in autoclaved eppendorf. To each of tube 2X kinase buffer (120 mM Tris-HCl, pH 8.5, 20 mM MgCl<sub>2</sub>, 20 mM dithiothreitol, 5  $\mu$ l), sterile water (22  $\mu$ l) and T<sub>4</sub> polynucleotide kinase (1  $\mu$ l, 500 u/ml) were added and centrifuged. Then 1  $\mu$ l [ $\gamma$ - $^{32}$ P]ATP (10  $\mu$ Ci) was added and centrifuged. It was then incubated at 37°C for 45 minutes. After this, 1  $\mu$ l of 0.5 M EDTA (pH 7-7.5), 2  $\mu$ l (0.15 M) NaCl, 2  $\mu$ g CT DNA, 80  $\mu$ l ethanol were added, centrifuged for 15 minutes. Supernatant liquid was removed and 30  $\mu$ l of water, 2  $\mu$ l NaCl (0.15 M) and 80  $\mu$ l ethanol were added mixed and kept it for precipitation at -70 °C for 1 hr. followed by centrifugation for 15 minutes. Supernatant was discarded and count was taken using LKB Scintillation counter (7.8 x 10<sup>5</sup> cpm).

### 5.5.18 Eco R1 digestion

The 5'-end labeled oligonucleotides **6**, **7** and **19** (0.06 O.D, A<sub>260</sub>) were treated with Eco R1 (12  $\mu$ l, activity 2 u/ $\mu$ g) in 1X buffer (50  $\mu$ l, Tris HCl 50 mM, NaCl 100 mM, MgCl<sub>2</sub> 10 mM, dithiothreitol 1mM, pH 7.5) and incubated at 37 °C for 48 hrs. The reaction was quenched by adding EDTA (1  $\mu$ l, 0.5 M) and the products were mixed with bromophenol blue dye-formamide (6  $\mu$ l, 0.5% BPB and 0.5% xylene cyanol) and loaded into different wells on a 20% polyacrylamide gel for analysis by electrophoresis at 400 V, 15 mA (buffer 1X Tris Borate, EDTA) until the dye reached about 75% of the gel length. The gels were visualized after autoradiography. It was then photographed on a UVP gel documentation system.

### 5.5.19 Sample preparation for melting experiments

The duplex DNA samples were prepared by mixing equimolar concentrations of the each DNA strand in a buffer, heating to 95°C and slow cooling to effect duplex formation. The self complementary sequences were used by dissolving in buffer and 0.3 to 0.6 OD units at (260 nm) of each sequence was used for melting experiments. The buffers used for spectroscopic measurements was

A, Tris-10mM, NaCl-80 mM, MgCl<sub>2</sub>-20 mM, pH-7.6.

Oligonucleotides **16** and **17** were mixed in equimolar proportion with its complementary sequence **20** and heated to 95 °C for 5 minutes. Then the sample was allowed to cool slowly in order to form duplex structure. Similarly duplex DNA was made by mixing **19** and **20**. 0.4 to 0.6 OD units of the duplex DNA was used for each experiment.

## 5.6 REFERENCES

1. (a) Ganem, B. *Acc. Chem. Res.* **1982**, *15*, 290. (b) Tabor, C. W.; Tabor, H. *Ann. Rev. Biochem.* **1984**, *53*, 749. (c) Pegg, A. E. *Biochem. J.* **1986**, *234*, 249. (d) Behr, J. -P. *Acc. Chem. Res.* **1993**, *26*, 274.
2. (a) Uhlmann, E.; Peyman, A. *Chem. Rev.*, **1990**, *90*, 544. (b) Riordan, M. L.; Martin, J. C. *Nature*, **1991**, *350*, 442.
3. (a) Fleischman, R. A.; Campbell, J. L.; Richardson, C. C. *J. Biol. Chem.*, **1976**, *251*, 1561. (b) Kaplan, D. A.; Nierlich, D. P. *J. Biol. Chem.*, **1975**, *250*, 2395.
4. (a) Kropinski, A. M. B.; Bose, R. J.; Warren, R. A. *J. Biochemistry*, **1973**, *12*, 151. (b) Miller, P. B.; Wakarchuk, W. W.; Warren, R. A. *J. Nucleic Acid Res.*, **1985**, *13*, 2559.
5. (a) MacMillan, A. M.; Verdine, G. L. *J. Org. Chem.*, **1990**, *55*, 5931-5933. (b) MacMillan, A. M.; Verdine, G. L. *Tetrahedron* **1991**, *47*, 2603.
6. Goodchild, J. *Bioconj.Chem.*, **1990**, *1*, 165.
7. (a) Haralambidis, J.; Chai, M.; Tregear, G. W. *Nucleic Acids Res.*, **1987**, *15*, 4857 (b)

- Zuckermann, R.; Corey, D.; Schultz, P. G. *Nucleic Acids Res.*, **1979**, *7*, 1485 (c)
- Agarwal, S.; Christodoulou, C.; Gait, M. J. *Nucleic Acids Res.*, **1986**, *14*, 6227 (c)
- Chu, B. C. F.; Wahl, G. M.; Orgel, L. E. *Nucleic Acids Res.*, **1983**, *11*, 6513.
8. (a) Moser, H. E.; Dervan, P. B. *Science (Washington D. C.)*, **1987**, *238*, 645 (b)
- Strobel, S. A.; Dervan, P. B. *Science (Washington D. C.)*, **1990**, *249*, 73 (c) Zuckermann, R. N.; Schultz, P. G. *J. Am. Soc.*, **1988**, *110*, 6592.
9. (a) Gillam, I. C.; Tener, G. M. *Anal. Biochem.*, **1986**, *157*, 199 (b) Urdea, M. S.; Warner, B. D.; Running, J. A. J.; Clyne Stempien, M. J.; Horn, T. *Nucleic Acids Res.*, **1988**, *16*, 4937.
10. (a) Gibson, K. J.; Benkovic, S. J. *Nucleic Acids Res.*, **1987**, *15*, 6455. (b) Xiao, L.; Swank, R. A.; Matthews, H. R. *Nucleic Acids Res.* **1991**, *19*, 3701. (c) Schmid, N.; Behr, J. -P. *Biochemistry* **1991**, *30*, 4357.
11. (a) Asseline, U.; Toulme, F.; Thuong, N. T.; Delarue, M.; Montenay-Garestier, T.; Helene, C. *EMBO J.*, **1984**, *3*, 795 (b) Asseline, U.; Delarue, M.; Lancelot, G.; Toulme, F.; Thuong, N. T.; Montenay-Garestier, T.; Helene, C. *Proc. Natl. Acad. Sci. U. S. A.*, **1984**, *81*, 3297 (c) Lancelot, G.; Asseline, U.; Thuong, N. T.; Helene, C. *Biochemistry*, **1985**, *24*, 2521.
12. Takeda, T.; Ikeda, K.; Mizuno, Y.; Ueda, T. *Chem. Pharm. Bull.*, **1987**, *36*, 3558.
13. (a) Sinha, N. D.; Binernat, J.; Koster, H. *Tetrahedron Lett.*, **1983**, *24*, 5843. (b) Sinha, N. D.; Biernat, J.; McManus, J.; Kosler, H. *Nucleic Acids Res.*, **1984**, *12*, 4539.
14. (a) Zhou, X. -X.; Chattopadhyaya, J. *Tetrahedron* **1986**, *42*, 5149.
15. (a) Pieleles, U.; Sproat, B. S.; Lamm, G. M. *Nucleic Acids Res.*, **1990**, *18*, 4355.
- (b) Sarfati, S. R.; Pochet, S.; Guerreiro, C.; Namane, A.; Huynh-Dinh, T.; Igoien, J. *Tetrahedron* **1987**, *43*, 3491.
16. Goody, R. S.; Walker, R. T. *Tet. Lett.*, **1967**, 289.
17. (a) Puglisi, J. D.; Tinoco Jr., I. *Methods in Enzymology*, **1989**, *180*, 304. (b) Cantoni, G. L.; Davies, D. R. *Procedures in Nucleic Acid Research*, Harper and Row: New

- York, **1971**, 11. (c) Holde, K. E. V.; Brahms, J.; Michelson, A. M. *J. Mol. Biol.*, **1965**, 12, 726. (d) Allen, F. S.; Gray, D. M.; Roberts, G. P.; Tinoco Jr., I. *Biopolymers*, **1972**, 11, 853. (e) Longfellow, C. E.; Kievzek, R.; Turner, D. H. *Biochemistry*, **1990**, 29, 278. (f) Duchesence, J.; *Physicochemical Properties of Nucleic Acids*, **1973**, II, Academic Press Inc. London.
18. Kyogoku, Y.; Lord, R. C.; Rich, A. *Proc. Natl. Acad. Sci., U. S. A.*, **1967**, 57, 250.
19. (a) Katz, L.; Penman, S. *J. Mol. Biol.*, **1966**, 15, 220. (b) Newmark, R. A.; Cantor, C. R. *J. Am. Chem. Soc.*, **1968**, 90, 5010.
20. Ogilvie, K. K. *Can. J. Chem.*, **1973**, 51, 3799.
21. Job, A. *Annales de Chim* **1928**, 9, 113.
22. Wilcox, C. S. "*Frontiers in Supramolecular Organic Chemistry and Photochemistry*", Schneider, H.; Durr, H.; Ed.; VCH, Weinheim, 1990.
23. Tavale, S. S.; Sobell, H. M. *J. Mol. Biol.* **1970**, 48, 109.
24. Gait, M. J. (ed) *Oligonucleotide synthesis: a practical approach*, IRL Press: Oxford, **1984**. (b) Gene assembler plus: Owners Manual Pharmacia, LKB Biotechnology **1991**.
25. Sambrook, J.; Fritsch, E. F.; Maniatis, T. *Molecular Cloning: A Laboratory Manual*, Cold Spring Harbour Laboratory Press, **1989**.